2012

From pincers to scorpionates: The synthesis and reactivity of oxazoline based transition metal and alkaline earth metal complexes

Steven Ryan Neal
Iowa State University

From pincers to scorpionates: The synthesis and reactivity of oxazoline based transition metal and alkaline earth metal complexes

by

Steven Ryan Neal

A dissertation submitted to the graduate faculty

in partial fulfillment for the degree of

DOCTOR OF PHILOSOPHY

Major: Organic Chemistry

Program of Study Committee:

Aaron D. Sadow, Major Professor

Malika Jeffries-EL

William Jenks

Gordon Miller

Nicola Pohl

Iowa State University

Ames, Iowa

2012

Table of Contents

Acknowledgments

My years in graduate school can be summed up as a crazy rollercoaster ride. During my orientation, I remember Erin Rockafellow drawing this graph of happiness versus year in grad school. It started out very high since all of us were excited about this new adventure we were about to embark on. It remained fairly steady with a few bumps along the way as research progressed…until the third year. The drastic drop coincided with our prelim-exam; after that it was a gradual (bumpy) increase until this point where we dropped precipitously while writing our dissertation. As silly as I thought this was at the time, I realize looking back how true, and fun, the ride has been.

At the helm of this rollercoaster is Dr. Aaron Sadow; how could I possibly have gotten anywhere without his advice, kind words, and "do more reactions?" There were days that I didn't want to see him because I might yell and scream at him, and I am sure he would say the same about me, and days that I couldn't wait for him to come by the lab to show him the latest spectra or kinetics plot. What I have learned from him can only be summarized by one word, everything; you have taught me everything I know about being a scientist. Thank you for being hard on me.

To my committee, Dr. Malika Jeffries-EL, Dr. Nicola Pohl, Dr. William Jenks, and Dr. Gordon Miller, thank you for your exceptionally valuable time for discussions, POS meetings, and last minute signatures.

The Sadow group, what do I say. I owe every one of you a huge thank you. To all past and present members – Dr. James Dunne, Ben Baird, Jiachun Su, KaKing Yan, Hung-An Ho, Ryang Kim, Dr. Andrew Pawlikowski, Stephanie Smith, Kuntal Manna, Debabrata Mukherjee, Songchen Xu, Dr. Barun Jana, Jing Zhu, Nicole Lampland, Naresh Eedugurala, Aradhana Pindwal, Zak Weinstein, Jacob Fleckenstein, Regina Reinig – you have had to put

up with my messy desk and bench for all these years. We have had way too many sandwiches from West Street Deli, enjoyed a few good beers at DG's, and many many late nights that I will never forget. I hope we cross paths again someday, until then…sleep less.

We have been blessed to have many undergraduates in the lab over the years – Shawna, Marlie, Tristan, Jared, Kate, Jooyoung, Brianna, Rick, Josh, Marissa, Megan, Yitzhak, Yixin, Jessica. While I hope I helped many of you become better scientists, you will never know just how much you taught me. Thank you for helping to keep me sane over the years, there is always time for a good laugh. Good luck to all of you in your adventures in life.

To all the students, past and present, in the chemistry department, your insightful discussions, chemistry and non-chemistry related, have played a very important role in all parts of my graduate career; thank you.

A huge thank you goes out to the staff of the chemistry department; we would all be completely lost without your constant reminders about seminars, deadlines, and the occasional open house participation request. You keep us all going.

My family – Mom, Dad, Erin, Barb, Alan, Tisha, Jennifer – you have been such a strong influence over the years; how can I ever thank you for your love, support, an ear to complain to, and frequent e-mail jokes.

And lastly, Ally…I don't know how you did it. From the day we visited Ames and I had to explain to you that what you were looking at is a snow blower to now where we just laugh at snow. You have put up with my late nights, early mornings, and constant 'yes I have to go back to work.' You are an amazing woman; I love you very much. Benton, your infectious smile and persistent "hi" has made the writing process so difficult and fun all at the same time. You have been a blessing to my life.

Abstract

Multidentate oxazoline based ligands have played a critical role in transition metal chemistry. They have several key advantages over many other ligands: (i) strong chelating ability, (ii) chiral versions readily synthesized from commercially available amino acids, (iii) the chirality is in close proximity to the metal center. With this in mind, we set out to design new bis(oxazoline) ligands that would cyclometalate with late-metal centers and tris(oxazoline) ligands for d^0 metal centers.

We synthesized new achiral [bis(4,4-dimethyl-2-oxazolinyl)propane], Probox^{Me2}, and chiral [bis(4*R*-phenyl-2-oxazolinyl)propane], Probox^{Ph}, ligands for use as pincer complex proligands. While the isopropyl derivative, Probox^{iPr}, was known, no transition metal complexes containing these ligands have been reported. We attempted to synthesize palladium pincer complexes with Probox^{Me2} and Probox^{iPr} but isolated thermally robust dipalladium(II) macrocycles of the form $[(Probox)PdCl_2]_2$. Attempts with rhodium provided a similar rhodium(I) macrocycle with Probox^{Ph}. Finally, a rhodium(III) pincer complex is obtained with Probox^{Me2}. The spectroscopic and structural characteristics along with their reactivity are described.

Since cyclometalation of Probox based ligands proved to be much more difficult than anticipated, we changed gears to tris(oxazolinyl)phenylborate ligands. Our group had reported the synthesis of achiral tris(4,4-dimethyl-2-oxazolinyl)phenylborate, To^M, and chiral tris(4*S*-isopropyl-2-oxazolinyl)phenylborate, To^P, along with the synthesis of several metal complexes containing these ligands. Unfortunately, we found that the isopropyl group in To^P, when coordinated to a metal, rotates away from the metal center, presumably to avoid steric interactions with the metal center, thus lessening the stereochemical control during asymmetric transformations. We decided to design a new chiral tris(oxazolinyl)phenylborate

ligand with *tert*-butyl groups at the 4-position on the oxazoline ring with the anticipation that the *tert*-butyl group will remain in close proximity to the metal center. Magnesium and calcium complexes bearing this ligand have been prepared and used as catalysts for the asymmetric hydroamination/cyclization of aminoalkenes with moderate success. We observed high conversion to the corresponding pyrrolidines with % ee's that were significantly higher than any other group 2-catalyst system to date.

$To^{M}MgMe$ was found to be an efficient precatalyst for the cross-dehydrocoupling of amines and silanes. With evidence gathered through kinetic investigations, including a Hammett plot, a new mechanism was proposed that involves a nucleophilic attack of the magnesium amide on the silane followed by hydrogen transfer to magnesium and displacement of the newly formed silazanes. Rapid protonolysis of the magnesium hydride with amine completed the catalytic cycle. Additionally, kinetic studies on the action of $To^{M}MgMe$ with $PhSiH_3$ were also conducted. These included Eyring analysis, isotope effect, and a Hammett plot; these data provided evidence that this process is very similar to the Si–N bond forming reactions catalyzed by $To^{M}MgMe$. Additionally, preliminary studies on catalytic hydrosilylation using $To^{M}MgMe$ and $To^{M}MgMe$ with $B(C_6F_5)_3$ as precatalysts are reported.

Chapter 1: Ligand effects on organomagnesium compounds

General Introduction

The design of new ligands for catalytic reactions is a continuous process because of the need to improve existing transformations while developing new reactions for organic synthesis. The synthesis of a single ligand class that can be easily modified to control the steric and electronic features of the metal complexes would be ideal. Additionally, a ligand that can stabilize reactive metal compounds (i.e. reaction intermediates) would be beneficial for mechanistic studies. In this vein, we have worked to synthesize new oxazoline based ligands for late transition metal and alkaline earth metal complexes. This thesis describes the synthesis of a new class of bis(oxazoline) ligands and their reactivity with palladium and rhodium metal centers; as well as the design of a new chiral tris(oxazolinyl)phenylborate ligand for magnesium and calcium and the action of these alkaline earth metal complexes in the hydroamination/cyclization of aminoalkenes. The design of these two ligands is centered on their ability to facially coordinate to the metal center.

Ever since Parkin and co-workers published their first work on isolated single site magnesium complexes containing the bulky tris(pyrazolyl)hydroborate ligands (Eq. 1-1),[1] a multitude of reports investigating the reactivity of well defined magnesium species have appeared.[2-23]

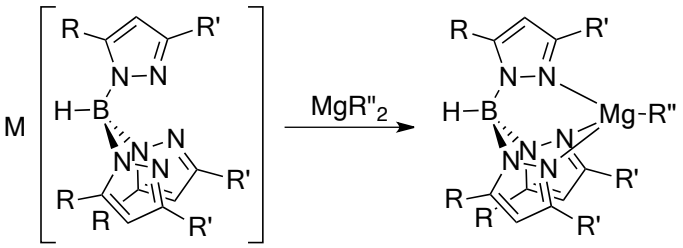

M = K, R = R' = Me, R" = Me
M = Tl, R = H, R' = tBu, R" = Me, Et

(Eq. 1-1)

Grignard reagents are very important tools in organic and organometallic chemistry; however, the development of new organomagnesium mediated reactions is complicated by the uncertainty of the active species in solution.[1, 24] Several monometallic solid state structures of Grignard reagents began to appear in the literature in the 1960's,[24] but the structure of Grignards in the solution state are more ambiguous for several reasons. First is the existence of the Schlenk equilibrium (Eq. 1-2)[25] and the several factors (e.g. solvent, temperature, and additional donor ligands)[26-27] that control the position of the equilibrium. Grignard reagents have a tendency to aggregate to form multimetallic complexes in donor solvents (e.g. Et_2O or THF), and form 'ate' complexes when mixed with alkali metal compounds (e.g. *n*-butyllithium).

$$2\ RMgX \rightleftharpoons R_2Mg + MgX_2$$

(Eq. 1-2)

The strong influence of the chelating ligand on the position of the Schlenk equilibrium is exemplified by the $Tp^{R}Mg$ chemistry. The very bulky $Tp^{tBu}MgMe$ (Tp^{tBu} = tris(3-*tert*-butylpyrazolyl)hydroborate) exists as a monomer in solution and in the solid state. Thermolysis of $Tp^{tBu}MgMe$ at 120 °C for 7 days results in isolation of only starting material. In contrast, Tp*MgMe (Tp* = tris(3,5-dimethylpyrazolyl)hydroborate) is isolated as a monomer but can be converted to $(Tp^*)_2Mg$ and $MgMe_2$ upon heating to 80 °C.

Parkin's first reports were focused on the synthesis of Tp^{tBu}MgR (R = CH_3, CH_2CH_3, $CH_2(CH_2)_2CH_3$, $CH(CH_3)_2$, $C(CH_3)_3$, $CH_2Si(CH_3)_3$, $CH{=}CH_2$, C_6H_5)[4] followed by reports focused on the stoichiometric reactivity of Tp^{tBu}MgR.[1-3, 5] As shown in (Eq. 1-3), Tp^{tBu}MgMe undergoes alkane elimination with a variety of protic reagents. Interestingly, Tp^{tBu}MgMe does not react with ketones (with α-protons) via 1,2-addition as is typical for Grignard reagents, but deprotonates the α-carbon on the ketone to generate the magnesium enolate complex.[5]

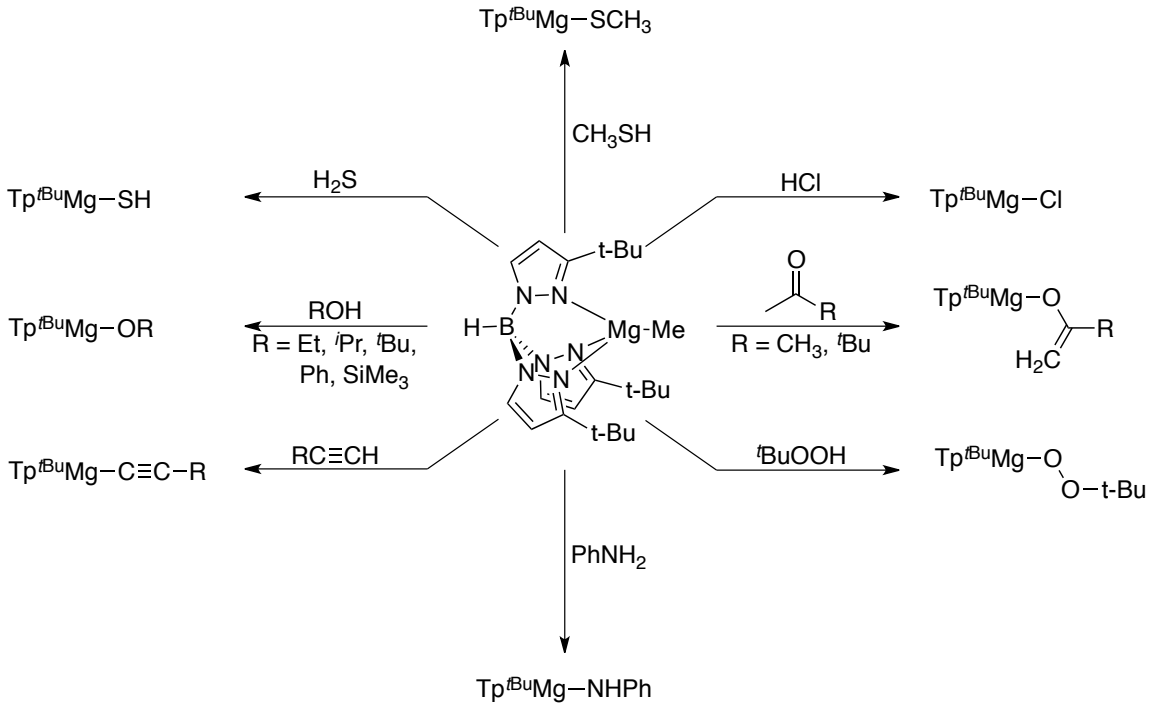

(Eq. 1-3)

Magnesium has been used as a catalyst for many decades, but its use was limited to heterogeneous catalysts generally consisting of magnesium oxide[28-30] and silica/alumina supported magnesium.[31-33] Remarkably, there was little development in the catalytic chemistry of isolated magnesium species until the work by Chisholm and co-workers. Using Tp^{tBu}MgOEt, they were able to achieve very high activity in the area of

ring-opening polymerization (ROP) of L-, *rac*- and *meso*-lactide such that only lanthanide alkoxides reported by scientists at DuPont were more active.[8-11, 34-35]

Concurrently, a different type of ligand was being used to isolate group 2 metal complexes. *β*-diketiminates with differing N-substituents were utilized to synthesize heteroleptic and homoleptic magnesium complexes (Eq. 1-4).[16, 36-37] *β*-diketiminate and similar aminotroponiminate[16, 38] ligands have been used to synthesize numerous group 2 metal complexes.[11, 17-19, 39]

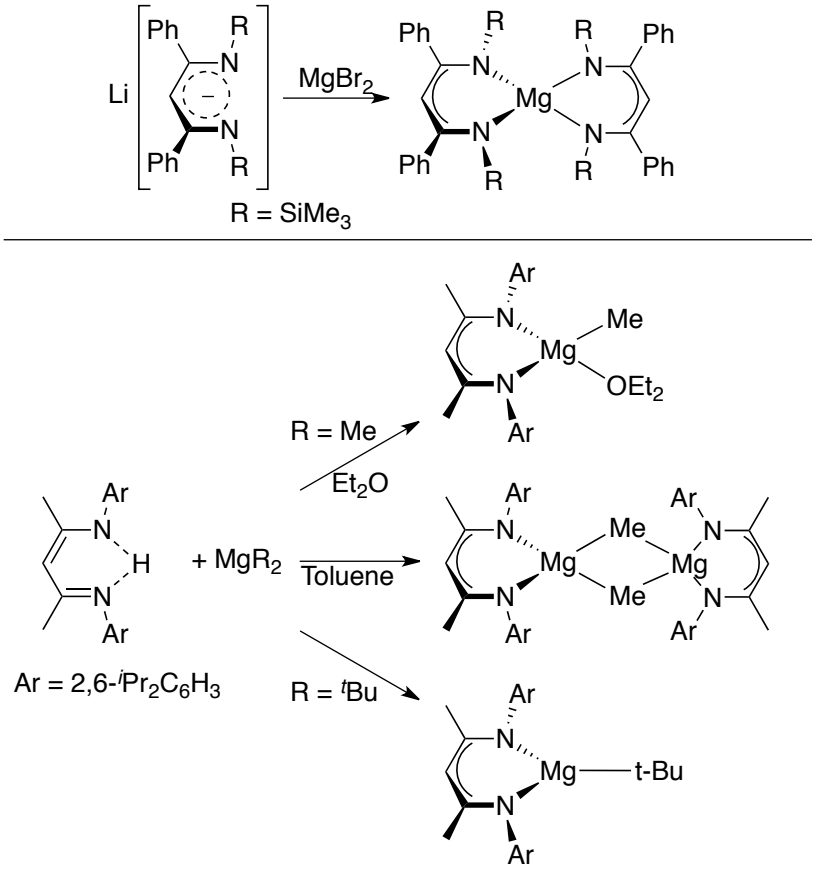

(Eq. 1-4)

Recently, Hill and co-workers reported the first example of group 2-catalyzed cyclization of aminoalkenes via hydroamination using *β*-diketiminate ligands on calcium,[40] and magnesium.[12] Further examples of group 2-catalyzed transformations in

recent years include hydrophosphination (Ca, Sr, Ba)[41-42], dearomatization of pyridine and pyridine derivatives (Mg),[13, 15] hydroboration (Mg),[14] dehydrocoupling of ammonia-borane (Mg, Ca),[22-23, 43-44] and hydrosilylation (Ca).[45]

Until very recently, calcium was the primary metal center for group 2-catalyzed transformations. However, the recent developments previously mentioned has prompted us to investigate magnesium-catalyzed transformations containing tris(oxazolinyl)phenylborate ligands developed in our research group.

Recently our group reported the synthesis of an achiral tris(4,4-dimethyl-oxazolinyl)phenylboratomagnesium methyl compound ($To^{M}MgMe$) that is active for the catalytic hydroamination/cyclization of aminoalkenes.[46] Based on kinetic studies and the isolation of magnesium amide intermediates, a concerted, non-insertive mechanism involving a six-membered transition state was favored over the proposed mechanism for rare earth/early metal catalyzed hydroamination/cyclization that consists of olefin insertion into the magnesium amide bond.[47]

Based on these developments, we began working on the synthesis of a new monoanionic bis(oxazoline) ligand that contained an aliphatic backbone. Upon cyclometalation, this ligand can adopt a *fac*-coordination geometry similar to To^{M}. Additionally, our group had synthesized a chiral version of To^{M} that contained isopropyl groups on the oxazoline ring; however, racemic pyrrolidines were obtained when $To^{P}Y(CH_2SiMe_3)_2$ (To^{P} = tris(4*S*-isopropyl-2-oxazolinyl)phenylborate) was used as the precatalyst for the hydroamination/cyclization of aminoalkenes.[48] Crystal structures of $To^{P}M(CO)_3$ (M = Re, Mn) revealed that the isopropyl groups are oriented such that the methine CH and not a methyl group on each oxazoline ring was directed toward the metal center.[49]

Therefore, we embarked on the synthesis of a *tert*-butyl substituted tris(oxazolinyl)phenylborate ligand for magnesium and calcium mediated enantioselective cyclization of aminoalkenes via hydroamination. Finally, the ability to isolate single site magnesium compounds bearing the To^M ligand allows us to study the reactions of magnesium alkyl and amide species with silanes and develop a mechanism for the Si–N and Si–C bond formation.

Thesis outline

This thesis is comprised primarily of a discussion of new oxazoline-based ligands and their transition metal and alkaline earth metal chemistry. Because the thesis contains a wide variety of topics, relevant literature is reviewed at the beginning of each chapter.

Chapter 2 examines the synthesis of new bis(oxazoline) ligands and attempts to synthesize pincer complexes of palladium and rhodium. The structural details of the metal complexes and their reactivity are discussed. Chapter 3 examines the difficulties encountered while attempting to synthesize a new chiral tris(oxazolinyl)phenylborate ligand and the method that is ultimately successful. Magnesium and calcium alkyl complexes of this new ligand are prepared and the structural details of the magnesium complex are discussed. Finally, asymmetric catalytic hydroamination/cyclization is investigated with these new chiral magnesium and calcium complexes.

Chapter 4 consists of collaborative work with Debabrata Mukherjee and Dr. James Dunne. Several new To^MMg complexes of nitrogen, phosphorus, and sulfur have been synthesized and their reactivity with silane explored. Kinetic studies on the catalytic reaction between *t*-$BuNH_2$ and $PhMeSiH_2$ with To^MMgMe as the precatalyst as well as insight gathered from a Hammett plot of phenyl(*para*-substituted-phenyl) silanes of the

form Ph(aryl)SiH_2 are discussed. This data allows us to propose a nucleophilic attack mechanism for the Si–N bond formation step. All contributions from Debabrata Mukherjee have been removed from this thesis. Some details of Dr. James Dunne's work, the scope of aminolysis of silanes as well as stoichiometric kinetics between To^MMgNH^tBu and $PhMeSiH_2$, are included for reference.

Finally, Chapter 5 discusses the reactivity of To^MMgMe in the presence of silanes and kinetic studies on the Si–C bond formation. Catalytic hydrosilylation using To^MMgMe as the precatalyst is studied as well as the effect of $B(C_6F_5)_3$ on both the stability of To^MMgH and the hydrosilylation catalysis. All work discussed in Chapter 5 was done by Steven Neal.

References

1. Han, R.; Looney, A.; Parkin, G., *J. Am. Chem. Soc.* **1989,** *111* (18), 7276.
2. Han, R.; Parkin, G., *J. Organomet. Chem.* **1990,** *393* (3), C43-C46.
3. Han, R.; Parkin, G., *J. Am. Chem. Soc.* **1990,** *112* (9), 3662-3663.
4. Han, R.; Parkin, G., *Organometallics* **1991,** *10* (4), 1010-1020.
5. Han, R.; Parkin, G., *J. Am. Chem. Soc.* **1992,** *114* (2), 748-757.
6. Ghosh, P.; Parkin, G., *Inorg. Chem.* **1996,** *35* (6), 1429.
7. Kisko, J. L.; Fillebeen, T.; Hascall, T.; Parkin, G., *J. Organomet. Chem.* **2000,** *596* (1-2), 22-26.
8. Chisholm, M. H.; Eilerts, N. W.; Huffman, J. C.; Iyer, S. S.; Pacold, M.; Phomphrai, K., *J. Am. Chem. Soc.* **2000,** *122* (48), 11845-11854.
9. Chisholm, M. H.; Huffman, J. C.; Phomphrai, K., *J. Chem. Soc., Dalton Trans.* **2001,** (3), 222-224.
10. Chisholm, M. H.; Gallucci, J.; Phomphrai, K., *Inorg. Chem.* **2002,** *41* (10), 2785-2794.
11. Chisholm, M. H.; Phomphrai, K., *Inorg. Chim. Acta* **2003,** *350* (0), 121-125.
12. Crimmin, M. R.; Arrowsmith, M.; Barrett, A. G. M.; Casely, I. J.; Hill, M. S.; Procopiou, P. A., *J. Am. Chem. Soc.* **2009,** *131* (28), 9670-9685.
13. Hill, M. S.; MacDougall, D. J.; Mahon, M. F., *Dalton Trans.* **2010,** *39* (46), 11129-11131.
14. Arrowsmith, M.; Hill, M. S.; Hadlington, T.; Kociok-Köhn, G.; Weetman, C., *Organometallics* **2011,** *30* (21), 5556-5559.
15. Hill, M. S.; Kociok-Kohn, G.; MacDougall, D. J.; Mahon, M. F.; Weetman, C., *Dalton Trans.* **2011,** *40* (46), 12500-12509.
16. Bailey, P. J.; Dick, C. M. E.; Fabre, S.; Parsons, S., *J. Chem. Soc., Dalton Trans.* **2000,** (10), 1655-1661.

17. Bailey, P. J.; Coxall, R. A.; Dick, C. M.; Fabre, S.; Parsons, S., *Organometallics* **2001,** *20* (4), 798-801.
18. Bailey, P. J.; Liddle, S. T.; Morrison, C. A.; Parsons, S., *Angew. Chem., Int. Ed. Engl.* **2001,** *40* (23), 4463-4466.
19. Bailey, P. J.; Coxall, R. A.; Dick, C. M.; Fabre, S.; Henderson, L. C.; Herber, C.; Liddle, S. T.; Loroño-González, D.; Parkin, A.; Parsons, S., *Chem. -Eur. J.* **2003,** *9* (19), 4820-4828.
20. Horrillo-Martínez, P.; Hultzsch, K. C., *Tetrahedron Lett.* **2009,** *50* (18), 2054-2056.
21. Zhang, X.; Emge, T. J.; Hultzsch, K. C., *Angew. Chem., Int. Ed. Engl.* **2012,** *51* (2), 394-398.
22. Spielmann, J.; Bolte, M.; Harder, S., *Chem. Commun.* **2009,** (45), 6934-6936.
23. Spielmann, J.; Piesik, D. F. J.; Harder, S., *Chem. -Eur. J.* **2010,** *16* (28), 8307-8318.
24. Jastrzebski, J. T. B. H.; Boersma, J.; van Koten, G., *The Chemistry of Organomagnesium Compounds*. Wiley: Hoboken, **2008**; Vol. 1.
25. Schlenk, W.; Schlenk, W., *Chem. Ber.* **1929,** *62* (4), 920-924.
26. Yousef, R. I.; Walfort, B.; Rüffer, T.; Wagner, C.; Schmidt, H.; Herzog, R.; Steinborn, D., *J. Organomet. Chem.* **2005,** *690* (5), 1178-1191.
27. Cannon, K. C.; Krow, G. R., *Handbook of Grignard Reagents*. Marcel Dekker: New York, **1996**.
28. Paskauskaite, L.; Mituzas, J., *Lietuvos TSR Mokslu Akad., Statybos, Architekt. Inst., Straipsniu Rinkinys* **1958,** *1*, 131-146;Russian summary 147.
29. Kontorovich, S. I.; Sandomirskaya, M. M.; Segalova, E. E., *Fiz.-Khim. Mekhan. Dispersnykh Struktur, Akad. Nauk SSSR, Sb. Statei* **1966**, 228-231.
30. Harkins, C. G.; Shang, W. W.; Leland, T. W., Jr., *J. Phys. Chem.* **1969,** *73*, 130-141.
31. Dzis'ko, V. A.; Borisova, M. S.; Karakchiev, L. G.; Makarov, A. D.; Kotsarenko, N. S.; Zusman, R. I.; Khripin, L. A., *Kinet. Katal.* **1965,** *6*, 1033-1040.
32. Dzisko, V. A., *Proc. Intern. Congr. Catalysis, 3rd, Amsterdam, 1964* **1965,** *1*, 422-431, discussion 431-422.
33. Zul'fugarov, L. S.; Dzhafarova, E. M.; Pis'man, I. I.; Zul'fugarov, Z. G., *Dokl. Akad. Nauk Azerb. SSR* **1968,** *24*, 20-26.
34. Mclain, S. J.; Ford, T. M.; Drysdale, N. E., *Polym. Prepr. (Am. Chem Soc. Div. Polym Chem.)* **1992,** *33* (2), 463-464.
35. McLain, S. J.; Ford, T. M.; Drysdale, N. E.; Jones, N.; McCord, E. F.; Shreeve, J. L.; Evans, W., *J. Polym. Prepr. (Am. Chem. Soc. Div. Polym. Chem.)* **1994,** *35* (2), 534-535.
36. F. Caro, C.; B. Hitchcock, P.; F. Lappert, M., *Chem. Commun.* **1999,** (15), 1433-1434.
37. Gibson, V. C.; Segal, J. A.; White, A. J. P.; Williams, D. J., *J. Am. Chem. Soc.* **2000,** *122* (29), 7120-7121.
38. Datta, S.; Gamer, M. T.; Roesky, P. W., *Organometallics* **2008,** *27* (6), 1207-1213.
39. Green, S. P.; Jones, C.; Stasch, A., *Angew. Chem., Int. Ed. Engl.* **2008,** *47* (47), 9079-9083.
40. Crimmin, M. R.; Casely, I. J.; Hill, M. S., *J. Am. Chem. Soc.* **2005,** *127* (7), 2042-2043.

41. Crimmin, M. R.; Barrett, A. G. M.; Hill, M. S.; Hitchcock, P. B.; Procopiou, P. A., *Organometallics* **2007,** *26* (12), 2953-2956.
42. Crimmin, M. R.; Barrett, A. G. M.; Hill, M. S.; Hitchcock, P. B.; Procopiou, P. A., *Organometallics* **2008,** *27* (4), 497-499.
43. Liptrot, D. J.; Hill, M. S.; Mahon, M. F.; MacDougall, D. J., *Chem. -Eur. J.* **2010,** *16* (28), 8508-8515.
44. Spielmann, J.; Harder, S., *J. Am. Chem. Soc.* **2009,** *131* (14), 5064-5065.
45. Buch, F.; Brettar, J.; Harder, S., *Angew. Chem., Int. Ed. Engl.* **2006,** *45* (17), 2741-2745.
46. Dunne, J. F.; Fulton, D. B.; Ellern, A.; Sadow, A. D., *J. Am. Chem. Soc.* **2010,** *132* (50), 17680-17683.
47. Gagne, M. R.; Stern, C. L.; Marks, T. J., *J. Am. Chem. Soc.* **1992,** *114* (1), 275-294.
48. Pawlikowski, A. V., Unpublished work.
49. Wu, K.; Mukherjee, D.; Ellern, A.; Sadow, A. D.; Geiger, W. E., *New J. Chem.* **2011,** *35*, 2169-2178.

Chapter 2: Palladium and rhodium complexes containing 1,3-bis(oxazolinyl)propyl (Probox) ligands: Macrocycles and pincer compounds

Modified from a paper published in *Polyhedron*[*]

Steven R. Neal[†], Jooyoung Yoo[‡], Arkady Ellern, Aaron D. Sadow

Iowa State University, Department of Chemistry, 1605 Gilman Hall, Ames, IA 50011

Abstract

New chiral 1,3-bis(4*R*-phenyl-2-oxazolinyl)propane (**Probox^{Ph}**) and achiral 1,3-bis(4,4-dimethyl-2-oxazolinyl)propane (**Probox^{Me2}**) ligands have been prepared by $Cd(OAc)_2$-catalyzed condensation reactions. These ligands, and the known isopropyl derivative Probox^{iPr}, react with $[PdCl_2(NCPh)_2]$ and $[RhCl(\eta^2\text{-}C_8H_{14})_2]_2$ to form 16-membered bimetallic macrocycles. Additionally, Probox^{Me2} and $RhCl_3$ react to form a new monoanionic 'NCN' pincer complex (κ^3-*N,C,N*-Probox^{Me2})$RhCl_2$. The structures of new palladium(II) and rhodium(I) macrocycles with the Probox ligands are confirmed by X-ray crystallography, and natural abundance ^{15}N 2D NMR experiments probe oxazoline coordination to the metal centers in solution. Addition of a weakly donating water ligand to (κ^3-*N,C,N*-Probox^{Me2})$RhCl_2$ gives a six-coordinate compound with a *mer*-Probox configuration, whereas PMe_3 coordination provides a single *fac*-coordinated Probox isomer.

---

[*] Reprinted from *Polyhedron*, *29*, Neal, S. R.; You, J.; Ellern, A.; Sadow, A. D., Palladium and rhodium complexes containing 1,3-bis(oxazolinyl)propyl (Probox) ligands: Macrocycles and pincer compounds, 544-552, *Copyright 2010, with permission from Elsevier*.

[†] Primary researcher and author

[‡] Undergraduate researcher

Introduction

Metal complexes containing tridentate mono-anionic ligands of the type L_2X having the generic form shown in Figure 2-1 are known as pincer compounds.[1] The tridentate ligand, also known as a pincer ligand, has a broad definition; generally it is comprised of a backbone that can be either aliphatic, aromatic, or a combination of the two and the donor atoms can be any atom that can bind strongly to the metal center. A key advantage to pincer complexes is their thermal stability and resistance to decomposition, thus permitting the use of more forcing conditions during catalysis.

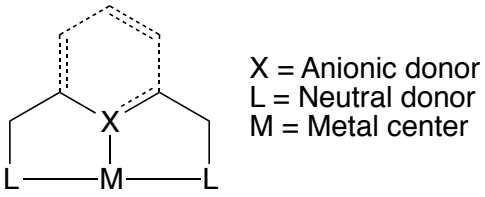

Figure 2-1. Generic form of a pincer complex

Ever since Shaw reported the first transition metal complex containing the ligand bis[(di-*tert*-butylphosphino)methyl]phenyl in 1976 (see Figure 2-2a),[2] the field of pincer chemistry has transformed from mere curiosity to the development of unprecedented catalytic transformations. Pincer complexes have been synthesized containing some early[3-7] and mid-transition metals,[7-16] while the vast majority of efforts have focused on late transition metals.[17-18] While there are reports of pincers complexes with a wide variety of neutral (L) and anionic (X) donor atoms, the most common pincer ligands utilize phosphorus or nitrogen for the neutral donor and carbon for the anionic donor; these complexes are most commonly known as 'PCP' and 'NCN' ligands respectively.

The synthesis of pincer complexes can take several routes depending on the nature of the metal center and the donor groups on the ligand.[18] Direct cyclometalation, the method Shaw used in the synthesis of the first pincer complex,[2] is a process where

the C–R bond is activated by the metal center and subsequent loss of RX (see Figure 2-2 a) results in the formation of the desired pincer complex. Generally, this process is facile for 'PCP' pincer complexes while direct cyclometalation of the analogous 'NCN' pincer ligands is less common.[19-23] This is proposed to be due to a lower bond strength of the M–N bond versus the M–P bond thus the initial coordination the two nitrogen groups on the ligand to the metal center is less favored. Therefore, regioselectivity is a significant problem requiring specific ligand modifications to control the location of the metal center (see Figure 2-2-b).[24] The difference in binding affinity between M–P and M–N is exemplified by the hemilabile 'PCN' pincer complexes reported my Milstein and co-workers.[25-26]

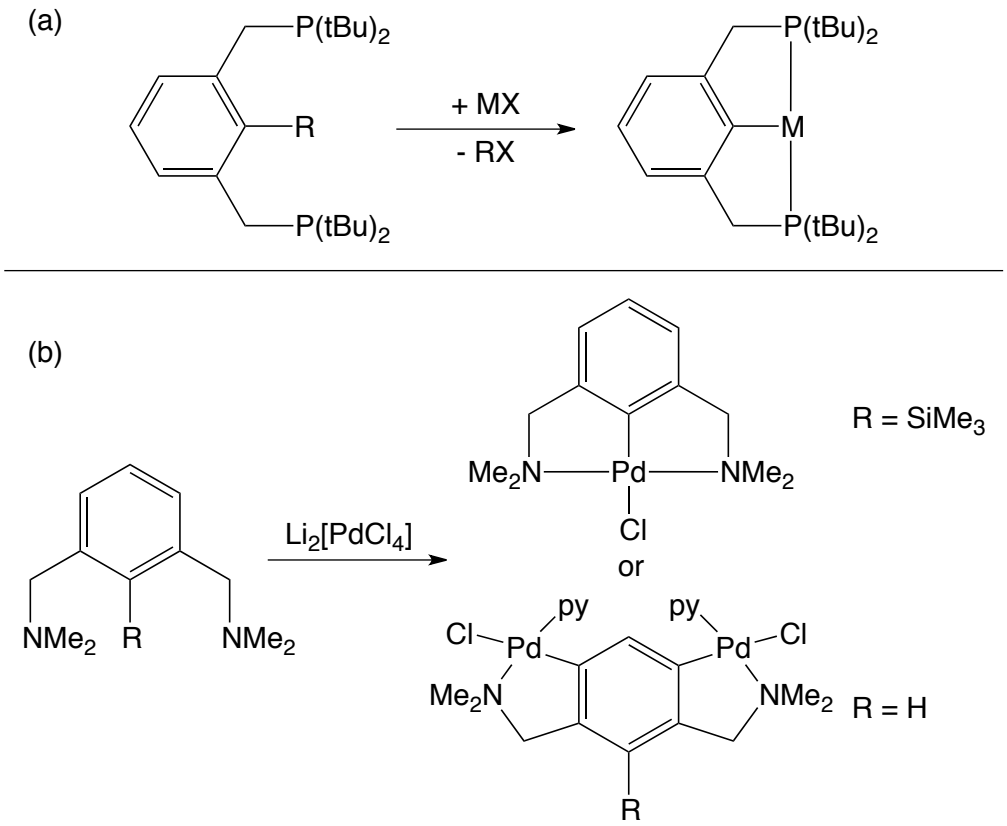

Figure 2-2. (a) Direct cyclometalation of phosphine based pincer ligands. (b) Difficulty in controlling regioselectivity in direct cyclometalation of nitrogen based pincer ligands.

The composition of the pincer backbone can also affect the ability of a ligand to undergo direct cyclometalation. For example, reacting 2,6-bis[(di-*tert*-butylphosphino)methyl]phenyl with $PdCl_2(NCPh)_2$ in refluxing 2-methoxyethanol provides the corresponding pincer complex ($PC_{Ar}P$)PdCl (Figure 2-3, top).[2] However, refluxing an ethanolic solution of 1,5-bis(di-*tert*-butylphosphino)pentane and $PdCl_2(NCPh)_2$ provides a dipalladium macrocycle as the major product.[27] The macrocycle converts, upon sublimation, to the pincer complex ($PC_{sp3}P$)PdCl (Figure 2-3, bottom).[27]

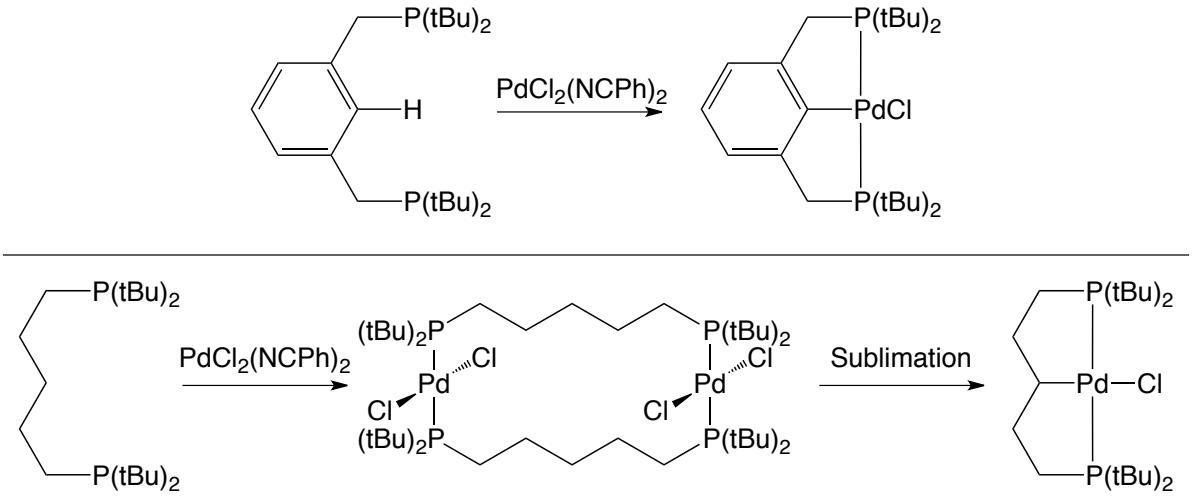

Figure 2-3. Comparison of direct cyclometalation between $PC_{Ar}P$ (top) and $PC_{sp3}P$ (bottom)

Finally, two other methods that arise from a similar ligand design have quite complementary chemistry. The first, oxidative addition, is a convenient method for the preparation of group 10 metal complexes from the corresponding aryl halide and low-valent metal center (see Figure 2-4). While the development of 'PCP' oxidative addition precursors has been limited, largely due to the success of direct cyclometalation of C_{Aryl}–H bonds, there has been significant work in the development of 'NCN' oxidative addition precursors and their corresponding nickel,[28-29] palladium and platinum[18] complexes. The second method, transmetalation, involves lithiation of the ligand followed by introduction of a metal halide to transfer the pincer ligand to the new metal center (see Figure 2-4).

This technique has been used to synthesize 'NCN' pincer complexes of both early[3, 5-6, 30] and late[30-36] transition metals.

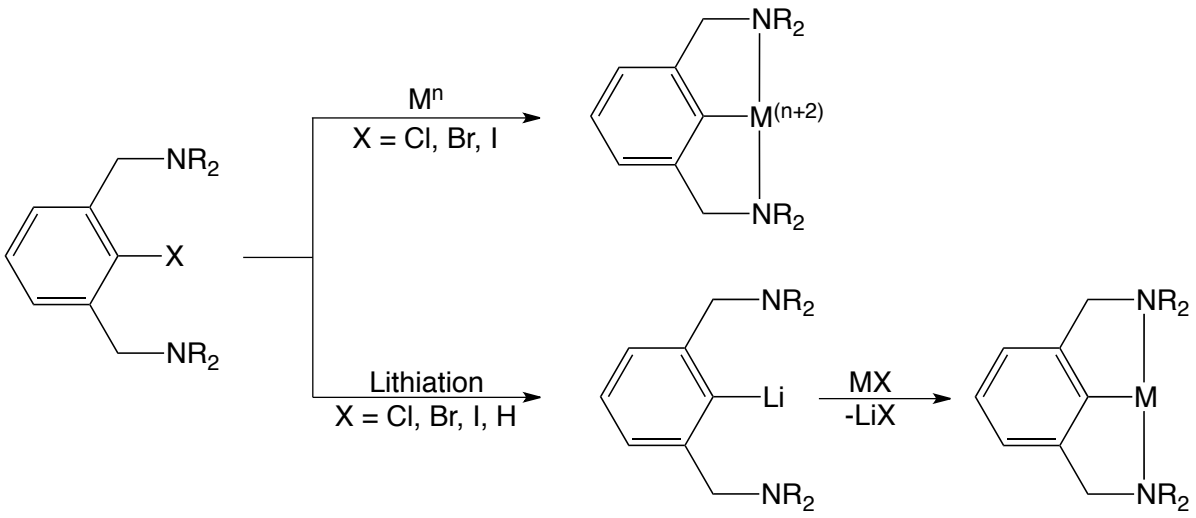

Figure 2-4. Top, oxidative addition of nitrogen based pincer ligands. Bottom, lithiation of nitrogen based pincer ligands followed by transmetalation.

There are many different ligand systems and metal centers explored in pincer chemistry,[1] Therefore, this discussion will focus on late metal (group 9 and 10) complexed 'PCP' and 'NCN' compounds as this more closely relates to the new chemistry presented in this thesis. As mentioned earlier, pincer complexes are generally thermally robust, thus allowing them to highly active catalysts in aldol condensations, allylation of aldehydes, allylic alkylation, cyclopropanation, dehydrogenation, Heck reaction, Kharasch additions, Michael reaction, Suzuki coupling, and transfer hydrogenation.[17, 37]

The reactivity of a pincer ligand is controlled by the backbone in addition to the donor groups. This relationship is exemplified by work reported by Goldman and Hartwig. Upon treating $(PC_{Ar}P)IrHCl(NH_3)$ with $KN(SiMe_3)_2$ at low temperature, $(PC_{Ar}P)Ir(H)NH_2$ is observed. After this species is allowed to warm to room temperature, the four-coordinate $(PC_{Ar}P)IrNH_3$ complex is isolated (see Figure 2-5-a).[38] However, the

reaction between $(PC_{sp3}P)IrHCl$ and ammonia followed by addition of $KN(SiMe_3)_2$ produces the iridium(III) hydridyl-amide $(PC_{sp3}P)Ir(H)NH_2$ that is robust at room temperature (see Figure 2-5-b).[39]

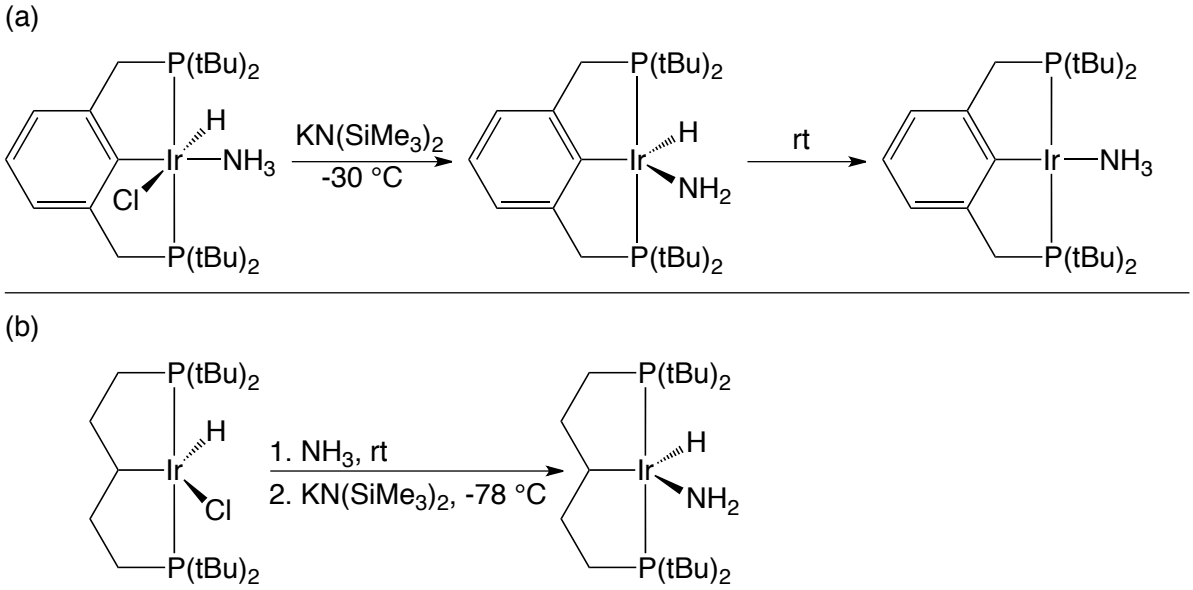

Figure 2-5. (a) $(PC_{Ar}P)Ir$ complex favoring NH_3 coordination. (b) $(PC_{sp3}P)Ir$ complex favoring N–H bond activation.

The difference in reactivity is attributed to the aliphatic backbone being more electron rich than the aromatic backbone. This makes the metal center more electron rich thus favoring insertion of the N–H bond over coordination of the highly electron donating NH_3 moiety. The comparison between pincers containing aliphatic versus aromatic backbones was the inspiration and a central focus of this thesis.

Another area of pincer chemistry that has received great attention is the development of chiral, non-racemic, ligands. There have been a variety of ligands designed (both 'PCP' and 'NCN') to address this need. The majority of these ligands can be grouped into three different categories; chirality on the backbone of the ligand, chirality on the arms, and chirality at the donor group itself (see Figure 2-6).[1] These

chiral pincer complexes have shown some success in enantioselective imine allylation,[40] aldol condensation of isonitriles with aldehydes,[41-46] Michael reaction,[47] and transfer hydrogenation.[43, 48]

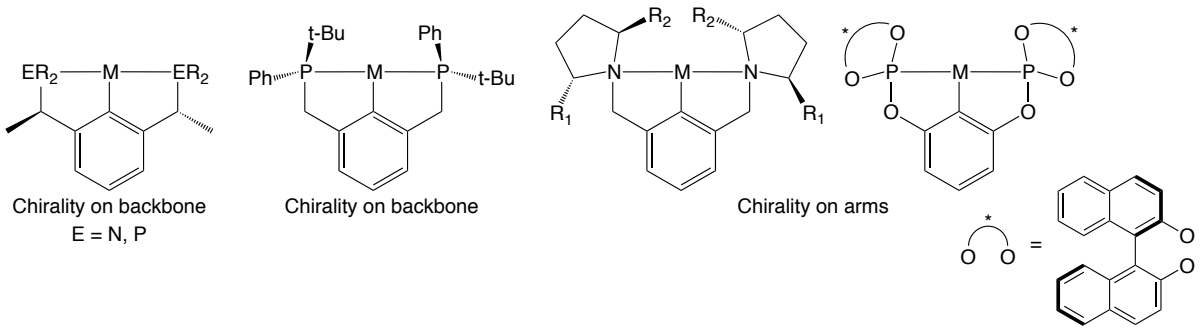

Figure 2-6. Types of chiral pincer complexes

Pincer ligands that contain oxazoline rings are another class of chiral pincer complexes. There are two types of oxazoline based pincer complexes, phebox[49] and benbox,[22] differentiated by the size of the metallacycles formed (see Figure 2-7). This class, which would fall under the chirality on the arms group, has advantages over the other chiral pincer complexes. In contrast to the complexes that have chiral centers on the backbone, the chiral center in bis(oxazolinyl) pincers is located in close proximity to the metal center. In addition, the introduction of the stereocenter is generally facile because oxazoline rings are commonly synthesized from a condensation reaction utilizing enantiopure amino alcohols derived from amino acids. The abundance of commercially available amino acids permits the development of a variety of oxazolines. Oxazoline based pincer complexes also provide significantly higher enantioselectivities for many of the same reaction types compared to the other chiral pincer complexes.[1]

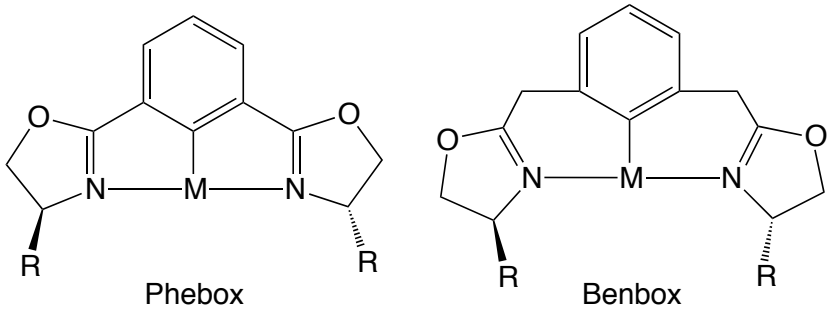

Figure 2-7. Oxazoline based '$NC_{Ar}C$' pincer complexes

While the chemistry of Phebox and Benbox pincer complexes has garnered a great deal of interest over the past 15 years,[20-23, 49-53] to our knowledge there have been no developments of oxazoline based pincer complexes bearing an aliphatic backbone. 1,3-bis(oxazolinyl)propane (Probox, see Figure 2-8) ligands were targeted because a five-membered ring would form upon cyclometalation; this is the favored ring size for 1,5-bis(phosphino)pentane ligands.[54] The isopropyl derivative, 1,3-bis(4*S*-isopropyl-2-oxazolinyl)propane (**Probox^{iPr}**), was initially prepared over 15 years ago,[55] but is the only species described. Our study has primarily focused on the synthesis and chemistry of the achiral derivative 1,3-bis(4,4-dimethyl-2-oxazolinyl)propane (**Probox^{Me2}**); a second chiral Probox ligand 1,3-bis(4*R*-phenyl-2-oxazolinyl)propane (**Probox^{Ph}**) was also synthesized.

To our knowledge, there are no reports of transition metal complexes containing Probox^{iPr}. Therefore, both optimization of the ligand synthesis as well as the coordination and cyclometalation chemistry with group 9 and 10 metals is studied. The presence of the strongly electron donating aliphatic backbone could greatly affect the reactivity, as seen in the ($PC_{sp3}P$)Ir chemistry shown in Figure 2-5, to permit the discovery of some very interesting chemistry.

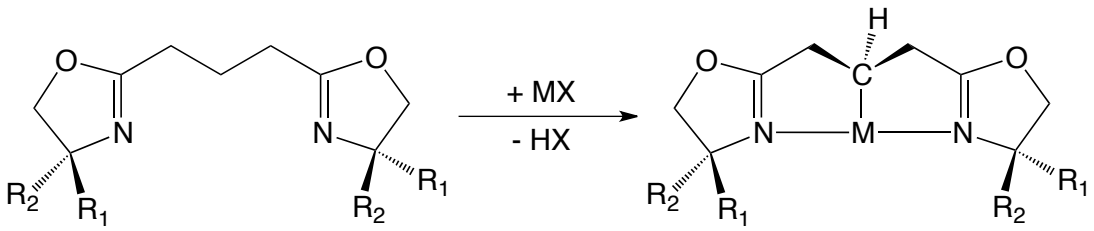

Figure 2-8. Oxazoline based '$NC_{sp3}C$' pincer complexes

Once pincer complexes of Probox are formed, *fac* and *mer* isomers are possible for five- and six-coordinate metal centers; the coordination geometry of the pincer complexes as well as possible interconversions between *fac* and *mer* configurations will be investigated. Both *fac*[39] and *mer*[27, 56-60] configurations have been observed for 1,5-bis(phosphino)pentane pincer complexes. Here we report the synthesis of two new Probox ligands and attempts to prepare the corresponding palladium and rhodium pincer complexes. A rhodium(III) *N,C,N*-Probox pincer complex is isolable and the geometry of the pincer ligand is controlled by the other ligands coordinated to the metal center.

Results and Discussion

Synthesis of Probox ligands

Optimization of the ligand synthesis and coordination chemistry began with achiral bis(4,4-dimethyl-2-oxazolinyl)propane (**Probox^{Me2}**). This ligand has advantages over the chiral derivative bis(4*S*-isopropyl-2-oxazolinyl)propane (**Probox^{iPr}**) previously synthesized by Bolm and coworkers.[55] First, achiral compounds are typically more easily crystallized than their chiral counterparts. Second, NMR investigations of the ligand and complexes containing the cyclometalated version of Probox^{Me2} should be more easily conducted, thus the ^{1}H NMR will be less complicated and determining if the propyl

backbone has been cyclometalated should be easier. In addition, with *fac* and *mer* isomers possible, the methyl resonances can be utilized via 2D NMR spectroscopy to determine spatial configuration in the solution state. More specifically, 2D-nOe (NOESY) spectroscopy can provide a crosspeak between the methyl resonances of the two different oxazoline rings indicating a *fac* configuration (Figure 2-9). The benzyl substituent on the oxazoline rings in a chiral phebox (Figure 2-7) structure are too far away (ca. 8.8 Å) from one another to observe any crosspeak in a NOESY spectrum.[20]

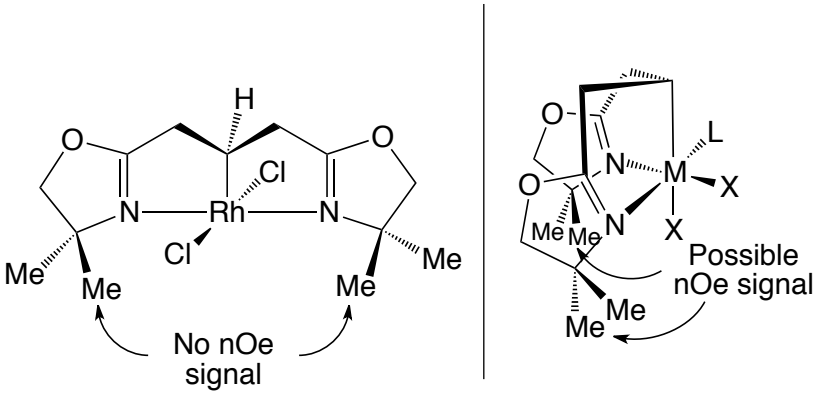

Figure 2-9. Possible nOe interaction with cyclometalated Probox^{Me2} complexes

The original synthesis of Probox^{iPr} utilized a $ZnCl_2$-catalyzed condensation.[55] This catalyst did not provide the desired Probox proligands in good yields. Mixtures of mono-oxazoline and bis-oxazoline products are obtained in the presence of a large excess (up to 4 equivalents) of amino alcohol (Eq. 2-1). Additional methods for the synthesis of bis-oxazolines include a stoichiometric $Zn(OTf)_2$-induced condensation for the synthesis of 1-methyl-1,1-bis-(2-oxazolinyl)ethane[61] and a $Cd(OAc)_2$-catalyzed condensation for the synthesis of benbox.[22]

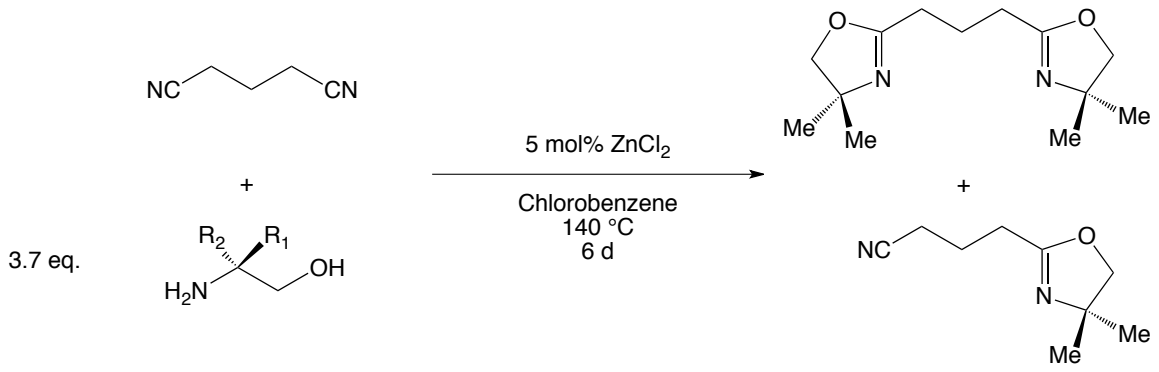

(Eq. 2-1)

The $Cd(OAc)_2$-catalyzed condensation provides the best results for the synthesis of Probox proligands. Thus, the reaction of 3.75 equivalents of 2-amino-2-methyl-1-propanol and glutaronitrile with five mol % $Cd(OAc)_2(H_2O)_2$ provides bis(4,4-dimethyl-2-oxazolinyl)propane (**Probox^{Me2}**) in 72% yield following distillation (Eq. 2-2). Optimized reaction conditions require excess amino alcohol, chlorobenzene, and refluxing temperatures.

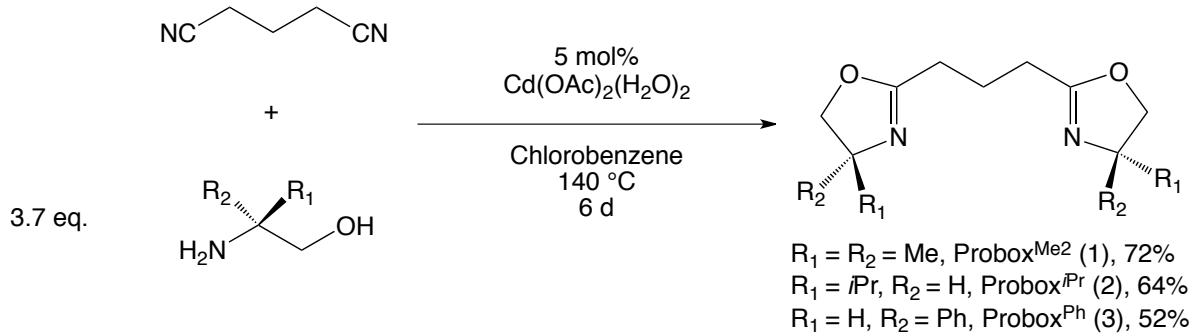

(Eq. 2-2)

Resonances at 1.08 (CH_2) and 3.52 ppm (CH_3) in the ^{1}H NMR spectrum of Probox^{Me2} in benzene-d_6 are assigned to the hydrogens on the oxazoline rings while resonances at 2.28 (α-CH_2) and 2.09 ppm (β-CH_2) are associated with the backbone hydrogens. Equivalent oxazolines are reflected in this ^{1}H NMR data, which suggests the

C_{2v}-symmetric structure expected for Probox^{Me2}. $^{1}H–^{15}N$ HMBC experiments provide natural abundance ^{15}N NMR chemical shift data for the Probox ligands as well as palladium and rhodium complexes bearing these ligands. Probox^{Me2} exhibits a crosspeak in the ^{1}H-^{15}N HMBC spectrum between the resonance corresponding to the methyl groups on the oxazoline ring and the imidine nitrogen providing the ^{15}N chemical shift at -137 ppm (in methylene chloride-d_2, relative to CH_3NO_2). This chemical shift data is informative because it indicates the bonding modes of the oxazoline rings (see Table 2-1).[62-65] For example, if one oxazoline is coordinated to a metal center and another is not, two ^{15}N chemical shifts are expected, assuming an equilibrium process is not involved. Two additional crosspeaks are observed in the ^{1}H-^{15}N HMBC spectrum for Probox^{Me2} between resonances corresponding to nitrogen and the methylene hydrogens on the oxazoline rings as well as between nitrogen and the α-methylene hydrogens on the propyl backbone.

Probox^{iPr} and 1,3-bis(4*R*-phenyl-2-oxazolinyl)propane (**Probox^{Ph}**) are synthesized in an analogous manner in 64 and 52% yields, respectively. Probox^{iPr} is C_2-symmetric in solution as evident by one set of oxazoline and α-methylene resonances. The ^{1}H NMR chemical shifts are consistent with those reported by Bolm[55] and the ^{15}N NMR chemical shift from a ^{1}H-^{15}N HMBC experiment is -160.1 ppm (in chloroform-*d*). Likewise, Probox^{Ph} is C_2-symmetric in solution with a ^{15}N chemical shift of -154.5 ppm (in methylene chloride-d_2).

Table 2-1. ^{15}N NMR chemical shift data, referenced to CH_3NO_2, colors represent observed correlations

Compound	^{15}N NMR Chemical Shift	^{1}H-^{15}N correlations
Probox^{Me2} (1)	-137.0	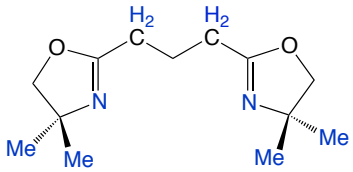
Probox^{iPr} (2)	-160.1	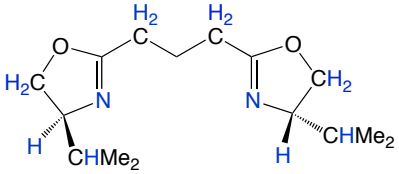
Probox^{Ph} (3)	-154.5	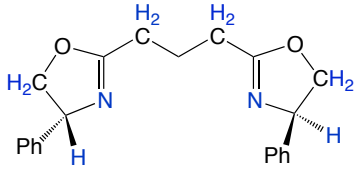
$[PdCl_2(\mu\text{-}N,N\text{-Probox}^{Me2})]_2$ (4)	-213.8	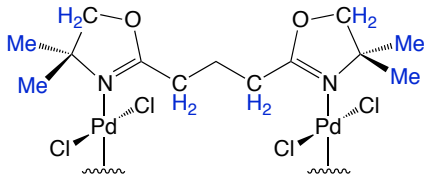
$[PdCl_2(\mu\text{-}N,N\text{-Probox}^{iPr})]_2$ (5)	-277.6	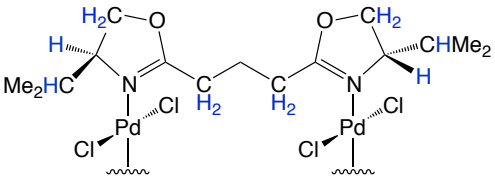
$[RhCl(\mu\text{-}N,N\text{-Probox}^{Ph})(\eta\text{-}^{2}C_8H_{14})]_2$ (6)	-209.9	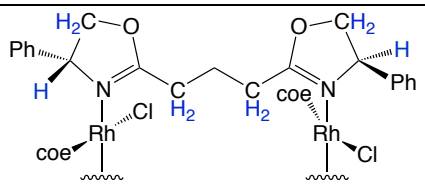
(κ^3-*N,C,N*-Probox^{Me2})$RhCl_2$ (7)	-211.9	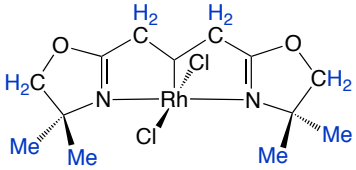
fac(κ^3-*N,C,N*-Probox^{Me2})$RhCl_2(PMe_3)$ (9)	-178.2 -207.3	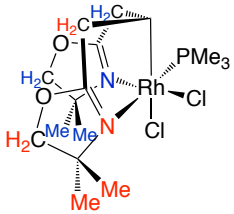

Coordination of Probox ligands to palladium(II)

Inspired by the success with 1,5-bis(di-*tert*-butyl-phosphino)pentane to form 5-membered palladacycles,[59-60] our initial attempts to prepare cyclometalated compounds of Probox^{Me2} began with square-planar palladium(II) complexes. Treatment of $[PdCl_2(NCPh)_2]$ and Probox^{Me2} in refluxing THF gives a new dipalladium compound $[PdCl_2(\mu\text{-}N,N,\text{-Probox}^{Me2})]_2$ (**2-1**) in 88% yield. The two palladium(II) centers are in square planar geometries (Eq. 2-3). The ^{1}H NMR spectrum of **2-1** is consistent with a C_{2v}-symmetric species in solution (methylene chloride-d_2) with one singlet resonance for the oxazolinyl methyl hydrogens and one singlet resonance for the oxazolinyl methylene hydrogens. This spectroscopy is not consistent with the desired cyclometalated Probox^{Me2}-palladium(II) pincer complex; that complex should be C_s-symmetric because the C_2 axis would be lost upon cyclometalation. Moreover, integration of the ^{1}H NMR spectrum of **2-1**, specifically the hydrogens on the α- and β-carbons, confirms that the isolated species is not cyclometalated. However, the oxazolines are clearly coordinated to palladium as evidenced by a ^{1}H-^{15}N HMBC experiment that provides one crosspeak corresponding to a ^{15}N chemical shift of -213.8 ppm, which was 141 ppm upfield of Probox^{Me2}. This significant difference in the ^{15}N chemical shift indicates that the oxazoline rings are coordinated to palladium through the imidine nitrogen.

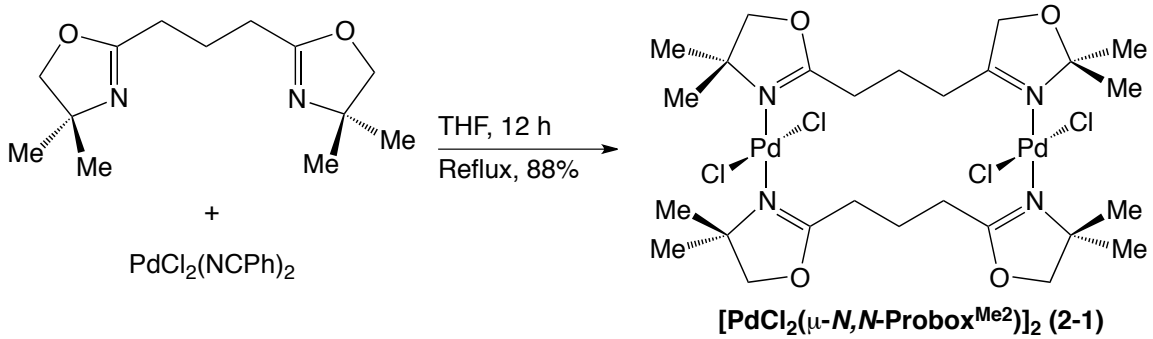

(Eq. 2-3)

X-ray quality crystals of $[PdCl_2(\mu\text{-}N,N,\text{-Probox}^{Me2})]_2$ are obtained by slow evaporation of a concentrated solution of **2-1** in methylene chloride; a single crystal diffraction study confirms the proposed macrocyclic dipalladium(II) structure (see ORTEP diagram of **2-1** plotted in Figure 2-10). The two palladium(II) centers are in an almost perfect square planar orientation; the sum of L–Pd–L angles for Pd1 and Pd2 are equal to 360.1(4)° and 360.2(4)°, respectively. The two oxazoline groups are coordinated *trans*, and ∠N1–Pd2–N2 and ∠N3–Pd1–N4 are 178.7(2)° and 175.6(2)°, respectively. The palladium–nitrogen bond distances are nearly identical as are the palladium–chlorine bond distances. Interestingly, planes defined by containing Pd1-Cl1-N4-Cl2-N3 (plane 1) and Pd2-Cl3-N1-Cl4-N2 (plane 2) are not parallel with one another but intersect at a 60.4° angle.

For comparison, there are four known dipalladium complexes containing 1,5-bis(phosphino)pentane ligands.[66-67] Each of these structures contain comparable planar intersection angles ranging from 56° to 63°; therefore the structure of **2-1** containing oxazoline rings is similar to the phosphine containing macrocycles. Five carbon atoms separate the donor groups in both Probox^{Me2} and 1,5-bis(phosphino)pentane, thus a direct comparison of the distance between the palladium center and the nearest central carbon atom in the backbone can be made. In $[PdCl_2(\mu\text{-}N,N,\text{-Probox}^{Me2})]_2$ this distance is long (Pd1–C12, 4.34 Å; Pd2–C25, 4.21 Å) while the distance in complexes of the type $[PdCl_2(R_2P(CH_2)_5PR_2)]_2$ (4.90-5.21 Å) is ca. 1 Å longer than **2-1**. Likely, the increased flexibility of the bis(phosphino) pentane ligand attributes to this increased distance; however, this cannot be the most important structural feature as these complexes will cyclize under photochemical conditions.

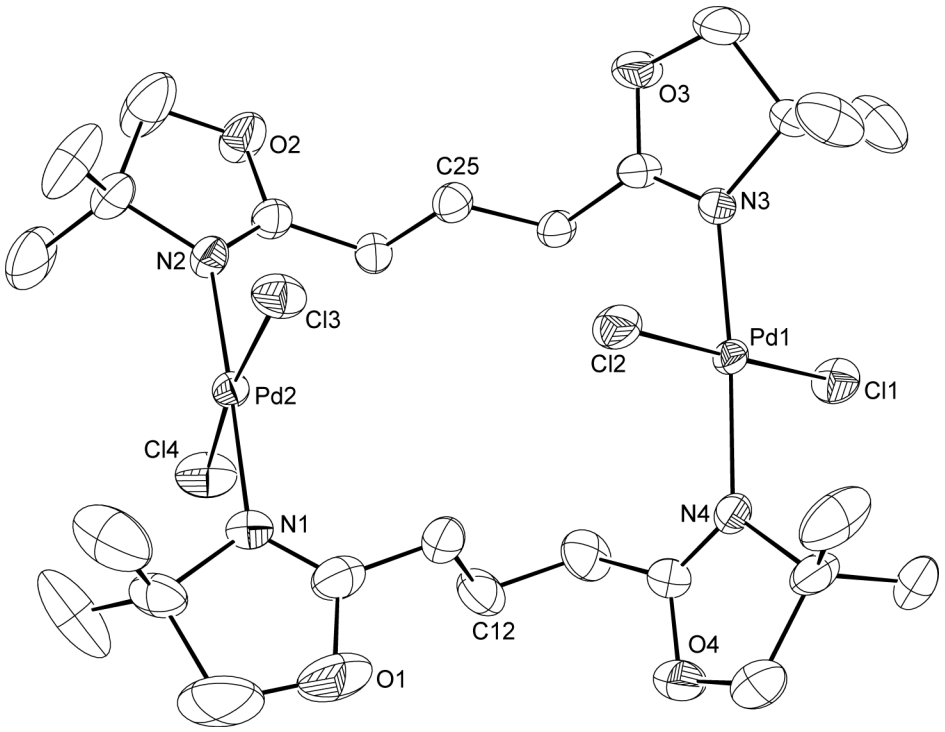

Figure 2-10. ORTEP plot of $[PdCl_2(\mu\text{-}N,N\text{-Probox}^{Me2})]_2$ (**2-1**). Ellipsoids are drawn at 50% probability. Hydrogen atoms and a disordered CH_2Cl_2 molecule are not included. Relevant bond distances (Å): Pd1-N3, 2.020(4); Pd1-N4, 2.033(4); Pd1-Cl1, 2.290(1); Pd1-Cl2, 2.299(1); Pd2-N1, 2.008(4); Pd2-N2, 2.014(4); Pd2-Cl3, 2.294(1); Pd2-Cl4, 2.300(2). Relevant bond angles (°): N1-Pd2-N2, 178.7(2); N3-Pd1-N4, 175.6(2).

The reaction of Probox^{iPr} and $PdCl_2(NCPh)_2$ in refluxing THF provides the optically active derivative $[PdCl_2(\mu\text{-}N,N\text{-Probox}^{iPr})]_2$ (**2-2**) in 84% yield. All spectroscopic data are consistent with a C_2-symmetric, non-cyclometalated species. The ^{1}H NMR spectrum of **2-2** contains two doublets corresponding to the two diastereotopic isopropyl methyl groups on the oxazoline ring. Thus the 4*S* stereocenters are maintained in the reaction with $PdCl_2(NCPh)_2$. The ^{15}N chemical shift of **2-2** at -277.6 ppm; is upfield compared to non-coordinated Probox^{iPr} (-177 ppm).

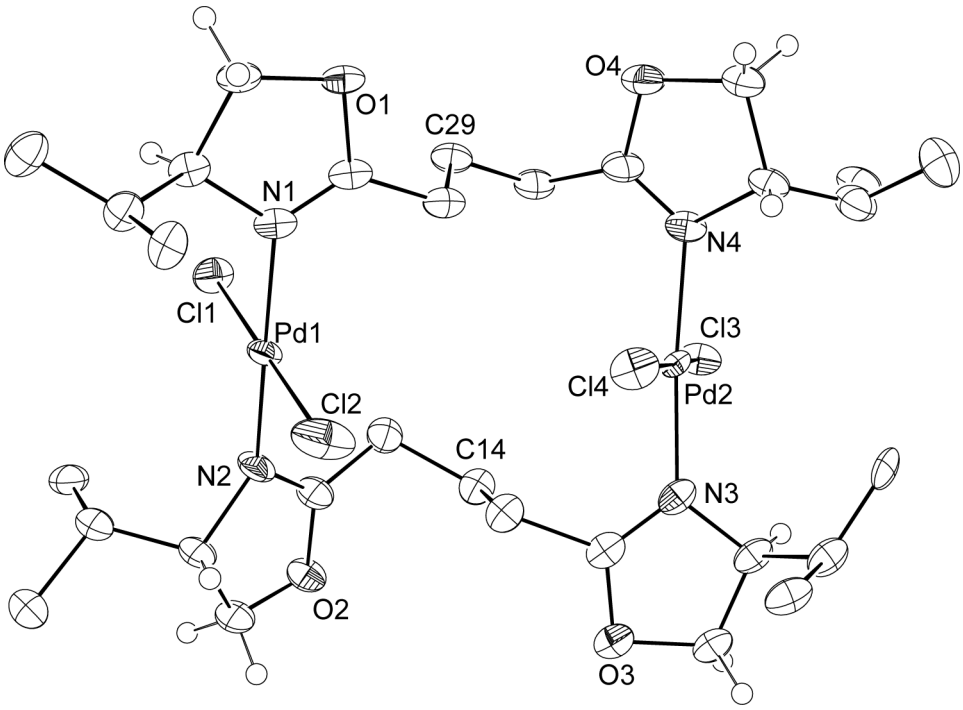

Figure 2-11. ORTEP diagram, drawn at 50% probability, of macrocycle **2-2A** (containing Pd1 and Pd2) of $[PdCl_2(\mu\text{-}N,N\text{-Probox}^{iPr})]_2$ (**2-2**) of two located in the asymmetric unit cell. Hydrogen atoms bonded to the oxazoline ring are shown to illustrate stereochemistry, but all other hydrogen atoms, the second macrocycle (containing Pd3 and Pd4), and disordered co-crystallized CH_2Cl_2 molecules are not illustrated. Relevant bond distances for **2-2A** (Å): Pd1-N1, 1.93(1); Pd1-N2, 2.05(1); Pd1-Cl1, 2.301(5); Pd1-Cl2, 2.290(6); Pd2-N3, 1.96(2); Pd2-N4, 2.02(1); Pd2-Cl3, 2.311(4); Pd2-Cl4, 2.285(4). Relevant bond angles for **2-2A** (°): N1-Pd1-N2, 178.6(6); N3-Pd2-N4, 174.9(6).

Crystals suitable for a single crystal X-ray diffraction study were obtained from a concentrated solution of **2-2** in toluene cooled to -30 °C. The connectivity of $[PdCl_2(\mu\text{-}N,N\text{-Probox}^{iPr})]_2$ is confirmed (see ORTEP diagram of **2-2** plotted in Figure 2-11). The structure contains two independent molecules per unit cell with only small differences in bond lengths and angles. The Pd–N distances (**2-2A**, 1.93(1) to 2.05(1) Å; **2-2B**, 1.99(1) to 2.06(2) Å) and the Pd–Cl distances (2.285(4) to 2.312(4) Å over the four palladium centers) are identical within 3σ error. The angles created by the square planes, defined by the atoms bound to palladium, in the two chiral macrocycles are more acute (**2-2A**,

40.2°; **2-2B**, 44.2°) compared to achiral macrocycle **2-1** (60.4°). The distance between Pd2–C14 (non bonding) is 3.75 Å, and is significantly shorter than those observed in **2-1**. The other non-bonding Pd–C (central carbon of the backbone) distances are larger than 4 Å.

Cyclometalation attempts

With these palladium macrocycles in hand, studies on promoting cyclometalation to form the desired 'NCN' pincer complexes were initiated. Only starting materials are observed by ^{1}H NMR spectroscopy when solutions of **2-1** in toluene or 2-methoxyethanol are heated to 120 °C for 3 days. Cyclometalation of $[PdCl_2(\mu\text{-}P,P\text{-}^t Bu_2P(CH_2)_5P^t Bu)]_2$ to form the pincer compound $[(\kappa^3\text{-PCP})PdCl]$ is achieved by photolytic sublimation.[59-60] However, **2-1** does not sublime under photolytic (450 watt mercury lamp) conditions. Addition of one equivalent of pyridine or triethylamine to reaction mixtures of Probox^{Me2} and $[PdCl_2(NCPh)_2]$ results in the formation of **2-1** with no evidence of cyclometalation. Attempts to alkylate **2-1** with MeLi or MeMgBr to form the corresponding Pd–Me complex to promote cyclization were not successful; only **2-1**, Probox^{Me2}, and palladium black are obtained. Similarly, treatment of Probox^{Me2} with (TMEDA)$PdMe_2$ (TMEDA = *N,N,N',N'*-tetramethylethylenediamine) results in the formation of palladium black and unchanged Probox^{Me2}. A report from Haraki and co-workers describes the preparation of an $[NC_{sp3}NPdCl]$ pincer complex from the reaction of 1,3-bis(2-pyridyl)propane with $Pd(OAc)_2$ in refluxing acetic acid (8 h) followed by anion exchange with LiCl in acetone.[68] However, only dipalladium dimer **2-1** is isolated under these reaction conditions.

Interaction of Probox ligands on rhodium

Given the lack of success in forming cyclometalated palladium complexes of Probox, we decided to try Rh(I) salts because C–H bond oxidative addition could be

more facile than direct cyclometalation. Unfortunately, reactions between Probox^{Me2} or Probox^{iPr} with $[RhCl(\eta^2\text{-}C_8H_{14})_2]_2$, $[RhCl(\eta^4\text{-}C_8H_{12})]_2$, or $[RhCl(\eta^2\text{-}C_2H_4)_2]_2$ were not successful. However, treating Probox^{Ph} with $[RhCl(\eta^2\text{-}C_8H_{14})_2]_2$ provides a new bis(oxazoline) species in 65% yield (Eq. 2-4); its structure is identified as the dirhodium macrocycle $[RhCl(\mu\text{-}N,N\text{-Probox}^{Ph})(\eta^2\text{-}C_8H_{14})]_2$ (**2-3**) reminiscent of **2-1** and **2-2**.

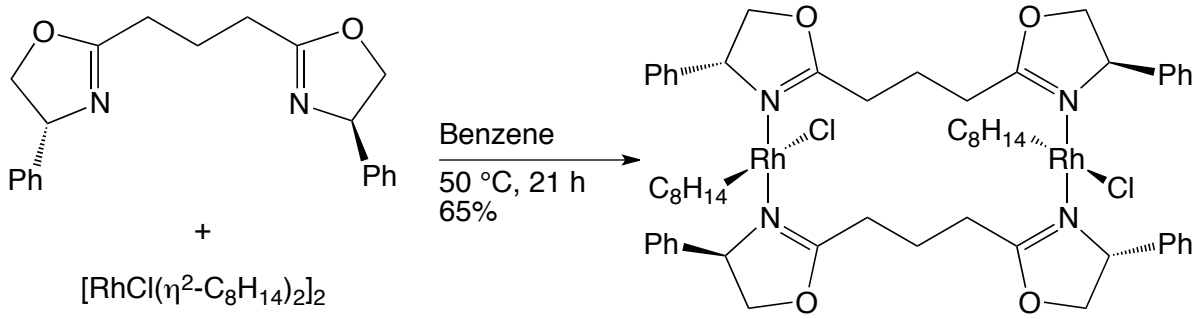

(Eq. 2-4)

The spectroscopy was initially misleading and suggested an NCN-pincer based on a Probox ligand had been obtained. Each of the two dipalladium macrocycles (**2-1** and **2-2**) contain a C_2 axis through the two palladium centers while no such symmetry is observed in **2-3**, thus the two Probox^{Ph} ligands are inequivalent in the NMR spectra of **2-3**. The key difference between the dipalladium and dirhodium macrocycles is the inequivalent substitution on rhodium (Cl and η^2-C_8H_{14}) versus palladium (two Cl). There are two sets of phenyl resonances and benzyl protons indicating that the two rhodium(I) centers are related by symmetry. In addition, there is only one set of cyclooctene resonances in the ^1H and $^{13}C\{^1H\}$ NMR spectra, further supporting the assessment of equivalent rhodium(I) centers in macrocycle (**2-3**). As earlier stated, compound **2-3** does not contain the same C_2 axis that is present in compounds **2-1** and **2-2**; this, as well as the presence of cyclooctene resonances, significantly complicated the analysis of the ^1H

and $^{13}C\{^{1}H\}$ NMR spectra. Additionally, the ^{15}N NMR chemical shift for **2-3** was found to be -209.9, which represents an upfield shift of 55.4 ppm from free Probox^{Ph}. A single crystal diffraction study of X-ray quality crystals provided unequivocal evidence for macrocycle formation.

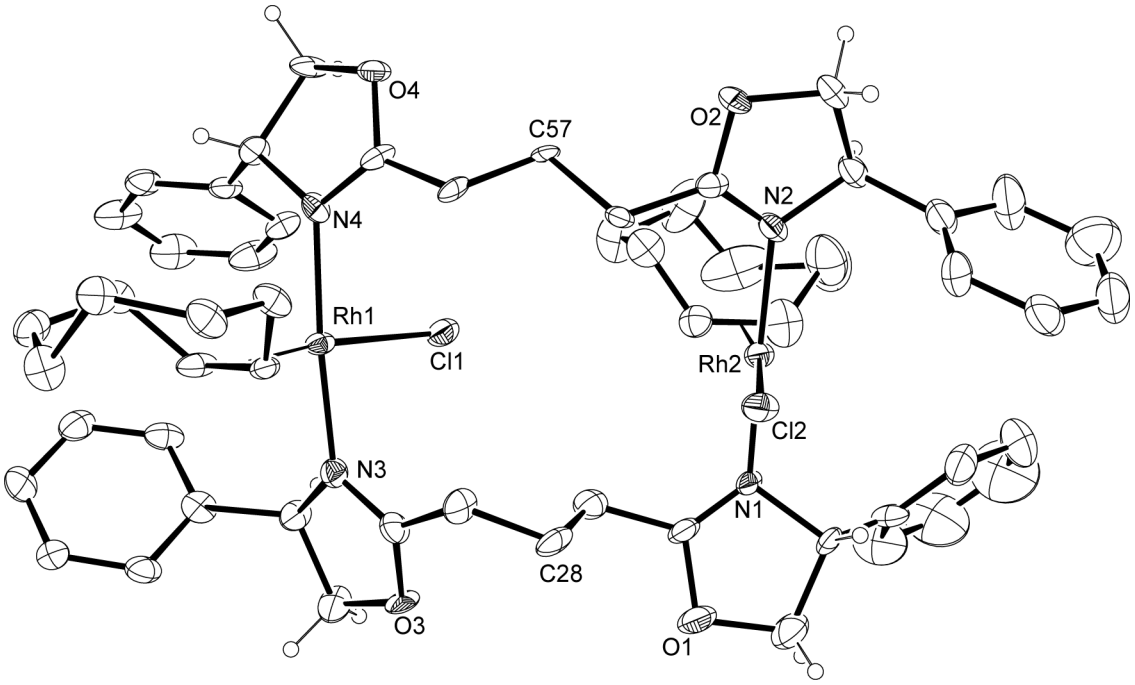

Figure 2-12. ORTEP diagram of [RhCl(m-N,N-ProboxPh)(h2-C8H14)]2 (**3**); ellipsoids are drawn at 30% probability and only hydrogen atoms bonded to oxazoline rings are illustrated. A co-crystallized benzene molecule is also not shown. Relevant bond distances (Å): Rh1-N3, 2.00(1); Rh1-N4, 2.05(1); Rh1-Cl1, 2.412(7); Rh2-N1, 2.01(1); Rh2-N2, 2.04(1); Rh2-Cl2, 2.404(5). Relevant bond angles (°): N3-Rh1-N4, 172.5(4); N1-Rh2-N2, 172.5(4).

The crystal structure (see ORTEP diagram of **2-3** plotted in Figure 2-12) shows the two rhodium(I) centers are square planar, as expected, and the two planes defined by Cl1–N3–N4 and Cl2–N1–N2 intersect with an angle of 46.4° (not refined). The ∠N3–Rh1–N4 and ∠N1–Rh2–N2 angles are identical (172.5(4)°) and more distorted from the idealized 180° than in dipalladium macrocycles **2-1** (178.7(2)° and 175.6(2)°) and **2-2** (**2-2A**, 174.9(6)° and 178.6(6)°; **2-2B**, 179.7(6)° and 177.7(6)°). This distortion is likely due

to unfavorable oxazoline–η^2-C_8H_{14} interactions. In the solid state, the distances between the rhodium centers and the nearest central carbon atom in the propyl backbone are long (4.33-4.66 Å, not refined) and the hydrogens on these two carbons (C28 and C57) are pointed outside of the macrocycle and away from the two rhodium centers. A comparison to 16-membered rhodium(I) macrocycles containing 1,5-bis(phosphino)pentane ligands is not available, thus making **2-3** a crystallographically unique structure in rhodium chemistry. Unfortunately, heating a solution of **2-3** for one day to promote cyclometalation proved futile because a black precipitate is formed and only free Probox^{Ph} is observed in ^{1}H NMR spectrum.

We were successful in isolating a cyclometalated compound from the reaction of Probox^{Me2} and $RhCl_3$ in low yield. Thus, a reaction between $RhCl_3$ and Probox^{Me2} affords the desired rhodium(III) cyclometalated complex (κ^3-*N,C,N*-Probox^{Me2})$RhCl_2$ after refluxing in ethanol for 18 hours (Eq. 2-5). **2-4** was purified by silica gel chromatography at 5 °C under an argon atmosphere. A large amount of black precipitate, presumed to be rhodium metal, is observed during the reaction. Large amounts of black precipitate also form in reactions in methanol and isopropanol. Only free ligand is isolated from reactions in non-protic solvents (benzene, methylene chloride, or THF). The decomposition to rhodium black likely arises from β-hydrogen elimination of a rhodium–solvent compound as an initial step. Switching to *tert*-butanol, to avoid the presence of β-hydrogens, prevents the formation of rhodium black; however, only non-coordinated Probox^{Ph} is isolated. A mixture of ethanol and *tert*-butanol provides isolable **2-4**, but rhodium black is observed and the yield is no better than pure ethanol. Modifying the reaction temperature, time, and concentration is ineffective in increasing the isolated yield of **2-4**.

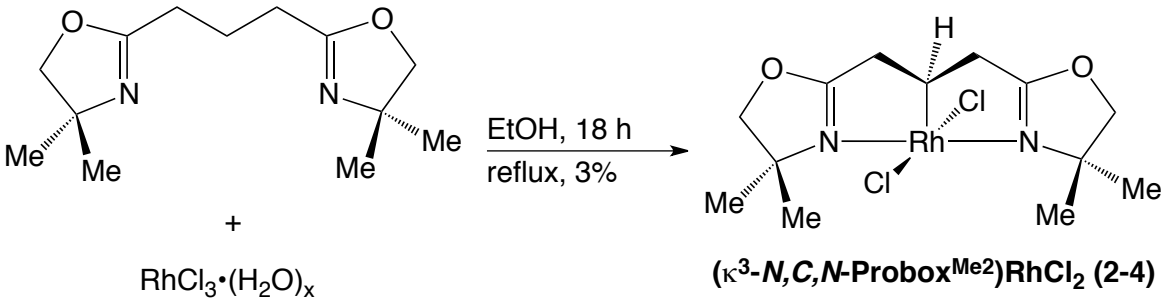

(Eq. 2-5)

The ^{1}H NMR spectrum of **2-4** is significantly different from the ^{1}H NMR spectrum of dipalladium macrocycle **2-1**. There was one ^{1}H NMR resonance at 5.85 ppm that appears as a multiplet assigned to the hydrogen on the cyclometalated carbon while a doublet ^{13}C{^{1}H} NMR resonance at 27.93 ppm ($^{1}J_{RhC}$ = 25 Hz) was assigned to the carbon bound to rhodium. Additionally, there were two sets of diastereotopic oxazolinyl methyl (1.47 and 1.44 ppm) and methylene (4.25 and 4.18 ppm) resonances in the ^{1}H NMR spectrum. One ^{15}N NMR crosspeak was observed in the ^{1}H–^{15}N HMBC experiment corresponding to a ^{15}N chemical shift of -211.9 ppm while a ^{1}H–^{15}N HSQC experiment provided an accurate rhodium–nitrogen coupling constant, $^{1}J_{RhN}$ = 24 Hz. This coupling constant is similar to a reported value for *trans*-[Rh(NC$_5$H$_5$)$_4$Cl$_2$]Cl ($^{1}J_{RhN}$ = 17.1 Hz).[69] Based on this NMR evidence, **2-4** is assigned as C_s-symmetric in solution (chloroform-d_1); however, both *fac* and *mer* isomers are possible. A NOESY experiment was performed to detect the presence of through-space interactions between methyl groups on opposite oxazoline rings, see Figure 2-9, but no crosspeak was detected. The geometry of **2-4** is assigned as *mer* based on the crystal structure of the water adduct **2-5** (vide infra).

Crystals suitable for an X-ray diffraction study are obtained by slow evaporation of a concentrated solution of **2-4** in methylene chloride. The resulting structure (see

ORTEP diagram of **2-5** plotted in Figure 2-13) confirms the presence of the Probox pincer complex, *mer*-(κ^3-*N,C,N*-Probox^{Me2})$RhCl_2(OH_2)$.

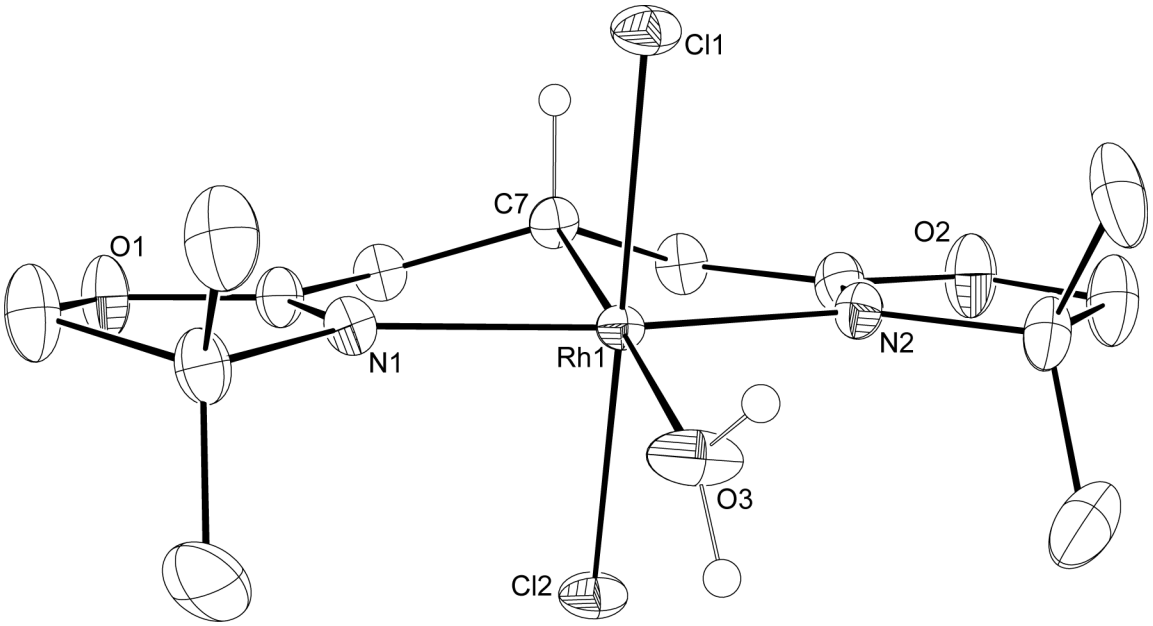

Figure 2-13. ORTEP diagram of (κ^3-*N,C,N*-Probox^{Me2})$RhCl_2(OH_2)$ (**2-5**). Hydrogen atoms, except those in the water ligand and on the metalated carbon, are not shown. The hydrogen atoms on OH_2 were found in the electron density map and refined. Ellipsoids are drawn at 35% probability. Relevant bond distances (Å): Rh1-C7, 2.022(3); Rh1-N1, 2.039(3); Rh1-N2, 2.048; Rh1-Cl1, 2.338(2); Rh1-Cl2, 2.358(2), Rh1-O3, 2.257(3). Relevant bond angles (°): N1-Rh1-N2, 164.6(1); N1-Rh1-C7, 82.3(1); N2-Rh1-C7, 82.5(1); Cl1-Rh1-Cl2, 178.86(3); C7-Rh-O3, 176.6(1).

The coordinated water molecule arose from the crystallization process because bench-grade methylene chloride was used and the crystallization was performed in air. Attempts to crystallize **2-4** in anhydrous/anaerobic conditions were not successful. The water molecule is not coordinated to the species obtained from the silica gel column as the two compounds, **2-4** and **2-5**, differ in their ^{1}H NMR spectra. A resonance at 1.62 ppm was assigned as the OH_2 ligand while the resonance corresponding to the hydrogen on C7 (see Figure 2-13) has a chemical shift of 5.77 ppm which was upfield of

the analogous hydrogen in **2-4** (vide supra) by 0.08 ppm. Additionally, elemental analysis of **2-4** is consistent with the five-coordinate *mer*-(κ^3-*N,C,N*-Probox^{Me2})$RhCl_2$.

Close examination of the crystal structure of **2-5** reveals that the Probox ligand is coordinated in a *mer* configuration with C7 *cis* to two mutually *trans* chlorides and *trans* to the water molecule. The nitrogen atoms in the oxazoline rings are "pulled back" toward C7, ∠N1–Rh–N2 angle is 164.6(1)° while the ∠N1–Rh-C7 and ∠N2–Rh–C7 angles are 82.3(1)° and 82.5(1)°, thus distorting the octahedral geometry expected for six-coordinate rhodium(III). The remaining angles around the rhodium center are close to the expected values. Interestingly, the rhodium–nitrogen interatomic distances in **2-5** are identical to those in rhodium macrocycle **2-3** even though the former is rhodium(III) and six-coordinate while the latter is rhodium(I) and four-coordinate. A comparison to other oxazoline based pincer complexes reveals that the Rh–C7 bond distance in *mer*-(κ^3-*N,C,N*-Probox^{Me2})$RhCl_2(OH_2)$, 2.022(3) Å, is 0.09 and 0.02 Å longer than the analogous distance in (Bn-Phebox)$RhCl_2(H_2O)$ (1.93(2) Å) and [$RhCl_2$(*S,S*-ip-benbox)Me_2)] (2.004(3) Å) respectively,[23,20] and the Rh-O distance for the water ligand (2.275(3) Å) is identical within 3σ error to the corresponding distance in (Bn-Phebox)$RhCl_2(H_2O)$.

The water ligand is *trans* to the cyclometalated carbon; exchanging this ligand for a strongly donating phosphine could force the Probox ligand to adopt a *fac* configuration, thus preventing two strongly donating ligands from being mutually *trans*. The reaction between **2-4** and PMe_3 in THF-d_8 produces a new bis(oxazoline) species in one hour at room temperature. The ^{31}P NMR spectrum of the reaction mixture contains one doublet resonance at 9.53 ppm ($^1J_{RhP}$ = 129 Hz) indicating that the phosphine is coordinated to the metal center, and a single isomer is obtained (Eq. 2-6).

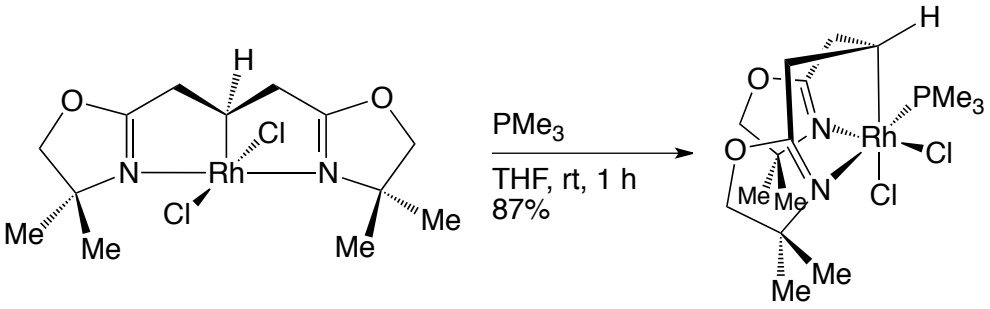

***fac*-(κ^3-*N,C,N*-Probox^{Me2})-RhCl$_2$(PMe$_3$) (2-6)**

(Eq. 2-6)

fac-(κ^3-*N,C,N*-Probox^{Me2})RhCl$_2$(PMe$_3$) (**2-6**) exists as a C_1-symmetric species in solution (methylene chloride-d_2) as evidenced by the presence of four resonances attributed to the oxazoline methyl (1.65, 1.60, 1.58, and 1.55 ppm) and methylene (4.23, 4.18, 4.12, and 4.00 ppm) hydrogens as well as four resonances (3.23, 2.84, 2.16, and 2.12 ppm) assigned to the hydrogens on the α-methylene carbon in the ^{1}H NMR spectrum. A chemical shift was observed at 3.00 ppm that corresponds to the hydrogen on the cyclometalated carbon in **2-6**; this significant upfield shift of 2.85 ppm from five-coordinate **2-4** (5.85 ppm) is due to the presence of an anionic ligand *trans* to carbon. The strong upfield shift of the hydrogen on the cyclometalated carbon was puzzling because the addition of PMe$_3$ was expected to necessitate a ligand rearrangement to prevent the two strongly donating groups, carbon and phosphorus, from being mutually *trans*. The geometry of the Probox ligand was initially assigned as *mer* on the basis of this strong upfield shift in the ^{1}H NMR spectrum. However, a ^{1}H–^{15}N HMBC experiment on **2-6** provides two ^{15}N chemical shifts correlating to two inequivalent imidine nitrogens. The ^{15}N chemical shifts, -178.2 and -207.3 ppm, were both significantly upfield of Probox^{Me2} (-137 ppm, Table 2-1); a doublet was observed in the ^{15}N dimension for the downfield resonance (-178.2 ppm, $^2J_{PN}$ = 104 Hz) that corresponds to phosphorus

coupling. This coupling constant is too large to be Rh–N coupling (vide supra) and is consistent with P–N coupling; more specifically, *trans*-P–N coupling.[70] Thus, one imidine nitrogen must be *trans* to phosphorus and the other *trans* to chloride. In addition, crosspeaks in the $^{1}H–^{15}N$ HMBC spectrum of **2-6** to oxazolinyl methyl and methylene hydrogens distinguished the two rings. This, in conjunction with a ^{1}H COSY experiment, allowed complete assignment of the ^{1}H NMR spectrum. The small P–C coupling ($^{2}J_{PC}$ = 7.7 Hz) for the cyclometalated carbon (18.94 ppm, $^{1}J_{RhC}$ = 21.2 Hz) was consistent with a *cis*-coordinated PMe_3. Based on the NMR evidence, the solution state structure is clarified; the Probox ligand must have adopted a *fac* configuration upon coordination of PMe_3.

Additional support for the solution state structure is obtained from a ^{1}H 2D-NOESY experiment. As shown in Figure 2-9, one would expect to observe a crosspeak between two methyl resonances on opposing oxazoline rings in the ^{1}H-NOESY experiment if the ligand is in a *fac* configuration. This is exactly what was observed; only one methyl-methyl inter-oxazoline crosspeak was detected, necessitating the oxazoline rings to be in close proximity. These two methyl groups are assigned as *endo* (see Figure 2-14). There were also crosspeaks between the two *endo* methyl groups on each oxazoline ring and the *endo* methylene resonance on the opposing oxazoline ring, thereby confirming the close proximity of the two oxazoline rings. Moreover, a crosspeak was observed between the methine proton on the backbone and the PMe_3 resonance, which confirmed the *cis* disposition of the metalated carbon and PMe_3. Through-space coupling was also observed between the PMe_3 resonance and one methyl resonance on an oxazoline ring that was defined as a *cis-exo* methyl resonance. Finally, through-space coupling was detected between one hydrogen on the propyl backbone (bound to the oxazoline ring *cis* to PMe_3) and the PMe_3 doublet allowing it to be assigned as the *exo*

methylene. The acquired NMR data allows for a full and complete assignment of the ^{1}H and $^{13}C\{^{1}H\}$ NMR spectra to conclude, unambiguously, the solution structure of *fac*-(κ^3-*N,C,N*-Probox^{Me2})$RhCl_2$-*cis*-(PMe_3).

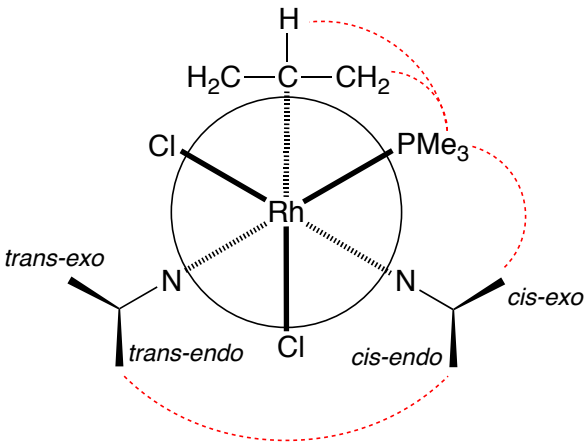

Figure 2-14. Newman projection illustrating the *fac* coordination of (κ^3-*N,C,N*-Probox^{Me2})$RhCl_2$-*cis*-(PMe_3) (2-6) and nOe through-space interactions observed via 2D-^{1}H-NOESY experiment. The substituents attached to nitrogen represent the methyl groups on the oxazoline ring and the $CH(CH_2)_2$ represents the cyclometalated carbon and α-methylene groups of the backbone. Other oxazoline carbons and hydrogens have been omitted for clarity.

Conclusion

We have synthesized two new 1,3-bis(oxazolinyl)propane ligands, achiral Probox^{Me2} and chiral Probox^{Ph}, and applied them to group 9 and 10 metals. Coordination of the Probox ligands to rhodium(I) and palladium(II) metal centers is facile and new 16-membered macrocycles are formed. Once formed, the palladium(II) macrocycles are highly resistant to cyclometalation compared to their 1,5-bis(phosphino)pentane counterparts. Reaction of Probox^{Me2} and $RhCl_3$ provides a cyclometalated rhodium(III) pincer complex under mild reducing conditions in low, but isolable, yield. The pincer ligand adopts a *mer*-configuration in the five-coordinate rhodium complex (and six-coordinate aqua complex) and a *fac* configuration in a PMe_3 adduct. Examination of the

structural data for the palladium(II) and rhodium(I) macrocycles and the rhodium(III) pincer compound does not reveal any significant bond length distortion in the later, although the *trans* N–Rh–N angles in the pincer structure are tied back by ca. 15° from 180°. The formation of cyclometalated species containing an aliphatic backbone is significantly more difficult with oxazoline donors than with phosphine or pyridine donors. Despite some success, further application of this chemistry requires increased yield of the desired NCN-pincer complex.

Experimental

General. All manipulations were performed using either Schlenk techniques or in a glovebox under an inert atmosphere of N_2 or argon unless otherwise indicated. Dry, oxygen-free solvents were used throughout. Benzene, toluene, methylene chloride, pentane, diethyl ether, and tetrahydrofuran were degassed by sparging with nitrogen, filtered through activated alumina columns, and stored under nitrogen. Benzene-d_6, toluene-d_8, and tetrahydrofuran-d_8 were vacuum transferred from Na/K alloy and stored under N_2 in the glovebox. Methylene chloride-d_2 was vacuum transferred from CaH_2 and stored under N_2 in the glovebox. All alcohols were dried over activated magnesium, distilled, and stored under N_2. Glutaronitrile was purchased from Acros, distilled under reduced pressure, and stored at 0 °C. 2-amino-2-methyl-1-propanol, L-valine, D-phenylglycine, $Cd(OAc)_2{\cdot}2H_2O$, and chlorobenzene were purchased from Acros and used as received. PMe_3 was purchased from Strem and vacuum transferred prior to use. Rhodium trichloride trihydrate was dehydrated immediately before use by dissolution in the alcohol solvent followed by removal of the alcohol in vacuo; this process is repeated three times. Probox$^{i\text{Pr}}$ was prepared using the $Cd(OAc_2)$-catalyzed method; the structural characterization has been previously reported.[55] ^1H, $^{13}C\{^1H\}$, and $^{31}P\{^1H\}$ spectra were

collected on either a Bruker DRX-400 spectrometer or a Bruker Avance-500 and 600 spectrometers. ^{15}N chemical shifts and ^{15}N-^{103}Rh coupling constants were determined by ^{1}H-^{15}N HMBC and ^{1}H-^{15}N HSQC experiments respectively on a Bruker Avance II 700 spectrometer with a Bruker Z-gradient inverse TXI $^{1}H/^{13}C/^{15}N$ 5mm cryoprobe, and chemical shifts were originally recorded with respect to liquid ammonia (machine calibration) and recalculated to the nitromethane chemical shift scale by adding -381.9 ppm.[71] The ^{1}H-^{15}N HSQC experiment utilized the Bruker hsqcetgp pulse program with correlation via double inept transfer, phase sensitive Echo/Antiecho-TPPI gradient, decoupling during acquisition, and trim pulses in inept transfer with a 6.0 ppm sweep width and 256 points in the ^{15}N dimension giving a FID resolution of 1.663 Hz.[69] Elemental analysis was performed on a Perkin-Elmer 2400 Series II CHN/S by the Iowa State Chemical Instrumentation Facility. High-resolution mass spectrometry performed on a Waters GCT TOF mass spectrometer equipped with an Agilent 6890 GC. X-ray diffraction data was collected on a Bruker-AXS SMART 1000 CCD diffractometer using Bruker-AXS SHELXTL software.

Probox^{Me2}. A 100 mL round bottom flask equipped with a magnetic stir bar was charged with glutaronitrile (0.97 g, 10.6 mmol) and 30 mL of chlorobenzene. Solid $Cd(OAc)_2{\cdot}2H_2O$ (0.144 g, 0.54 mmol) was added to the flask followed by and a solution of 2-amino-2-methyl-1-propanol (3.55 g, 39.7 mmol) in 20 mL of chlorobenzene. The flask was then equipped with a reflux condenser and an argon inlet, and the mixture was heated at reflux for 6 days. Upon cooling, saturated sodium bicarbonate solution (75 mL) was added, and the mixture was stirred for 30 minutes and then filtered. The filtrate was washed with brine (3 × 50 mL), and the aqueous layer was then back-extracted with ethyl acetate. The organic layers were combined, dried with sodium sulfate, and the volatile components were removed using a rotary evaporator. Probox^{Me2} was purified by

distillation, (86 °C, 2 × 10^{-3} mmHg) to give a colorless oil (1.76 g, 7.38 mmol, 72 %). ^{1}H NMR (benzene-d_6, 400 MHz): δ 3.52 (s, 4 H, $CH_2(CH_2CNCMe_2CH_2O)_2$), 2.28 (t, $^{3}J_{HH}$ = 7.19 Hz, 4 H, $CH_2(CH_2CNCMe_2CH_2O)_2$), 2.09 (pent, $^{3}J_{HH}$ = 7.19 Hz, 2 H, $CH_2(CH_2CNCMe_2CH_2O)_2$), 1.08 (s, 12 H, $CH_2(CH_2CNCMe_2CH_2O)_2$). $^{13}C\{^{1}H\}$ NMR (benzene-d_6, 100 MHz): δ 164.7 ($CH_2(CH_2CNCMe_2CH_2O)_2$), 79.62 ($CH_2(CH_2CNCMe_2CH_2O)_2$), 67.29 ($CH_2(CH_2CNCMe_2CH_2O)_2$), 28.54 ($CH_2(CH_2CNCMe_2CH_2O)_2$), 27.37 ($CH_2(CH_2CNCMe_2CH_2O)_2$), 22.76 ($CH_2(CH_2CNCMe_2CH_2O)_2$). ^{15}N NMR (methylene chloride-d_2, 71 MHz): δ -137.0. IR (neat, cm^{-1}): 2958 m, 2905 m, 2873 m, 1668 s (ν_{CN}), 1468 w, 1385 w, 1366 w, 1233 w, 1173 w, 984 m, 915 w. Anal. Calcd. for $C_{13}H_{22}N_2O_2$: C, 65.51; H, 9.30; N, 11.75. Found: C, 65.12; H, 9.32; N, 11.58.

Probox^{iPr}. A 100 mL round bottom flask equipped with a magnetic stir bar was charged with glutaronitrile (1.00 g, 10.7 mmol) and 30 mL of chlorobenzene. Solid $Cd(OAc)_2{\cdot}2H_2O$ (0.144 g, 0.54 mmol) was added to the flask followed by a solution of L-valinol (4.13 g, 40.0 mmol) in 20 mL of chlorobenzene. The flask was then equipped with a reflux condenser and an argon inlet, and the mixture was heated at reflux for 6 days. Upon cooling, saturated sodium bicarbonate solution (75 mL) was added, and the mixture was stirred for 30 minutes and then filtered. The filtrate was washed with brine (3 × 50 mL), and the aqueous layer was then back-extracted with ethyl acetate. The organic layers were combined, dried with sodium sulfate, and the volatile components were removed using a rotary evaporator. Probox^{iPr} was purified by distillation, (140 °C, 3.9 × 10^{-2} mmHg) to give a colorless oil (1.82 g, 6.83 mmol, 64 %). ^{1}H and $^{13}C\{^{1}H\}$ NMR spectra are identical with the literature values.[55] ^{15}N NMR (chloroform-d_1, 71 MHz): δ -160.1.

Probox^{Ph}. A 1 L, 3-neck round bottom flask was equipped with a magnetic stir bar and a reflux condenser connected to an argon purge. Glutaronitrile (7.63 g, 81.5 mmol) and 100 mL of chlorobenzene were added, followed by $Cd(OAc)_2{\cdot}2H_2O$ (1.09 g, 4.09 mmol) and an additional 100 mL of chlorobenzene. D-phenylglycinol (41.2 g, 0.301 mol) in 175 mL of chlorobenzene was then added to the stirring solution. The reaction mixture was heated at reflux for 6 days. After cooling to room temperature, the reaction was stirred with 500 mL of brine for 1 h. The mixture was extracted with ethyl acetate and washed with sodium bicarbonate. A white voluminous solid precipitated upon addition of sodium bicarbonate and was removed with the aqueous layer. The organic layer was dried with sodium sulfate, and the volatile components were removed using a rotary evaporator to yield a yellow oil. The product was purified by flash chromatography on silica gel (hexane:ethyl acetate:triethyl amine = 10:3:1 R_f = 0.7) to give Probox^{Ph} as a yellow oil in 52% yield (14.2 g, 42.43 mmol). ^{1}H NMR (chloroform-d_1, 400 MHz): δ 7.30 (t, $^3J_{HH}$ = 7.4 Hz, 4 H, *meta*-C_6H_5), 7.23 (t, $^3{}_{JHH}$ = 8.8 Hz, 4 H, *ortho*-C_6H_5), 7.23 (d, $^3J_{HH}$ = 9.2 Hz, 2 H, *para*-C_6H_5), 5.13 (t, $^3J_{HH}$ = 9.2 Hz, 2 H, $CH_2(CH_2CNCPh(H)CH_2O)_2$), 4.54 (dd, $^2J_{HH}$ = 10 Hz, $^3J_{HH}$ = 8.4 Hz, 2 H, $CH_2(CH_2CNCPh(H)CH_2O)_2$), 4.02 (vt, J_{HH} = 8.4 Hz, 2 H, $CH_2(CH_2CNCPh(H)CH_2O)_2$), 2.50 (t, $^3J_{HH}$ = 7.6 Hz, 4 H, $CH_2(CH_2CNCPh(H)CH_2O)_2$), 2.12 (pent, $^3J_{HH}$ = 7.6 Hz, 2 H, $CH_2(CH_2CNCPh(H)CH_2O)_2$). $^{13}C\{^1H\}$ NMR (chloroform-d_1, 100 MHz): δ 167.96 ($CH_2(CH_2CNCPh(H)CH_2O)_2$), 142.36 (*ipso*-$C_6H_5$), 128.70 (*meta*-$C_6H_5$), 127.42 (*para*-$C_6H_5$), 126.48 (*ortho*-$C_6H_5$), 74.47, ($CH_2(CH_2CNCPh(H)CH_2O)_2$), 69.51 ($CH_2(CH_2CNCPh(H)CH_2O)_2$), 27.30 ($CH_2(CH_2CNCPh(H)CH_2O)_2$), 22.46 ($CH_2(CH_2CNCPh(H)CH_2O)_2$). ^{15}N NMR (methylene chloride-d_2, 71 MHz): δ -154.5. IR (neat, cm^{-1}): 3057 w, 3023 w, 2958 m, 2894 m, 1662 s (ν_{CN}), 1492 m, 1452 m, 1164 m, 979 m, 698 s. MS (EI) exact mass Calculated for $C_{21}H_{22}N_2O_2$: m/e 334.1861 ($[M]^+$), Found: 334.1681.

[$PdCl_2$(μ-*N,N*-Probox^{Me2})]2 (2-1). A Schlenk flask was charged with $PdCl_2(NCPh)_2$ (1.81 g, 4.73 mmol) in air. The flask was connected to a Schlenk manifold and an argon atmosphere was established. THF (75 mL) was added via cannula transfer. A solution of Probox^{Me2} (1.13 g, 4.74 mmol) in THF (10 mL) was quickly added to the stirring $PdCl_2(NCPh)_2$ solution via cannula, and the color immediately changed from dark red to orange. The solution was stirred at room temperature for 1 h and then heated at reflux overnight. The mixture was cooled to room temperature and concentrated to ca. 10 mL to give an orange solid. This solid was filtered on a frit, washed with pentane, and dried under vacuum for 24 h to yield **2-1** (1.74 g, 2.09 mmol, 88%). Slow evaporation of a solution of **2-1** in methylene chloride at room temperature provided X-ray quality crystals. ^{1}H NMR (methylene chloride-d_2, 600 MHz): δ 4.14 (s, 8 H, $CH_2(CH_2CNCMe_2CH_2O)_2$), 3.43 (t, $^3J_{HH}$ = 7.8 Hz, 8 H, $CH_2(CH_2CNCMe_2CH_2O)_2$), 2.23 (pent, $^3J_{HH}$ = 7.8 Hz, 4 H, $CH_2(CH_2CNCMe_2CH_2O)_2$), 1.59 (s, 24 H, $(CH_2(CH_2CNCMe_2CH_2O)_2)$. $^{13}C\{^1H\}$ NMR (methylene chloride-d_2, 150 MHz): δ 169.68 ($CH_2(CH_2CNCMe_2CH_2O)_2$), 81.00 ($CH_2(CH_2CNCMe_2CH_2O)_2$), 68.61 ($CH_2(CH_2CNCMe_2CH_2O)_2$), 31.56 ($CH_2(CH_2CNCMe_2CH_2O)_2$), 28.88 ($CH_2(CH_2CNCMe_2CH_2O)_2$), 22.36 ($CH_2(CH_2CNCMe_2CH_2O)_2$). ^{15}N NMR (methylene chloride-d_2, 70.9 MHz): δ -213.8. IR (KBr, cm^{-1}): 2967 m, 2925 m, 1652 s (ν_{CN}), 1457 m, 1378 m, 1004 m, 971 m. Anal. Calcd. for $C_{26}H_{44}Cl_4N_4O_4Pd_2$: C, 37.6; H, 5.33; N, 6.74. Found C, 38.0; H, 5.43; N, 6.58. mp 185-188 °C (dec).

[$PdCl_2$(μ-*N,N*-Probox^{iPr})]$_2$ (2-2). A 100 mL Schlenk flask was charged with $PdCl_2(NCPh)_2$ (1.45 g, 3.78 mmol), attached to a Schlenk manifold, and filled with an argon atmosphere. THF (30 mL) was added via cannula, followed by a THF (20 mL) solution of Probox^{iPr} (1.00 g, 3.77 mmol). The solution changed from deep red to yellow.

The yellow solution was stirred at room temperature for 1 h and then heated at reflux for 18 h. The solvent was removed under vacuum to yield a yellow solid that was then extracted with 3 × 20 mL of toluene. The orange toluene solution was concentrated to ca. 10 mL and cooled to -30 °C. Compound **2-2** was collected after 1 day at -30 °C as a yellow crystalline solid (1.42 g, 1.60 mmol, 84 %). ^{1}H NMR (methylene chloride-d_2, 600 MHz): δ 4.40 (dd, $^{2}J_{HH}$ = 10.2 Hz, $^{3}J_{HH}$ = 9.0 Hz, 4 H, $CH_2(CH_2CNC(CHMe_2)HCH_2O)$, 4.23 (vt, J_{HH} = 8.4 Hz, 4 H, $CH_2(CH_2CNC(CHMe_2)HCH_2O)$, 4.16 (m, 4 H, $CH_2(CH_2CNC(CHMe_2)HCH_2O)$, 3.94 (dt, $^{2}J_{HH}$ = 14.4 Hz, $^{3}J_{HH}$ = 8.4 Hz, 4 H, $CH_2(CH_2CNC(CHMe_2)HCH_2O)$, 2.85 (m, 4 H, $CH_2(CH_2CNC(CHMe_2)HCH_2O)$, 2.62 (m, 4 H, $CH_2(CH_2CNC(CHMe_2)HCH_2O)$, 2.29 (pent, $^{3}J_{HH}$ = 7.8 Hz, 4 H, $CH_2(CH_2CNC(CHMe_2)HCH_2O)$, 1.10 (d, $^{3}J_{HH}$ = 7.2 Hz, 12 H, $CH_2(CH_2CNC(CHMe_2)HCH_2O)$, 1.07 (d, $^{3}J_{HH}$ = 7.3 Hz, 12 H, $CH_2(CH_2CNC(CHMe_2)HCH_2O)$. $^{13}C\{^{1}H\}$ NMR (methylene chloride-d_2, 150 MHz): δ 171.17 ($CH_2(CH_2CNC(CHMe_2)HCH_2O)$, 70.67 ($CH_2(CH_2CNC(CHMe_2)HCH_2O)$, 70.57 ($CH_2(CH_2CNC(CHMe_2)HCH_2O)$, 30.85 ($CH_2(CH_2CNC(CHMe_2)HCH_2O)$, 30.77 ($CH_2(CH_2CNC(CHMe_2)HCH_2O)$, 22.94 ($CH_2(CH_2CNC(CHMe_2)HCH_2O)$, 19.22 ($CH_2(CH_2CNC(CHMe_2)HCH_2O)$, 16.38 ($CH_2(CH_2CNC(CHMe_2)HCH_2O)$. ^{15}N NMR (benzene-$d_6$, 70.9 MHz): δ -277.6. IR (KBr, cm^{-1}): 2952 m, 2925 m, 2871 m, 1650 s (ν_{CN}), 1481 m, 1465 m, 1389 m, 1373 m, 1247 m, 1232 m, 997 m, 952 m. Anal. Calcd. for $C_{30}H_{52}Cl_4N_4O_4Pd_2$: C, 40.6; H, 5.91; N, 6.31. Found C, 40.6; H, 5.97; N, 6.21. mp 174-177 °C (dec).

[RhCl(μ-*N*,*N*-Probox^{Ph})(η^2-C$_8$H$_{14}$)]$_2$ (2-3). A 200 mL Schlenk flask was charged with $[RhCl(\eta^2\text{-}C_8H_{14})_2]_2$ (0.85 g, 1.18 mmol) in the glovebox. The flask was attached to a Schlenk manifold and benzene (90 mL) was added via cannula to give a suspension. A

benzene solution of Probox^{Ph} (0.76 g, 2.27 mmol) was then added via cannula to the stirring rhodium suspension. The mixture was heated to 50 °C to give a brown solution. After 21 h, the brown solution was filtered to remove a precipitate, and the precipitate was extracted with benzene (3 × 15 mL). The solvent was evaporated to afford 0.857 g of **2-3** (0.735 mmol, 65%) as a brown air-sensitive solid. Cooling a toluene solution of **2-3** at -30 °C for two weeks provided X-ray quality crystals. ^{1}H NMR (benzene-d_6, 400 MHz): δ 7.88 (d, $^{3}J_{HH}$ = 7.5 Hz, 4 H, *ortho*-C_6H_5), 7.47 (t, $^{3}J_{HH}$ = 7.5 Hz, 4 H, *meta*-C_6H_5), 7.30 (t, $^{3}J_{HH}$ = 7.5 Hz, 2 H, *para*-C_6H_5), 7.23 (d, $^{3}J_{HH}$ = 7.5 Hz, 4 H, *ortho*-C_6H_5), 7.13 (t, $^{3}J_{HH}$ = 7.5 Hz, 2 H, *para*-C_6H_5) 7.05 (t, $^{3}J_{HH}$ = 7.5 Hz, 4 H, *meta*-C_6H_5), 5.24 (vt, $^{3}J_{HH}$ = 10.5 Hz, 2 H, $CH_2(CH_2CNCPh(H)CH_2O)_2$), 4.61 (br m, 2 H, $CH_2(CH_2CNCPh(H)CH_2O)_2$), 4.53 (br m, 2 H, $CH_2(CH_2CNCPh(H)CH_2O)_2$), 4.33 (vt, $^{3}J_{HH}$ = 10.5 Hz, 2 H, $CH_2(CH_2CNCPh(H)CH_2O)_2$), 3.90 (vt, $^{3}J_{HH}$ = 8.5 Hz, 2 H, $CH_2(CH_2CNCPh(H)CH_2O)_2$), 3.89 (vt, $^{3}J_{HH}$ = 9.0 Hz, 2 H, $CH_2(CH_2CNCPh(H)CH_2O)_2$), 3.77 (vt, $^{3}J_{HH}$ = 9.0 Hz, 2 H, $CH_2(CH_2CNCPh(H)CH_2O)_2$), 3.62 (dd, $^{3}J_{HH}$ = 10.5 Hz, $^{2}J_{HH}$ = 9.0 Hz, 2 H, $CH_2(CH_2CNCPh(H)CH_2O)_2$), 3.10 (br m, 4 H, C_8H_{14}), 2.74 (br m, 2 H, $CH_2(CH_2CNCPh(H)CH_2O)_2$), 2.70 (br m, 2 H, $CH_2(CH_2CNCPh(H)CH_2O)_2$), 2.66 (br m, 2 H, $CH_2(CH_2CNCPh(H)CH_2O)_2$), 2.44 (br m, 2 H, $CH_2(CH_2CNCPh(H)CH_2O)_2$), 1.71 (br m, 8 H, C_8H_{14}), 1.49 (br m, 8 H, C_8H_{14}), 1.24 (br m, 8 H, C_8H_{14}). $^{13}C\{^{1}H\}$ NMR (benzene-d_6, 125 MHz): δ 172.10 ($CH_2(CH_2CNCPh(H)CH_2O)_2$), 169.96 ($CH_2(CH_2CNCPh(H)CH_2O)_2$), 140.24 (*ipso*-$C_6H_5$), 138.92 (*ipso*-$C_6H_5$), 130.93 (*ortho*-$C_6H_5$), 129.81 (*ortho*-$C_6H_5$), 128.92 (*meta*-$C_6H_5$), 128.76 (*meta*-$C_6H_5$), 128.50 (*para*-$C_6H_5$), 128.30 (*para*-$C_6H_5$), 76.21 ($CH_2(CH_2CNCPh(H)CH_2O)_2$), 72.50 ($CH_2(CH_2CNCPh(H)CH_2O)_2$), 71.26 ($CH_2(CH_2CNCPh(H)CH_2O)_2$), 60.67 (d, $^{1}J_{RhC}$ = 16.6 Hz, C_8H_{14}), 33.84 ($CH_2(CH_2CNCPh(H)CH_2O)_2$), 31.41 ($C_8H_{14}$), 30.19 ($CH_2(CH_2CNCPh(H)CH_2O)_2$), 27.81

(C_8H_{14}), 27.14 (C_8H_{14}), 23.26 ($CH_2(CH_2CNCPh(H)CH_2O)_2$), 22.61 ($CH_2(CH_2CNCPh(H)CH_2O)_2$). ^{15}N NMR (benzene-$d_6$, 70.9 MHz): δ -209.9. IR (KBr, cm^{-1}): 3066 m, 3030 m, 2919 m, 2845 m, 1645 s (ν_{CN}), 1455 m, 1379 m, 1232 m, 990 m, 697 m. Anal. Calcd. for $C_{58}H_{72}Cl_2N_4O_4Rh_2$: C, 59.7; H, 6.22; N, 4.81. Found: C, 59.4; H, 5.83; N, 4.98. mp 230-235 °C (dec).

***mer*-(κ^3-*N*,*C*,*N*-Probox^{Me2})RhCl$_2$ (2-4).** Rhodium trichloride hydrate (0.629 g, 2.34 mmol) was dissolved in ethanol (200 mL) and heated to 80 °C. A solution of Probox^{Me2} (0.507 g, 2.13 mmol) in ethanol was added, and this mixture was heated at reflux for 18 h under argon. After cooling to room temperature, the suspension was filtered to remove a black precipitate (Rh metal). The precipitate was extracted with methylene chloride (3 × 20 mL), and the combined ethanol and methylene chloride filtrates were evaporated. Residual ethanol was removed by lyophilization with benzene (2 × 20 mL) to give a reddish-brown solid. The solid was purified by chromatography (silica gel 1" × 5") at 5 °C (using a 3' long jacketed column with an argon inlet and ground glass joint on the collection end of the column) under an argon atmosphere. The desired *mer*-(κ^3-*N*,*C*,*N*-Probox^{Me2})RhCl$_2$ was collected with methylene chloride:2-propanol (200:1) as a yellow band. After removing the solvent under vacuum, **2-4** was isolated as a yellow-orange solid 0.030 g (0.07 mmol, 3.4%). A solution of **2-4** in methylene chloride was cooled to -30 °C for one week to provide X-ray quality crystals of water adduct, **2-5**. ^{1}H NMR (chloroform-d_1, 600 MHz): δ 5.85 (m, 1 H, RhC*H*($CH_2CNCMe_2CH_2O)_2$), 4.25 (d, $^2J_{HH}$ = 8.4 Hz, 2 H, RhCH($CH_2CNCMe_2CH_2O)_2$), 4.18 (d, $^2J_{HH}$ = 8.4 Hz, 2 H, RhCH($CH_2CNCMe_2CH_2O)_2$), 3.28 (dd, $^2J_{HH}$ = 16.8 Hz, $^3J_{HH}$ = 10.2 Hz, 2 H, RhCH($CH_2CNCMe_2CH_2O)_2$), 2.10 (dd, $^2J_{HH}$ = 17.4 Hz, $^3J_{HH}$ = 6.0 Hz, 2 H, RhCH($CH_2CNCMe_2CH_2O)_2$), 1.47 (s, 6 H, RhCH($CH_2CNCMe_2CH_2O)_2$), 1.44 (s, 6 H,

RhCH($CH_2CNCMe_2CH_2O$)$_2$). $^{13}C\{^1H\}$ NMR (chloroform-d_1, 150 MHz): δ 171.61 (d, $^2J_{RhC}$ = 3.15 Hz, RhCH($CH_2CNCMe_2CH_2O$)$_2$), 82.00 (RhCH($CH_2CNCMe_2CH_2O$)$_2$), 67.09 (RhCH($CH_2CNCMe_2CH_2O$)$_2$), 38.08 (RhCH($CH_2CNCMe_2CH_2O$)$_2$), 27.93 (d, $^1J_{RhC}$ = 25.7 Hz, Rh*C*H($CH_2CNCMe_2CH_2O$)$_2$), 27.84 (RhCH(CH_2CNC*Me*$_2CH_2O$)$_2$), 27.39 (RhCH(CH_2CNC*Me*$_2CH_2O$)$_2$). ^{15}N NMR (methylene chloride-d_2, 70.9 MHz): δ -211.9 (d, $^1J_{RhN}$ = 24 Hz). IR (KBr, cm^{-1}): 2966 m, 2923 m, 2902 m, 1656 s (ν_{CN}), 1390 m, 1394 m, 1328 m, 1259 m, 1201 m, 1002 m, 800 m. Anal. Calcd. for $C_{13}H_{21}Cl_2N_2O_2Rh$: C, 38.0; H, 5.15; N, 6.81. Found: C, 38.0; H, 4.85; N, 6.62. mp 213-215 °C (dec).

***fac*-(κ^3-*N,N,C*-Probox^{Me2})RhCl$_2$(PMe$_3$) (2-6).** *mer*-(κ^3-*N,C,N*-Probox^{Me2})$RhCl_2$ (**2-4**) (0.025 g, 0.06 mmol) was placed in a vial in the glovebox and dissolved in THF (10 mL). Trimethylphosphine (0.007 mL, 0.07 mmol) was added, and the solution was stirred at room temperature for 1 h. The solvent was removed under vacuum to yield *fac*-(κ^3-*N,C,N*-Probox^{Me2})RhCl$_2$(PMe$_3$) as a yellow solid (0.026 g, 0.053 mmol, 87%). ^1H NMR (methylene chloride-d_2, 400 MHz): δ 4.23 (d, $^2J_{HH}$ = 8.0 Hz, 1 H, *trans-exo*-RhCH($CH_2CNCMe_2CH_2O$)$_2$), 4.18 (d, $^2J_{HH}$ = 8.4 Hz, 1 H, *cis-endo*-RhCH($CH_2CNCMe_2CH_2O$)$_2$), 4.12 (d, $^2J_{HH}$ = 8.4 Hz, 1 H, *cis-exo*-RhCH($CH_2CNCMe_2CH_2O$)$_2$), 4.00 (d, $^2J_{HH}$ = 8.0 Hz, 1 H, *trans-endo*-RhCH($CH_2CNCMe_2CH_2O$)$_2$), 3.23 (dd, $^2J_{HH}$ = 18.4 Hz, $^3J_{HH}$ = 9.2 Hz, 1H, *trans-endo*-RhCH($CH_2CNCMe_2CH_2O$)$_2$), 3.00 (m, 1 H, RhC*H*($CH_2CNCMe_2CH_2O$)$_2$), 2.84 (dd, $^2J_{HH}$ = 18.8 Hz, $^3J_{HH}$ = 9.6 Hz, 1 H, *cis-exo*-RhCH($CH_2CNCMe_2CH_2O$)$_2$), 2.16 (d, $^2J_{HH}$ = 17.6 Hz, 1 H, *cis-endo*-RhCH($CH_2CNCMe_2CH_2O$)$_2$), 2.12 (d, $^2J_{HH}$ = 18.4 Hz, 1 H, *trans-exo*-RhCH($CH_2CNCMe_2CH_2O$)$_2$), 1.65 (s, 3 H, *trans-endo*-RhCH(CH_2CNC*Me*$_2CH_2O$)$_2$), 1.60 (s, 3 H, *cis-exo*-RhCH(CH_2CNC*Me*$_2CH_2O$)$_2$), 1.58 (s, 3 H, *trans-exo*-RhCH(CH_2CNC*Me*$_2CH_2O$)$_2$), 1.55 (s, 3 H, *cis-endo*-RhCH(CH_2CNC*Me*$_2CH_2O$)$_2$), 1.50 (d,

$^{2}J_{PH}$ = 11.2 Hz, 9H, P*Me*$_3$). $^{13}C\{^{1}H\}$ NMR (methylene chloride-d_2, 100 MHz): δ 176.26 (d, $^{2}J_{RhC}$ = 4.3 Hz, *cis*-RhCH(CH$_2$*C*NCMe$_2$CH$_2$O)$_2$), 175.22 (vt, $^{2}J_{RhC}$ = 5.8 Hz, $^{3}J_{PC}$ = 2.7 Hz, *trans*-RhCH(CH$_2$*C*NCMe$_2$CH$_2$O)$_2$), 83.15 (*cis*-RhCH(CH$_2$CNCMe$_2$*C*H$_2$O)$_2$), 82.54 (d, *J* = 4.3 Hz, *trans*-RhCH(CH$_2$CNCMe$_2$*C*H$_2$O)$_2$), 70.87 (d, *J* = 4.0 Hz, *trans*-RhCH(CH$_2$CN*C*Me$_2$CH$_2$O)$_2$), 68.78 (d, *J* = 1.0 Hz, *cis*-RhCH(CH$_2$CN*C*Me$_2$CH$_2$O)$_2$), 40.70 (*cis*-RhCH(*C*H$_2$CNCMe$_2$CH$_2$O)$_2$), 40.22 (*trans*-RhCH(*C*H$_2$CNCMe$_2$CH$_2$O)$_2$), 30.19 (*cis-endo*-RhCH(CH$_2$CNC*Me$_2$*CH$_2$O)$_2$), 28.88 (*trans-exo*-RhCH(CH$_2$CNC*Me$_2$*CH$_2$O)$_2$), 28.16 (*trans-endo*-RhCH(CH$_2$CNC*Me$_2$*CH$_2$O)$_2$), 27.64 (*cis-exo*-RhCH(CH$_2$CNC*Me$_2$*CH$_2$O)$_2$), 18.94 (dd, $^{1}J_{RhC}$ = 21.2 Hz, $^{2}J_{PC}$ = 7.7 Hz, Rh*C*H(CH$_2$CNCMe$_2$CH$_2$O)$_2$), 15.45 (d, $^{1}J_{PC}$ = 36.0 Hz, P*Me*$_3$). ^{15}N NMR (methylene chloride-d_2, 71 MHz): δ -178.2 (d, $^{2}J_{PN}$ = 104 Hz, *N-trans* to PMe$_3$), -207.3 (s, *N-trans* to Cl). $^{31}P\{^{1}H\}$ NMR (methylene chloride-d_2, 161.9 MHz): δ 9.53 (d, $^{1}J_{RhP}$ = 129 Hz). IR (KBr, cm^{-1}): 2967 m, 2909 m, 1653 s (ν_{CN}), 1465 m, 1419 m, 1378 m, 1261 m, 1200 m, 1181 m, 981 m, 957 s. Anal. Calcd. for $C_{16}H_{30}Cl_2N_2O_2PRh(C_6H_6)_{0.5}$: C, 43.4; H, 6.32; N, 5.32. Found: C, 43.4; H, 5.83; N, 4.98. mp 215-218 °C (dec).

References

1. Jensen, C.; Morales-Morales, D., *The Chemistry of Pincer Compounds*. Elsevier: Amsterdam, **2007**.
2. Shaw, B. L.; Moulton, C. J., *J. Chem. Soc., Dalton Trans.* **1976**, 1020-1024.
3. Donkervoort, J. G.; Jastrzebski, J. T. B. H.; Deelman, B.-J.; Kooijman, H.; Veldman, N.; Spek, A. L.; van Koten, G., *Organometallics* **1997,** *16* (19), 4174-4184.
4. Weng, W.; Yang, L.; Foxman, B. M.; Ozerov, O. V., *Organometallics* **2004,** *23* (20), 4700-4705.
5. Brandts, J. A. M.; Gossage, R. A.; Boersma, J.; Spek, A. L.; van Koten, G., *Organometallics* **1999,** *18* (14), 2642-2648.
6. Brandts, J. A. M.; Kruiswijk, E.; Boersma, J.; Spek, A. L.; van Koten, G., *J. Organomet. Chem.* **1999,** *585* (1), 93-99.
7. Contel, M.; Stol, M.; Casado, M. A.; van Klink, G. P. M.; Ellis, D. D.; Spek, A. L.; van Koten, G., *Organometallics* **2002,** *21* (21), 4556-4559.
8. Donkervoort, J. G.; Vicario, J. L.; Jastrzebski, J. T. B. H.; van Koten, G.; Cahiez, G., *Recueil des Travaux Chimiques des Pays-Bas* **1996,** *115* (11-12), 547-548.

9. Vila, J.; Gayoso, M.; Pereira, M. T.; López Torres, M.; Fernández, J. J.; Fernández, A.; Ortigueira, J. M., *J. Organomet. Chem.* **1996,** *506* (1–2), 165-174.
10. Rietveld, M. H. P.; Nagelholt, L.; Grove, D. M.; Veldman, N.; Spek, A. L.; Rauch, M. U.; Herrmann, W. A.; van Koten, G., *J. Organomet. Chem.* **1997,** *530* (1–2), 159-167.
11. de Koster, A.; Kanters, J. A.; L., S. A.; van der Zeuden, A. A. H.; van Koten, G.; Vrieze, K., *Acta Crystallogr., Sect. C* **1985,** *41*, 893-895.
12. Beley, M.; Chodorowski-Kimmes, S.; Collin, J.-P.; Lainé, P.; Launay, J.-P.; Sauvage, J.-P., *Angew. Chem., Int. Ed. Engl.* **1994,** *33* (17), 1775-1778.
13. Beley, M.; Collin, J. P.; Sauvage, J. P., *Inorg. Chem.* **1993,** *32* (21), 4539-4543.
14. Çelenligil-Çetin, R.; Watson, L. A.; Guo, C.; Foxman, B. M.; Ozerov, O. V., *Organometallics* **2004,** *24* (2), 186-189.
15. van der Boom, M. E.; Kraatz, H.-B.; Hassner, L.; Ben-David, Y.; Milstein, D., *Organometallics* **1999,** *18* (19), 3873-3884.
16. Gauvin, R. M.; Rozenberg, H.; Shimon, L. J. W.; Milstein, D., *Organometallics* **2001,** *20* (9), 1719-1724.
17. van der Boom, M. E.; Milstein, D., *Chem. Rev.* **2003,** *103* (5), 1759-1792.
18. Albrecht, M.; van Koten, G., *Angew. Chem., Int. Ed. Engl.* **2001,** *40* (20), 3750-3781.
19. Steenwinkel, P.; Gossage, R. A.; van Koten, G., *Chem. -Eur. J.* **1998,** *4* (5), 759-762.
20. Motoyama, Y.; Okano, M.; Narusawa, H.; Makihara, N.; Aoki, K.; Nishiyama, H., *Organometallics* **2001,** *20* (8), 1580-1591.
21. Motoyama, Y.; Kawakami, H.; Shimozono, K.; Aoki, K.; Nishiyama, H., *Organometallics* **2002,** *21* (16), 3408-3416.
22. Gerisch, M.; Krumper, J. R.; Bergman, R. G.; Tilley, T. D., *J. Am. Chem. Soc.* **2001,** *123* (24), 5818-5819.
23. Gerisch, M.; Krumper, J. R.; Bergman, R. G.; Tilley, T. D., *Organometallics* **2003,** *22*, 47-58.
24. Steenwinkel, P.; Gossage, R. A.; Maunula, T.; Grove, D. M.; van Koten, G., *Chem. -Eur. J.* **1998,** *4* (5), 763-768.
25. Poverenov, E.; Gandelman, M.; Shimon, L. J. W.; Rozenberg, H.; Ben-David, Y.; Milstein, D., *Organometallics* **2005,** *24* (6), 1082-1090.
26. Poverenov, E.; Leitus, G.; Shimon, L. J. W.; Milstein, D., *Organometallics* **2005,** *24* (24), 5937-5944.
27. Al-Salem, N. A.; Empsall, H. D.; Markham, R.; Shaw, B. L.; Weeks, B., *J. Chem. Soc., Dalton Trans.* **1979**, 1972-1982.
28. Grove, D. M.; Van Koten, G.; Ubbels, H. J. C.; Zoet, R.; Spek, A. L., *Organometallics* **1984,** *3* (7), 1003-1009.
29. Van Beek, J. A. M.; Van Koten, G.; Ramp, M. J.; Coenjaarts, N. C.; Grove, D. M.; Goubitz, K.; Zoutberg, M. C.; Stam, C. H.; Smeets, W. J. J.; Spek, A. L., *Inorg. Chem.* **1991,** *30* (15), 3059-3068.
30. Sutter, J.-P.; James, S. L.; Steenwinkel, P.; Karlen, T.; Grove, D. M.; Veldman, N.; Smeets, W. J. J.; Spek, A. L.; van Koten, G., *Organometallics* **1996,** *15* (3), 941-948.
31. Van der Zeijden, A. A. H.; Van Koten, G.; Luijk, R.; Nordemann, R. A.; Spek, A. L., *Organometallics* **1988,** *7* (7), 1549-1556.

32. Kleij, A. W.; Gossage, R. A.; Klein Gebbink, R. J. M.; Brinkmann, N.; Reijerse, E. J.; Kragl, U.; Lutz, M.; Spek, A. L.; van Koten, G., *J. Am. Chem. Soc.* **2000,** *122* (49), 12112-12124.
33. Grove, D. M.; Van Koten, G.; Louwen, J. N.; Noltes, J. G.; Spek, A. L.; Ubbels, H. J. C., *J. Am. Chem. Soc.* **1982,** *104* (24), 6609-6616.
34. Terheijden, J.; Van Koten, G.; Muller, F.; Grove, D. M.; Vrieze, K.; Nielsen, E.; Stam, C. H., *J. Organomet. Chem.* **1986,** *315* (3), 401-417.
35. Van der Zeijden, A. A. H.; Van Koten, G., *Inorg. Chem.* **1986,** *25* (26), 4723-4725.
36. Van der Zeijden, A. A. H.; Van Koten, G.; Nordemann, R. A.; Kojic-Prodic, B.; Spek, A. L., *Organometallics* **1988,** *7* (9), 1957-1966.
37. John T, S., *Tetrahedron* **2003,** *59* (11), 1837-1857.
38. Kanzelberger, M.; Zhang, X.; Emge, T. J.; Goldman, A. S.; Zhao, J.; Incarvito, C.; Hartwig, J. F., *J. Am. Chem. Soc.* **2003,** *125* (45), 13644-13645.
39. Zhao, J.; Goldman, A. S.; Hartwig, J. F., *Science* **2005,** *307* (5712), 1080-1082.
40. Wallner, O. A.; Olsson, V. J.; Eriksson, L.; Szabó, K. J., *Inorg. Chim. Acta* **2006,** *359* (6), 1767-1772.
41. Gorla, F.; Togni, A.; Venanzi, L. M.; Albinati, A.; Lianza, F., *Organometallics* **1994,** *13* (5), 1607-1616.
42. Longmire, J. M.; Zhang, X.; Shang, M., *Organometallics* **1998,** *17* (20), 4374-4379.
43. Albrecht, M.; Kocks, B. M.; Spek, A. L.; van Koten, G., *J. Organomet. Chem.* **2001,** *624* (1–2), 271-286.
44. Gosiewska, S.; Veld, M. H. i. t.; de Pater, J. J. M.; Bruijnincx, P. C. A.; Lutz, M.; Spek, A. L.; van Koten, G.; Klein Gebbink, R. J. M., *Tetrahedron Asymmetry* **2006,** *17* (4), 674-686.
45. Soro, B.; Stoccoro, S.; Minghetti, G.; Zucca, A.; Cinellu, M. A.; Manassero, M.; Gladiali, S., *Inorg. Chim. Acta* **2006,** *359* (6), 1879-1888.
46. Williams, B. S.; Dani, P.; Lutz, M.; Spek, A. L.; van Koten, G., *Helv. Chim. Acta* **2001,** *84* (11), 3519-3530.
47. Takenaka, K.; Minakawa, M.; Uozumi, Y., *J. Am. Chem. Soc.* **2005,** *127* (35), 12273-12281.
48. Medici, S.; Gagliardo, M.; Williams, S. B.; Chase, P. A.; Gladiali, S.; Lutz, M.; Spek, A. L.; van Klink, G. P. M.; van Koten, G., *Helv. Chim. Acta* **2005,** *88* (3), 694-705.
49. Motoyama, Y.; Makihara, N.; Mikami, Y.; Aoki, K.; Nishiyama, H., *Chemistry Letters* **1997,** *26* (9), 951-952.
50. Motoyama, Y.; Shimozono, K.; Aoki, K.; Nishiyama, H., *Organometallics* **2002,** *21* (8), 1684-1696.
51. Jun-ichi Ito, T. S. H. N., *Adv. Synth. Catal.* **2006,** *348* (10-11), 1235-1240.
52. Nishiyama, H., *Chem. Soc. Rev.* **2007,** *36*, 1133-1141.
53. Krumper, J. R.; Gerisch, M.; Suh, J. M.; Bergman, R. G.; Tilley, T. D., *J. Org. Chem.* **2003,** *68* (25), 9705-9710.
54. Canty, A. J.; Patel, J.; Skelton, B. W.; White, A. H., *J. Organomet. Chem.* **2000,** *607* (1-2), 194-202.
55. Bolm, C.; Weickhardt, K.; Zehnder, M.; Ranff, T., *Chem. Ber.* **1991,** *124* (5), 1173-1180.

56. Crocker, C.; Errington, R. J.; McDonald, W. S.; Odell, K. J.; Shaw, B. L.; Goodfellow, R. J., *J. Chem. Soc., Chem. Commun.* **1979,** *J. Chem. Soc., Chem Commun.*, 498-499.
57. Crocker, C.; Empsall, H. D.; Errington, R. J.; Hyde, E. M.; Mcdonald, W. S.; Markham, R.; Norton, M. C.; Shaw, B. L.; Weeks, B., *J. Chem. Soc., Dalton Trans.* **1982**, 1217.
58. Errington, R. J.; McDonald, W. S.; Shaw, B. L., *J. Chem. Soc., Dalton Trans.* **1982**, 1829-1835.
59. Seligson, A. L.; Trogler, W. C., *Organometallics* **1993,** *12* (3), 738-743.
60. Seligson, A. L.; Trogler, W. C., *Organometallics* **1993,** *12* (3), 744-751.
61. Cornejo, A.; Fraile, J. M.; Garcia, J. I.; Gil, M. J.; Martinez-Merino, V.; Mayoral, J. A.; Pires, E.; Villalba, I., *Synlett* **2005,** *15*, 2321-2324.
62. Bucher, U. E.; Fassler, T. F.; Hunzinker, M.; Nesper, R.; Ruegger, H.; Venanzi, L. M., *Gazz. Chim. Ital.* **1995,** *125* (4), 181-188.
63. Bucher, U. E.; Currao, A.; Nesper, R.; Rueegger, H.; Venanzi, L. M.; Younger, E., *Inorg. Chem.* **1995,** *34* (1), 66-74.
64. Carole Foltz, M. E., Stéphane Bellemin-Laponnaz, Hubert Wadepohl, Lutz H. Gade,, *Chem. -Eur. J.* **2007,** *13* (21), 5994-6008.
65. Baird, B.; Pawlikowski, A. V.; Su, J.; Wiench, J. W.; Pruski, M.; Sadow, A. D., *Inorg. Chem.* **2008,** *47* (22), 10208-10210.
66. Molander, G. A.; Burke, J. P.; Carroll, P. J., *J. Org. Chem.* **2004,** *69* (23), 8062-8069.
67. Samar, D.; Fortin, J.-F.; Fortin, D.; Decken, A.; Harvey, P. D., *Journal of Inorganic and Organometallic Polymers and Materials* **2005,** *15* (4), 411-429.
68. Hiraki, K.; Fuchita, Y.; Matsumoto, Y., *Chem. Lett.* **1984**, 1947-1948.
69. Pazderski, L.; Toušek, J.; Sitkowski, J.; Kozerski, L.; Marek, R.; Szłyk, E., *Magn. Reson. Chem.* **2007,** *45* (1), 24-36.
70. Otting, G.; Messerle, B. A.; Soler, L. P., *J. Am. Chem. Soc.* **1997,** *119* (23), 5425-5434.
71. Witanowski, M.; Stefaniak, L.; Webb, G. A., *Ann. Rep. NMR Spectrosc.* Academic Press: London, **1993**; Vol. 25.

Chapter 3: Optically active, bulky tris(oxazolinyl)borato magnesium and calcium compounds for asymmetric hydroamination/cyclization

Modified from a paper published in *Journal of Organometallic Chemistry*[*]

Steven R. Neal, Arkady Ellern, Aaron D. Sadow

Department of Chemistry, Iowa State University, Ames, IA 50011, USA

Abstract

The synthesis of the new chiral, pseudo-C_3-symmetric, monoanionic ligand tris(4*S*-*tert*-butyl-2-oxazolinyl)phenylborate $[To^T]^-$ is reported. The steric bulk, tridentate coordination, and anionic charge of $[To^T]^-$ are suitable for formation of complexes of the type To^TMX, where one valence is available for reactivity. With this point in mind, we prepared magnesium and calcium To^T complexes that resist redistribution to $(To^T)_2M$ compounds. Both To^TMgMe and $To^TCaC(SiHMe_2)_3$ contain tridentate To^T-coordination to the metal center, as shown by NMR spectroscopy, infrared spectroscopy, and X-ray crystallography. These compounds are active catalysts for the cyclization of three aminoalkenes to pyrrolidines, and provide non-racemic mixtures of pyrrolidines in enantiomeric excesses up to 36%.

Introduction

Group 2 organometallic compounds have potential advantages in homogeneous catalysis, as organomagnesium and organocalcium compounds are inexpensive, their

---

[*] Reprinted from *J. Organomet. Chem.*, *696*, Neal, S. R.; Ellern, A.; Sadow, A. D., Optically active, bulky tris(oxazolinyl)borato magnesium and calcium compounds for asymmetric hydroamination/cyclization, 228-234, *Copyright 2011 with permission from Elsevier*.

starting materials are readily available, both metals are physiologically benign, and techniques for their manipulation are typically similar to those developed for Grignard reagents. However, their ionic bonding, facile configurational and structural exchange reactions, and thermodynamic stability of oxide and halide salts due to high lattice energies are particular challenges that inhibit the application of group 2 metal compounds in catalysis.

In this regard, the discovery by Parkin and co-workers that tris(pyrazolyl)borato magnesium(II) compounds are resistant toward disproportionation reactions and provide compounds with well-defined coordination constitutions and geometries offers opportunities for organomagnesium compounds in catalysis.[1-4] Later, Chisholm reported achiral C_{3v} and chiral C_3-symmetric tris(pyrazolyl)borato magnesium(II) catalysts for lactide ring-opening polymerization.[5] More recently, magnesium and calcium *β*-diketiminate compounds (e.g. {nacnac}MR) have been shown to be highly active in hydroamination/cyclization of aminoalkenes[6-9] where sterically demanding substituents on the *β*-diketiminate ligands hinder the formation of bis(diketiminate)magnesium and calcium complexes.[10] Additionally, interesting zwitterionic bis (carbene)-[11-14] and tris(carbene)borato alkaline earth metal compounds have been reported and applied in hydroamination/cyclization.[15-17] At the time of publication, a few reports of stereoselective hydroamination with calcium and magnesium based catalysts have provided % ee's up to 6% and 14%, respectively.[18-19] Recently, Hultzsch and co-workers have reported a phenoxyamine magnesium catalyst capable of cyclizing aminoalkenes with % ee's up to 90%.[20]

Recent reports form our group describe the synthesis of the achiral monoanionic tris(4,4-dimethyl-2-oxazolinly)phenylborate $[To^M]^-$ and its chemistry in zirconium,[21]

iridium, aluminum, and yttrium complexes,[22-24] where the latter yttrium species is a catalyst for the hydroamination/cyclization of aminoalkenes to pyrrolidines.[25-26]

These tridentate monoanionic ligands are electronically similar to the well-known tris(pyrazolyl)borate ligands.[27-28] The tridentate monoanionic oxazolinylborate ligands also may be compared to Gade's neutral tridentate tris(oxazolinyl)ethane ligands (trisox)[29-30] whereas the anionic borate center in the tris(oxazolinyl)borates provides an additional electrostatic component to their interaction with metal centers. Compounds with the formula$[\{trisox\}LnR]^{2+}$ (Ln = Sc, Y, Lu, Tm, Er, Ho, Dy) generated in situ from $\{trisox\}LnR_3$ and $[Ph_3C][B(C_6F_5)_4]$, are catalysts for stereospecific polymerization of α-olefins.[31-33] Neutral tris(oxazolinyl)borate compounds of divalent metal centers, such as magnesium, calcium, and zinc, are isoelectronic with the putative dicationic trisox rare earth alkyls and might provide reactive complexes. In this context, we recently described a series of achiral tris(oxazolinyl)borato zinc compounds containing chloride, hydride, alkoxide, and disilazide ligands.[34] Tris(oxazolinyl)borato magnesium and calcium compounds could behave similarly, and provide robust compounds that might still access open coordination sites for chemical reactivity. Here we report the synthesis of tris(4*S*-*tert*-butyl-2-oxazolinyl)phenylborate $[To^T]^-$, its complexes with magnesium(II) and calcium(II), and their reactivity as catalysts for the hydroamination/cyclization of aminoalkenes.

Results and Discussion

Ligand synthesis

The preparation of $Li[To^M]$ involves the in situ deprotonation of 2-H-4,4-dimethyl-2-oxazoline with *n*-butyllithium followed by the addition of 0.30 equivalents of $PhBCl_2$ (Eq. 3-1).[21]

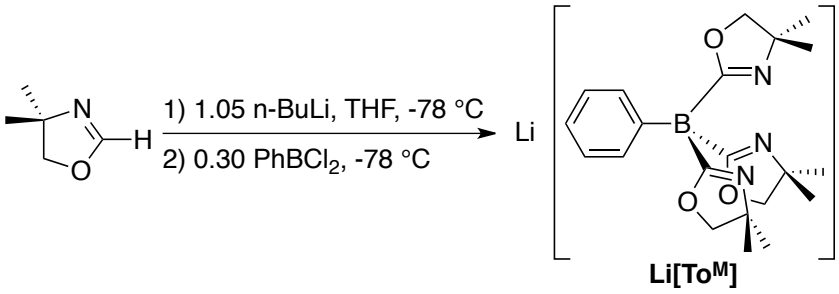

(Eq. 3-1)

A chiral analog of Li[To^{M}], tris(4*S*-isopropyl-2-oxazolinyl)phenylborate [To^{P}]$^{-}$,[35] has also been prepared. However, unlike the synthesis of Li[To^{M}], the one-pot synthesis of Li[To^{P}] is not successful because 2-H-4*S*-isopropyl-oxazoline is not completely deprotonated with *n*-butyllithium.[36-37] Deprotonation of 2-H-4*S*-isopropyl-oxazoline with LiN(SiMe$_3$)$_2$ provides 2-Li-4*S*-isopropyl-oxazolide in good yield; treating the isolated oxazolide with 0.31 equivalents of PhBCl$_2$ gives Li[To^{P}] in 92% yield (Eq. 3-2).[35] It is evident that each tris(oxazolinyl)phenylborate ligand will likely require optimization to achieve good yields rather than follow a generic synthetic scheme. This optimization is markedly different from the synthesis of similar bis(oxazolinyl)borates described by Pfaltz that are prepared by the in situ reaction of 2-H-oxazolines, *tert*-butyllithium, and Ph$_2$BCl.[38-39]

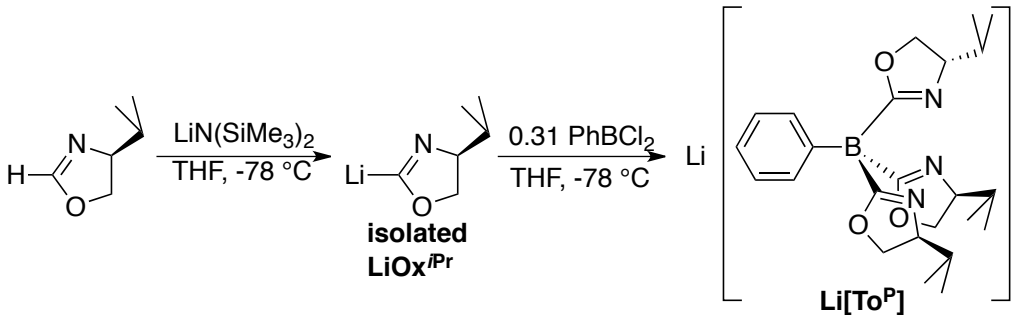

(Eq. 3-2)

Reactions of 2-H-4*S*-*tert*-butyl-oxazoline and $LiN(SiMe_3)_2$ provide 2-Li-4*S*-*tert*-butyl-oxazolide (**LiOx^{tBu}**, (Eq. 3-3) in quantitative yield in micromolar scale reactions. The IR spectrum of LiOx^{tBu} (KBr) contains both isocyanide (2000 cm^{-1}) and oxazolide (1635 cm^{-1}) bands, which is consistent with previous reports with 2-lithio-4,4-dimethyl-oxazolide and 4*S*-isopropyl-2-lithio-oxazolide.[35, 40] Unlike the deprotonation of LiOx^{iPr}, isolation of LiOx^{tBu} from the $HN(SiMe_3)_2$ byproduct proves difficult because the latter is highly soluble in hydrocarbon and ethereal solvents. The difference in solubility between 4*S*-*tert*-butyl-oxazolide and 4*S*-isopropyl- or 4,4-dimethyl-oxazolides is puzzling. THF could be coordinating to the *tert*-butyl-oxazolide, thus increasing the solubility; however, no evidence of such interaction is observed in the ^1H NMR spectrum. A sample of LiOx^{tBu} is reacted with methanol-d_4 as solvent, and the NMR spectrum of the resulting 2-D-4*S*-*tert*-butyl-oxazoline contains no resonances attributed to diethyl ether or THF. Likewise, no resonances corresponding to coordinated or free THF are present in the NMR spectrum of LiOx^{tBu} in benzene-d_6, and the addition of THF-d_8 to the benzene-d_6 sample of LiOx^{tBu} does not affect a change in the chemical shift of the oxazolide resonances. The ^7Li NMR spectrum of LiOx^{tBu} contains one resonance (1.22 ppm) in benzene-d_6 and does not shift upon addition of THF.

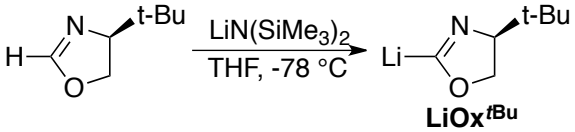

(Eq. 3-3)

The high solubility of LiOx^{tBu} is in sharp contrast to 2-Li-4,4-dimethyl-oxazolide (**LiOx^{Me2}**) and 2-Li-4*S*-isopropyl-oxazolide (**LiOx^{iPr}**) that, once isolated, are insoluble in hydrocarbons, diethyl ether, and THF. Isolated LiOx^{Me2} is not useful in the preparation of Li[To^M], while the addition of $PhBCl_2$ to a THF suspension of LiOx^{iPr} does yield Li[To^P].

Unfortunately, the high solubility of LiOx^{tBu} makes its use as a precursor for Li[To^{T}] impossible because the procedure for isolating LiOx^{iPr} from the deprotonation byproduct, $HN(SiMe_3)_2$, involves repeated washing of the oxazolide with diethyl ether. Additionally, neither repeated crystallizations nor exposure to high vacuum (10^{-5} Torr) for extended times (2 days) is successful in improving the purity of LiOx^{tBu}.

A one-pot procedure for the synthesis of lithium tris(4*S*-*tert*-butyl-2-oxazolinyl)phenyl borate (**Li[To^{T}]**) requires deprotonation of 2-H-4*S*-*tert*-butyl-oxazoline with *tert*-butyllithium at -78 °C then adding 0.31 equivalents of $PhBCl_2$ (Eq. 3-4). A single ^{11}B resonance at -17.0 ppm in methanol-d_4 is consistent with the formation of a four-coordinate borate. The ^{1}H NMR spectrum of crude Li[To^{T}] is consistent with a pseudo-C_3-symmetric species due to the presence of one set of oxazoline resonances at 0.86 (CH_3), 3.75 (CH), and 3.89 ppm (CH_2). The syntheses of Li[To^{M}] and Li[To^{P}] require a 26-hour reaction time while full conversion of LiOx^{tBu} to Li[To^{T}] requires a significantly increased reaction time (72 hours). This increased reaction time is needed due to the increased steric bulk of the 4-S-*tert*-butyl group on the oxazoline ring compared to the 4,4-dimethyl or 4*S*-isopropyl substituents on the oxazoline rings in Li[To^{M}] and Li[To^{P}] respectively. It is evident that the yield of in situ generated LiOx^{tBu}, obtained from deprotonation of 2H-4*S*-*tert*-buyl-oxazoline with *tert*-butyllithium, is much improved compared to the in situ generated LiOx^{iPr}.[36-37] Apparently, the formation of a quaternary borate with three boron–oxazoline bonds requires pure oxazolide anion and cannot tolerate the lower yield of LiOx^{iPr} (via in situ deprotonation) or small amounts of $HN(SiMe_3)_2$ byproduct. A pure sample of Li[To^{T}] suitable for combustion analysis could not be isolated due to contamination by LiCl. During the synthesis of Li[To^{M}], removal of the reaction solvent, THF, followed by extraction with hot toluene provides an analytically

pure species; however, this extraction technique was not suitable for Li[To^T] due to its high solubility and coordination of LiCl.

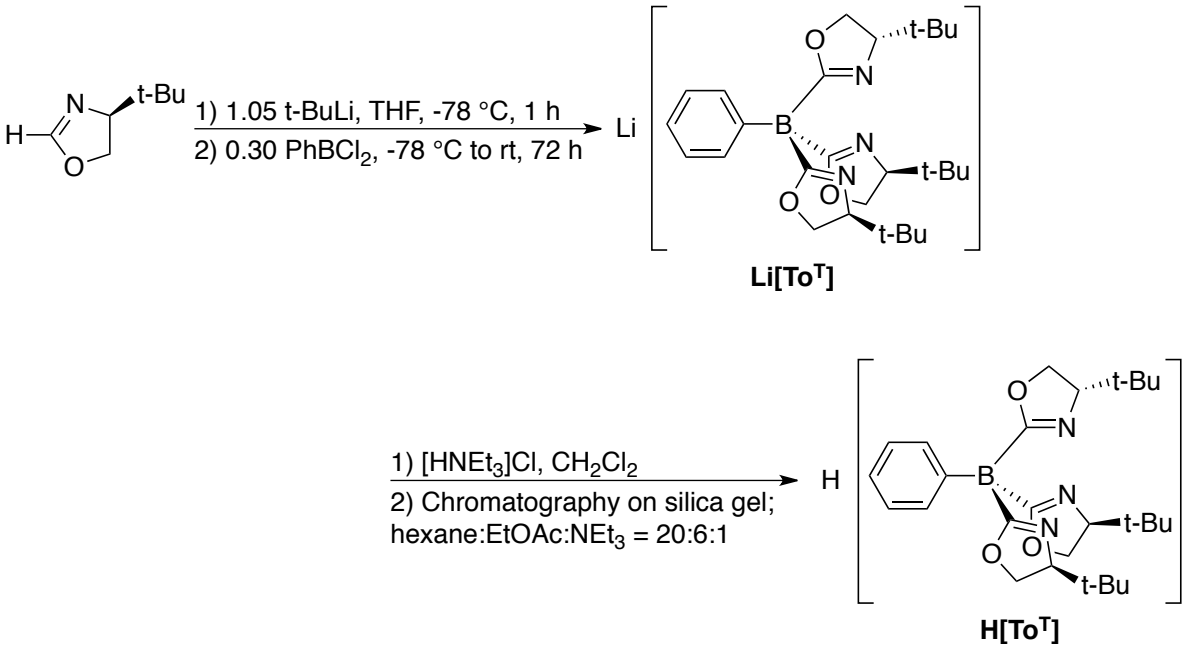

(Eq. 3-4)

A crude sample of Li[To^T] (contaminated with LiCl) is treated with triethylammonium chloride in methylene chloride to provide hydrogen tris(4*S*-*tert*-butyl-2-oxazolinyl)phenyl borate (**H[To^T]**) after filtration through a short plug of grade-III neutral alumina (Eq. 3-4). Analytically pure H[To^T] is isolated after silica gel column chromatography. The four-coordinate borate structure is maintained as evidenced by a single resonance in the ^{11}B NMR spectrum at -16.5 ppm. The ^{1}H NMR spectrum of H[To^T] is consistent with a single diastereomeric species with pseudo-C_3 symmetry in solution (benzene-d_6) due to the presence of three oxazoline resonances at 0.80 (CH_3), 3.44 (CH), and 3.78 ppm (CH_2).

The presence of only one ν_{CN} band at 1601 cm^{-1} indicates that H[To^M] is also pseudo-C_{3v} symmetric in the solid state. This is an interesting contradiction to the solid

state structure of H[To^{M}], the analogous protonated form of Li[To^{M}], which exhibits two ν_{CN} bands (1627, 1594 cm^{-1}) in the IR spectrum. Analysis of a single crystal X-ray diffraction study shows the presence of two coplanar oxazoline rings in a geometry consistent with coordination to a proton (not observable in an X-ray diffraction study) with the third oxazoline ring rotated away from the indicated proton.[21] The origination of this difference is unknown but likely a result of steric interactions between the substituents at the 4-position of the oxazoline ring. Similar to H[To^{T}], the IR spectrum of H[To^{P}] contains only one ν_{CN} band at 1594 cm^{-1} in the solid state indicating all three oxazoline rings are equivalent. As was observed in [To^{P}]$^{-}$ chemistry, the oxazoline groups in *S,S,S*-H[To^{T}] are optically pure because small amounts of 4*R*-*tert*-buyl-oxazoline would give diastereomers (e.g. *S,S,R*) that would have a ^{1}H NMR spectrum that is distinct from the *S,S,S*-H[To^{T}] diastereomer.

The attempted synthesis of a chiral tris(oxazolinyl)phenylborate bearing a phenyl group on the oxazoline ring, tris(4*R*-phenyl-2-oxazolinyl)phenylborate (**Li[To^{Ph}]**) began with isolation of the corresponding 2-Li-4*R*-phenyl-oxazolide (**LiOx^{Ph}**). Deprotonating 2-H-4*R*-phenyl-oxazoline[40] with LiN(SiMe$_3$)$_2$ provides LiOx^{Ph} in quantitative yield on micromolar scale. Unfortunately, the solubility of LiOx^{Ph} is very similar to the solubility of LiOx^{tBu} and isolation from the HN(SiMe$_3$)$_2$ byproduct is not successful. Additionally, in situ deprotonation of 2-H-4*R*-phenyl-oxazoline with *n*-butyllithium or *tert*-butyllithium does not provide sufficiently pure tris(oxazolinyl)phenyl borate.

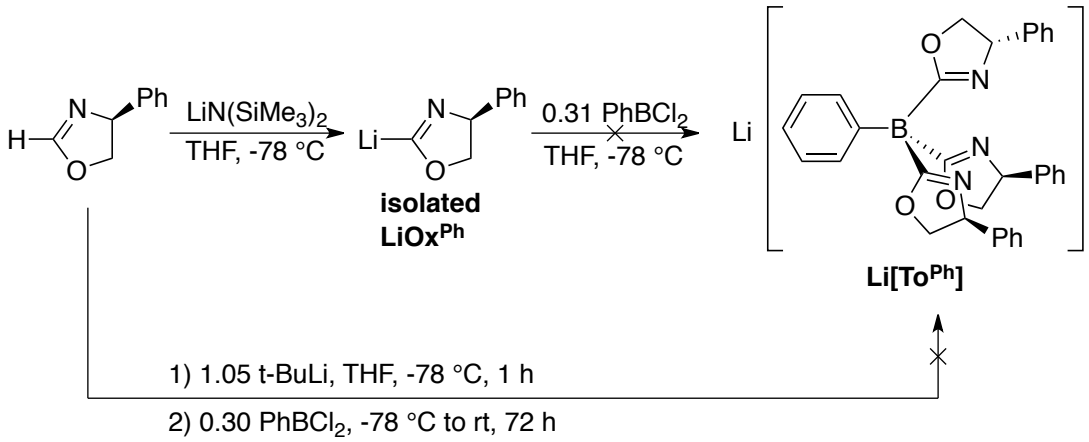

(Eq. 3-5)

The thallium version of $[To^T]^-$ is synthesized via transmetalation from $Li[To^T]$ with TlOAc in methylene chloride, similar to the preparation of $Tl[To^P]$[28] (Eq. 3-6). The ^{11}B NMR spectrum of thallium tris(4*S*-*tert*-butyl-2-oxazolinyl)phenylborate (**$Tl[To^T]$**) in benzene-d_6 displays a characteristic broad resonance at -17.1 ppm of a tris(oxazolinyl)phenyl borate.[28] A pseudo-C_3 symmetric species is observed in the ^1H NMR spectrum of $Tl[To^T]$ with resonances at 0.73 (CH_3), 3.39 (CH), and 3.67 ppm (CH_2). The IR spectrum of $Tl[To^T]$ contains one ν_{CN} band (1588 cm^{-1}) indicating that the three imidine nitrogens are coordinated to the thallium center in the solid state consistent with both $Tl[To^M]$ and $Tl[To^P]$.[28] The synthesis of $Tl[To^T]$ has two advantages over the synthesis of $H[To^T]$. The yield of $Tl[To^T]$ is higher than the yield of $H[To^T]$, and the synthesis and purification is entirely anaerobic thus not requiring a drying step before treating with air and moisture sensitive reagents.

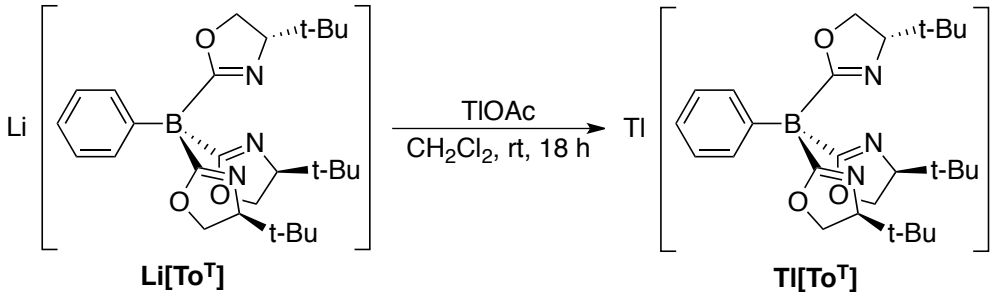

Li[To^T] **Tl[To^T]**

(Eq. 3-6)

X-ray quality crystals are obtained by slow evaporation of a solution of Tl[To^T] in benzene. A single crystal diffraction study confirms the structure of Tl[To^T] (see ORTEP diagram of Tl[To^T] plotted in Figure 3-1) with the tris(oxazolinyl)phenylborate ligand bound tridentate to the metal center. The chiral $P2_12_12_1$ space group is consistent with the presence of only one enantiomer of Tl[To^T] in the solid state.

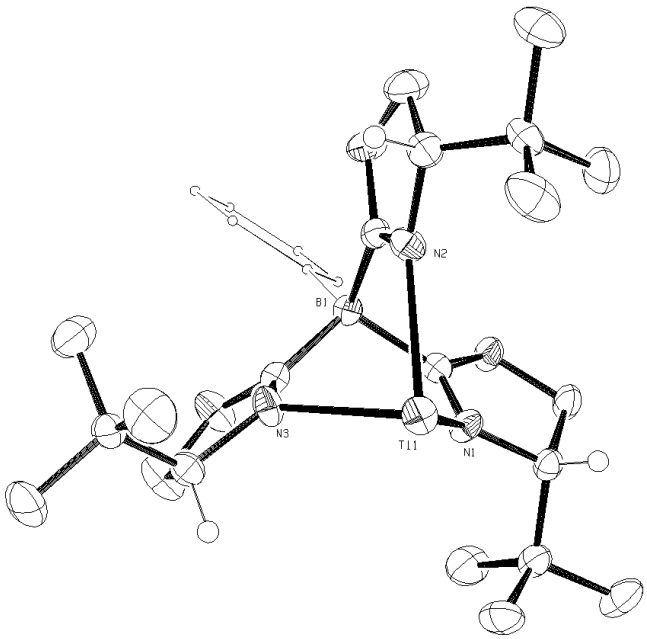

Figure 3-1. An ORTEP diagram of Tl[To^T], drawn at 50% probability. Hydrogen atoms on the stereogenic centers are shown to highlight the configuration, and the C_6H_5 group is represented by a ball and stick structure (without the hydrogens) for clarity. Relevant bond distances (Å) Tl1–N1, 2.557(2); Tl1–N2, 2.570(2); Tl1–N3, 2.505(2). Relevant bond angles (°) N1–Tl1–N2, 78.02(7); N1–Tl1–N3, 77.47(7); N2–Tl1–N3, 75.61(7).

Synthesis and characterization of To^{T}MgMe and To^{T}CaC(SiHMe$_2$)$_3$

The reaction of H[To^T] and $MgMe_2{\cdot}(O_2C_4H_8)_2$ in benzene affords To^{T}MgMe in 81% yield (Eq. 3-7). The oxazoline rings in To^{T}MgMe are equivalent in the ^{1}H NMR spectrum indicating the magnesium compound is pseudo-C_3 symmetric in solution (benzene-d_6). One resonance was observed at 0.72 ppm corresponding to the *tert*-butyl moiety and three resonances assigned to the methine and two diastereotopic methylene hydrogens on the oxazoline ring at 3.45, 3.59, and 3.72 ppm. Additionally, the resonance assigned to Mg–CH_3 appeared at -0.65 ppm; the integrated ratio of this resonance versus the *tert*-butyl resonance was the expected 3 H: 27 H. A ^{1}H–^{15}N HMBC experiment provides a single natural abundance ^{15}N chemical shift (-178.2 ppm) indicating tridentate coordination of [To^T]$^-$ to magnesium. Crosspeaks were observed between the imidine nitrogen and the oxazoline methylene and methine resonances; there was no crosspeak detected between the imidine nitrogen and the magnesium-bound methyl. The ^{15}N chemical shift was only slightly upfield of that for H[To^T] (-174.5 ppm), but was significantly upfield of 2-H-4*S*-*tert*-butyl-oxazoline (-148.0 ppm). The IR spectrum further supported the tridentate coordination of [To^T]$^-$ to magnesium with the presence of only one ν_{CN} band at 1585 cm^{-1}. The large size of the [To^T]$^-$ ligand provides significant steric shielding around the magnesium(II) center, thus preventing coordination of THF or dioxane in the bulk sample.

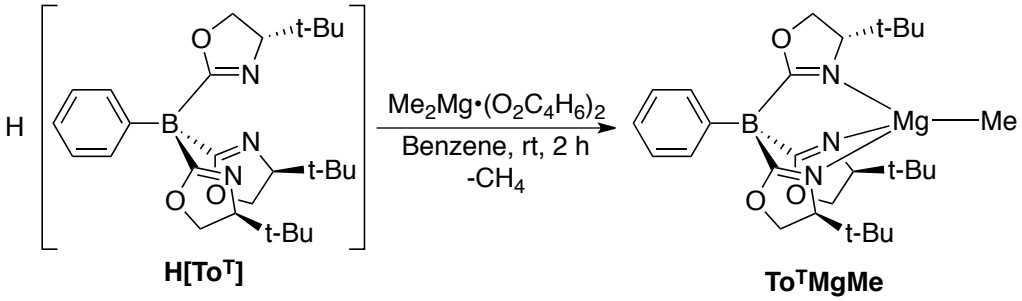

H[To^T] **To^{T}MgMe**

(Eq. 3-7)

X-ray quality crystals are obtained by cooling a $To^{T}MgMe$ solution in toluene to -78 °C. A single crystal diffraction study confirms the structure of $To^{T}MgMe$ (see ORTEP diagram of $To^{T}MgMe$ plotted in Figure 3-2). The tris(oxazolinyl)phenylborate ligand is coordinated tridentate to magnesium and adopts pseudo-C_3-symmetry with the C_3-axis coincident with the B–Mg vector. Thus, the $[To^{T}]^{-}$ ligand forms a propeller-type shape around the magnesium center. The space group ($P2_12_12_1$) is identical to that observed for $Tl[To^{T}]$ and is consistent with the presence of only one enantiomer of $To^{T}MgMe$ in the solid state.

The Mg1–C26 bond length is 2.102(1) Å; the Mg1–N1 and Mg1–N3 bond lengths are identical within 3σ error (2.108(1) and 2.109(1) Å) while the Mg1–N2 bond length is slightly longer (2.118(1) Å). All of the Mg–N bond lengths are significantly shorter (ca. 0.4 Å) than those in $Tl[To^{T}]$. The steric bulk and chelating $[To^{T}]^{-}$ ligand distort the bond angles of the Mg center from tetrahedral, as expected for a highly ionic compound. For example, the ∠N–Mg–N angles are close to 90° (89.74(4) to 91.56(4)°) whereas the ∠N–Mg–C26 angles are more obtuse, ranging from 121.13(6) to 127.84(6)°. The analogous ∠N–Tl–N angles for $Tl[To^{T}]$ are considerably more acute (75.61(7) to 78.02(7)°) than those in $To^{T}MgMe$ due to the increased M–N bond distances in the former. Comparing $To^{T}MgMe$ and the related tris(pyrazolyl)borate compound $Tp^{tBu}MgMe$ (Tp^{tBu} = tris(3-*tert*-butyl-pyrazolyl)borate) reveals that the Mg–C bond distance in $Tp^{tBu}MgMe$ (2.12(1) Å) is the same, within 3σ error, and the Mg–N bond distances (2.13(1), 2.137(7), and 2.137(7) Å) are also essentially identical with those in $To^{T}MgMe$.[1-4] The ∠N–Mg–N and ∠N–Mg–C bond angles are also similar (90.6(4) to 91.3(3)°) and (122.7(4) to 125.4(2)°) respectively. The similarity of Mg–N bonds lengths in $To^{T}MgMe$ and $Tp^{tBu}MgMe$, where 4*S*-*tert*-butyl-oxazolinyl and 3-*tert*-butyl-pyrazolyl are expected to have distinct electronic

properties, further emphasizes the substantial ionic character of these four-coordinate magnesium compounds.

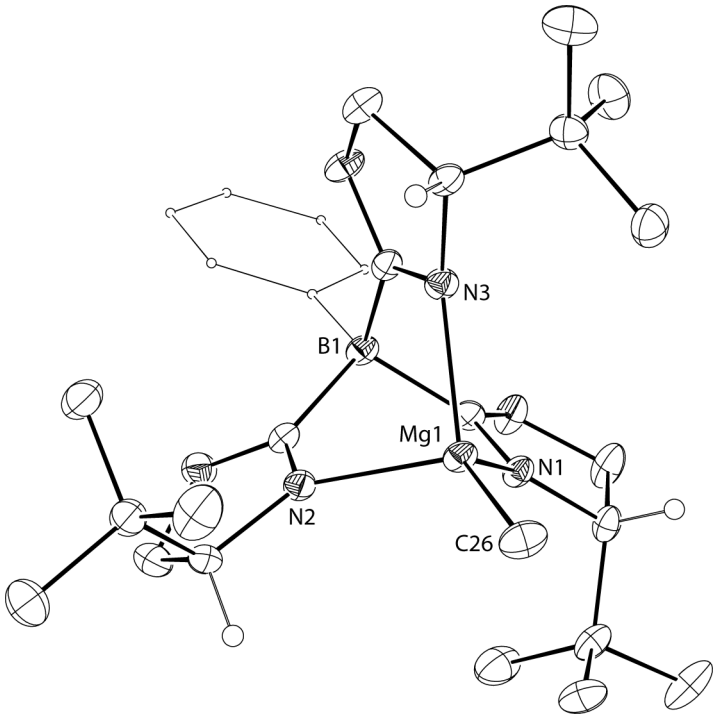

Figure 3-2. An ORTEP diagram of To^{T}MgMe, drawn at 50% probability. Hydrogen atoms on the stereogenic centers are shown to highlight the configuration, and the C_6H_5 group is represented by a ball and stick structure (without the hydrogens) for clarity.

A better comparison between To^{T}MgMe and Tp^{tBu}MgMe involves their relative steric properties. The cone angle of Tp^{tBu} was previously estimated at 244°,[1-4] whereas the cone angle of [To^{T}] in To^{T}MgMe was estimated to be 233°. The cone angle measures the extent to which the substituents on the pyrazole ring or oxazoline ring (i.e., *tert*-butyl) extend past the magnesium center. Another method for examining the steric effects of a ligand on a metal center is the solid angle. This method treats the metal center as a point source of light and the complex is encompassed by an imaginary sphere;[41-42] the solid angle is then defined as the overall surface of the sphere shaded by the ligand. The advantage of using solid angles to investigate the size of a ligand over cone angles

arises when the ligand is multi-haptic and does not contain free rotation about the metal–element bond.[43] The solid angles of $[To^T]^-$ and Tp^{tBu} are calculated from their X-ray coordinates to be 7.8 steradians (the percentage of the shaded surface is 62%) and 8.9 steradians (71%) respectively using the program Solid-G.[44-45] Therefore, the effective size of $[To^T]^-$ is smaller than Tp^{tBu}, this size difference is proposed to be due to the hybridization of the carbons on the heterocyclic rings. The planar sp^2-hybridized C3 in the pyrazole directs the *tert*-butyl group past the magnesium center while the sp^3-hybridized C4 in the oxazoline ring directs the *tert*-butyl group toward the backside of one of the adjacent oxazoline rings rather than in front of the metal center. For a stereoselective reaction (such as insertion) in which a substrate must penetrate the space between two oxazoline rings, the steric properties of $[To^T]^-$ are expected to make a significant steric distinction between prochiral faces.

Furthermore, the solid angles of both $[To^T]^-$ and Tp^{tBu} indicate that $(To^T)_2Mg$ and $(Tp^{tBu})_2Mg$ are not sterically reasonable complexes, at least when both ligands are bonded in a tridentate fashion. Thus, the moniker 'tetrahedral enforcer' often applied to Tp^{tBu},[1-4] is also an appropriate descriptor of the steric properties of $[To^T]^-$. Consistently, To^TMgMe is thermally robust in solution, and no decomposition, assessed by ^1H NMR spectroscopy in toluene-d_8, is observed when heated at 120 °C for five days. Additionally, To^TMgMe is stored in the solid state in the absence of air and moisture for extended periods without observable decomposition.

A related calcium compound is accessible by reaction of $H[To^T]$ and $Ca[C(SiHMe_2)_3]_2(THF)_2$[46] in benzene, which yields $To^TCaC(SiHMe_2)_3$ and $HC(SiHMe_2)_3$ as a non-coordinating byproduct that can be removed under vacuum (Eq. 3-8). All starting materials are consumed within five minutes and only the presence of free,

uncoordinated, THF is observed by ^{1}H NMR spectroscopy in micromolar scale reactions; the reaction is stirred for one hour in larger scale reaction to insure complete conversion.

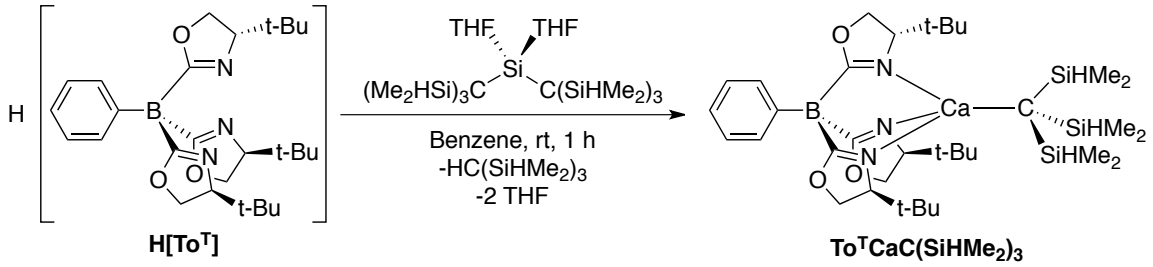

H[To^T] **To^{T}CaC(SiHMe$_2$)$_3$**

(Eq. 3-8)

The lack of solvent coordination to To^{T}CaC(SiHMe$_2$)$_3$ is intriguing because the implication is that calcium(II) is 4-coordinate; however, the –C(SiHMe$_2$)$_3$ alkyl group has been shown to stabilize (formally) low-coordinate yttrium,[47] ytterbium, and calcium[46] complexes via *β*-agostic SiH interactions. Thus, the δ_{SiH} and $^1J_{SiH}$ values of 4.89 ppm and 153 Hz from the ^{1}H NMR spectrum of To^{T}CaC(SiHMe$_2$)$_3$ as well as the ν_{SiH} values of 2106 and 1877 cm^{-1} in the IR spectrum are indicative of the presence of a *β*-agostic SiH interaction.[48] For comparison, the *β*-agostic ν_{SiH} bands for Y[C(SiHMe$_2$)$_3$]$_3$,[47] Ca[C(SiHMe$_2$)$_3$]$_2$(THF)$_2$, and Yb[C(SiHMe$_2$)$_3$]$_2$(THF)$_2$[46] are 1845, 1905, and 1890 cm^{-1} respectively. This indicates the presences of at least one *β*-agostic SiH interaction in both the solution state and solid state structures of To^{T}CaC(SiHMe$_2$)$_3$. The presence of only one δ_{SiH} in the ^{1}H NMR spectrum indicates that the compound is fluxional on the NMR timescale but not the IR timescale (due to the presence of both agostic and non-agostic ν_{SiH} bands). Additionally, no ν_{CN} bands from 1630 to 1615 cm^{-1} were detected indicative of oxazoline ring dissociation in the solid state;[49] only a single ν_{CN} band at 1569 cm^{-1} was detected and assigned as the symmetric normal stretching mode.

Hydroamination/cyclization of aminoalkenes

We investigated our new optically active complexes $To^{T}MgMe$ and $To^{T}CaC(SiHMe_2)_3$ as catalysts for the hydroamination/cyclization of the aminopentenes 2,2-diphenyl-1-amino-pent-4-ene, 2,2-dimethyl-1-amino-pent-4-ene, and C-(1-allyl-cyclohexyl)-methylamine as test substrates. The results are summarized in Table 3-1 to Table 3-3.

Table 3-1. Enantioselective hydroamination/cyclization of 2,2-diphenyl-4-penten-1-amine catalyzed by $To^{T}MgMe$ and $To^{T}CaC(SiHMe_2)_3$

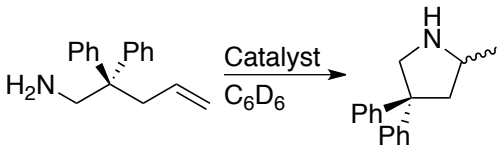

Entry	Catalyst[a]	Time	Temperature	Conversion[b]	% ee
1	$To^{T}MgMe$	24 h	RT	89%	0%
2	$To^{T}MgMe$	12 h	60 °C	≥99%	0%
3	$To^{T}CaC(SiHMe_2)_3$	5 min	RT	≥99%	0%

[a] 10 mol % catalyst. [b] Conversion was determined by ^{1}H NMR spectroscopy.

In general, the calcium compound $To^{T}CaC(SiHMe_2)_3$ catalyzes the cyclization of all three substrates at a significantly greater rate than hydroaminations catalyzed by $To^{T}MgMe$. The presumed catalyst intermediate, $To^{T}M–NHCH_2CR_2CH_2CH=CH_2$ (R_2 = Ph_2, $–(CH_2)_5–$, Me_2), should be more reactive for M = Ca versus M = Mg based on size and related rates of hydroamination catalyzed by *β*-diketiminate calcium and magnesium complexes;[6-7] however, initiation of $To^{T}CaC(SiHMe_2)_3$ is surprisingly fast given the unusual properties of the $–C(SiHMe_2)_3$ group.[46-47] This alkyl ligand is both sterically encumbered and relatively non-basic at the central carbon, and as a result Lewis acids such as $B(C_6F_5)_3$ react with a peripheral SiH rather than abstract the alkyl group in the typical fashion.[50]

Although To^TMgMe and $To^TCaC(SiHMe_2)_3$ are efficient catalysts for the cyclization of 2,2-diphenyl-1-amino-pent-4-ene, the corresponding pyrrolidine product is obtained as a racemic mixture (See Table 3-1). More promising results are observed with C-(1-allyl-cyclohexyl)-methylamine, which is cyclized by To^TMgMe at 60 °C and by $To^TCaC(SiHMe_2)_3$ at room temperature to give the spiro-pyrrolidine product in 36% and 18% ee, respectively (See Table 3-2).

Table 3-2. Enantioselective hydroamination/cyclization of C-(1-allyl-cyclohexyl)-methylamine catalyzed by To^TMgMe and $To^TCaC(SiHMe_2)_3$

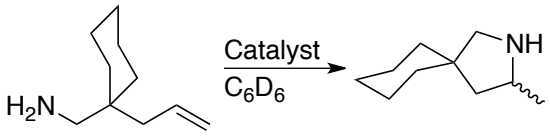

Entry	Catalyst[a]	Time	Temperature	Conversion[b]	% ee[c]
1	To^TMgMe	24 h	RT	No conversion	N/A
2	To^TMgMe	26 h	60 °C	93%	36% (*R*)
3	$To^TCaC(SiHMe_2)_3$	5 min	RT	≥99%	18% (*S*)
4[d]	$To^TCaC(SiHMe_2)_3$	7 d	80 °C	≤10%	N/A

[a] 10 mol % catalyst loading. [b] Conversion was determined by ^1H NMR spectroscopy. [c] % ee values were determined by ^{19}F NMR spectroscopy of Mosher amide derivatives. Absolute configuration in parentheses; assignments based on literature values.[51-52] [d] 1 mol % $To^TCaC(SiHMe_2)_3$

Additionally, the substrate 2,2-dimethyl-1-amino-pent-4-ene is cyclized by To^TMgMe in 27% ee and by $To^TCaC(SiHMe_2)_3$ in 18% ee (See Table 3-3). Interestingly, hydroamination/cyclization of 2,2-dimethyl-1-amino-pent-4-ene and C-(1-allyl-cyclohexyl)-methylamine with To^TMgMe gives rise to the *R* pyrrolidines whereas $To^TCaC(SiHMe_2)_3$ gives rise to the *S* pyrrolidines. Such differences in absolute configuration have been observed in rare earth and transition metal complex-catalyzed hydroaminations with scandium providing a different absolute configuration than larger metal centers[53] as well as in our lab with zirconium and yttrium catalyzed hydroaminations.[54-55] Thus, the substituents on the alkyl chain appear to be the most important component of the aminoalkenes for stereoselectivity in these cyclizations.

Table 3-3. Enantioselective hydroamination/cyclization of 22-dimethyl-4-penten-1-amine catalyzed by $To^{T}MgMe$ and $To^{T}CaC(SiHMe_2)_3$

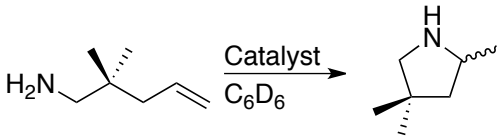

Entry	Catalyst[a]	Time	Temperature	Conversion[b]	% ee[c]
1	$To^{T}MgMe$	7 d	RT	No conversion	NA
2	$To^{T}MgMe$	5 d	80 °C	80%	27% (*R*)
3	$To^{T}CaC(SiHMe_2)_3$	5 min	RT	≥99%	18% (*S*)

[a] 10 mol % catalyst loading. [b] Conversion was determined by ^{1}H NMR spectroscopy [c] % ee values were determined by ^{19}F NMR spectroscopy of Mosher amide derivatives. Absolute configuration in parentheses; assignments based on literature values.[51-52]

While the enantioselectivity of $To^{T}MgMe$ and $To^{T}CaC(SiHMe_2)_3$ are relatively low in comparison to the highly selective catalysts of Sadow (Zr and Y)[54-55] Hultzsch (Sc and Lu)[51] and Schafer (Zr),[52] they provided the highest reported % ee's for group 2-catalyzed hydroamination/cyclization reported at the time of publication. At that time, there were only two reports of group 2 catalysts that provided any enantioselectivity for the hydroamination/cyclization of aminopentene substrates. Hultzsch and co-workers described chiral binaphthyl-derived tetraamine dimagnesium complexes that cyclized 2,2-diphenyl-1-amino-pent-4-ene with 14% ee, though 2,2-dimethyl-1-amino-pent-4-ene (4% ee) and C-(1-allyl-cyclohexyl)-methylamine (6% ee) were less successful.[19] Additionally, Harder and co-workers reported that bis(oxazoline) disilazidocalcium catalyzed the cyclization of 2,2-diphenyl-1-amino-pent-4-ene in up to 10% ee.[18] Very recently, Hultzsch and co-workers reported a chiral phenoxyamine magnesium catalyst that was highly active for the hydroamination of several aminopentenes; specifically 2,2-diphenyl-1-amino-pent-4-ene (80% ee), 2,2-dimethyl-1-amino-pent-4-ene (79% ee), and C-(1-allyl-cyclohexyl)-methylamine (90% ee).[20]

Conclusion

The contrasting stereoselectivity between the neutral group 2 tris(oxazolinyl)borate catalyzed hydroamination/cyclization described here and the dicationic trisox scandium alkyls that polymerize α-olefins with high stereoregularity is striking. Both reactions are presumed to involve insertion of an olefin into an M–E bond, albeit Mg/Ca–N versus Sc–C bonds and intramolecular cyclization versus a chain and/or ligand mediated intermolecular process. Clearly, the factors that control stereoselective insertion in olefin polymerization are significantly different from the factors that influence cyclization of aminoalkenes in hydroamination reactions. A related comparison was considered by Marks and co-workers, who investigated C_1-symmetric and chiral *ansa*-lanthanoidocene complexes $Me_2Si(C_5Me_4)(C_5H_3R^*)LnR$ as catalysts for enantioselective hydrogenation and hydroamination/cyclization.[56] In those cases, good enantioselectivities were obtained for both reactions (up to 74% for hydroamination and up to 96% for hydrogenation), and olefin insertion was proposed as the stereochemistry defining step for both catalytic transformations.

Experimental

General. All manipulations were performed using either Schlenk techniques or in a glovebox under an inert atmosphere of N_2 or argon unless otherwise indicated. Dry, oxygen-free solvents were used throughout. Benzene, toluene, pentane, diethyl ether, and tetrahydrofuran were degassed by sparging with nitrogen, filtered through activated alumina columns, and stored under nitrogen. Benzene-d_6, toluene-d_8, and tetrahydrofuran-d_8 were vacuum transferred from Na/K alloy and stored under N_2 in the glovebox. $Ca[C(SiHMe_2)_3]_2(THF)_2$,[46] $Me_2Mg\cdot(O_2C_4H_8)_2$,[57] 2,2-diphenyl-4-penten-1-amine,[58] 2,2-dimethyl-4-penten-1-amine,[58] and C-(1-allyl-cyclohexyl)-methylamine[59] were

prepared by published procedures. All the aminoalkenes were degassed and stored with 4 Å molecular sieves in a glovebox prior to use. All other chemicals were obtained from commercial sources and used as received. ^{1}H, ^{7}Li, ^{11}B, $^{13}C\{^{1}H\}$, $^{19}F\{^{1}H\}$, and $^{29}Si\{^{1}H\}$ NMR spectra were collected on a Bruker DRX-400 spectrometer, a Varian VXR-400 spectrometer, or a Bruker Avance II 700 spectrometer with a Bruker Z-gradient inverse TXI $^{1}H/^{13}C/^{15}N$ 5mm cryoprobe. ^{15}N chemical shifts were also determined on the Bruker Avance II 700 spectrometer by ^{1}H-^{15}N HMBC experiments; ^{15}N chemical shifts were originally referenced to liquid NH_3 and recalculated to the CH_3NO_2 chemical shift scale by adding -381.9 ppm. ^{7}Li NMR spectra were referenced to an external sample of 9.7 M LiCl in D_2O, ^{11}B NMR spectra were referenced to an external sample of $BF_3{\cdot}Et_2O$, and $^{29}Si\{^{1}H\}$ NMR spectra were referenced to an external sample of tetramethylsilane. Accurate mass ESI mass spectrometry was performed using the Agilent QTOF 6530 equipped with the Jet Stream ESI source. An Agilent ESI test mix was used for tuning and calibration. Accurate mass data was obtained in the positive ion mode using a reference standard with ions at 121.05087 and 922.00979. The mass resolution (FWHM) was maintained at 18,000.

[LiOx^{tBu}]. A Schlenk flask containing a stir bar was charged with hexamethyldisilazane (1.0 mL, 4.80 mmol) followed by 15 mL of THF. The solution was cooled to -78 °C, and *n*-butyllithium (1.92 mL, 4.80 mmol) was added slowly. The solution was allowed to stir for 45 minutes then a THF (5 mL) solution of degassed 4*S*-*tert*-butyl-2-oxazoline was added slowly via cannula. The solution immediately turned bright yellow. The yellow solution was stirred at -78 °C for 1 h then warmed to room temperature and allowed to stir for an additional 2 h. All volatiles were removed under vacuum. The resulting yellow solid was dissolved in warm hexane and cooled to -30 °C. The resulting off-white solid

was filtered under argon at -30 °C and dried under vacuum to yield 0.461 g (3.46 mmol, 76%) of crude LiOx^{tBu}. ^{1}H NMR (400 MHz, tetrahydrofuran-d_8): δ 4.02 (br, d, J_{HH} = 8.4 Hz, 1 H, LiCNCHCMe$_3$C*H*$_2$O), 3.74 (t, $^{2}J_{HH}$ = 9.6 Hz, 1 H, LiCNC*H*CMe$_3$CH$_2$O), 3.23 (br, d, J_{HH} = 7.2 Hz, 1 H, LiCNCHCMe$_3$C*H*$_2$O), 0.95 (s, LiCNCHC*Me*$_3$CH$_2$O). ^{13}C{^{1}H} NMR (100 MHz, tetrahydrofuran-d_8): δ 156.98 (Li*C*NCHCMe$_3$CH$_2$O), 73.54 (LiCN*C*HCMe$_3$CH$_2$O), 65.64 (LiCNCHCMe$_3$*C*H$_2$O), 33.48 (LiCNCH*C*Me$_3$CH$_2$O), 27.27 (LiCNCHC*Me*$_3$CH$_2$O).

Li[To^{T}]. 4*S*-*tert*-butyl-2-oxazoline (2.771 g, 21.8 mmol) was added to a Schlenk flask under argon. THF (100 mL) was added, and the colorless solution was cooled to -78 °C. *tert*-Butyllithium (13.6 mL, 23.1 mmol, 1.7 M) was added dropwise, and the solution turned from colorless to bright yellow. The reaction mixture was allowed to stir for 30 min at -78 °C, and $PhBCl_2$ (0.88 mL, 6.78 mmol) was added slowly. The yellow solution was allowed to warm to room temperature and stir for 72 h. The volatiles were removed under vacuum, and the resulting yellow solid was extracted with diethyl ether to yield crude Li[To^{T}] (2.23 g, 4.71 mmol, 65 %). ^{1}H NMR (methanol-d_4): δ 7.42 (d, $^{2}J_{HH}$ = 5.6 Hz, 2 H, *ortho*-C_6H_5), 7.02 (t, $^{2}J_{HH}$ = 7.2 Hz, 2 H, *meta*-C_6H_5), 6.94 (t, $^{2}J_{HH}$ = 7.2 Hz, 1 H, *para*-C_6H_5), 3.89 (d, J_{HH} = 8.0 Hz, 6 H, CNCHCMe$_3$C*H*$_2$O), 3.75 (t, $^{2}J_{HH}$ = 8.4 Hz, 3 H, CNC*H*CMe$_3$CH$_2$O), 0.86 (s, 27 H, CNCHC*Me*$_3$CH$_2$O). ^{11}B NMR (128 MHz, methanol-d_4): δ -17.0.

H[To^{T}]. Crude Li[To^{T}] (1.316 g, 2.78 mmol) was placed in Schlenk flask and dissolved in methylene chloride (50 mL). [HNEt$_3$]Cl (0.455 g, 3.31 mmol) was added, and the resulting yellow suspension was allowed to stir overnight at room temperature. All volatile materials were evaporated under reduced pressure. The resulting pale yellow solid was re-dissolved in a minimal amount of methylene chloride and passed through a

plug of grade-III neutral alumina (16 mm × 76 mm) using methylene chloride (100 mL) as the eluent. The solvent was removed under vacuum to yield a pale yellow solid, which was extracted with benzene (3 × 15 mL) to remove residual $[HNEt_3]Cl$. The filtrate was collected, and the solvent was removed under vacuum to yield a pale yellow solid. This crude product was purified by silica gel chromatography (16 mm × 140 mm, hexane:EtOAc:NEt_3 = 20:10:1, R_f = 0.27) to afford 0.714 g (1.53 mmol, 55%) of hydrogen tris(*4S*-*tert*-butyl-2-oxazolinyl)phenylborate ($H[To^T]$). $H[To^T]$ was further dried over P_2O_5 in benzene without loss of yield. ^1H NMR (400 MHz, benzene-d_6): δ 8.12 (d, $^2J_{HH}$ = 7.2 Hz, 2 H, *ortho*-C_6H_5), 7.46 (t, $^2J_{HH}$ = 7.6 Hz, 2 H, *meta*-C_6H_5), 7.25 (t, $^2J_{HH}$ = 7.2 Hz, 2 H, *para*-C_6H_5), 3.78 (m, 6 H, CNCHCMe$_3$C*H*$_2$O), 3.44 (dd, J_{HH} = 10.2 Hz, 7.6 Hz, 3 H, CNC*H*CMe$_3$CH$_2$O), 0.80 (s, 27 H, CNCHC*Me*$_3$CH$_2$O). $^{13}C\{^1H\}$ NMR (175 MHz, benzene-d_6): δ 134.99 (*ortho*-C_6H_5), 127.88 (*meta*-C_6H_5), 126.36 (*para*-C_6H_5), 73.18 (CN*C*HCMe$_3$CH$_2$O), 39.16 (CNCHCMe$_3$*C*H$_2$O), 33.86 (CNCH*C*Me$_3$CH$_2$O), 26.14 (CNCHC*Me*$_3$CH$_2$O). ^{11}B NMR (128 MHz, benzene-d_6): δ -16.5. ^{15}N NMR (70.9 MHz, benzene-d_6): δ -174.5. IR (KBr, cm^{-1}): 3069 w, 3045 w, 2955 s, 2901 m, 2869 m, 1601 s (ν_{CN}), 1478 m, 1423 m, 1392 w, 1362 w, 1208 w, 1176 w, 969 m. MS (ESI) exact mass Calculated for $C_{27}H_{42}BN_3O_3$: m/e 468.3392 ($[M^+]$), Found: 468.3398 (Δ -1.29 ppm). mp 98-102 °C.

Tl[To^T]. Li[To^T] (0.976 g, 2.06 mmol) and TlOAc (0.823 g, 3.12 mmol) were added to a 100 mL Schlenk flask inside the glove box. The flask was placed on a Schlenk line and 50 mL of CH_2Cl_2 was added via cannula. The yellow solution with white precipitate slowly turned milky over the course of one hour. The suspension was allowed to stir overnight. The reaction mixture was filtered, and the solid extracted with 100 mL of CH_2Cl_2. The resulting yellow solution was evaporated to dryness yielding a yellow

powder. Tl[To^{T}] was extracted from this yellow powder with pentane (3 × 30 mL) and recrystallized at -30 °C. Subsequent recrystallizations of the mother liquor resulted in the isolation of Tl[To^{T}] as a white powder (0.938 g, 1.40 mmol, 68 %). ^{1}H NMR (400 MHz, benzene-d_6): δ 8.25 (d, $^{3}J_{HH}$ = 7.6 Hz, 2 H, *ortho*-C_6H_5), 7.54 (t, $^{3}J_{HH}$ = 7.6 Hz, 2 H, *meta*-C_6H_5), 7.32 (t, $^{3}J_{HH}$ = 7.6 Hz, 1 H, *para*-C_6H_5), 3.67 (d, $^{3}J_{HH}$ = 8.4 Hz, 6 H, CNCHCMe$_3$C*H$_2$*O), 3.39 (t, $^{3}J_{HH}$ = 8.4 Hz, 3 H, CNC*H*CMe$_3$CH$_2$O), 0.73 (s, CNCHC*Me$_3$*CH$_2$O). ^{13}C{^{1}H} NMR (100 MHz, benzene-d_6): δ 191.71 (br, *C*NCHCMe$_3$CH$_2$O), 146.97 (br, *ipso*-C_6H_5), 136.37 (*ortho*-C_6H_5), 127.07 (*meta*-C_6H_5), 125.50 (*para*-C_6H_5), 74.88 (CN*C*HCMe$_3$CH$_2$O), 68.99 (CNCHCMe$_3$*C*H$_2$O), 33.98 (CNCH*C*Me$_3$CH$_2$O), 26.45 (CNCHC*Me$_3$*CH$_2$O). ^{11}B NMR (128 MHz, benzene-d_6): δ -17.1. IR (KBr, cm^{-1}): 3079 w, 3040 w, 2961 m, 2899 m, 2866 m, 1588 s (ν_{CN}), 1477 m, 1464 m, 1430 w, 1393 w, 1361 w, 1346 w, 1328 w, 1285 w, 1262 w, 1173 w, 1063 w, 1038 w, 1025 w, 997 w, 968 m, 932 w, 873 w, 848 w, 824 w, 791 w, 745 w, 726 w, 700 w. Anal. Calcd. for $C_{27}H_{41}BN_3O_3Tl$: C, 48.34; H, 6.16; N, 6.26. Found: C, 48.47; H, 6.27; N, 5.99. mp 190-194 °C (dec).

To^{T}MgMe. A yellow benzene solution of H[To^{T}] (0.441 g, 0.943 mmol) was slowly added to a rapidly stirring suspension of $Me_2Mg{\cdot}(O_2C_4H_8)_2$ (0.241 g, 1.04 mmol) in benzene at room temperature. Vigorous bubbling was observed upon addition. After addition was complete, the suspension was allowed to stir for 2 h; excess $Me_2Mg{\cdot}(O_2C_4H_8)_2$, which is insoluble under reaction conditions, was removed by filtration. The filtrate was evaporated under reduced pressure, and the resulting solid was washed with pentane to yield To^{T}MgMe (0.384 g, 0.759 mmol, 80.5%). X-ray quality crystals are obtained by cooling a concentrated toluene solution of To^{T}MgMe to -80 °C. ^{1}H NMR (700 MHz, benzene-d_6): δ 8.22 (d, $^{2}J_{HH}$ = 7.7 Hz, 2 H, *ortho*-C_6H_5), 7.52 (t, $^{2}J_{HH}$ = 7.7 Hz, 2 H, *meta*-

C_6H_5), 7.33 (t, $^2J_{HH}$ = 7.4 Hz, 1 H, *para*-C_6H_5), 3.72 (dd, $^2J_{HH}$ = 9.8 Hz, $^3J_{HH}$ = 5.6 Hz, 3 H, CNCHCMe$_3$C*H$_2$*O), 3.59 (t, J_{HH} = 9.8 Hz, 3 H, CNCHCMe$_3$C*H$_2$*O), 3.45 (dd, $^2J_{HH}$ = 9.8 Hz, $^2J_{HH}$ = 5.6 Hz, 3 H, CNC*H*CMe$_3$CH$_2$O), 0.72 (s, 27 H, CNCHC*Me$_3$*CH$_2$O), -0.65 (s, MgMe). $^{13}C\{^1H\}$ NMR (175 MHz, benzene-d_6): δ 193.76 (br, *C*NCHCMe$_3$CH$_2$O), 136.44 (*ortho*-C_6H_5), 127.23 (*meta*-C_6H_5), 126.16 (*para*-C_6H_5), 73.59 (CN*C*HCMe$_3$CH$_2$O), 70.28 (CNCHCMe$_3$*C*H$_2$O), 34.11 (CNCH*C*Me$_3$CH$_2$O), 26.28 (CNCHC*Me$_3$*CH$_2$O), -13.69 (MgMe). ^{11}B NMR (128 MHz, benzene-d_6): δ -17.1. ^{15}N NMR (70.9 MHz, benzene-d_6): δ -178.2. IR (KBr, cm^{-1}): 3045 w, 2958 m, 2869 m, 1585 s (ν_{CN}), 1478 m, 1396 w, 1365 m, 1196 s, 966 m. Anal. Calcd. for $C_{28}H_{44}BMgN_3O_3$(-$C_4H_8O_2$): C, 64.72; H, 8.83; N, 7.08. Found C, 64.44; H, 8.87; N, 7.52. mp 238 °C (dec).

To^{T}CaC(SiHMe$_2$)$_3$. Ca[C(SiHMe$_2$)$_3$]$_2$(THF)$_2$ (0.086 g, 0.153 mmol) was placed in a vial and dissolved in 5 mL of benzene. In a separate vial, H[To^T] (0.054 g, 0.116 mmol) was dissolved in 5 mL of benzene and added to the Ca[C(SiHMe$_2$)$_3$]$_2$(THF)$_2$ solution. An additional 5 mL of benzene was added, and the reaction mixture was stirred for 1 h. All the volatiles were removed under vacuum to yield an orange solid. To^{T}CaC(SiHMe$_2$)$_3$ was extracted with pentane. The pentane solvent and HC(SiHMe$_2$)$_3$ byproduct were removed under vacuum overnight to yield a pale yellow solid. (49.2 mg, 0.071 mmol, 61%). ^1H NMR (400 MHz, benzene-d_6): δ 8.11 (d, $^2J_{HH}$ = 7.2 Hz, 2 H, *ortho*-C_6H_5), 7.49 (t, $^2J_{HH}$ = 7.2 Hz, 2 H, *meta*-C_6H_5), 7.30 (t, $^2J_{HH}$ = 7.2 Hz, 1 H, *para*-C_6H_5), 4.89 (d, sept, $^1J_{SiH}$ = 153 Hz, $^3J_{HH}$ = 3.2 Hz, 3 H, SiH), 3.72 (dd, $^2J_{HH}$ = 9.2 Hz, $^3J_{HH}$ = 4 Hz, 3 H, CNCHCMe$_3$C*H$_2$*O), 3.67 (dd, $^3J_{HH}$ = 9.2 Hz, $^3J_{HH}$ = 4 Hz, 3 H, CNC*H*CMe$_3$CH$_2$O), 3.48 (t, J_{HH} = 9.2 Hz, 3 H, CNCHCMe$_3$C*H$_2$*O), 0.73 (s, 27 H, CNCHC*Me$_3$*CH$_2$O), 0.52 (d, $^3J_{HH}$ = 3.2 Hz, 9 H, SiHC*H$_3$*), 0.50 (d, $^3J_{HH}$ = 3.2 Hz, 9 H, SiHC*H$_3$*). $^{13}C\{^1H\}$ NMR (100 MHz, benzene-d_6): δ 135.97 (*ortho*-C_6H_5), 126.83 (*meta*-C_6H_5), 125.59 (*para*-C_6H_5), 74.15

(CN*C*HCMe$_3$CH$_2$O), 68.91 (CNCHCMe$_3$*C*H$_2$O), 34.02 (CNCH*C*Me$_3$CH$_2$O), 25.84 (CNCHC*Me$_3$*CH$_2$O), 4.18 (*C*(SiHMe$_2$)$_3$), 3.73 (C(SiH*Me$_2$*)$_3$). ^{11}B NMR (128 MHz, benzene-d_6): δ -16.7. ^{15}N NMR (70.9 MHz, benzene-d_6): δ -163.7. ^{29}Si{^{1}H} NMR (79.5 MHz, benzene-d_6): δ -20.4. IR (KBr, cm^{-1}): 3044 w, 3074 w, 2958 m, 2903 m, 2870 w, 2106 m (ν_{SiH}), 1877 w (ν_{SiH}) 1569 m (ν_{CN}), 1478 w, 1254 w. Anal. Calcd. for $C_{34}H_{62}BCaN_3O_3Si_3$(HC(SiHMe$_2$)$_3$): C, 55.55; H, 9.55; N, 4.74. Found C, 55.67; H, 9.44; N, 4.61. mp 226-227 °C (dec).

General conditions for hydroamination/cyclization. In a glove box, To^{T}MgMe or To^{T}CaC(SiHMe$_2$)$_3$ catalyst (1 equivalent) and aminoalkene (10 equivalents) were massed in separate test tubes. To^{T}MgMe was dissolved in benzene-d_6 and transferred to the test tube containing the aminoalkene. This solution was either added to a dry NMR tube and capped with a septa for room temperature reactions or added to a dry NMR tube fitted with a J-Young valve for reactions at elevated temperatures. ^{1}H NMR spectra were taken at regular intervals.

Determination of % ee for cyclohexyl- and dimethyl-pyrrolidine: The NMR sample was transferred to a flask and all volatiles were vacuum transferred via high vacuum. The solution is then transferred to an NMR tube. The amount of pyrrolidine is calculated from the ^{1}H NMR spectrum using tetrakis(trimethylsilyl)silane as an internal standard. Hünig's base (2 equivalents) and (*S*)-(+)-Mosher's chloride (1.2 equivalents) were added to the NMR tube. After 20 minutes, the NMR sample was added to a vial and all volatiles were removed under vacuum. The pyrrolidine-Mosher amide was extracted with pentane (3 × 2 mL) and the volatiles were removed. The % ee was then determined by integration of the ^{19}F{^{1}H} NMR spectrum at 60 °C in chloroform-*d*.

Determination of % ee for diphenyl-pyrrolidine: The NMR sample was transferred to a small flask and the product, 4,4-diphenyl-2-methylpyrrolidine, was vacuum distilled using a Kugelrohr (~120 °C, 10^{-6} Torr). The distillate was then transferred to an NMR tube with chloroform-*d*. The amount of pyrrolidine product was calculated from the ^{1}H NMR spectrum using tetrakis(trimethylsilyl)silane as an internal standard. Hünig's base (2 equivalents) and (*S*)-(+)-Mosher's chloride (1.2 equivalents) were added to the NMR tube. After 20 minutes, all volatiles were removed under vacuum. The amide product was extracted with pentane (3 x 2 mL) and the volatiles were removed. The % ee was then determined by integration of the ^{1}H NMR spectrum at ambient temperature in chloroform-*d*.

References

1. Han, R.; Looney, A.; Parkin, G., *J. Am. Chem. Soc.* **1989,** *111* (18), 7276.
2. Han, R.; Parkin, G., *J. Organomet. Chem.* **1990,** *393* (3), C43-C46.
3. Han, R.; Parkin, G., *Organometallics* **1991,** *10* (4), 1010-1020.
4. Han, R.; Parkin, G., *J. Am. Chem. Soc.* **1992,** *114* (2), 748-757.
5. Chisholm, M. H.; Eilerts, N. W.; Huffman, J. C.; Iyer, S. S.; Pacold, M.; Phomphrai, K., *J. Am. Chem. Soc.* **2000,** *122* (48), 11845-11854.
6. Crimmin, M. R.; Arrowsmith, M.; Barrett, A. G. M.; Casely, I. J.; Hill, M. S.; Procopiou, P. A., *J. Am. Chem. Soc.* **2009,** *131* (28), 9670-9685.
7. Crimmin, M. R.; Casely, I. J.; Hill, M. S., *J. Am. Chem. Soc.* **2005,** *127* (7), 2042-2043.
8. Harder, S., *Chem. Rev.* **2010,** *110* (7), 3852-3876.
9. Barrett, A. G. M.; Crimmin, M. R.; Hill, M. S.; Procopiou, P. A., *Proc. R. Soc. A* **2010,** *466* (2116), 927-963.
10. Harder, S.; Brettar, J., *Angew. Chem., Int. Ed. Engl.* **2006,** *45* (21), 3474-3478.
11. Spielmann, J.; Harder, S., *Eur. J. Inorg. Chem.* **2008,** *2008* (9), 1480-1486.
12. Crimmin, M. R.; Barrett, A. G. M.; Hill, M. S.; Hitchcock, P. B.; Procopiou, P. A., *Organometallics* **2008,** *27* (4), 497-499.
13. Barrett, A. G. M.; Crimmin, M. R.; Hill, M. S.; Hitchcock, P. B.; Procopiou, P. A., *Dalton Trans.* **2008,** (33).
14. Barrett, A. G. M.; Crimmin, M. R.; Hill, M. S.; Hitchcock, P. B.; Lomas, S. L.; Mahon, M. F.; Procopiou, P. A.; Suntharalingam, K., *Organometallics* **2008,** *27* (23), 6300-6306.
15. Nieto, I.; Cervantes-Lee, F.; Smith, J. M., *Chem. Commun.* **2005,** (30).
16. Arrowsmith, M.; Heath, A.; Hill, M. S.; Hitchcock, P. B.; Kociok-Köhn, G., *Organometallics* **2009,** *28* (15), 4550-4559.

17. Arrowsmith, M.; Hill, M. S.; Kociok-Köhn, G., *Organometallics* **2009,** *28* (6), 1730-1738.
18. Buch, F.; Harder, S., *Z. Naturforsch* **2008,** *63b*, 169-177.
19. Horrillo-Martínez, P.; Hultzsch, K. C., *Tetrahedron Lett.* **2009,** *50* (18), 2054-2056.
20. Zhang, X.; Emge, T. J.; Hultzsch, K. C., *Angew. Chem., Int. Ed. Engl.* **2012,** *51* (2), 394-398.
21. Dunne, J. F.; Su, J.; Ellern, A.; Sadow, A. D., *Organometallics* **2008,** *27* (11), 2399-2401.
22. Pawlikowski, A. V.; Ellern, A.; Sadow, A. D., *Inorg. Chem.* **2009,** *48* (16), 8020-8029.
23. Pawlikowski, A. V.; Gray, T. S.; Schoendorff, G.; Baird, B.; Ellern, A.; Windus, T. L.; Sadow, A. D., *Inorg. Chim. Acta* **2009,** *362* (12), 4517-4525.
24. Dunne, J. F.; Manna, K.; Wiench, J. W.; Ellern, A.; Pruski, M.; Sadow, A. D., *Dalton Trans.* **2010,** *39* (2), 641-653.
25. Gagne, M. R.; Marks, T. J., *J. Am. Chem. Soc.* **1989,** *111* (11), 4108-4109.
26. Gagne, M. R.; Stern, C. L.; Marks, T. J., *J. Am. Chem. Soc.* **1992,** *114* (1), 275-294.
27. Tellers, D. M.; Skoog, S. J.; Bergman, R. G.; Gunnoe, T. B.; Harman, W. D., *Organometallics* **2000,** *19* (13), 2428-2432.
28. Ho, H.-A.; Dunne, J. F.; Ellern, A.; Sadow, A. D., *Organometallics* **2010,** *29* (18), 4105-4114.
29. Bellemin-Laponnaz, S.; Gade, L. H., *Chem. Commun.* **2002,** (12), 1286-1287.
30. Bellemin-Laponnaz, S.; Gade, L. H., *Angew. Chem., Int. Ed. Engl.* **2002,** *41* (18), 3473-3475.
31. Ward, B. D.; Bellemin-Laponnaz, S.; Gade, L. H., *Angew. Chem., Int. Ed. Engl.* **2005,** *44* (11), 1668-1671.
32. Lukesova, L.; Ward, B. D.; Bellemin-Laponnaz, S.; Wadepohl, H.; Gade, L. H., *Dalton Trans.* **2007,** (9).
33. Lukešová, L.; Ward, B. D.; Bellemin-Laponnaz, S.; Wadepohl, H.; Gade, L. H., *Organometallics* **2007,** *26* (18), 4652-4657.
34. Mukherjee, D.; Ellern, A.; Sadow, A. D., *J. Am. Chem. Soc.* **2010,** *132* (22), 7582-7583.
35. Baird, B.; Pawlikowski, A. V.; Su, J.; Wiench, J. W.; Pruski, M.; Sadow, A. D., *Inorg. Chem.* **2008,** *47* (22), 10208-10210.
36. Silks, L. A.; Peng, J.; Odom, J. D.; Dunlap, R. B., *J. Org. Chem.* **1991,** *56* (24), 6733-6736.
37. Ollivault-Shiflett, M.; Kimball, D. B.; Silks, L. A. P., *J. Org. Chem.* **2004,** *69* (15), 5150-5152.
38. Mazet, C.; Köhler, V.; Pfaltz, A., *Angew. Chem., Int. Ed. Engl.* **2005,** *44* (31), 4888-4891.
39. Köhler, V.; Mazet, C.; Toussaint, A.; Kulicke, K.; Häussinger, D.; Neuburger, M.; Schaffner, S.; Kaiser, S.; Pfaltz, A., *Chem. -Eur. J.* **2008,** *14* (28), 8530-8539.
40. Leonard, W. R.; Romine, J. L.; Meyers, A. I., *J. Org. Chem.* **1991,** *56* (5), 1961-1963.
41. White, D.; Taverner, B. C.; Leach, P. G. L.; Coville, N. J., *J. Comput. Chem.* **1993,** *14* (9), 1042-1049.
42. White, D.; Coville, N. J., *Adv. Organomet. Chem.* **1994,** *Volume 36*, 95-158.

43. White, D. P.; Anthony, J. C.; Oyefeso, A. O., *J. Org. Chem.* **1999,** *64* (21), 7707-7716.
44. Guzei, I. A.; Wendt, M. *Solid-G*, UW-Madison, WI, 2004.
45. Guzei, I. A.; Wendt, M., *Dalton Trans.* **2006,** (33).
46. Yan, K.; Upton, B. M.; Ellern, A.; Sadow, A. D., *J. Am. Chem. Soc.* **2009,** *131* (42), 15110-15111.
47. Yan, K.; Pawlikowski, A. V.; Ebert, C.; Sadow, A. D., *Chem. Commun.* **2009,** (6).
48. Corey, J. Y.; Braddock-Wilking, J., *Chemical Reviews* **1998,** *99* (1), 175-292.
49. Dunne, J. F.; Fulton, D. B.; Ellern, A.; Sadow, A. D., *J. Am. Chem. Soc.* **2010,** *132* (50), 17680-17683.
50. Yang, X.; Stern, C. L.; Marks, T. J., *J. Am. Chem. Soc.* **1994,** *116* (22), 10015-10031.
51. Gribkov, D. V.; Hultzsch, K. C.; Hampel, F., *J. Am. Chem. Soc.* **2006,** *128* (11), 3748-3759.
52. Wood, M. C.; Leitch, D. C.; Yeung, C. S.; Kozak, J. A.; Schafer, L. L., *Angew. Chem., Int. Ed. Engl.* **2007,** *46* (3), 354-358.
53. Yu, X.; Marks, T. J., *Organometallics* **2006,** *26* (2), 365-376.
54. Manna, K.; Kruse, M. L.; Sadow, A. D., *ACS Catal.* **2011,** *1* (11), 1637-1642.
55. Manna, K.; Xu, S.; Sadow, A. D., *Angew. Chem., Int. Ed. Engl.* **2011,** *50* (8), 1865-1868.
56. Giardello, M. A.; Conticello, V. P.; Brard, L.; Gagne, M. R.; Marks, T. J., *J. Am. Chem. Soc.* **1994,** *116* (22), 10241-10254.
57. Tobia, D.; Baranski, J.; Rickborn, B., *J. Org. Chem.* **1989,** *54* (17), 4253-4256.
58. Bexrud, J. A.; Beard, J. D.; Leitch, D. C.; Schafer, L. L., *Org. Lett.* **2005,** *7* (10), 1959-1962.
59. Martinez, P. H.; Hultzsch, K. C.; Hampel, F., *Chem. Commun.* **2006,** (21).

Chapter 4: Synthesis of tris(oxazolinyl)boratomagnesium complexes of nitrogen, phosphorus, and sulfur: A reactivity study of silicon–heteroatom bond formation and a mechanistic study of Si–N bond formation via cross–dehydrocoupling

Contains results reported in a paper published in *Journal of the American Chemical Society*[*]

James F. Dunne, Steven R. Neal, Joshua Engelkemier, Arkady Ellern, Aaron D. Sadow

Department of Chemistry, Iowa State University, Ames, Iowa 50011, United States

and

From a paper to be submitted for publication

Abstract

We describe the continuing study of $To^{M}MgMe$ (To^{M} = tris(4,4-dimethyl-2-oxazolinyl)phenylborate) as a precatalyst for the cross–dehydrocoupling of Si–H and E–H bonds to give Si–E bonds and H_2. While Si–N bond formation with primary aliphatic and aromatic amines is facile with $To^{M}MgMe$ as the precatalyst, $To^{M}MgMe$ is not a suitable precatalyst for Si–N bond formation with indole and *para*-toluenesulfonamide as well as Si–O, Si–P, and Si–S bond formations. Kinetic studies of the overall catalytic cycle as well as stoichiometric Si–N bond forming reactions with (p-XC_6H_4)$PhSiH_2$ suggest a nucleophilic attack by a magnesium amide as the turnover-limiting step.

---

[*] Reproduced in part with permission from Dunne, J. F.; Neal, S. R.; Engelkemier, J.; Ellern, A.; Sadow, A. D. *J. Am. Chem. Soc.* **2011**, *133*, 16782-16785. Copyright 2011 American Chemical Society. Contributions from the specific authors are listed in the thesis outline section and will not be repeated here.

Introduction

Compounds containing Si–N bonds have important applications in synthetic chemistry as bases,[1] silylating agents,[2-5] ligands for metal centers, and polymeric precursors for ceramic materials.[6-7] Current examples for Si–N bond formation involve supported palladium,[8] ruthenium,[9-13] rhodium,[14] chromium,[15] titanium,[16-17] copper,[18] and uranium;[19] moreover, there are two reports of group 2-catalyzed Si–N bond formation. The first example is a stoichiometric reaction between [(^{Dipp}nacnac)CaN(SiMe$_3$)$_2$(THF)] (^{Dipp}nacnac = [(2,6-diisopropyl-phenyl)NC-Me]$_2$CH) and $PhSiH_3$ yielding $PhH_2SiN(SiMe_3)_2$ and [(^{Dipp}nacnac)CaH(THF)]$_2$.[20] The second is a catalytic synthesis of silazanes with the azametallacyclopropane catalyst Ca(η^2-Ph$_2$CNPh)(HMPA)$_3$ (HMPA = hexamethylphosphoramide). This catalyst provides the dehydrogenative silylation products from aryl and aliphatic amines with Ph_3SiH.[21] Neither of these reports provides insight into the mechanism of Si–N bond formation.

Additionally, several reports have recently appeared in the literature involving isoelectronic C–N bond formation via hydroamination/cyclization of aminoalkenes.[22-27] In these reactions, a magnesium alkyl undergoes protonolysis with the amine substrate to form the corresponding magnesium amide followed by a C–N bond formation step. Both experimental[22, 24] and theoretical[28] evidence provide support for conflicting mechanisms; the implication from these investigations is that a general mechanism for group 2-catalyzed bond formations cannot be generated and detailed studies on each system is required.

To^{M}MgMe (To^M = tris(4,4-dimethyl-2-oxazolinyl)phenyl borate)[24] is an effective precatalyst for the cross–dehydrocoupling of Si–H bonds in organosilanes and N–H bonds in amines to give Si–N bonds and H_2. With this catalyst system, a range of silazanes can be prepared in high conversion and high yield (see Table 4-1).[29]

Table 4-1. To^{M}MgMe catalyzed aminolysis of silanes[a]

$$R_3Si\text{-}H + H\text{-}NHR' \xrightarrow[\text{benzene}]{To^{M}MgMe\ catalyst} R_3Si\text{-}NHR'$$

Amine (equiv.)	Silane	Product	% yield (isolated)
n-$PrNH_2$ (3.5)	$PhSiH_3$	(*n*-PrNH)$_3$SiPh	99 (99)
n-$PrNH_2$ (3.0)	$PhMeSiH_2$	(*n*-PrNH)$_2$SiMePh	99 (90)
n-$PrNH_2$ (0.5)	$PhMeSiH_2$	*n*-PrHNSiHMePh	99 (78)
n-$PrNH_2$ (3.0)	Ph_2SiH_2	(*n*-PrNH)$_2$SiPh$_2$	99 (99)
n-$PrNH_2$ (0.5)	Ph_2SiH_2	*n*-PrHNSiHPh$_2$	99 (96)
i-$PrNH_2$ (2.5)	$PhSiH_3$	(*i*-PrNH)$_2$SiHPh	99 (99)
i-$PrNH_2$ (0.5)	$PhSiH_3$	*i*-PrHNSiH$_2$Ph	99 (45)
i-$PrNH_2$ (2.0)	$PhMeSiH_2$	*i*-PrHNSiHMePh	89 (67)
i-$PrNH_2$ (2.0)	Ph_2SiH_2	*i*-PrHNSiHPh$_2$	99 (97)
t-$BuNH_2$ (2.5)	$PhSiH_3$	*t*-BuHNSiH$_2$Ph	99 (90)
t-$BuNH_2$ (2.0)	$PhMeSiH_2$	*t*-BuHNSiHMePh	90 (60)
t-$BuNH_2$ (2.0)	Ph_2SiH_2	*t*-BuHNSiHPh$_2$	99 (81)
$PhNH_2$ (2.5)	$PhSiH_3$	(PhNH)$_2$SiHPh	99 (97)
$PhNH_2$ (2.0)	$PhMeSiH_2$	PhHNSiHMePh	43[b] (19)
$PhNH_2$ (2.0)	Ph_2SiH_2	PhHNSiHPh$_2$	53[b] (19)

[a] Conditions: 5 mol % To^{M}MgMe, C_6H_6, 24 h, room temperature. [b] 60 °C.

Important to note is the comparison between the reactions of *tert*-butyl amine and aniline with organosilanes. *tert*-Butyl amine reacts with $PhMeSiH_2$ and Ph_2SiH_2 in 24 hours at room temperature to give the corresponding monosilazanes in quantitative yield. However, reactions between aniline and $PhMeSiH_2$ and Ph_2SiH_2 require heating to 60 °C for 24 hours to obtain ca. 50% conversion. This difference in reactivity is puzzling and will be an area of focus in this thesis.

The overall catalytic cycle (shown in Scheme 4-1 for *tert*-butyl amine and $PhMeSiH_2$) is proposed to proceed through initial protonolysis of To^{M}MgMe by amine to provide To^{M}MgNH^{t}Bu followed by introduction of silane and loss of silazane. Finally, protonolysis of To^{M}MgH with *tert*-butyl amine will generate one equivalent of H_2 and regenerate To^{M}MgNH^{t}Bu.

Scheme 4-1. Catalytic cycle for organosilane aminolysis

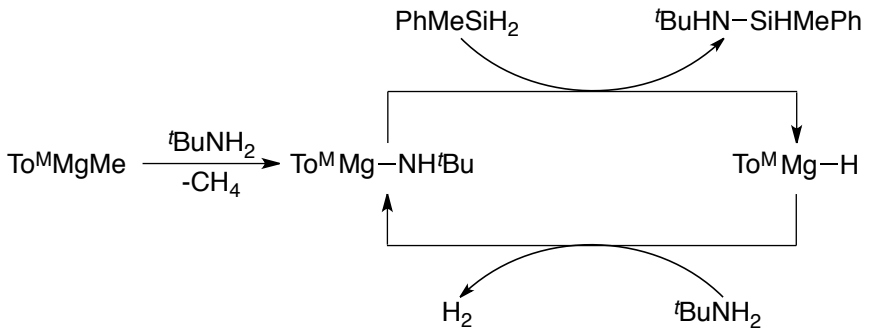

$To^{M}MgNH^{t}Bu$ is isolable and reacts with $PhMeSiH_2$ in a reaction that models Si–N formation in the catalytic cycle. The ability to isolate $To^{M}MgNH^{t}Bu$ permits the detailed investigation of the Si–N bond formation step. Thus, linear second-order integrated rate law plots of ln([$PhMeSiH_2$]/[$To^{M}MgNH^{t}Bu$]) versus time provide the rate law in (Eq. 4-1) with k_{obs} = (3.9 ± 0.3) × 10^{-3} $M^{-1}{\cdot}s^{-1}$ at 273 K.

$$-\frac{d[To^{M}MgNH^{t}Bu]}{dt} = k_{obs}[To^{M}MgNH^{t}Bu][PhMeSiH_2]$$

(Eq. 4-1)

Activation parameters were obtained from a plot of ln(*k*/T) versus 1/T from –20 to 80 °C for the reaction of $To^{M}MgNH^{t}Bu$ and $PhMeSiH_2$ ($\Delta H^{\ddagger H}$ = 5.9(2) kcal·mol^{-1} and $\Delta S^{\ddagger H}$ = –46.5(8) cal·$mol^{-1}{\cdot}K^{-1}$. These values suggest a highly ordered transition state.[30] A primary isotope effect of k_H/k_D = 1.0(2) at 0 °C was measured for the reaction of $To^{M}MgNH^{t}Bu$ and $PhMeSiD_2$. This small primary isotope effect was essentially temperature-independent from –20 to 80 °C, and the activation parameters for $PhMeSiD_2$ ($\Delta H^{\ddagger D}$ = 5.7(2) kcal·mol^{-1} and $\Delta S^{\ddagger D}$ = –46.1(8) cal·$mol^{-1}{\cdot}K^{-1}$) are identical to those obtained for $PhMeSiH_2$. For comparison, kinetic studies of Si–C bond formations mediated by early transition metals and rare-earth elements, which are proposed to involve concerted, four-center transition states (i.e. σ-bond metathesis), have primary isotope effects for Si–C bond formation of ca. 1.1,[31-32] highly negative $\Delta S^{\ddagger}$ values, and

small $\Delta H^{\ddagger}$ values that are similar to those for the magnesium-mediated Si–N bond formation.

Scheme 4-2. Proposed mechanisms for $To^{M}Mg$–mediated Si–N bond formation; Concerted σ-bond metathesis (Mechanism A) versus nucleophilic attack (Mechanism B)

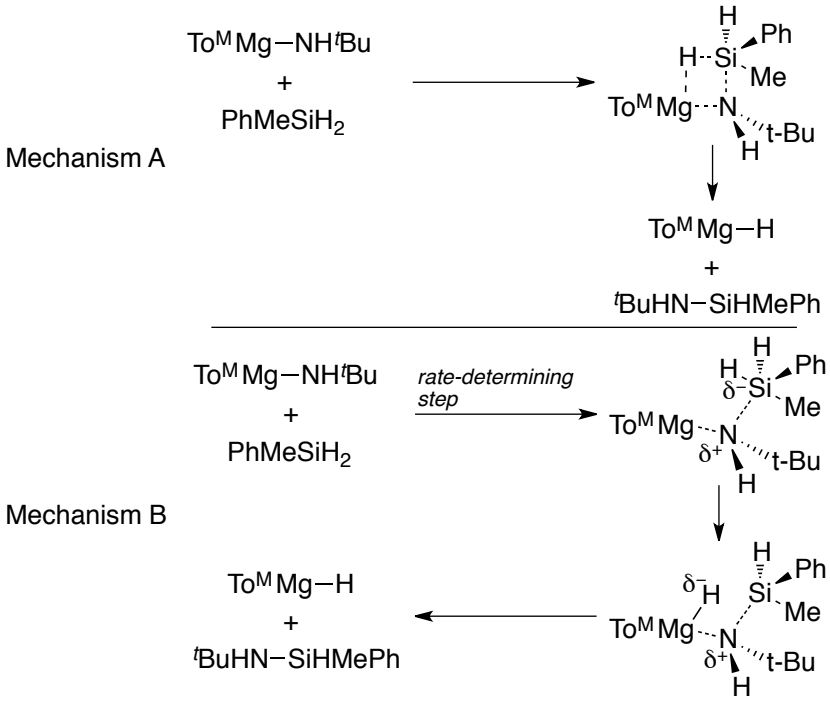

Two possible mechanisms for magnesium-mediated Si–N bond formation have been considered. The first is a concerted, four-center transition state (Scheme 4-2, Mechanism A) that is similar to the mechanism reported by Tilley and co-workers for scandium-catalyzed Si–C bond formation.[32] The second is a nucleophilic attack of the magnesium amide on silicon followed by hydrogen transfer from silicon to magnesium and subsequent loss of the silazane (Scheme 4-2, Mechanism B). The mechanism of nucleophilic substitution at silicon and the role of electrophilic assistance has been debated in the literature and is primarily based on observing the retention or inversion of stereochemistry of chiral silicon centers.[33]

Preference for one mechanism over the other cannot be made solely based on the data collected from the stoichiometric kinetic studies. However, establishing the rate law for the overall catalytic cycle is needed to verify that the stoichiometric reaction of $To^{M}MgNH^{t}Bu$ and $PhMeSiH_2$ is an effective model of the reaction under catalytic conditions. Additionally, a key difference between the two possible mechanisms depicted in Scheme 4-2 is the buildup of charge on the silane in the nucleophilic attack mechanism compared to the σ-bond metathesis mechanism. Therefore, Hammett plots could provide support for one pathway over another, and we set out to study the effect of substituted aryl silanes on the Si–N bond formation step. Lastly, a nucleophilic attack mechanism should be highly susceptible to the nucleophilicity of the amine in comparison to a σ-bond metathesis mechanism. Thus, the synthesis of the magnesium amides of *n*-propyl amine, isopropyl amine, and aniline and their comparison to $To^{M}MgNH^{t}Bu$ could prove informative.

The stoichiometric reactivity of single site magnesium complexes with amines has been studied; Parkin and coworkers reported the first studies on the stoichiometric reactivity amines utilizing tris(pyrazolyl)borate ligands to stabilize the metal center.[34-38] Their studies show that the magnesium alkyl species react via protonolysis to yield the corresponding magnesium amides. For example, reacting $Tp^{tBu}MgMe$ (Tp^{tBu} = tris(3-*tert*-butyl-pyrazolyl)borate) with aniline provides $Tp^{tBu}MgNHPh$ in good yield after heating at 60 °C for one day.[38] Similar reactivity was observed with alcohols and thiols to yield magnesium alkoxides and sulfides respectively.[37] Surprisingly absent from the stoichiometric studies was any reaction between $Tp^{tBu}MgMe$ and phosphines (either primary or secondary phosphines).

In this vein, we began synthesizing several $To^{M}MgE$ (E = NHR, NRR', PHR, SR) complexes and studying of their interactions with organosilanes as a route to new

silicon–heteroatom bonds. Studies on the mechanism of magnesium-mediated Si–N bond formation provides significant evidence to support a mechanism consisting of a nucleophilic attack of the Mg–N bond on silicon followed by hydrogen transfer from silicon to magnesium (Scheme 4-2, Mechanism B).

Results and discussion

Kinetic investigations of Si–N bond formation

In catalytic reactions, the consumption of organosilane and the formation of the silazane product are evident from the SiH resonances, which shift downfield as the hydrides are replaced with amides. Additionally, the $^{3}J_{HH}$ coupling constants (~3 Hz) between the SiH and NH groups give rise to doublet SiH resonances in RH_2SiNHR' and triplets in $RHSi(NHR')_2$, and therefore, the SiH signal assists in product identification.

$$\text{PhMeHSi-H} + \text{H-NH}^{t}\text{Bu} \xrightarrow[\text{benzene}]{\text{To}^{M}\text{MgMe catalyst}} \text{PhMeHSi-NH}^{t}\text{Bu}$$

(Eq. 4-2)

Establishing the rate law for the catalytic reaction, (Eq. 4-2), begins by monitoring the concentration of $PhMeSiH_2$. A plot of $\ln[PhMeSiH_2]$ versus time is linear over three half-lives indicating the catalytic reaction is first-order in silane. Plots of $\ln[PhMeSiH_2]$ versus time at different [*t*-$BuNH_2$] provide linear correlations that have the same slope; therefore, the catalytic reaction is zeroth-order in amine. Finally, plots of $\ln[PhMeSiH_2]$ versus time at different [$To^{M}MgMe$] provide linear correlations that do not have the same slope (Figure 4-1), and a plot of the k_{obs} values obtained under these conditions versus [$To^{M}MgMe$] provides a linear relationship indicating the catalytic reaction is first-order in magnesium (Figure 4-2). Therefore, the overall catalytic reaction is second-order with the rate law given in (Eq. 4-3), with $k' = 0.060(4)\ M^{-1}\ s^{-1}$ at 335 K.

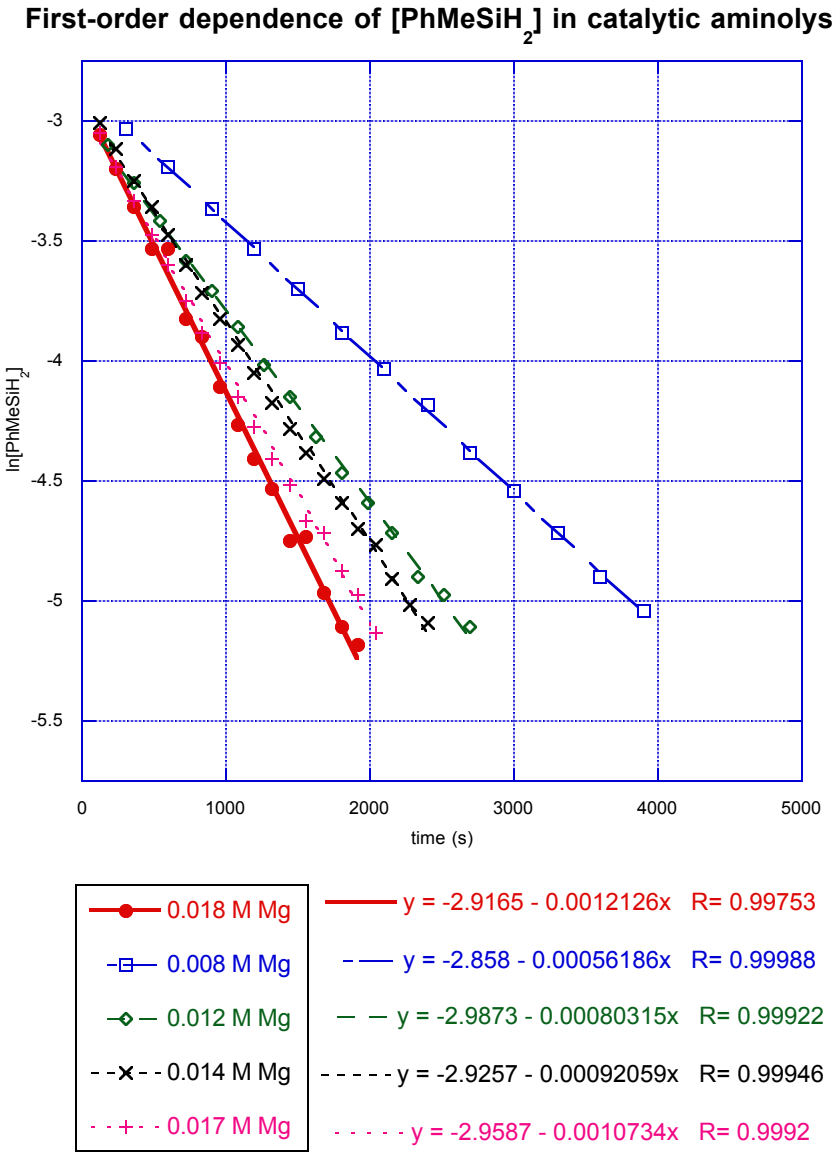

Figure 4-1. Plots of ln[$PhMeSiH_2$] versus time showing first-order dependence for the $To^{M}MgMe$ catalyzed reaction of $PhMeSiH_2$ and *t*-$BuNH_2$ (benzene-d_6, 335 K). Each set of data represents a particular catalyst concentration ranging from 0.008 M to 0.018 M; reactions were performed in the presence of a large excess of *t*-$BuNH_2$ (~ 1.2 M). The curves are linear least-squares best fits of the data to the equation ln[$PhMeSiH_2$] = constant + $k_{obs}t$.

$$-\frac{d[\mathrm{PhMeSiH_2}]}{dt} = k'[\mathrm{To^M MgNH}t\text{-Bu}]^1[\mathrm{PhMeSiH_2}]^1[t\text{-BuNH}_2]^0$$

(Eq. 4-3)

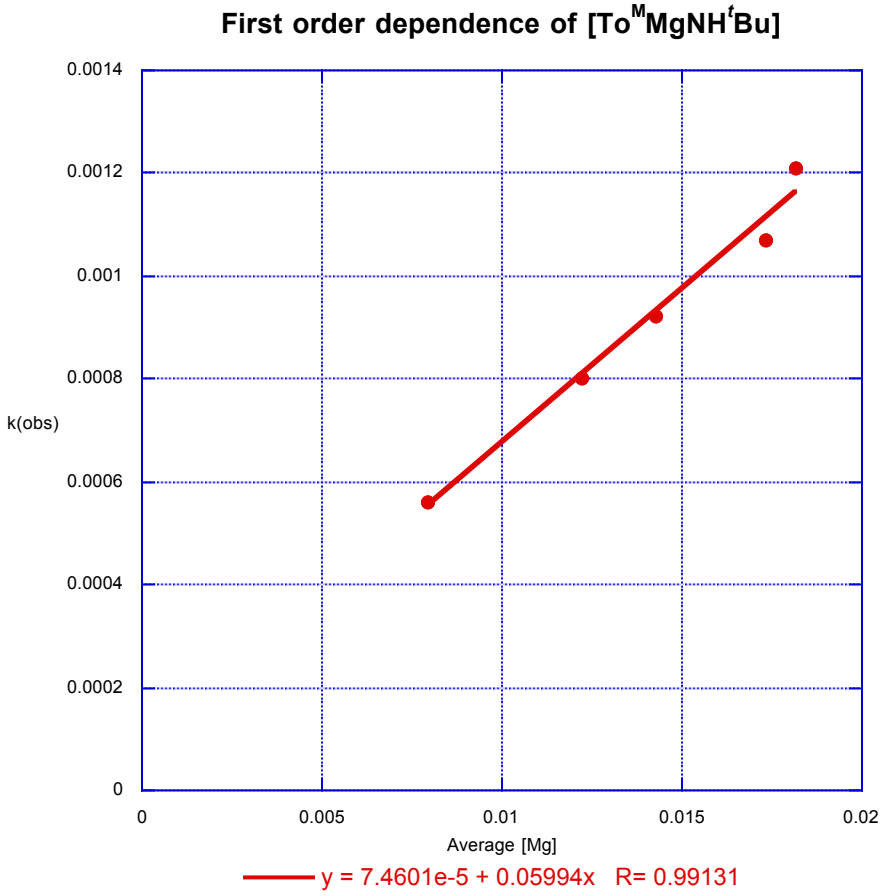

Figure 4-2. Plot of k_{obs} versus average [Mg] concentration showing the first-order dependence for the To^MMgMe catalyzed reaction of $PhMeSiH_2$ and *t*-$BuNH_2$ (benzene-d_6, 335 K). Each k_{obs} value is obtained from the plots of ln[$PhMeSiH_2$] versus time shown in **Figure 4-1**.

The rate law in (Eq. 4-3) indicates that the turnover-limiting step involves an interaction of the catalyst and $PhMeSiH_2$; zeroth-order dependence on the concentration of *tert*-butyl amine denotes that it is not present in the turnover-limiting step. ^{1}H NMR spectra of the catalytic mixture contain only one set of To^M resonances corresponding to To^MMgNH^tBu, thus suggesting that To^MMgNH^tBu is the catalyst resting state. These

observations are consistent with the general mechanism shown in Scheme 4-1, in which both steps are irreversible, and the reaction between To^{M}MgNHtBu and PhMeSiH$_2$ is turnover-limiting. The correlation between the *k*' value obtained from under catalytic conditions (0.060 $M^{-1}\cdot s^{-1}$) and the calculated value for k_{obs} in the stoichiometric reaction between To^{M}MgNH^{t}Bu and PhMeSiH$_2$ (k_{obs} = 0.04 $M^{-1}\cdot s^{-1}$ at 335 K; obtained from a linear regression analysis of a plot of ln(*k*/T) versus 1/T) is significant because it validates the use of the stoichiometric reaction between To^{M}MgNH^{t}Bu and PhMeSiH$_2$ as a model of the overall catalytic cycle.

Electronic studies on Si–N bond formation

A few studies probing electronic effects in σ-bond metathesis have shown small changes in rate with electron-donating or electron-withdrawing groups, consistent with small polarization in the transition state.[39] Similarly small electronic effects were observed in the [2σ + 2π] four-center transition state of styrene insertion into Zr–H bonds [Figure 4-3; ρ = –0.46(1)], whereas β-elimination provides a large negative ρ value of –1.8(5) and large KIEs (k_H/k_D = 3.9 to 4.5).[40] The aryl group is pendent from the β-position of the four-center transition state in both of these transformations.

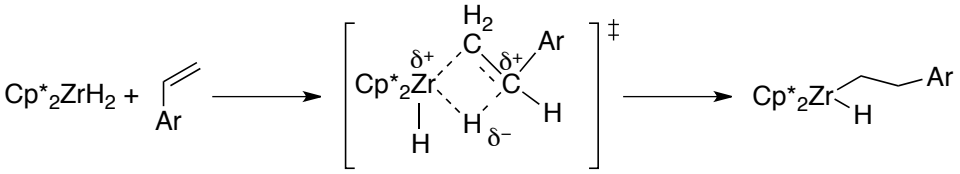

Figure 4-3. Styrene insertion via σ-bond metathesis

Second-order rate constants were determined for the reaction of To^{M}MgNH^{t}Bu and several Ph(aryl)SiH$_2$ (aryl = Ph, *p*-FC_6H_4, *p*-$CH_3C_6H_4$, *p*-$OCh_3C_6H_4$, *p*-$CF_3C_6H_4$). For all Ph(aryl)SiH$_2$ except *p*-$CF_3C_6H_4$, the rate constants used were average values determined from second-order integrated rate law plots of ln{[Ph(*p*-

$XC_6H_4)SiH_2]/[To^MMgNH^tBu]\}$ versus time (X = OCH_3, Me, H, F) for reactions at 313 K. For Ph(*p*-$CF_3C_6H_4$)SiH_2, the rate constant was calculated from an Eyring plot (see Figure 4-5 in the experimental section) for reactions measured over the range 245 K to 304 K because the rate at 313 K was sufficiently high to require verification.

The organosilanes with electron-withdrawing groups react more rapidly than those with electron-donating groups. A Hammett plot (Figure 4-4) of $\log(k_X/k_H)$ versus σ_p[41] provides a positive slope (ρ = 1.4). Thus, the activation barrier is decreased with electron-withdrawing substituents on silicon. This effect is consistent with a reaction pathway involving a five-coordinate silicon species $To^MMgH^tBuN–SiPh(aryl)H_2$ that is stabilized by electron-withdrawing groups. Importantly, the magnitude of the inductive electronic effect is less consistent with a concerted bond-breaking and bond-forming process; electron-withdrawing groups are expected to have counteracting effects on bond formation and bond cleavage by simultaneously increasing the barrier for hydride transfer to magnesium while stabilizing the five-coordinate silicon center. The temperature-independent primary isotope effect of unity further supports little Si–H bond cleavage in the transition state.

Based on the kinetic data, we suggest that these reactions involve nucleophilic attack of the amide on silicon to form a five-coordinate silicon center in the rate-determining step, which is followed by rapid hydrogen transfer to magnesium in a step reminiscent of β-elimination (Scheme 4-1, Mechanism B).

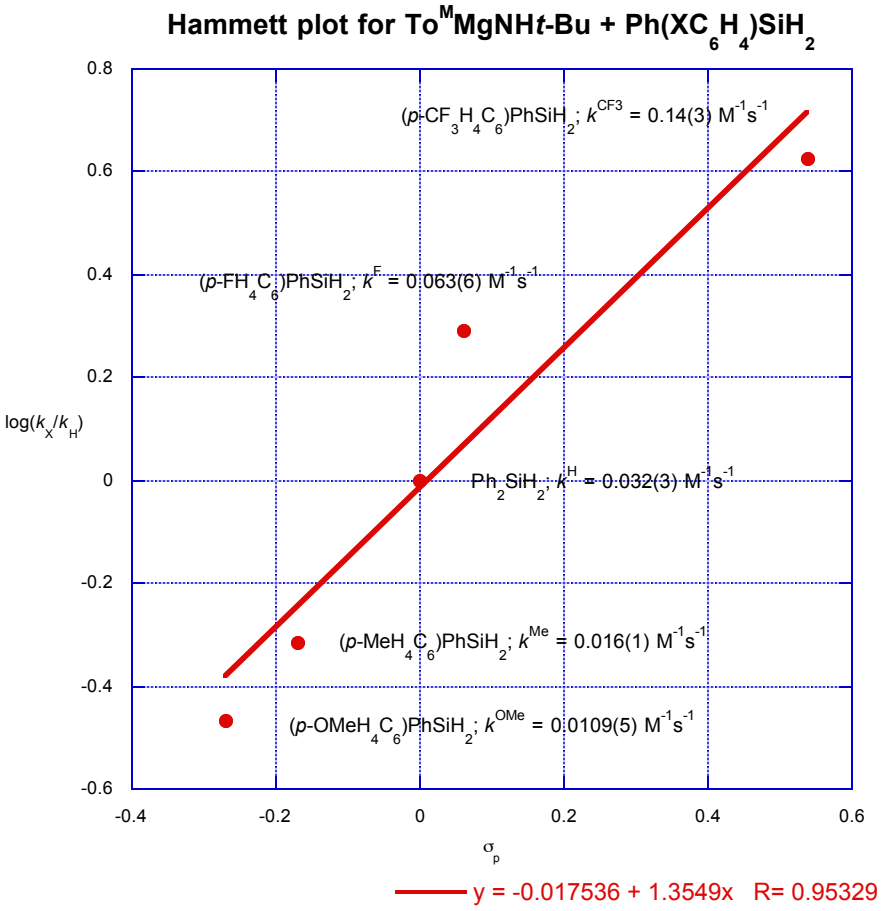

Figure 4-4. Hammett plot showing the reaction rate acceleration with electron-withdrawing groups on the silane for the reaction of To^{M}MgNH^{t}Bu and Ph(*p*-XH$_4$C$_6$)SiH$_2$. Each log (k_X/k_H) point represents the average k_{obs} value obtained from several runs.

Two additional observations suggest that this mechanism is more reasonable than the concerted four-centered transition-state-like pathway. First, the decrease in reaction rate for aniline versus *tert*-butyl amine is consistent with nucleophilic attack playing an important role in the rate-limiting step because aniline is less nucleophilic than *tert*-butyl amine. Second, zeroth-order amine concentration dependence was observed in the catalytic rate law even at very high concentrations with no evidence of inhibition by amine coordination. Thus, these reactions may be performed even in liquid NH_3. In

contrast, intermolecular σ-bond metathesis reactions require coordinative unsaturation and are inhibited by coordinating groups.[39, 42] Hydroamination studies from our lab, utilizing $To^{M}MgMe$ as the precatalyst, suggest that amines coordinate to the magnesium center in $To^{M}MgNHR$ compounds, either to give a five-coordinate magnesium or substitute an oxazoline.[24, 43] Thus, the zeroth-order amine dependence (rather than an inverse dependence) suggests that an open coordination site is not important in the current Si–N bond formation.

Synthesis of magnesium amides

Micromolar scale reactions involving $To^{M}MgMe$ and *n*-propyl amine give methane and a single new To^{M} species with ^{1}H NMR chemical shifts at 3.56 and 1.13 ppm for the oxazolinyl methylene and methyl moieties respectively. One set of amide resonances is also observed at 2.51 α-CH_2, 1.37 β-CH_2, 0.86 CH_3, and -0.94 ppm NH (Eq. 4-4). However, a solid precipitate forms, and the To^{M} resonances disappear from the ^{1}H NMR spectrum of the reaction mixture upon standing for one hour. A white solid that is insoluble in benzene is isolated in larger scale reactions. An IR spectrum of the white solid exhibits diagnostic ν_{CN} bands for the oxazoline rings at 1627, 1594, and 1565 cm^{-1}. The presence of multiple ν_{CN} bands is typical for a bidentate To^{M} species ($[\kappa^2\text{-}To^{M}]_2Mg$, ν_{CN} 1602 and 1555 cm^{-1}).[24] Thorough washing and drying of the solid material provides analytically pure material consistent with the empirical formula for $To^{M}MgNH(n\text{-}C_3H_7)$. Because $To^{M}MgNH(n\text{-}C_3H_7)$ is insoluble in benzene-d_6, it is not monomeric in solution and thus not suitable for kinetic studies. $To^{M}MgNH(n\text{-}C_3H_7)$ likely exists as a dimer based on previous experiments with hydroamination substrates and the formation of dimeric $[(\kappa^2\text{-}To^{M})MgNHCH_2C(CH_2)_5CH_2CH{=}CH_2]_2$.[44]

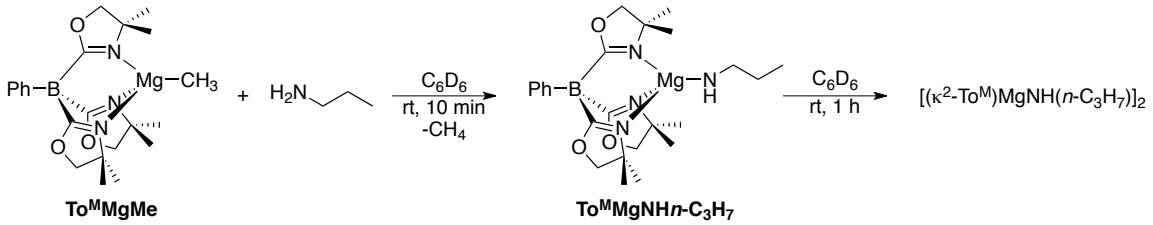

$To^{M}MgMe$ **$To^{M}MgNHn\text{-}C_3H_7$**

(Eq. 4-4)

$To^{M}MgNH(i\text{-}C_3H_7)$ is also a presumed intermediate in the catalytic cycle for Si–N bond formation. The reaction between $To^{M}MgMe$ and isopropyl amine produces methane and a new To^{M} species as evidenced by ^1H NMR spectroscopy (Eq. 4-5). To^{M} resonances at 3.52 (CH_2) and 1.08 ppm (CH_3) and amide resonances at 3.87 (CH), 1.54 (CH_3), and -0.26 ppm (NH) indicate that the species is pseudo-C_{3v} symmetric in solution. Unfortunately, the compound precipitates upon standing for two hours and all To^{M} resonances disappear from the ^1H NMR spectrum of the reaction mixture. Preparative scale reactions provide a white solid that is insoluble in benzene, similar to the reaction with *n*-propyl amine. The IR spectrum of the white solid also contains three ν_{CN} bands at 1625, 1594, and 1565 cm^{-1}. Elemental microanalysis provides an empirical formula consistent with $To^{M}MgNH(i\text{-}C_3H_7)$.

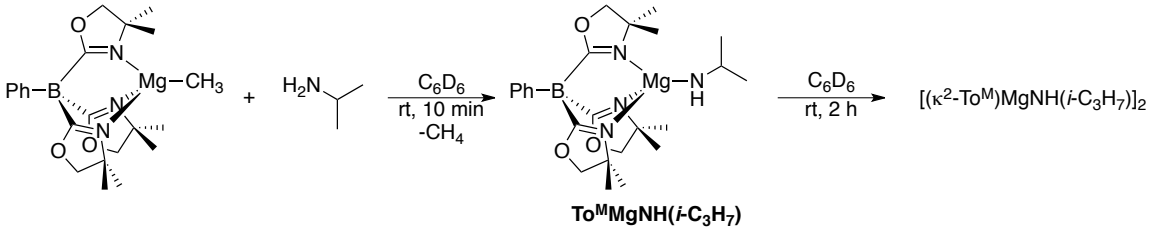

$To^{M}MgNH(i\text{-}C_3H_7)$

(Eq. 4-5)

The reaction of $To^{M}MgMe$ and aniline in benzene-d_6 provides $To^{M}MgNHPh$ in quantitative yield (Eq. 4-6). After several hours, $To^{M}MgNHPh$ remains in solution. The ^1H NMR spectrum in benzene-d_6 contains resonances attributed to a pseudo-C_{3v} symmetric

species with one set of To^M resonances at 3.36 (CH_2) and 0.97 ppm (CH_3). Upon standing overnight, the resonances corresponding to To^MMgNHPh decrease and only broad, uninterpretable resonances are present which is consistent with decomposition. Additionally, preparative scale reactions provide impure samples of To^MMgNHPh, and the isolated solid gradually darkens over the course of a day. Thus, To^MMgNHPh appears unstable under a nitrogen atmosphere. Aniline is described as being light sensitive and changes color upon decomposition (similar to the color change observed for To^MMgNHPh). Therefore, the stability of To^MMgNHPh in the absence of light was investigated. Performing a micromolar scale reaction between To^MMgMe and aniline while keeping the NMR tube wrapped in foil to exclude light affords To^MMgNHPh in quantitative yield as expected. The ^{1}H NMR spectrum does not change upon standing for several days in the absence of light. Likewise, isolated To^MMgNHPh is robust at room temperature if protected from light.

The origin of the light sensitivity is of interest because, to the best our knowledge, there are no examples of light sensitive metal–anilides in the literature. To^MMgNHPh is a white solid and shouldn't absorb visible light. Therefore, the absorption properties of To^MMgNHPh were studied. The UV-Vis spectrum in benzene contains one absorption band at 325 nm (ϵ = 2,376 M^{-1} cm^{-1}); this band is believed to arise from a $\pi \rightarrow \pi^*$ transition involving aniline.

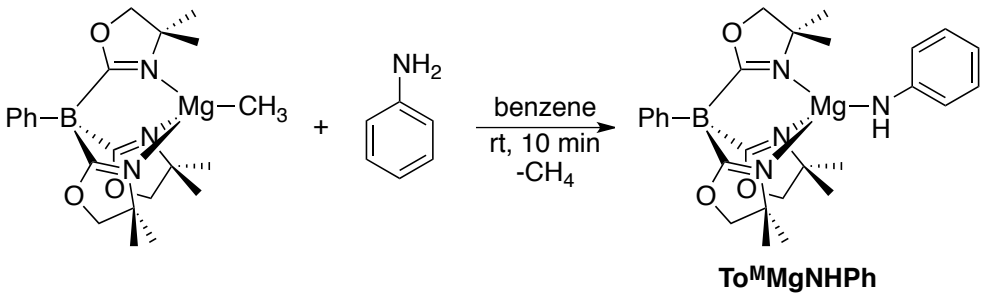

To^MMgNHPh

(Eq. 4-6)

Based on the success in generating a Hammett plot for the reaction between $To^{M}MgNH^{t}Bu$ and substituted organosilanes, a similar investigation with substituents on the aniline moiety could provide additional support for the nucleophilic attack mechanism. Therefore, the synthesis of a series of anilides ($To^{M}MgNH(p\text{-}XC_6H_4)$; X = OCH_3, CH_3, Cl, CF_3) was initiated. Reactions of $To^{M}MgMe$ and either *para*-toluidine or *para*-chloroaniline give methane and single pseudo-C_{3v} symmetric, tridentate-To^{M} species (Eq. 4-7). The ^1H NMR spectrum of each compound is similar to $To^{M}MgNHPh$ with one set of oxazoline methyl and methylene resonances at 1.00 and 3.39 ppm for $To^{M}MgNH(p\text{-}CH_3C_6H_4)$ and 0.92 and 3.35 ppm for $To^{M}MgNH(p\text{-}ClC_6H_4)$ respectively. Both compounds are robust at room temperature in the absence of light.

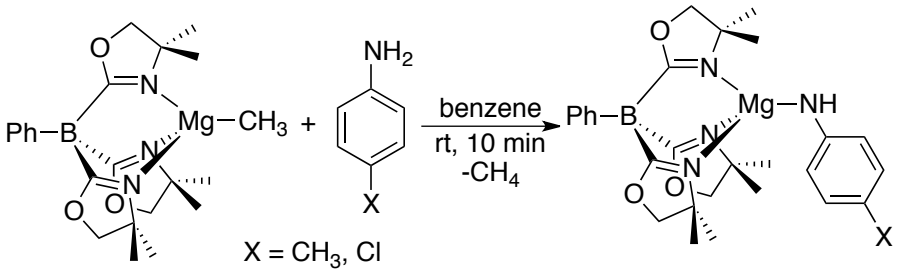

(Eq. 4-7)

The reaction of $To^{M}MgMe$ and anisidine produces a strikingly different product. The anticipated tridentate-To^{M} species was not observed; instead, the ^1H NMR spectrum contained five distinct sets of oxazoline resonances. There were five singlet resonances in the methyl region (0.9 and 1.5 ppm) and five resonances in the methylene region (3.25 to 3.70 ppm). One methylene resonance is a singlet while the other four are doublets with a relative integration of 2:1:1:1:1. Meanwhile, there is only one set of boron-bound aryl resonances and one set of anilide resonances. This data is consistent with a C_1 symmetric, bidentate-To^{M} species that likely exists as a binuclear dimer (Eq.

4-8). Due to the asymmetric substitution on magnesium, the inner and outer methyl/methylene hydrogens on the bound oxazoline rings are inequivalent.

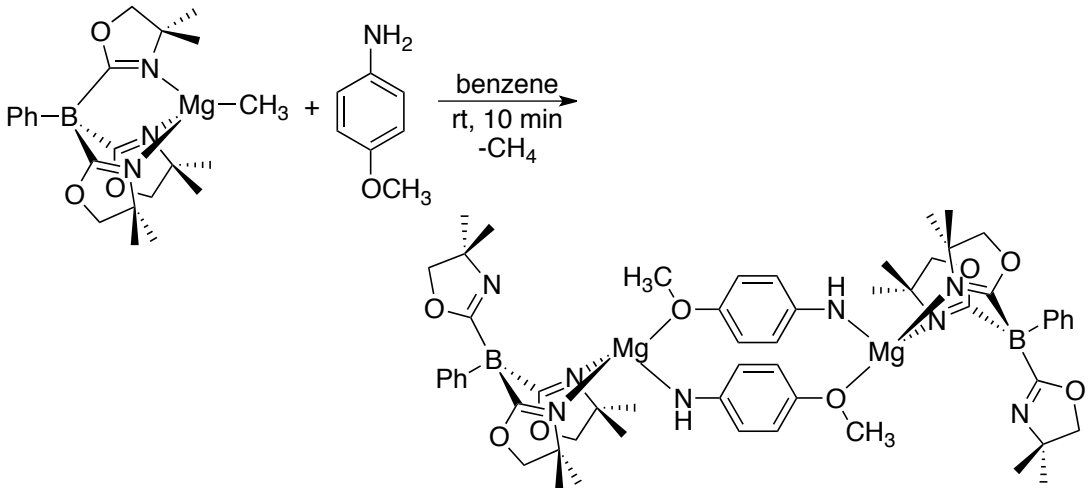

(Eq. 4-8)

Unfortunately, attempts to isolate X-ray quality crystals have been unsuccessful. Based on the lack of dimerization with other aniline derivatives (Ph, *p*-$CH_3C_6H_4$, *p*-ClC_6H_4), the dimerization of $To^MMgNH(p\text{-}OCH_3C6H_4)$ likely occurs through the *para*-methoxy substituent forming the 14-membered dimagnesium macrocycle (Eq. 4-8). A variable temperature NMR study reveals that the dimer remains intact at 60 °C, thus making $To^MMgNH(p\text{-}OCH_3C_6H_4)$ unsuitable for use in the Hammett plot.

A micromolar scale reaction between To^MMgMe and (*p*-trifluoromethyl)aniline produces methane and a new To^M species consistent with $To^MMgNH(p\text{-}CF_3C_6H_4)$. The ^1H NMR spectrum contained one set of To^M resonances; however, upon standing for 10 minutes, a bright orange solid precipitates from solution and all To^M resonances disappear from the ^1H NMR spectrum. Unfortunately, the synthesis of $To^MMgNHAr$ complexes for a Hammett plot was abandoned because a suitable quantity of anilides was unavailable.

More acidic amines were sought in order to expand the scope of amine cross-dehydrocoupling,. $To^{M}MgMe$ reacts with indole at room temperature to produce $To^{M}MgN(C_8H_6)$ in 94% yield (Eq. 4-9). The ^1H NMR spectrum in benzene-d_6 contains one set of To^{M} resonances at 0.98 ppm (CH_3), and 3.34 ppm (CH_2) and is consistent with a pseudo-C_{3v} symmetric structure. Only starting materials are observed when a benzene solution of $To^{M}MgN(C_8H_6)$ and $PhSiH_3$ are heated to 80 °C for several days. The lack of reactivity with secondary amines using $To^{M}MgMe$ as the precatalyst is not unprecedented; diphenylamine undergoes only one turnover with $PhSiH_3$ while diisopropylamine is inert to $PhSiH_3$.

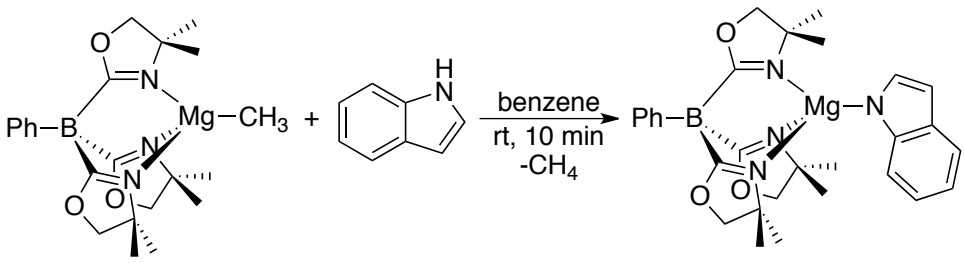

(Eq. 4-9)

A primary amine that is more acidic than aniline was studied due to the lack of reactivity between secondary amines and silanes. $To^{M}MgMe$ reacts with *para*-toluenesulfonamide in benzene at room temperature over eight hours to yield $To^{M}MgNHTs$ in 96% yield (Eq. 4-10). The long reaction time is likely needed because *para*-toluenesulfonamide exhibits low solubility in benzene. $To^{M}MgNHTs$ is pseudo-C_{3v} symmetric in solution with ^1H NMR resonances at 1.12 (CH_3) and 3.44 ppm (CH_2) for To^{M}. A micromolar scale reaction between $To^{M}MgNHTs$ with $PhMeSiH_2$ at 80 °C for two days provides no Si–N dehydrocoupled product, and the ^1H NMR spectrum of the stoichiometric reaction mixture contains only starting materials. For comparison,

$To^{M}MgNHPh$ reacts with $PhMeSiH_2$ under stoichiometric conditions within one day at 60 °C.

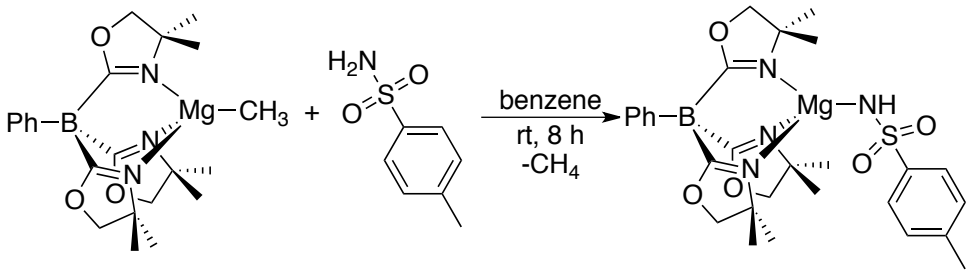

(Eq. 4-10)

Attempted cross-dehydrocoupling to form other Si–E bonds

$To^{M}ZnH$ catalyzes the cross-dehydrocoupling of alcohols and organosilanes to form the corresponding silyl ethers.[45] In light of our success with silazane formation, we were interested to investigate the possibility of $To^{M}MgOR$ compounds as catalysts for this transformation. Using $To^{M}MgMe$ as the precatalyst, the reactivity of aliphatic and aromatic alcohols with $PhSiH_3$ was surveyed. In all cases, protonolysis of $To^{M}MgMe$ was rapid. ^1H NMR spectra of reaction mixtures (prior to addition of silane) contain only resonances for free alcohol and a new To^{M} species. The resonances for the new To^{M} species integrate correctly for the anticipated alkoxide, $To^{M}MgOR$. No change in the ^1H NMR spectrum of the catalytic reaction mixtures is observed upon addition of $PhSiH_3$, and heating the micromolar scale reaction at 80 °C for several days does not promote Si–O bond formation.

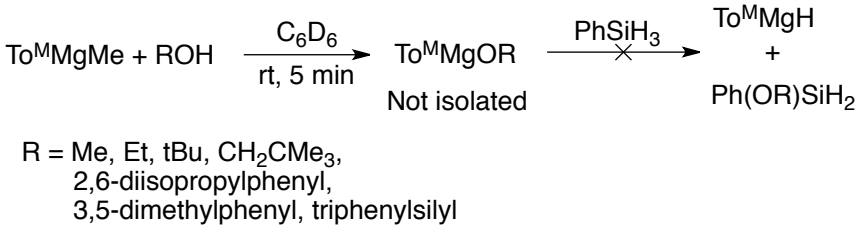

(Eq. 4-11)

For all alcohols, except methanol and ethanol, the To^{M}MgOR species that are formed upon protonolysis of To^{M}MgMe remain soluble in benzene-d_6. None of the alkoxides have been isolated, but their ^{1}H NMR spectra display pseudo-C_{3v} symmetry in solution. Samples of To^{M}MgOR (R = Me, Et) do not remain in solution upon protonolysis of To^{M}MgMe with alcohol. ^{1}H NMR spectra indicate they are initially pseudo-C_{3v} symmetric but a white precipitate forms rapidly leaving only broad, uninterpretable resonances. This is consistent with physical and spectroscopic properties observed with To^{M}MgNHR (R = *n*-propyl, isopropyl, *tert*-butyl, Ph) where the *n*-propyl and isopropyl amides dimerize rapidly and precipitate from the benzene-d_6 solution while the larger *tert*-butyl and phenyl amides remain soluble and pseudo-C_{3v} symmetric in benzene-d_6.

Expanding to row three elements, we next looked at magnesium-phosphorus bond formation and subsequent cross-dehydrocoupling with silane. Reacting To^{M}MgMe with phenylphosphine at room temperature yields To^{M}MgPHPh in 75% yield (Eq. 4-12). Unexpectedly, the protonolysis of To^{M}MgMe is much slower with $PhPH_2$ than with $PhNH_2$. The ^{1}H NMR spectrum of To^{M}MgPHPh is very similar to that of To^{M}MgNHPh with a doublet resonance for the P–H at 3.16 ppm ($^{1}J_{PH}$ = 173 Hz). The $^{31}P\{^{1}H\}$ NMR spectrum contains only one resonance at -135.8 ppm.

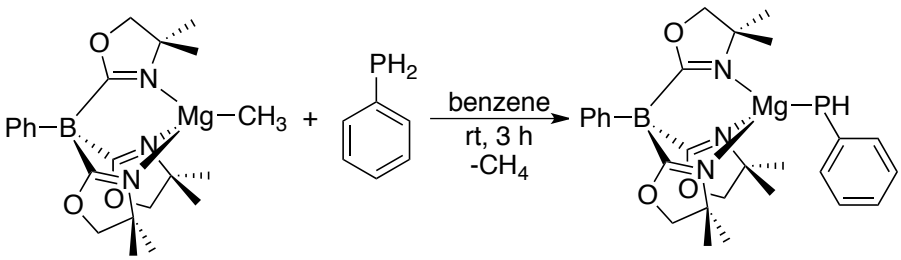

(Eq. 4-12)

No P–Si bond formation is observed in a room temperature reaction between $PhPH_2$ and $PhSiH_3$ in the presence of 10 mol % To^{M}MgMe. ^{1}H and $^{31}P\{^{1}H\}$ NMR spectra

of reaction mixture only contain resonances for $PhPH_2$, $PhSiH_3$, and $To^MMgPHPh$. Heating the reaction mixture for two days at 120 °C produces two small ^{31}P NMR resonances at -141 and -192 ppm along with two small Si-H signals in the ^1H NMR spectrum at 5.6 and 4.7 ppm. The signals at -141 ppm in the $^{31}P\{^1H\}$ NMR spectrum and 4.7 ppm in the ^1H NMR spectrum correlated to the reported values for $PhHP-SiH_2Ph$.[46] The other species is tentatively assigned as $PhP(SiH_2Ph)_2$; this assignment is based on $^2J_{PH}$ coupling (21 Hz) observed in the ^1H NMR spectrum for the SiH resonance at 5.6 ppm. Suppressing the phosphorus coupling by acquiring a $^1H\{^{31}P\}$ NMR spectrum results in a singlet for the SiH resonance at 5.6 ppm, thus supporting the assignment of $PhP(SiH_2Ph)_2$. However, neither species could be formed in large enough quantities to be isolated or characterized.

To^MMgMe reacts with MeSH (1 atmosphere) to produce methane and To^MMgSMe in 60 % yield (Eq. 4-13). The ^1H NMR in benzene-d_6 supports a pseudo-C_{3v} symmetric structure in solution as indicated by the presence of only one resonance each for the oxazoline methyl, sulfide methyl, and oxazoline methylene hydrogens at 1.06, 2.49, and 3.39 ppm. There is no change in the ^1H NMR spectrum upon heating a solution of To^MMgSMe in benzene-d_6 or allowing the NMR sample to stand overnight. This indicates that, unlike the oxygen analog To^MMgOMe, To^MMgSMe remains a monomer in solution. Only starting materials are evident in the ^1H NMR spectrum of a reaction mixture of To^MMgSMe and $PhSiH_3$. Heating the solution for two days at 120 °C produces no change in the ^1H NMR spectrum.

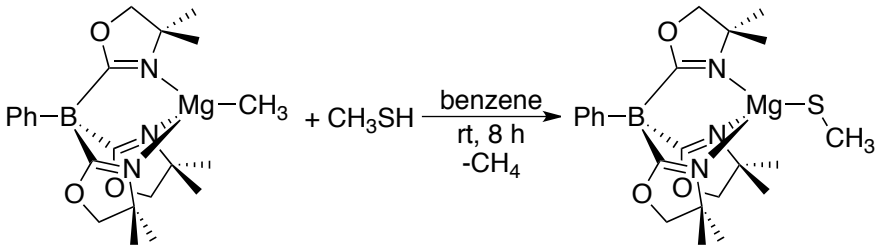

(Eq. 4-13)

Conclusion

To^{M}MgMe was previously shown to be a viable precatalyst for the cross-dehydrocoupling of N–H bonds with Si–H bonds; in particular, primary aliphatic amines and aniline have shown high reactivity with organosilanes in the presence of To^{M}MgMe as the precatalyst. Previous stoichiometric kinetic studies on Si–N bond formation in conjunction with newly acquired kinetic data for the overall catalytic cycle and insight gained through a Hammett plot of *para*-substituted silanes has provided evidence supporting a nucleophilic attack mechanism in which the turnover-limiting step involves the nucleophilic attack of the magnesium amide at the silicon center. The contrasting reactivity of To^{M}MgNH^{t}Bu and To^{M}MgNHTs toward silane is intriguing, while To^{M}MgNH^{t}Bu is more bulky than To^{M}MgNHTs, the former reacts rapidly with $PhMeSiH_2$ while the latter does not react with $PhMeSiH_2$.

The viability of To^{M} supported magnesium complexes for Si–E (E = O, P, S) bond formation has also been investigated. In situ generated To^{M}MgOR complexes are inert to reactions with silane but display interesting spectroscopic characteristics similar to those observed for To^{M}MgNHR complexes. Smaller aliphatic alkoxides/amides readily precipitate from solution and are speculated to be dimeric/oligomeric in the solid state, while larger aliphatic and aromatic alkoxides/amides remain pseudo-C_{3v} symmetric and soluble in benzene-d_6. Isolated To^{M}MgSMe displays no reactivity with silane, but differs

significantly from in situ generated To^{M}MgOMe because it remains soluble in benzene-d_6 and thus likely monomeric. While isolated To^{M}MgPHPh does appear to react with $PhSiH_3$, very little dehydrocoupling product is detected. According to our observations and mechanistic model for Si–N bond formation, an increase in nucleophilicity from aniline to *tert*-butyl amine results in an increase in reaction rate. However, the differing reactivity between Mg–N and Mg–P bonds toward dehydrocoupling with silanes is very interesting as the translation down the periodic table, in the same family, usually indicates an increase in nucleophilicity.

Experimental

General. All reactions were performed under an inert atmosphere using standard Schlenk techniques or in a glovebox unless otherwise indicated. All glassware was pre-treated with a solution of 10% trimethylchlorosilane in chloroform, rinsed with water and acetone, and dried overnight in an oven. Dry, oxygen-free solvents were used throughout. Benzene, toluene, pentane, diethyl ether, and tetrahydrofuran were degassed by sparging with nitrogen, filtered through activated alumina columns, and stored under N_2. Dioxane was dried over purple Na/benzophenone, distilled, and stored under N_2. Benzene-d_6 and toluene-d_8 were vacuum transferred from Na/K alloy and stored under N_2 in the glovebox. Dichlorophenylmethylsilane and dichlorodiphenylsilane were purchased from Gelest and reduced with $LiAlH_4$ to their corresponding silanes. LiCl used to synthesize the substituted silanes was dried overnight in an oven and pumped into the glovebox while hot and stored under N_2. Grignards used to synthesize the substituted silanes were either purchased from Aldrich or prepared according to standard procedure using I_2 to activate the magnesium. To^{M}MgMe was prepared according to the published procedure.[24] Ph(p-$OCH_3C_6H_4$)SiH_2,[47] Ph(p-$CH_3C_6H_4$)SiH_2,[48]

Ph(*p*-FC_6H_4)SiH_2,[49] and Ph(*p*-$CF_3C_6H_4$)SiH_2 were synthesized following analogous literature procedures and compared to available literature data.[50] All other reagents were purchased from standard suppliers and used as received.

^1H, $^{13}C\{^1H\}$, ^{11}B, ^{19}F, $^{29}Si\{^1H\}$, and $^{31}P\{^1H\}$ NMR spectra were collected on a Bruker DRX400 spectrometer, Agilent MR400 spectrometer, or Bruker Avance III 600 spectrometer with a Bruker BBFO SmartProbe. ^{11}B NMR spectra were referenced to an external sample of $BF_3{\cdot}Et_2O$, ^{19}F NMR spectra were referenced to an external sample of $C_6H_5CF_3$, and $^{31}P\{^1H\}$ spectra were referenced to an external sample of H_3PO_4. ^{15}N chemical shifts were determined either by ^1H–^{15}N CIGARAD experiments on the Agilent spectrometer or ^1H-^{15}N HMBC experiments on the Bruker Avance spectrometer; ^{15}N chemical shifts were originally referenced to liquid NH_3 and recalculated to the CH_3NO_2 chemical shift scale by adding -381.9 ppm. Elemental analyses were performed using a Perkin-Elmer 2400 series II CHN/S by the Iowa State Chemical Instrumentation Facility. Accurate mass ESI mass spectrometry was performed using the Agilent QTOF 6530 equipped with the Jet Stream ESI source. An Agilent ESI test mix was used for tuning and calibration. Accurate mass data was obtained in the positive ion mode using a reference standard with ions at 121.05087 and 922.00979. The mass resolution (FWHM) was maintained at 18,000.

To^{M}MgNH(*n*-C_3H_7). Monomeric To^{M}MgNH(*n*-C_3H_7) is soluble in benzene and generated as follows: To^{M}MgMe (0.015 g, 0.036 mmol) was dissolved in 0.6 mL of benzene-d_6 and added to an NMR tube. Propylamine (0.002 mL, 0.024 mmol) was added. Formation of To^{M}MgNH(*n*-C_3H_7) was evident after 10 minutes. ^1H NMR (benzene-d_6, 600 MHz): δ 7.99 (d, $^3J_{HH}$ = 7.2 Hz, 2 H, *ortho*-C_6H_5), 7.41 (t, $^3J_{HH}$ = 7.2 Hz, 2 H, *meta*-C_6H_5), 7.22 (t, $^3J_{HH}$ = 7.2 Hz, 1 H, *para*-C_6H_5), 3.56 (s, 6 H, $CNCMe_2CH_2O$), 2.51 (quint, J_{HH} = 7.5 Hz, 2

H, NHC*H*$_2$CH$_2$CH$_3$), 1.37 (sextet, $^3J_{HH}$ = 7.5 Hz, 2 H, NHCH$_2$C*H*$_2$CH$_3$), 1.13 (s, 18 H, CNC*Me*$_2$CH$_2$O), 0.86 (t, $^3J_{HH}$ = 7.5 Hz, 3 H, NHCH$_2$CH$_2$C*H*$_3$), -0.94 (t, $^3J_{HH}$ = 7.5 Hz, N*H*CH$_2$CH$_2$CH$_3$). ^{13}C{^{1}H} NMR (benzene-d_6, 150 MHz, determined from a ^{1}H-^{13}C HMQC experiment): δ 134.3 (*ortho*-C$_6$H$_5$), 127.4 (*meta*-C$_6$H$_5$), 125.8 (*para*-C$_6$H$_5$), 78.3 (CNCMe$_2$*C*H$_2$O), 48.2 (NH*C*H$_2$CH$_2$CH$_3$), 31.9 (NHCH$_2$*C*H$_2$CH$_3$), 29.0 (CNC*Me*$_2$CH$_2$O), 11.7 (NHCH$_2$CH$_2$*C*H$_3$).

[To^{M}MgNH(*n*-C$_3$H$_7$)]$_n$. To^{M}MgMe (0.076 g, 0.180 mmol) was dissolved in 2 mL of benzene, and propylamine (0.030 mL, 0.365 mmol) was added. The solution was allowed to stand for 2 h during which time a white precipitate formed. The solution was decanted, and the white solid was washed with pentane (2 × 1 mL) and dried under vacuum to yield [To^{M}MgNH(*n*-C$_3$H$_7$)]$_n$ (0.063 g, 0.136 mmol, 75%). IR (KBr, cm^{-1}): 3035 w, 2963 s, 2930 m, 2883 m, 1627 sh (ν_{CN}), 1594 s (ν_{CN}), 1565 s (ν_{CN}), 1462 m, 1430 w, 1365 m, 1267 m, 1197 m, 1152 m, 1100 w, 1064 w, 1003 m, 966 w, 892 w, 840 w, 809 w, 752 w, 713 m, 701 sh, 656 s, 594 w. Anal. Calc. for C$_{24}$H$_{37}$BMgN$_4$O$_3$: C, 62.03; H, 8.03; N, 12.06. Found C, 62.05; H, 7.83; N, 10.95. mp 205-210 °C (dec).

To^{M}MgNH(*i*-C$_3$H$_7$). The generation and isolation of To^{M}MgNH(*i*-C$_3$H$_7$) follows that of To^{M}MgNH(*n*-C$_3$H$_7$). To^{M}MgMe (0.010 g, 0.024 mmol) was dissolved in 0.6 mL of benzene-d_6 and added to an NMR tube. Isopropylamine (0.0023 mL, 0.027 mmol) was added. Formation of pseudo-C_{3v} symmetric To^{M}MgNH(*i*-C$_3$H$_7$) was evident after 10 minutes. ^{1}H NMR (benzene-d_6, 600 MHz): δ 8.08 (d, $^3J_{HH}$ = 7.2 Hz, 2 H, *ortho*-C$_6$H$_5$), 7.46 (t, $^3J_{HH}$ = 7.4 Hz, 2 H, *meta*-C$_6$H$_5$), 7.45 (t, $^3J_{HH}$ = 7.4 Hz, 1 H, *para*-C$_6$H$_5$), 3.87 (m, 1 H, NHC*H*Me$_2$), 3.52 (s, 6 H, CNCMe$_2$C*H*$_2$O), 1.54 (d, $^3J_{HH}$ = 6.0 Hz, 6 H, NHCH*Me*$_2$), 1.08 (s, 18 H, CNC*Me*$_2$CH$_2$O), -0.26 (br, N*H*CHMe$_2$). ^{13}C{^{1}H} NMR (benzene-d_6, 150

MHz, determined from a ^{1}H-^{13}C HMQC experiment): δ 134.4 (*ortho*-C_6H_5), 127.7 (*meta*-C_6H_5), 125.9 (*para*-C_6H_5), 80.4 ($CNCMe_2CH_2O$), 34.1 ($NHCHMe_2$), 28.4 ($CNCMe_2CH_2O$).

$[To^{M}MgNH(i\text{-}C_3H_7)]_n$. Upon standing, a solution of monomeric $To^{M}MgNH(i\text{-}C_3H_7)$ precipitates to give isolable, insoluble material following the procedure: $To^{M}MgMe$ (0.048 g, 0.116 mmol) was dissolved in 2 mL of benzene, and isopropylamine (0.020 mL, 0.233 mmol) was added. The solution was allowed to stand for 2 h during which time a white precipitate formed. The solution was decanted, and the white solid was washed with pentane (2 × 1 mL) and dried under vacuum to yield $[To^{M}MgNH(i\text{-}C_3H_7)]_n$ (0.042 g, 0.090 mmol, 78%). The structural change upon precipitation is evident from the IR spectrum that shows a C_s symmetric tris(oxazolinyl)borate ligand. IR (KBr, cm^{-1}): 3035 w, 2964 s, 2884 m, 1625 sh (ν_{CN}), 1594 s (ν_{CN}), 1565 s (ν_{CN}), 1463 m, 1431 w, 1365 m, 1267 m, 1197 m, 1152 m, 1065 w, 1006 m, 966 s, 893 w, 840 w, 810 w, 768 w, 749 w, 702 m, 664 s, 638 s, 596 w. Anal. Calc. for $C_{24}H_{37}BMgN_4O_3(0.5\ C_6H_6)$: C, 64.38; H, 8.00; N, 11.12. Found C, 64.45; H, 8.02; N, 11.25. mp 210-212 °C (dec).

$To^{M}MgNHC_6H_5$. $To^{M}MgMe$ (0.073 g, 0.174 mmol) was dissolved in 2 mL of benzene, and aniline (0.030 mL, 0.329 mmol) was added. The solution was allowed to stir for 1 h in the absence of light. All volatile materials were removed under vacuum to yield an off-white solid of $To^{M}MgNHC_6H_5$ (0.081 g, 0.163 mmol, 93.5%). ^{1}H NMR (benzene-d_6, 400 MHz): δ 8.26 (d, $^{3}J_{HH}$ = 7.2 Hz, 2 H, *ortho*-C_6H_5), 7.54 (t, $^{3}J_{HH}$ = 7.6 Hz, 2 H, *meta*-C_6H_5), 7.36 (t, $^{3}J_{HH}$ = 7.6 Hz, 1 H, *para*-C_6H_5), 7.32 (t, $^{3}J_{HH}$ = 7.6 Hz, *meta*-NH-C_6H_5), 6.87 (d, $^{3}J_{HH}$ = 7.6 Hz, 2 H, *ortho*-NH-C_6H_5), 6.68 (t, $^{3}J_{HH}$ = 7.6 Hz, 1 H, *para*-NH-C_6H_5), 3.36 (s, 6 H, $CNCMe_2CH_2O$), 3.21 (s, 1 H, N*H*), 0.97 (s, 18 H, $CNCMe_2CH_2O$). $^{13}C\{^{1}H\}$ NMR (benzene-d_6, 100 MHz): δ 192.17 (br, $CNCMe_2CH_2O$), 160.58 (*ipso*-NHC_6H_5), 142.4 (br, *ipso*-BC_6H_5), 136.37 (*ortho*-BC_6H_5), 130.18 (*meta*-NHC_6H_5), 127.25 (*meta*-BC_6H_5), 126.36 (*para*-BC_6H_5), 116.68 (*ortho*-NHC_6H_5), 112.30 (*para*-NHC_6H_5), 80.54

(CNCMe$_2$*C*H$_2$O), 65.69 (CN*C*Me$_2$CH$_2$O), 28.50 (CNC*Me$_2$*CH$_2$O). ^{11}B NMR (benzene-d_6, 128 MHz): δ -18.1. ^{15}N NMR (benzene-d_6, 41 MHz): δ -159.1 (C*N*CMe$_2$CH$_2$O), -303.0 (*N*HC$_6$H$_5$). IR (KBr, cm^{-1}): 2963 w, 2835 w, 1594 s (ν_{CN}), 1497 w, 1465 w, 1365 w, 1349 w, 1267 m, 1197 m, 1152 m, 965 m, 891 w, 810 w, 747 w, 702 m, 657 m, 637 m. UV-Vis (benzene, nm): 325 (ϵ = 2376 M^{-1} cm^{-1}). Anal. Calc. for C$_{27}$H$_{35}$BMgN$_4$O$_3$: C, 65.03; H, 7.07; N, 11.23. Found: C, 64.50; H, 7.02; N, 11.32. mp 190-192 °C (dec).

To^{M}MgNH(*p*-CH$_3$C$_6$H$_4$). To^{M}MgMe (0.202 g, 0.479 mmol) was added to a vial and dissolved in 5 mL of benzene. *para*-Toluidine (0.103 g, 0.96 mmol) was dissolved in 3 mL of benzene and transferred to the vial; gas evolution was observed immediately. The solution was allowed to stir for 1 h in the absence of light. The solution was filtered, and all volatiles were removed under vacuum to yield an off-white solid. Recrystallization from toluene at -30 °C yielded To^{M}MgNH(*p*-CH$_3$C$_6$H$_4$) as a white, light sensitive solid (0.080 g, 0.156 mmol, 33 % yield). ^{1}H NMR (benzene-d_6, 400 MHz): δ 8.23 (d, $^3J_{HH}$ = 7.2 Hz, 2 H, *ortho*-C$_6$H$_5$), 7.50 (t, $^3J_{HH}$ = 7.6 Hz, 2 H, *meta*-C$_6$H$_5$), 7.32 (t, $^3J_{HH}$ = 7.3 Hz, 1 H, *para*-C$_6$H$_5$), 7.08 (d, $^3J_{HH}$ = 8.0 Hz, 2 H, MgNH(*p*-CH$_3$C$_6$H$_4$, *meta*-NH)), 6.78 (d, $^3J_{HH}$ = 8.1 Hz, 2 H, MgNH(*p*-CH$_3$C$_6$H$_4$, *ortho*-NH)), 3.39 (s, 6 H, CNCMe$_2$C*H$_2$*O), 3.09 (s, 1 H, N*H*), 2.33 (s, 3 H, NHC$_6$H$_4$C*H$_3$*), 1.00 (s, 18 H, CNC*Me$_2$*CH$_2$O). ^{13}C{^{1}H} NMR (benzene-d_6, 100 MHz): δ 192.20 (br, *C*NCMe$_2$CH$_2$O), 158.16 (MgNH(*p*-CH$_3$C$_6$H$_4$, *ipso*-NH)), 142.6 (br, *ipso*-C$_6$H$_5$), 136.37 (*ortho*-C$_6$H$_5$), 130.69 (MgNH(*p*-CH$_3$C$_6$H$_4$, *meta*-NH)) , 127.24 (*meta*-C$_6$H$_5$), 126.34 (*para*-C$_6$H$_5$), 120.08 (MgNH(*p*-CH$_3$C$_6$H$_4$, *ipso*-CH$_3$)), 116.51 (MgNH(*p*-CH$_3$C$_6$H$_4$, *ortho*-NH)), 80.55 (CNCMe$_2$*C*H$_2$O), 65.71 (CN*C*Me$_2$CH$_2$O), 28.51 (CNC*Me$_2$*CH$_2$O), 21.12 (MgNH(*p*-*C*H$_3$C$_6$H$_4$)). ^{11}B NMR (benzene-d_6, 128 MHz): δ -18.18 (br, s). ^{15}N NMR (benzene-d_6, 41 MHz): δ -159.5 (C*N*CMe$_2$CH$_2$O), -307.0 (Mg*N*H(*p*-CH$_3$C$_6$H$_4$)). IR (KBr, cm^{-1}): 3043 w, 2965 s, 1583 s (ν_{CN}), 1505 s, 1462 w, 1388 w, 1367 m, 1351 m, 1298 s, 1198 s, 1107 w, 964 s, 846 w, 811 m, 759 w, 747 w, 704 m, 654 m,

637 m, 619 w. Anal. Calc. for $C_{28}H_{37}O_3N_4BMg$: C, 65.59; H, 7.27; N, 10.93. Found: C, 65.45; H, 7.25; N, 10.98. mp 153-155 °C (dec).

To^{M}MgNH(*p*-ClC$_6$H$_4$). To^{M}MgMe (0.078 g, 0.185 mmol) was added to a vial and dissolved in 5 mL of benzene. 4-Chloroaniline (0.038 g, 0.296 mmol) was dissolved in 3 mL of benzene and transferred to the vial. The solution was allowed to stir for 1 h in the absence of light. The solution was filtered, and all volatiles were removed under vacuum to yield a white solid. Recrystallization from toluene at -30 °C yielded To^{M}MgNH(*p*-ClC$_6$H$_4$) as a white, light sensitive solid (0.025 g, 0.046 mmol, 25 % yield). ^{1}H NMR (benzene-d_6, 600 MHz): δ 8.24 (d, $^3J_{HH}$ = 6.9 Hz, 2 H, *ortho*-C$_6$H$_5$), 7.54 (t, $^3J_{HH}$ = 7.5 Hz, 2 H, *meta*-C$_6$H$_5$), 7.36 (tt, $^3J_{HH}$ = 7.3 Hz, $^4J_{HH}$ = 1.2 Hz, 1 H, *para*-C$_6$H$_5$), 7.22 (d, $^3J_{HH}$ = 8.6 Hz, MgNH(*p*-ClC$_6$H$_4$, *meta*-NH), 6.60 (d, $^3J_{HH}$ = 8.8 Hz, 2 H, MgNH(*p*-ClC$_6$H$_4$, *ortho*-NH)), 3.35 (s, 6 H, CNCMe$_2$C*H$_2$*O), 3.11 (s, 1 H, MgN*H*(*p*-ClC$_6$H$_4$)), 0.921 (s, 18 H, CNC*Me$_2$*CH$_2$O). ^{13}C{^{1}H} NMR (benzene-d_6, 151 MHz): δ 192.6 (br, *C*NCMe$_2$CH$_2$O), 159.14 (MgNH(*p*-ClC$_6$H$_4$, *ipso*-NH)), 142.1 (br, *ipso*-C$_6$H$_5$), 136.33 (*ortho*-C$_6$H$_5$), 129.89 (MgNH(*p*-ClC$_6$H$_4$, *meta*-NH)), 127.31 (*meta*-C$_6$H$_5$), 126.48 (*para*-C$_6$H$_5$), 117.51 (MgNH(*p*-ClC$_6$H$_4$, *ortho*-NH)), 116.17 (MgNH(*p*-ClC$_6$H$_4$, *ipso*-Cl)), 80.51 (CNCMe$_2$*C*H$_2$O), 65.61 (CN*C*Me$_2$CH$_2$O), 28.47 (CNC*Me$_2$*CH$_2$O). ^{11}B NMR (benzene-d_6, 193 MHz): δ -18.24 (br, s). ^{15}N NMR (benzene-d_6, 61 MHz): δ -303.3 (Mg*N*H(*p*-ClC$_6$H$_4$)), -159.9 (C*N*CMe$_2$CH$_2$O). IR (KBr, cm^{-1}): 2963 s, 2885 w, 1594 s (ν_{CN}), 1494 s, 1366 w, 1302 w, 1269 m, 1197 m, 1155 m, 965 m, 892 w, 814 w, 746 w, 702 w, 669 w, 638 w. Anal. Calc. for $C_{27}H_{34}O_3N_4BMg$: C, 60.82; H, 6.43; N, 10.51. Found: C, 60.27; H, 6.36; N, 10.45. mp 160-163 °C (dec).

To^{M}MgNH(*p*-OCH$_3$C$_6$H$_4$). To^{M}MgMe (0.212 g, 0.500 mmol) was added to a vial and dissolved in 5 mL of benzene. Anisidine (0.123 g, 1.00 mmol) was dissolved in 3 mL of benzene and transferred to the vial; gas evolution was observed immediately. The

solution was allowed to stir for 1 h in the absence of light. The solution was filtered, and all volatiles were removed under vacuum to yield an off-white solid. Recrystallization from toluene at -30 °C yielded $To^{M}MgNH(p\text{-}OCH_3\text{-}C_6H_4)$ as a white, light sensitive solid (0.049 g, 0.091 mmol, 18 % yield). ^{1}H NMR (benzene-d_6, 600 MHz): δ 8.10 (d, $^{3}J_{HH}$ = 7.0 Hz, 2 H, *ortho*-C_6H_5), 7.44 (t, $^{3}J_{HH}$ = 7.5 Hz, 2 H, *meta*-C_6H_5), 7.25 (t, $^{3}J_{HH}$ = 7.3 Hz, 1 H, *para*-C_6H_5), 6.72 (d, $^{3}J_{HH}$ = 8.8 Hz, 2 H, MgNH(*p*-$OCH_3C_6H_4$, *meta*-NH), 6.33 (d, $^{3}J_{HH}$ = 8.5 Hz, 2 H, MgNH(*p*-$OCH_3C_6H_4$, *ortho*-NH), 3.69 (s, 3 H, pendant, $CNCMe_2CH_2O$), 3.48 (d, $^{2}J_{HH}$ = 8.4 Hz, 1 H, ring B-bound, $CNCMe_2CH_2O$), 3.37 (s, 3 H, MgNH(*p*-$OCH_3C_6H_4$)), 3.34 (d, $^{2}J_{HH}$ = 8.4 Hz, 1 H, ring A-bound, $CNCMe_2CH_2O$), 3.30 (d, $^{2}J_{HH}$ = 8.4 Hz, 1 H, ring B-bound, $CNCMe_2CH_2O$), 3.29 (d, $^{2}J_{HH}$ = 8.4 Hz, 1 H, ring A-bound, $CNCMe_2CH_2O$), 2.67 (br, 1 H, NH), 1.30 (br, s, 9 H, pendant, $CNCMe_2CH_2O$), 1.30 (br, s, 3 H, ring B-bound, $CNCMe_2CH_2O$), 1.23 (s, 3 H, ring A-bound, $CNCMe_2CH_2O$), 1.11 (s, 3 H, ring B-bound, $CNCMe_2CH_2O$), 0.93 (s, 3 H, ring A-bound, $CNCMe_2CH_2O$). $^{13}C\{^{1}H\}$ NMR (benzene-d_6, 151 MHz): δ 196.0 (ring A-bound, $CNCMe_2CH_2O$), 194.6 (ring B-bound, $CNCMe_2CH_2O$), 176.4 (pendant, $CNCMe_2CH_2O$), 153.58 (MgNH(*p*-$OCH_3C_6H_4$, *ipso*-OCH_3), 147.6 (br, *ipso*-C_6H_5), 141.14 (MgNH(*p*-$OCH_3C_6H_4$, *ipso*-NH), 134.49 (*ortho*-C_6H_5), 127.71 (*meta*-C_6H_5), 126.07 (*para*-C_6H_4), 116.69 (MgNH(*p*-$OCH_3C_6H_4$, *ortho*-NH), 115.42 (MgNH(*p*-$OCH_3C_6H_4$, *meta*-NH), 79.01 (ring B-bound, $CNCMe_2CH_2O$), 78.48 (ring A-bound, $CNCMe_2CH_2O$), 77.31 (pendant, $CNCMe_2CH_2O$), 68.29 (pendant, $CNCMe_2CH_2O$), 66.84 (ring B-bound, $CNCMe_2CH_2O$), 66.16 (ring A-bound, $CNCMe_2CH_2O$), 55.60 (OCH_3), 29.50 (pendant, $CNCMe_2CH_2O$), 28.94 (ring B-bound, $CNCMe_2CH_2O$), 28.86 (ring B-bound, $CNCMe_2CH_2O$), 28.30 (ring A-bound, $CNCMe_2CH_2O$), 26.44 (ring A-bound, $CNCMe_2CH_2O$). ^{11}B NMR (benzene-d_6, 193 MHz): δ -16.86 (br, s). ^{15}N NMR (benzene-d_6, 61 MHz): δ -121.3 (pendant, $CNCMe_2CH_2O$), -171.8 (ring B-bound, $CNCMe_2CH_2O$), -172.1 (ring A-bound, $CNCMe_2CH_2O$). IR (KBr, cm^{-}

^{1}): 3068 w, 3043 w, 2966 s, 2932 m, 2883 m, 2832 w, 1595 s (ν_{CN}), 1556 s (ν_{CN}), 1512 s, 1464 s, 1369 w, 1360 w, 1275 m, 1239 s, 1197 m, 1181 w, 1150 m, 1031 w, 1000 m, 967 s, 892 w, 827 w, 744 w, 710 m, 652 w, 593 w. Anal. Calc. for $C_{28}H_{37}O_4N_4BMg$: C, 63.60; H, 7.05; N, 10.60. Found: C, 63.66; H, 6.78; N, 10.58. mp 110-115 °C (dec).

To^{M}MgN(C_8H_6). To^{M}MgMe (0.117 g, 0.278 mmol) was dissolved in 5 mL of benzene. Solid indole (0.032 g, 0.277 mmol) was added, and the solution was stirred for 5 min. The cloudy solution was filtered, and the solvent removed under vacuum. To^{M}MgN(C_6H_8) was isolated as a white solid (0.136 g, 0.260 mmol, 94 %). ^{1}H NMR (benzene-d_6, 400 MHz): δ 8.24 (d, $^{2}J_{HH}$ = 7.2 Hz, 2 H, *ortho*-C_6H_5), 8.14 (d, $^{2}J_{HH}$ = 7.6 Hz, 1 H, C_6H_8, H4), 7.85 (d, $^{2}J_{HH}$ = 8.0 Hz, 1 H, C_6H_8, H7), 7.79 (d, $^{2}J_{HH}$ = 2.4 Hz, 1 H, C_6H_8, H2), 7.54 (t, $^{2}J_{HH}$ = 7.6 Hz, 2 H, *meta*-C_6H_5), 7.43 (t, $^{2}J_{HH}$ = 8.0 Hz, 1 H, C_6H_8, H6), 7.38 (t, $^{2}J_{HH}$ = 7.2 Hz, 1 H, C_6H_8, H5), 7.36 (t, $^{2}J_{HH}$ = 7.2 Hz, 1 H, *para*-C_6H_5), 7.14 (d, $^{2}J_{HH}$ = 2.0 Hz, 1 H, C_6H_8, H3), 3.34 (s, 6 H, CNCMe$_2$C*H$_2$*O), 0.89 (s, 18 H, CNC*Me$_2$*CH$_2$O). ^{13}C{^{1}H} NMR (benzene-d_6, 100 MHz): δ 192.52 (br, *C*NCMe$_2$CH$_2$O), 146.67 (C_6H_8, C8), 142.04 (br, *ipso*-C_6H_5), 136.35 (*ortho*-C_6H_5), 134.92 (C_6H_8, C2), 132.51 (C_6H_8, C9), 127.33 (*meta*-C_6H_5), 126.53 (*para*-C_6H_5), 121.33 (C_6H_8, C4), 119.34 (C_6H_8, C6), 118.45 (C_6H_8, C5), 115.23 (C_6H_8, C7), 103.12 (C_6H_8, C3), 80.71 (CNCMe$_2$*C*H$_2$O), 65.84 (CN*C*Me$_2$CH$_2$O), 28.46 (CNC*Me$_2$*CH$_2$O). ^{11}B NMR (benzene-d_6, 128 MHz): δ -18.18. ^{15}N NMR (benzene-d_6, 41 MHz): δ -160.3 (C*N*CMe$_2$CH$_2$O). IR (KBr, cm^{-1}): 3043 w, 2963 s, 2929 m, 2884 m, 1595 s (ν_{CN}), 1577 s, 1495 w, 1463 m, 1444 m, 1385 w, 1367 m, 1351 m, 1268 s, 1196 s, 1156 s, 963 s, 933 m, 894 w, 839 w, 812 w, 744 s, 704 s, 657 s, 638 s. Anal. Calc. for $C_{29}H_{35}O_3N_4BMg$: C, 66.63; H, 6.75; N, 10.72. Found: C, 66.94; H, 6.34; N, 10.37. mp 118-122 °C (dec).

To^{M}MgNHTs. To^{M}MgMe (0.105 g, 0. 25 mmol) was added to a vial and dissolved in 5 mL of benzene. Solid *p*-toluenesulfonamide (0.045 g, 0.27 mmol) was added to the vial,

and methane was observed immediately. The suspension was allowed to stir for 8 h then filtered. The solvent was removed under vacuum to yield To^{M}MgNHTs (0.138 g, 0.24 mmol, 96%) as a white solid. ^{1}H NMR (benzene-d_6, 400 MHz): δ 8.37 (d, $^{3}J_{HH}$ = 6.8 Hz, 2 H, *ortho*-C_6H_5), 8.04 (d, $^{3}J_{HH}$ = 8.4 Hz, 2 H, NHTs), 7.56 (t, $^{3}J_{HH}$ = 6.8 Hz, 2 H, *meta*-C_6H_5), 7.37 (t, $^{3}J_{HH}$ = 6.8 Hz, 1 H, *para*-C_6H_5), 6.88 (d $^{3}J_{HH}$ = 8.0 Hz, 2 H, NHTs), 3.44 (s, 6 H, CNCMe$_2$C*H$_2$*O), 3.03 (br, s, 1 H, NH), 1.95 (s, 3 H, NHTs, C*H$_3$*), 1.12 (s, 18 H, CNC*Me$_2$*CH$_2$O). ^{13}C{^{1}H} NMR (benzene-d_6, 151 MHz): δ 191.53 (br, *C*NCMe$_2$CH$_2$O), 143.9 (br, *ipso*-C_6H_5), 143.9 (NHTs, *ipso*-SO_2), 141.7 (NHTs, *ipso*-Me) 136.57 (*ortho*-C_6H_5), 129.66 (NHTs, *meta*-SO_2), 127.15 (*meta*-C_6H_5), 126.99 (NHTs, *ortho*-SO_2), 126.14 (*para*-C_6H_5), 80.60 (CNCMe$_2$*C*H$_2$O), 66.02 (CN*C*Me$_2$CH$_2$O), 28.34 (CNC*Me$_2$*CH$_2$O), 21.42 (NHTs, *C*H$_3$). ^{11}B NMR (benzene-d_6, 128 MHz): δ -18.04. ^{15}N NMR (benzene-d_6, 61 MHz): δ 223.8 (C*N*CMe$_2$CH$_2$O). IR (KBr, cm^{-1}): 3317 m (ν_{NH}), 3039 w, 2968 s, 2928 m, 2891 m, 1588 s (ν_{CN}), 1496 w, 1462 m, 1386 w, 1367 w, 1351 w, 1251 br s, 1193 s, 1158 s, 1119 s, 1088 s, 1022 s, 972 w, 894 w, 841 w, 814 m, 745 w, 703 m, 681 s, 638 m. Anal. Calc. for $C_{28}H_{37}O_5N_4SBMg$: C, 58.30; H, 6.47; N, 9.71; S, 5.56. Found: C, 58.13; H, 6.54; N, 9.76; S, 5.60. mp 212-217 °C (dec).

To^{M}MgPHPh. To^{M}MgMe (0.090 g, 0.214 mmol) was added to a vial and dissolved in 5 mL of benzene. Phenylphosphine (0.060 mL, 0.545 mmol) was added to the vial, and the solution was allowed to stir overnight. The solution was filtered, and all volatiles were removed under vacuum to yield an off-white solid. Recrystallization from toluene at -30 °C yielded To^{M}MgPHPh as a white solid (0.083 g, 0.161 mmol, 75 % yield). ^{1}H NMR (benzene-d_6, 600 MHz): δ 8.23 (d, $^{3}J_{HH}$ = 4.5 Hz, 2 H, *ortho*-C_6H_5), 7.72 (m, 2 H, MgPHPh, *ortho*), 7.51 (t, $^{3}J_{HH}$ = 7.7 Hz, 2 H, *meta*-C_6H_5), 7.34 (tt, $^{3}J_{HH}$ = 7.3 Hz, $^{4}J_{HH}$ = 1.3 Hz, 1 H, *para*-C_6H_5), 7.08 (t, $^{3}J_{HH}$ = 7.3 Hz, 2 H, MgPHPh, *meta*), 6.91 (t, $^{3}J_{HH}$ = 7.4 Hz, 1 H, MgPHPh, *para*), 3.35 (s, 6 H, CNCMe$_2$C*H$_2$*O), 3.16 (d, $^{1}J_{PH}$ = 173.5 Hz, 1 H,

MgP*H*Ph), 0.94 (s, 18 H, CNC*Me*$_2$CH$_2$O). ^{13}C{^{1}H} NMR (benzene-d_6, 151 MHz): δ 192.2 (br, *C*NCMe$_2$CH$_2$O), 145.73 (d, $^1J_{PC}$ = 30.2 Hz, MgPHPh, *ipso*), 142.2 (*ipso*-C$_6$H$_5$), 136.37 (*ortho*-C$_6$H$_5$), 132.40 (d, $^2J_{PC}$ = 14.6 Hz, MgPHPh, *ortho*), 128.68 (MgPHPh, *meta*), 127.25 (*meta*-C$_6$H$_5$), 126.41 (*para*-C$_6$H$_5$), 122.97 (MgPHPh, *para*), 80.64 (CNCMe$_2$*C*H$_2$O), 65.61 (CN*C*Me$_2$CH$_2$O), 28.43 (CNC*Me*$_2$CH$_2$O). ^{11}B NMR (benzene-d_6, 193 MHz): δ -18.24 (br, s). ^{15}N NMR (benzene-d_6, 61 MHz): δ -159.0 (C*N*CMe$_2$CH$_2$O). ^{31}P{^{1}H} NMR (benzene-d_6, 243 MHz): δ -135.86. IR (KBr, cm^{-1}): 3056 w, 2968 m, 2926 w, 2895 w, 2257 m (ν_{PH}), 1586 s (ν_{CN}), 1460 w, 1431 w, 1387 w, 1368 w, 1352 w, 1271 m, 1194 m, 1159 w, 1024 w, 956 s, 894 w, 842 w, 815 w, 741 w, 708 w, 675 w, 659 w, 638 w, 619 w. Anal. Calc. for C$_{27}$H$_{35}$O$_3$N$_3$PBMg: C, 62.89; H, 6.84; N, 8.15. Found: C, 63.23; H, 6.84; N, 8.23. mp 98-100 °C (dec).

To^{M}MgSMe. To^{M}MgMe (0.248 g, 0.588 mmol) was dissolved in 20 mL of benzene and transferred to a flask with a Teflon seal. The solution was degassed via three freeze-pump-thaw cycles then one atmosphere of methylmercaptan was added. The solution was allowed to stir overnight then filtered, and the solvent was removed under vacuum to yield To^{M}MgSMe. Recrystallization from toluene at -30 °C yielded pure To^{M}MgSMe as a white solid (0.159 g, 0.350 mmol, 60 %). ^{1}H NMR (benzene-d_6, 600 MHz): δ 8.25 (d, $^3J_{HH}$ = 7.0 Hz, 2 H, *ortho*-C$_6$H$_5$), 7.53 (t, $^3J_{HH}$ = 7.7 Hz, 2 H, *meta*-C$_6$H$_5$), 7.35 (tt, $^3J_{HH}$ = 7.3 Hz, $^4J_{HH}$ = 1.4 Hz, 1 H, *para*-C$_6$H$_5$), 3.39 (s, 6 H, CNCMe$_2$C*H$_2$*O), 2.49 (s, 3 H, S*Me*), 1.06 (s, 18 H, CNC*Me*$_2$CH$_2$O). ^{13}C{^{1}H} NMR (benzene-d_6, 151 MHz): δ 192.34 (br, *C*NCMe$_2$CH$_2$O), 142.1 (br, *ipso*-C$_6$H$_5$), 136.38 (*ortho*-C$_6$H$_5$), 127.26 (*meta*-C$_6$H$_5$), 126.40 (*para*-C$_6$H$_5$), 80.64 (CNCMe$_2$*C*H$_2$O), 65.66 (CN*C*Me$_2$CH$_2$O), 28.53 (CNC*Me*$_2$CH$_2$O), 7.41 (br, S*Me*). ^{11}B NMR (benzene-d_6, 199 MHz): δ -18.17. ^{15}N NMR (benzene-d_6, 61 MHz): δ -159.16. IR (KBr, cm^{-1}): 3039 w, 2964 s, 2927 m, 2885 w, 1590 s, (ν_{CN}), 1492 w, 1432 w,

1384 w, 1365 w, 1351 w, 1269 s, 1195 s, 1152 s, 967 s, 894 w, 839 w, 810 w, 746 w, 704 m, 659 m, 638 m. Anal. Calc. for $C_{22}H_{32}O_3N_3SBMg$: C, 58.24; H, 7.11; N, 9.26; S, 7.07. Found: C, 57.94; H, 7.18; N, 9.26; S, 6.21. mp 165-170 °C (dec).

General procedure for Ph(*p*-XC_6H_4)SiH_2 synthesis.[50] *p*-XC_6H_4MgBr and LiCl (0.065 g, 1.53 mmol) were added to a Schlenk flask. THF (10 mL) was added and the solution was cooled to -20 °C. $PhSiH_3$ (0.60 mL, 4.86 mmol) in 2 mL of THF was slowly added to the stirring solution. The solution was allowed to stir at this temperature for 2 h. The reaction was quenched by the addition of aqueous NH_4Cl (5 mL). The suspension was filtered through Celite, which was subsequently washed with ca. 100 mL of diethyl ether. The organic phase was dried over Na_2SO_4, and the solvent was removed by rotary evaporation. The product was purified by either Kugelrohr distillation at 100 °C/0.1 mmHg or recrystallization.

Ph(*p*-$OCH_3C_6H_4$)SiH_2. *p*-$OCH_3C_6H_4MgBr$ (12.5 mL, 6.25 mmol) yielded Ph(*p*-$OCH_3C_6H_4$)SiH_2 (0.544 g, 2.54 mmol, 52.2%) after recrystallization from pentane/methanol. ^{1}H NMR (benzene-d_6, 400 MHz): δ 7.56 (m, 2 H, *ortho*-C_6H_5), 7.46 (d, $^3J_{HH}$ = 8.4 Hz, 2 H, *p*-$OCH_3C_6H_4$), 7.14 (br, m, 3 H, *para*- and *meta*-C_6H_5), 6.77 (d, $^3J_{HH}$ = 8.4 Hz, 2 H, *p*-$OCH_3C_6H_4$), 5.14 (s, $^1J_{SiH}$ = 197 Hz, 2 H, SiH), 3.45 (s, 3 H, O*C*H_3). $^{13}C\{^1H\}$ NMR (benzene-d_6, 100 MHz): δ 162.16 (*p*-$OCH_3C_6H_4$), 138.00 (*p*-$OCH_3C_6H_4$), 136.36 (*ortho*-C_6H_5), 132.77 (*ipso*-C_6H_5), 130.40 (*para*-C_6H_5), 128.78 (*meta*-C_6H_5), 122.42 (*p*-$OCH_3C_6H_4$), 114.81 (*p*-$OCH_3C_6H_4$), 54.88 (O*C*H_3). $^{29}Si\{^1H\}$ NMR (benzene-d_6, 79 MHz): δ -34.3.

Ph(*p*-$CH_3C_6H_4$)SiH_2. *p*-$CH_3C_6H_4MgBr$ (12.5 mL, 6.25 mmol) yielded Ph(*p*-$CH_3C_6H_4$)SiH_2 (0.535 g, 2.69 mmol, 55.3%) after distillation. ^{1}H NMR (benzene-d_6, 400 MHz): δ 7.57 (m, 2 H, *ortho*-C_6H_5), 7.49 (d, $^3J_{HH}$ = 7.5 Hz, 2 H, *p*-$CH_3C_6H_4$), 7.15 (m, 3 H, *para*- and

meta-C_6H_5), 7.00 (d, $^3J_{HH}$ = 7.5 Hz, 2 H, *p*-$CH_3C_6H_4$), 5.14 (s, $^1J_{SiH}$ = 198 Hz, 2 H, SiH), 2.08 (s, 3 H, CH_3). $^{13}C\{^1H\}$ NMR (benzene-d_6, 100 MHz): δ 140.33 (*p*-$CH_3C_6H_4$), 136.51 (*p*-$CH_3C_6H_4$), 136.37 (*ortho*-C_6H_5), 132.47 (*ipso*-C_6H_5), 130.40 (*para*-C_6H_5), 129.68 (*p*-$CH_3C_6H_4$), 128.77 (*meta*-C_6H_5), 127.56 (*p*-$CH_3C_6H_4$), 21.78 (s, CH_3). $^{29}Si\{^1H\}$ NMR (benzene-d_6, 79 MHz): δ -34.4.

Ph(*p*-FC_6H_4)SiH_2. *p*-FC_6H_4MgBr (4.8 mL, 4.8 mmol) yielded Ph(*p*-FC_6H_4)SiH_2 (0.215 g, 1.06 mmol, 22%) as a colorless oil after distillation. ^1H NMR (benzene-d_6, 400 MHz): δ 7.47 (d, $^3J_{HH}$ = 7.6 Hz, 2 H, *ortho*-C_6H_5), 7.27 (m, 2 H, *p*-FC_6H_4), 7.18 (d, $^3J_{HH}$ = 7.6 Hz, 1 H, *para*-C_6H_5), 7.14 (t, $^3J_{HH}$ = 7.6 Hz, 2 H, *meta*-C_6H_5), 6.79 (m, 2 H, *p*-FC_6H_4), 5.0 (s, $^1J_{SiH}$ = 199 Hz, 2 H, SiH). $^{13}C\{^1H\}$ NMR (benzene-d_6, 100 MHz): δ 165.07 (d, $^1J_{FC}$ = 249.7 Hz, *p*-FC_6H_4), 138.43 (d, $^3J_{FC}$ = 7.6 Hz, *p*-FC_6H_4), 136.29 (*ortho*-C_6H_5), 131.81 (*ipso*-C_6H_5), 130.62 (*para*-C_6H_5), 128.85 (*meta*-C_6H_5), 127.47 (d, $^4J_{FC}$ = 3.9 Hz, *p*-FC_6H_4), 116.01 (d, $^2J_{FC}$ = 19.7 Hz, *p*-FC_6H_4). ^{19}F NMR (benzene-d_6, 376 MHz): δ -110.22 (tt, $^3J_{HF}$ = 9.1 Hz, $^4J_{HF}$ = 6.0 Hz). $^{29}Si\{^1H\}$ NMR (benzene-d_6, 79 MHz): δ -34.7. IR (neat, cm^{-1}): 3068 w, 3022 w, 2141 s (ν_{SiH}), 1588 s, 1498 s, 1429 m, 1387 w, 1232 s, 1163 s, 1119 s, 936 s, 848 s, 820 s. MS (ESI) exact mass Calculated for $C_{12}H_{10}FSi$: m/z 201.0536 ([H^+-H_2]), Found: 201.0525 (Δ 2.66).

Ph(*p*-$CF_3C_6H_4$)SiH_2. Magnesium (0.148 g, 6.09 mmol) and LiCl (0.231 g, 5.45 mmol) were placed in a 100 mL Schlenk flask. The flask was heated at 130 °C under vacuum for 1 h. A crystal of iodine was added and the flask heated slightly under argon. THF (20 mL) was then added and the flask cooled to 0 °C. *p*-$CF_3C_6H_4Br$ was added dropwise via syringe. The red solution turned colorless initially upon addition of the aryl bromide then slowly turned dark red-orange. The flask was warmed to room temperature and stirred for 1.5 h. *p*-$CF_3C_6H_4MgBr$ was used in the general procedure with no additional LiCl

yielding Ph(*p*-$CF_3C_6H_4$)SiH_2 (0.830 g, 3.29 mmol, 67.7%) after distillation. ^{1}H NMR chemical shifts match reported values.[49]

Procedure for kinetic measurements

All kinetics measurements were conducted by monitoring the reaction with ^{1}H NMR spectroscopy using a Bruker DRX 400 MHz spectrometer. The reaction was monitored by taking a single ^{1}H NMR scans at regular preset intervals. Concentrations of the reactants and products were determined by integration of resonances corresponding to the species of interest and integration of a 1,3,5-trimethoxybenzene standard of known concentration. Stock solutions of 1,3,5-trimethoxybenzene (10 to 30 mM) in the appropriate solvent (benzene-d_6 or toluene-d_8) were prepared and used for a series of experiments and rate constants were obtained reproducibly through several batches of stock solutions. The NMR probe was pre-heated (or pre-cooled) to the desired temperature, and the probe temperature was calibrated using either an 80% ethylene glycol sample in 20% DMSO-d_6 for temperature over 300 K or a 100% methanol sample for temperatures under 300 K. The temperature was monitored during the course of the measurements using a thermocouple.

Procedure for catalytic Si–N measurements

In a typical experiment, 7 μmol To^{M}MgMe was dissolved in a 0.7 mL sample of a stock solution containing 1.0 M *t*-BuNH_2 and 50 mM Ph$MeSiH_2$ and added to a J. Young style NMR tube with a resealable Teflon valve. The solution was frozen in liquid nitrogen, and was only thawed immediately prior to being inserted into the NMR probe. Rate constants were obtained by a nonweighted linear least-squares regression analysis of the integrated first-order rate law:

$$\ln([\mathrm{PhMeSiH_2}]) = \text{constant} - kt$$

Procedure for Si–N Hammett measurements

In a typical experiment, 0.7 mL of a stock solution containing 10–20 mM To^{M}MgNH^{t}Bu was added to a septa capped NMR tube. The sample was inserted into the probe, locked, and shimmed. The sample was removed from the probe and placed in an ice bath at 0 °C. The appropriate silane was added via syringe through the septa cap. The NMR tube was quickly shaken and placed back in the probe. Rate constants were obtained by a nonweighted linear least-squares regression analysis of the integrated second-order rate law:

$$\ln\left(\frac{[\mathrm{Ph(aryl)SiH_2}]}{[\mathrm{To^{M}MgNH}t\text{-Bu}]}\right) = \ln\left(\frac{[\mathrm{Ph(aryl)SiH_2}]_0}{[\mathrm{To^{M}MgNH}t\text{-Bu}]_0}\right) + k\Delta_0 t$$

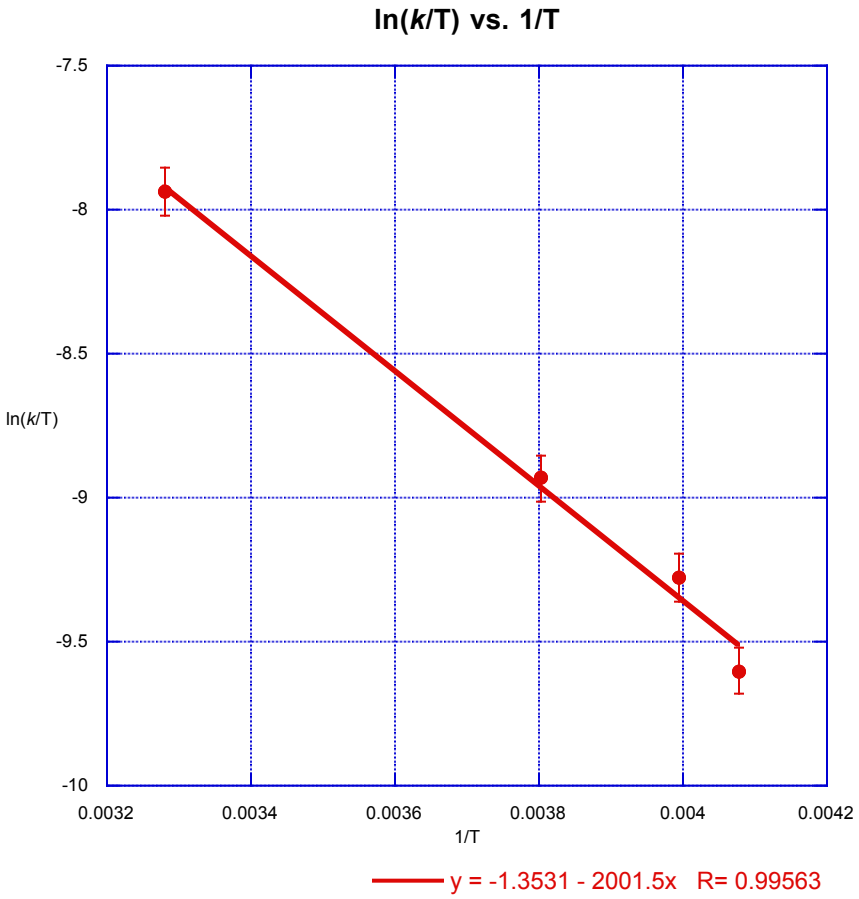

Figure 4-5. Plot showing the temperature dependence for the reaction of To^{M}MgNH^{t}Bu and Ph(*p*-$CF_3C_6H_4$)SiH_2 from 245 K to 304 K. Each ln(*k*/T) value is obtained from a linear-least squares fit of ln([Ph(*p*-$CF_3C_6H_4$)SiH_2]/[To^{M}MgNH^{t}Bu]) versus time.

References

1. Fieser, L. F.; Fieser, M., *Reagents in Organic Chemistry*. Wiley: New York, **1967**; Vol. 1.
2. Roth, C. A., *Product R&D* **1972,** *11* (2), 134-139.
3. Tanabe, Y.; Misaki, T.; Kurihara, M.; Iida, A.; Nishii, Y., *Chem. Commun.* **2002,** (15), 1628-1629.
4. Tanabe, Y.; Murakami, M.; Kitaichi, K.; Yoshida, Y., *Tetrahedron Lett.* **1994,** *35* (45), 8409-8412.
5. Iida, A.; Horii, A.; Misaki, T.; Tanabe, Y., *Synthesis* **2005,** *2005* (EFirst), 2677,2682.
6. Neugebauer, P.; Jaschke, B., *The Chemistry of Organic Silicon Compounds*. Wiley: Chichester, England, **1989**; Vol. 3.
7. Armitage, D. A., *The Silicon - Heteroatom Bond*. Wiley: Chichester, England, **1991**.
8. Sommer, L. H.; Citron, J. D., *J. Org. Chem.* **1967,** *32* (8), 2470-2472.

9. Blum, Y.; Laine, R. M., *Organometallics* **1986,** *5* (10), 2081-2086.
10. Chow, A. W.; Hamlin, R. D.; Blum, Y.; Laine, R. M., *J. Polym. Sci., Part C.: Polym. Lett.* **1988,** *26* (2), 103-108.
11. Laine, R. M., *Platinum Metals Rev.* **1988,** *32* (2), 64-71.
12. Youngdahl, K. A.; Laine, R. M.; Kennish, R. A.; Cronin, T. R.; Balavoine, G. A., *Better Ceramics through Chemistry III*. Materials Research Society: Warrendale, PA, **1988**.
13. Blum, Y. D.; Schwartz, K. B.; Laine, R. M., *J. Mater. Sci.* **1989,** *24* (5), 1707-1718.
14. Wang, W. D.; Eisenberg, R., *Organometallics* **1991,** *10* (7), 2222-2227.
15. Matarasso-Tchiroukhine, E., *J. Chem. Soc., Chem. Commun.* **1990,** (9), 681-682.
16. Liu, H. Q.; Harrod, J. F., *Organometallics* **1992,** *11* (2), 822-827.
17. He, J.; Liu, H. Q.; Harrod, J. F.; Hynes, R., *Organometallics* **1994,** *13* (1), 336-343.
18. Liu, H. Q.; Harrod, J. F., *Can. J. Chem.* **1992,** *70* (1), 107-110.
19. Wang, J. X.; Dash, A. K.; Berthet, J. C.; Ephritikhine, M.; Eisen, M. S., *J. Organomet. Chem.* **2000,** *610* (1-2), 49-57.
20. Harder, S.; Brettar, J., *Angew. Chem., Int. Ed. Engl.* **2006,** *45* (21), 3474-3478.
21. Buch, F.; Harder, S., *Organometallics* **2007,** *26* (21), 5132-5135.
22. Crimmin, M. R.; Arrowsmith, M.; Barrett, A. G. M.; Casely, I. J.; Hill, M. S.; Procopiou, P. A., *J. Am. Chem. Soc.* **2009,** *131* (28), 9670-9685.
23. Horrillo-Martínez, P.; Hultzsch, K. C., *Tetrahedron Lett.* **2009,** *50* (18), 2054-2056.
24. Dunne, J. F.; Fulton, D. B.; Ellern, A.; Sadow, A. D., *J. Am. Chem. Soc.* **2010,** *132* (50), 17680-17683.
25. Neal, S. R.; Ellern, A.; Sadow, A. D., *J. Organomet. Chem.* **2011,** *696* (1), 228-234.
26. Zhang, X.; Emge, T. J.; Hultzsch, K. C., *Angew. Chem., Int. Ed. Engl.* **2012,** *51* (2), 394-398.
27. Buch, F.; Harder, S., *Z. Naturforsch* **2008,** *63b*, 169-177.
28. Tobisch, S., *Chem. -Eur. J.* **2011,** *17* (52), 14974-14986.
29. Dunne, J. F.; Neal, S. R.; Engelkemier, J.; Ellern, A.; Sadow, A. D., *J. Am. Chem. Soc.* **2011,** *133* (42), 16782-16785.
30. Espenson, J. H., *Chemical Kinetics and Reaction Mechanisms*. 2nd ed.; McGraw-Hill: New York, **1995**.
31. Gountchev, T. I.; Tilley, T. D., *Organometallics* **1999,** *18* (26), 5661-5667.
32. Sadow, A. D.; Tilley, T. D., *J. Am. Chem. Soc.* **2005,** *127* (2), 643-656.
33. Bassindale, A. R.; Taylor, P. G., *The Chemistry of Organic Silicon Compounds*. Wiley: New York, **1989**; Vol. 3.
34. Han, R.; Looney, A.; Parkin, G., *J. Am. Chem. Soc.* **1989,** *111* (18), 7276.
35. Han, R.; Parkin, G., *J. Organomet. Chem.* **1990,** *393* (3), C43-C46.
36. Han, R.; Parkin, G., *J. Am. Chem. Soc.* **1990,** *112* (9), 3662-3663.
37. Han, R.; Parkin, G., *Organometallics* **1991,** *10* (4), 1010-1020.
38. Han, R.; Parkin, G., *J. Am. Chem. Soc.* **1992,** *114* (2), 748-757.
39. Thompson, M. E.; Baxter, S. M.; Bulls, A. R.; Burger, B. J.; Nolan, M. C.; Santarsiero, B. D.; Schaefer, W. P.; Bercaw, J. E., *J. Am. Chem. Soc.* **1987,** *109* (1), 203-219.
40. Chirik, P. J.; Bercaw, J. E., *Organometallics* **2005,** *24* (22), 5407-5423.

41. Hansch, C.; Leo, A.; Taft, R. W., *Chem. Rev.* **1991,** *91* (2), 165-195.
42. Watson, P. L.; Parshall, G. W., *Acc. Chem. Res.* **1985,** *18* (2), 51-56.
43. Dunne, J. F.; Su, J.; Ellern, A.; Sadow, A. D., *Organometallics* **2008,** *27* (11), 2399-2401.
44. Dunne, J. F. Stoichiometric and catalytc reactivity of tris(oxazolinyl)borate main group metal compounds. Dissertation, Iowa State University, **2011**.
45. Mukherjee, D.; Thompson, R. R.; Ellern, A.; Sadow, A. D., *ACS Catal.* **2011,** *1* (7), 698-702.
46. Roering, A. J.; MacMillan, S. N.; Tanski, J. M.; Waterman, R., *Inorg. Chem.* **2007,** *46* (17), 6855-6857.
47. Gilman, H.; Zuech, E. A., *J. Am. Chem. Soc.* **1959,** *81* (22), 5925-5928.
48. Friedrich, G.; Bartsch, R.; Ruehlmann, K., *Pharmazie* **1977,** *32*, 394-397.
49. Peyronel, J. F.; Fiaud, J. C.; Kagan, H. B., *J. Chem. Research* **1980**, (S) 320, (M) 4057-4080.
50. Hirone, N.; Sanjiki, H.; Tanaka, R.; Hata, T.; Urabe, H., *Angew. Chem., Int. Ed. Engl.* **2010,** *49* (42), 7762-7764.

Chapter 5: Tris(oxazolinyl)boratomagnesium mediated Si–C bond formation: A reactivity and mechanistic study

Modified from a paper to be submitted for publication

Steven R. Neal,* Debabrata Mukherjee,† James F. Dunne,‡ Arkady Ellern, Aaron D. Sadow

Department of Chemistry, Iowa State University, Ames, IA 50011, USA

Abstract

$To^{M}MgMe$ (To^{M} = tris(4,4-dimethyl-2-oxazolinyl)phenylborate) reacts with primary and secondary aryl silanes to transfer the methyl group from magnesium to silicon. Kinetic studies on the Si–C bond formation step provide evidence for a mechanism involving nucleophilic attack of the $Mg–CH_3$ bond on silicon. As a result of the methyl group transfer to silicon, hydrogen transfer from silicon to magnesium will generate $To^{M}MgH$. The use of this magnesium hydride as a potential hydrosilylation catalyst is discussed. Finally, preliminary evidence of a magnesium hydride stabilized by $B(C_6F_5)_3$ and its catalytic reactivity in the hydrosilylation of *tert*-butyl acrylate is reported.

Introduction

Organomagnesium reagents are very important tools in organic synthesis. Ever since Grignard reagents were first introduced in 1900 there has been a myriad of reports on their usefulness.[1-2] A key difficulty encountered with expanding the utility of Grignard reagents is the ambiguity associated with their solution state structure. To better

---

* Primary researcher and author

† Performed reactions of $To^{M}MgMe$ and O_2

‡ Performed initial reaction between $To^{M}MgMe$ and $PhSiH_3$

correlate structure and reactivity, well-defined and solvent free organomagnesium complexes have been targeted.[3-14] Another advantage of generating well-defined magnesium species is the ability to use organomagensium complexes as catalysts for organic transformations. These catalysts can be tuned to control reactivity and stereoselectivity.

In this vein, our group began investigating tris(oxazolinyl)phenylboratomagnesium alkyl complexes as precatalysts for the cyclization of aminoalkenes via intramolecular hydroamination.[15-16] An optically active magnesium complex bearing a *tert*-butyl substituted tris(oxazolinyl)phenylborate ligand can produce pyrrolidines via hydroamination/cyclization with % ee's up to 36%. In addition, kinetic studies on achiral tris(oxazolinyl)phenylboratomagnesium alkyl and amide complexes provided significant evidence favoring a concerted, non-insertive mechanism over the general insertion mechanism proposed for rare earth metal catalyzed hydroamination.[15, 17-18]

$To^{M}MgMe$ (To^{M} = tris(4,4-dimethyl-2-oxazolinyl)phenylborate) was shown to be a potent precatalyst for the cross-dehydrocoupling of primary amines, hydrazine, and ammonia with silanes.[19] In these studies, the combination of careful control over the stoichiometry and the availability of a well-defined, single site catalyst permitted the isolation of single products when multiple dehydrocoupling species were possible. The ability to isolate $To^{M}MgNH^{t}Bu$ and study the kinetics of the Si–N bond formation step assists in the proposal of a mechanism for the silane/amine dehydrocoupling in which the magnesium amide undergoes a nucleophilic attack at the silicon center followed by hydrogen transfer. With the usefulness of $To^{M}MgMe$ as a precatalyst for Si–N bond formation established, we began to investigate other possible silicon–element bond formations.

Metal catalyzed hydrosilylation of C=X (X = C, N, O) multiple bonds is a common silicon–element bond formation reaction that has significant utility in the silicone industry.[20-21] Late metals have been known to catalyze the hydrosilylation of olefins and carbonyl containing functional groups for over 50 years.[22-25] Developments over the past two decades have shown that a variety of other metals are competent hydrosilylation catalysts.[26-35] Moreover, Piers and co-workers have described the use of $B(C_6F_5)_3$ as a Lewis acid catalyst with high activity for imine and carbonyl hydrosilylation over the last decade.[36-39] Gevorgyan and co-workers have also reported that $B(C_6F_5)_3$ was an effective catalyst for the hydrosilylation of activated and unactivated olefins.[40]

The catalytic hydrosilylation of olefins with group 3 and rare earth metals has been investigated. The kinetic studies suggest that the turnover-limiting step is the Si–C bond formation that proceeds via a concerted, four-centered transition state (i.e. σ-bond metathesis).[41-45] The Si–C bond formation step can be modeled by the reactions of rare earth metal alkyls and organosilanes. These reactions have been shown to be highly dependent on the steric properties of the ancillary ligands and the organosilane such that either Si–C bond formation or Ln–Si bond formation can occur.[41, 46-51] For example, when $Cp^*_2ScMe(THF)$ (Cp^* = η^5-C_5Me_5) is treated with $PhSiH_3$, the scandium hydride (Cp^*_2ScH) and $PhMeSiH_2$ are produced, whereas the reaction with $MesSiH_3$ (Mes = 2,4,6-trimethylphenyl) produces methane and the scandium silyl, $Cp^*_2ScSiH_2Mes$. The mechanism for the Si–C bond formation step is also proposed to proceed through σ-bond metathesis based on kinetic data.

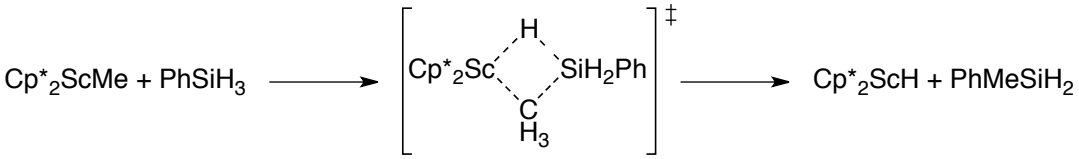

Figure 5-1. Proposed σ-bond metathesis mechanism for $Cp^*_2ScH/PhMeSiH_2$ formation

Recently, Harder and co-workers reported the first group 2 catalyst system that was competent for the hydrosilylation of olefins[52] and ketones.[53] The ketone hydrosilylation catalyst is a stable, bimetallic calcium hydride complex generated by treating [(^{Dipp}nacnac)CaN(SiMe$_3$)$_2$(THF)] (^{Dipp}nacnac = [(2,6-diisopropyl-phenyl)NC-Me]$_2$CH) with PhSiH$_3$.[54-55] Jones and co-workers generate [(^{Dipp}nacnac)Mg(μ-H)$_2$]$_2$ as a stable, bimetallic magnesium hydride from the reaction of [(^{Dipp}nacnac)Mg*n*Bu] and PhSiH$_3$ in a synthetic strategy similar to that of Harder and co-workers.[56-57] In the last few years, Hill and co-workers have used [(^{Dipp}nacnac)Mg(μ-H)$_2$]$_2$ in an attempt to hydrosilylate pyridine and quinoline derivatives.[10, 58] So far, they have only isolated dearomatized pyridine and quinoline bound magnesium species and have not succeeded in completing the hydrosilylation catalytic cycle.

A study of To^{M}MgMe as a precatalyst for hydrosilylation and the stoichiometric reactivity of To^{M}MgMe with organosilanes as a model for the Si–C bond formation step are discussed. In addition, initial studies on magnesium mediated hydrosilylation in the presence of B(C$_6$F$_5$)$_3$ are presented. Finally, kinetic studies with To^{M}MgMe on the Si–C bond formation step allows us to propose a mechanism that is similar to the mechanism of To^{M}MgMe promoted Si–N bond formation.

Results and discussion

Si–C bond formation: reactivity and kinetic studies

The reaction of PhSiH$_3$ and To^{M}MgMe gives PhMeSiH$_2$ in quantitative yield after heating at 100 °C for three hours. Based on mass balance, To^{M}MgH is expected to be the resulting magnesium species. When monitoring the reaction between To^{M}MgMe and PhSiH$_3$, the only resonances detected in the ^{1}H NMR spectrum are consistent with starting materials and PhMeSiH$_2$ while a black precipitate forms as the reaction

proceeds. This contrasts the reaction between $To^{M}MgNH^{t}Bu$ and organosilanes where a new set of To^{M} resonances is observed in the NMR spectrum of reaction mixtures. Thus far, attempts to isolate the magnesium hydride provide only intractable solids.

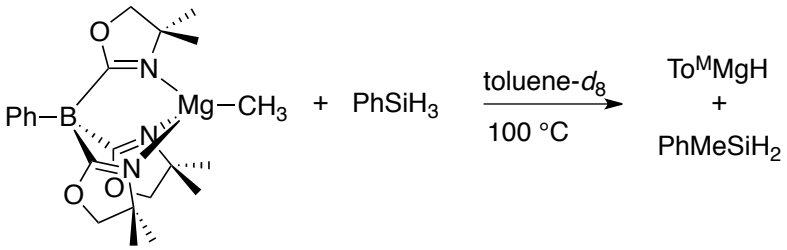

(Eq. 5-1)

Ph_2SiH_2 also reacts with $To^{M}MgMe$; this reaction requires three days in toluene-d_8 at 120 °C to yield Ph_2MeSiH quantitatively. In contrast, only starting materials are observed after heating a toluene-d_8 solution of $To^{M}MgMe$ and $PhMeSiH_2$ for several days. Similarly only starting materials are observed when $To^{M}MgMe$ is heated with tertiary silanes, $BnMe_2SiH$, $(C_3H_5)Me_2SiH$, or Et_3SiH (Bn = CH_2Ph) at 120 °C for one week.

Kinetic studies on the reactions between $To^{M}MgMe$ and organosilanes were conducted in order to better understand the mechanism of magnesium mediated Si–C bond formation and compare our system to group 3 and rare earth metal mediated Si–C bond formation (see Figure 5-1). Isolated $To^{M}MgMe$ reacts quantitatively with $PhSiH_3$ to yield $PhMeSiH_2$ (Eq. 5-1). The in situ concentrations of $To^{M}MgMe$, $PhSiH_3$ and $PhMeSiH_2$ in the stoichiometric reactions were monitored by ^{1}H NMR spectroscopy. Under conditions of a slight excess of $PhSiH_3$ (1.7 to 2.0 equivalents versus $To^{M}MgMe$), second-order integrated rate law plots of $\ln\{[PhSiH_3]/[To^{M}MgMe]\}$ versus time (Figure 5-2) are linear through three half-lives over the temperature range studied (343 K to 402 K) and provide the rate law shown in (Eq. 5-2), with $k' = 2.633(4) \times 10^{-3}\ M^{-1}s^{-1}$ at 373 K.

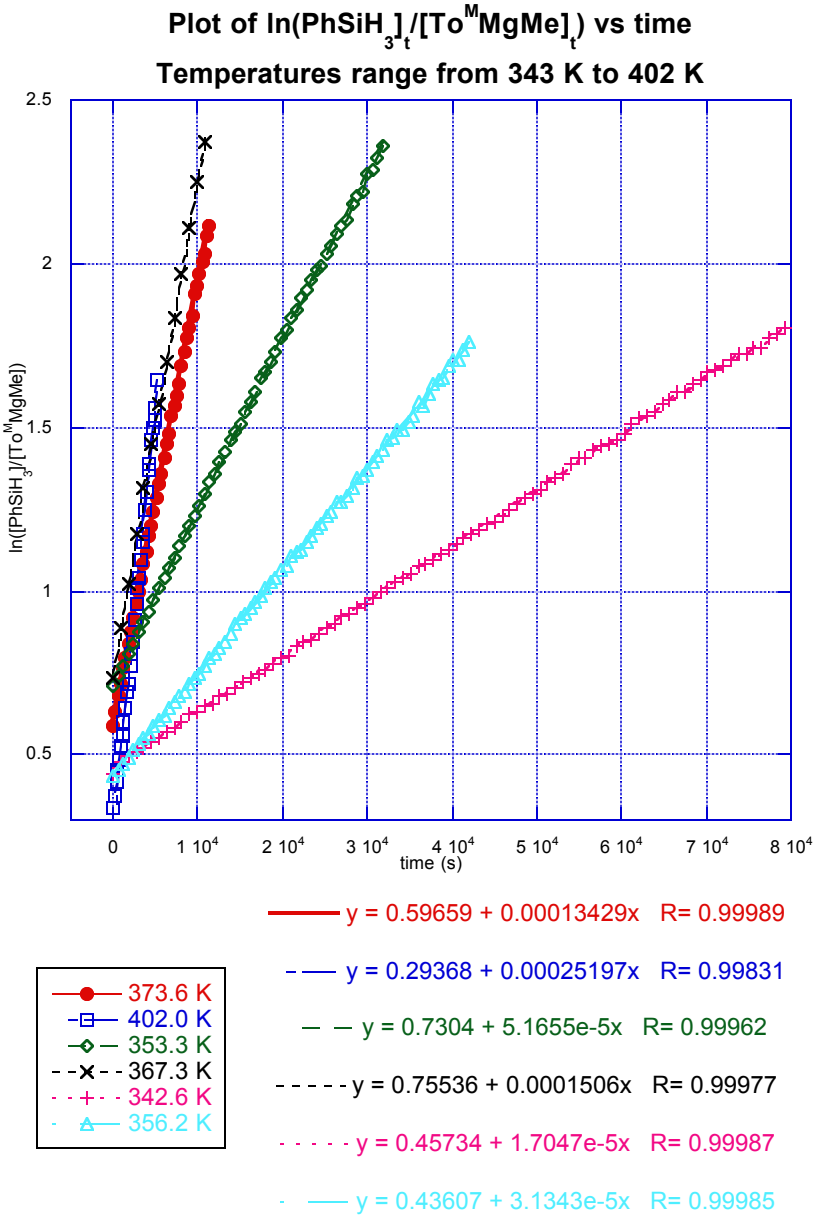

Figure 5-2. Second-order plots of ln([$PhSiH_3$]/[$To^{M}MgMe$]) vs. time for the reaction of $To^{M}MgMe$ and $PhSiH_3$. The curves represent non-weighted linear least squares best fits of the data to the equation: $\ln([PhSiH_3]_t/[To^{M}MgMe]_t) = \ln([PhSiH_3]_0/[To^{M}MgMe]_0) + k\Delta_0 t$. Δ_0(342 K) = 0.0342 M; Δ_0(353 K) = 0.0679 M; Δ_0(356 K) = 0.0361 M; Δ_0(367 K) = 0.0818 M; Δ_0(374 K) = 0.0431 M; Δ_0(402 K) = 0.0102 M.

$$-\frac{d[\mathrm{PhSiH_3}]}{dt} = k'[\mathrm{To^{M}MgMe}]^1[\mathrm{PhSiH_3}]^1$$

(Eq. 5-2)

This rate law indicates the rate-limiting step involves both $To^{M}MgMe$ and $PhSiH_3$; Scheme 5-1 depicts the two possible mechanisms considered for this transformation. Further kinetic studies are needed at this point to make a determination between σ-bond metathesis and nucleophilic attack.

Scheme 5-1. Proposed mechanism for $To^{M}MgMe$ + $PhSiH_3$: Concerted σ-bond metathesis (Mechanism A) versus nucleophilic attack (Mechanism B)

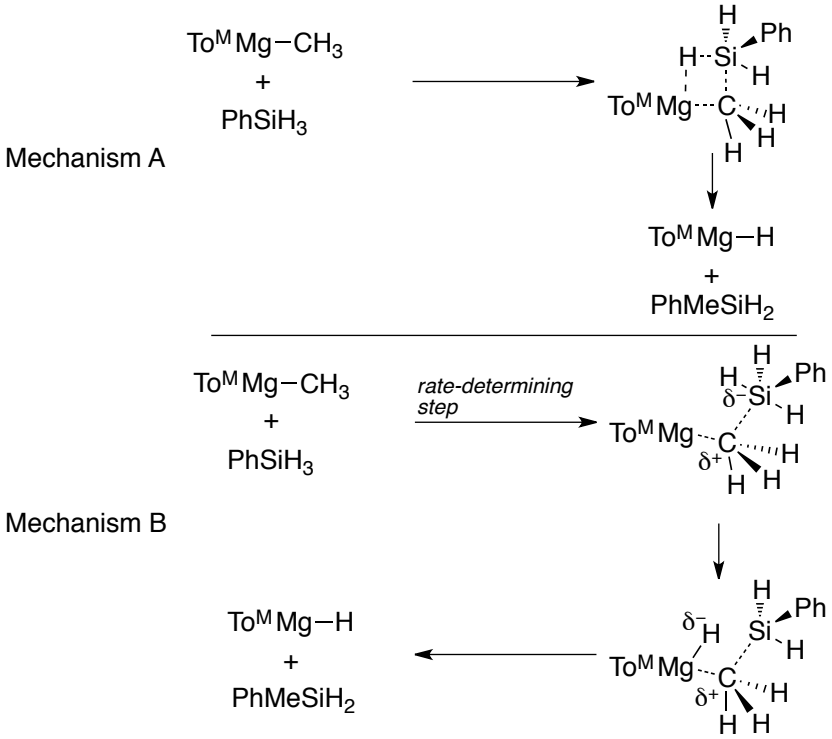

A report from Tilley and co-workers on yttrium-catalyzed hydrosilylation proposes that the Si–C bond formation step is turnover-limiting and proceeds via a metathesis mechanism. The reaction solvent has a pronounced effect on rate of reaction; thus, the reaction is significantly slower when the reaction is run in THF-d_8 versus benzene-d_6.[41] The origin of this rate difference is proposed to be due to the need for coordinative unsaturation at the metal center for metathesis to occur; thus, the metal center is coordinatively saturated in the presence of a high concentration of THF.

Because the nucleophilic attack mechanism should not be affected by coordinative saturation at the metal center, the effect of THF on the reaction between To^{M}MgMe and $PhSiH_3$ was studied. Reactions were run under conditions such that [THF] ranged from 0 to 2.1 M (0 to 40 equivalents versus To^{M}MgMe). A plot of [THF] versus k_{obs} (Figure 5-3) shows that the rate remains constant over the measured [THF] concentration range, which indicates that there is no inhibition by THF.

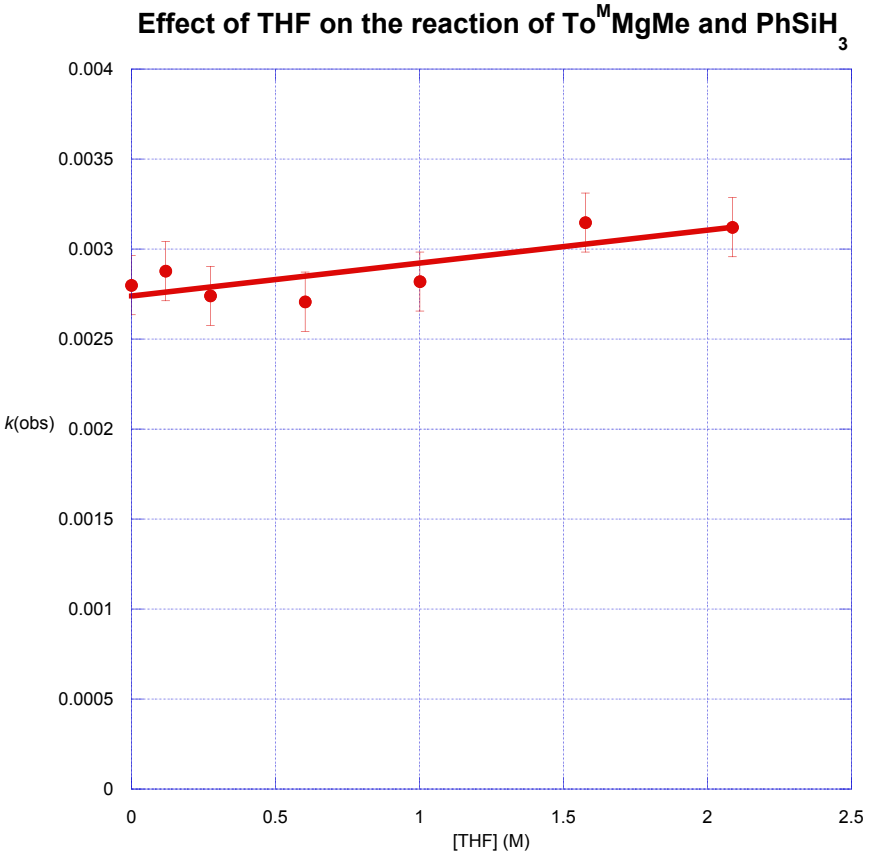

Figure 5-3. Plot showing the lack of impact on the rate of reaction by THF for the reaction of To^{M}MgMe and $PhSiH_3$. Each k_{obs} value is obtained from a linear-least-squares fit of ln([$PhSiH_3$]/[To^{M}MgMe]) versus time.

Reactions of To^{M}MgMe and (p-$CH_3C_6H_4$)SiH_3 were monitored under conditions analogous to the reaction of To^{M}MgMe and $PhSiH_3$ while varying the temperature from 77 to 127 °C. The activation parameters for the protio-silane are calculated from a plot of

ln(*k*/T) versus 1/T (Figure 5-4) giving $\Delta H^{\ddagger H}$ = 15(1) kcal·mol^{-1} and $\Delta S^{\ddagger H}$ = –30(3) cal·mol^{-1}·K^{-1}. The large negative value for the entropy of activation is similar to that observed in the magnesium-mediated Si–N bond formation ($\Delta S^{\ddagger H}$ = -46.5(8) cal·mol^{-1}·K^{-1}) and implies that both reactions have highly ordered transitions states.[59] A primary kinetic isotope effect of k_H/k_D = 1.04(3) at 100 °C was measured for the reaction of To^{M}MgMe and (*p*-$CH_3C_6H_4$)SiD_3. This small primary isotope effect was essentially temperature-independent from 77 to 127 °C (Figure 5-4). The activation parameters calculated for (*p*-$CH_3C_6H_4$)SiD_3 ($\Delta H^{\ddagger D}$ = 16(2) kcal·mol^{-1} and $\Delta S^{\ddagger D}$ = -29(5) cal·mol^{-1}·K^{-1}) are identical, within error, to those calculated for (*p*-$CH_3C_6H_4$)SiH_3.

As a comparison, kinetic studies on rare earth and early transition metal catalyzed Si–C bond formations, which propose concerted, four-center transition states (i.e. σ–bond metathesis), have primary kinetic isotope effects for Si–C bond formation of ca. 1.1,[41, 47] highly negative $\Delta S^{\ddagger}$ values and small $\Delta H^{\ddagger}$ values. The kinetic isotope effect of unity and the highly negative $\Delta S^{\ddagger}$ value are similar to those for both rare earth/early transition metal-mediated Si–C bond formations and magnesium-mediated Si–N bond formation. The value for $\Delta H^{\ddagger}$ in magnesium-mediated Si–C bond formation is significantly larger than the value for $\Delta H^{\ddagger}$ in either the rare earth/early transition metal-mediated Si–C bond formation or the magnesium-mediated Si–N bond formation processes. This implies that bond cleavage/formation makes a significant contribution to the reaction barrier (i.e. the reaction is “less concerted” with respect to σ-bond metathesis).

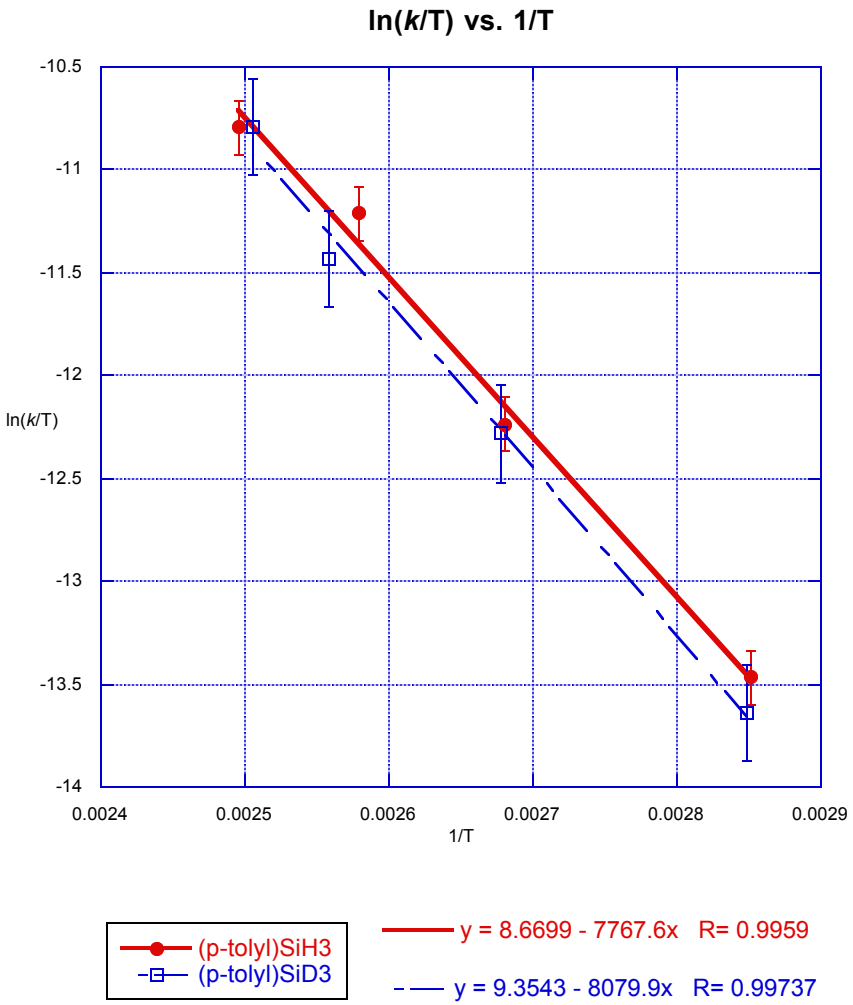

Figure 5-4. Plot showing the temperature dependence for the reaction of To^{M}MgMe and (p-$CH_3C_6H_4$)SiH_3 (Red circle) and To^{M}MgMe and (p-$CH_3C_6H_4$)SiD_3 (Blue square) from 351 K to 400 K. Each ln(k/T) value is obtained from a linear-least-squares fit of ln([(p-$CH_3C_6H_4$)Si(H/D)$_3$]/[To^{M}MgMe]) vs. time.

Second-order rate constants were then determined for the reaction of To^{M}MgMe and (aryl)SiH_3 (aryl = Ph, p-FC_6H_4, p-$CH_3C_6H_4$, p-$OCH_3C_6H_4$, p-$CF_3C_6H_4$). For all (aryl)SiH_3 except p-$CF_3C_6H_4$, the rate constants used are average values determined from second-order integrated rate law plots of ln{[(XC_6H_4)SiH_3]/[To^{M}MgMe]} versus time (X = OCH_3, CH_3, H, F) for reactions at 373 K. The rate constant for (p-$CF_3C_6H_4$)SiH_3 at 373 K was calculated from an Eyring plot (see Figure 5-7 in the experimental section) for

reactions measured over the range 310 to 353 K because the rate at 373 K was sufficiently high to require verification. A Hammett plot of $\log(k_X/k_H)$ versus σ_p[60] provides a straight line with a positive slope and a ρ value of 1.5(2) ($\rho_{MgNHtBu}$ = 1.4).

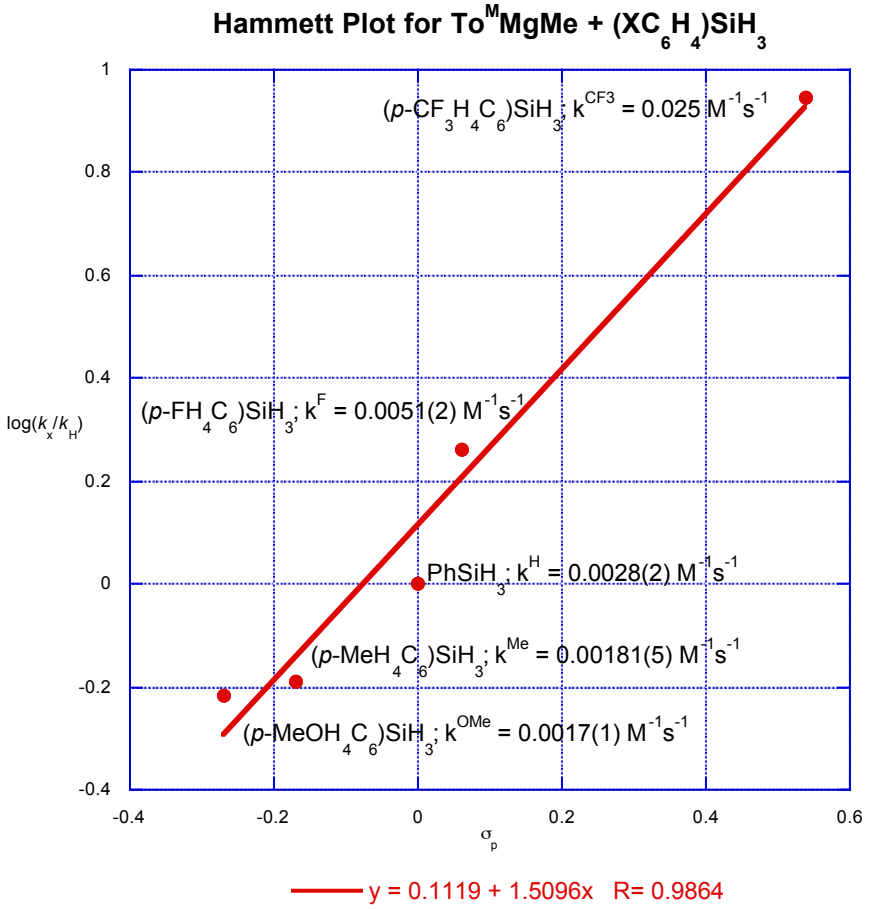

Figure 5-5. Hammett plot showing the reaction rate acceleration with electron-withdrawing groups on the silane for the reaction of To^{M}MgMe and (p-XC_6H_4)SiH_3. Each log (k_X/k_H) point represents the average k_{obs} value obtained from several runs.

Silanes with electron-withdrawing groups reacted more rapidly than those with electron-donating groups, as was observed for Si–N bond formation. Therefore, the barrier of activation is decreased for silanes containing electron-withdrawing groups, which is consistent with a pathway involving a five coordinate silicon species in To^{M}MgH_3C–Si(aryl)H_3. The ρ value of 1.5(2) is less consistent with a concerted bond-

breaking and bond-forming process where the electron-withdrawing groups should have a negative impact on the hydride transfer from silicon to magnesium thus increasing the activation barrier while simultaneously having a positive impact on the formation of the five-coordinate silicon center thus decreasing the activation barrier. One would expect this counteracting effect would cause the overall reaction to have little to no rate enhancement from substituted aryl silanes. This, coupled with the lack of any primary isotope effect, suggests the rate-determining step does not involve Si–H bond cleavage in the transition state.

To further differentiate between the nucleophilic attack and σ-bond metathesis mechanisms, the effect of adding fluoride to the reaction of $To^{M}MgMe$ and $PhSiH_3$ was studied. The added fluoride could coordinate to the silicon center, making silicon five-coordinate and thus more electrophilic. Based on the Hammett plot, the reaction is accelerated by electron-withdrawing groups on the silane, which makes the silane more electrophilic. Unfortunately, independent reactions between either $To^{M}MgMe$ or $PhMeSiH_2$ (the product of the reaction between $To^{M}MgMe$ and $PhSiH_3$) and $[Ph_3SiF_2]^-[Bu_4N]^+$ led to decomposition of both $To^{M}MgMe$ and $PhMeSiH_2$.

The accumulated evidence including (1) an isotope effect of unity, (2) the reaction rate not affected by THF concentration, and (3) a Hammett plot indicating negative charge buildup on silicon in the transition state, we propose that the reaction between $To^{M}MgMe$ and silane involves the Mechanism B shown in Scheme 5-1. A nucleophilic attack of the $Mg–CH_3$ bond on silicon forms a five-coordinate silicon center with a three-centered two-electron interaction at carbon in the rate-determining step. This is followed by a rapid hydrogen transfer from silicon to magnesium and loss of organosilane. A linear dependence on silane concentration is observed when a large excess of $PhSiH_3$ is used (13 to 69 equivalents versus $To^{M}MgMe$, see Figure 5-8 in

experimental section); this implies that the initial Mg···C···Si adduct formation step is irreversible. Additionally, the observation that $To^{M}MgMe$ reacts with Ph_2SiH_2 but not with $PhMeSiH_2$ is consistent with the proposed mechanism; compared to Ph_2SiH_2, $PhMeSiH_2$ is more electron rich and thus less susceptible to nucleophilic attack.

Magnesium-mediated hydrosilylation

Although $To^{M}MgH$ has not yet proven isolable, a magnesium hydride should be formed when $To^{M}MgMe$ reacts with $PhSiH_3$. Therefore, we began to investigate the viability of $To^{M}MgMe$ as a precatalyst for hydrosilylation. When $To^{M}MgMe$ is treated with 10 equivalents of $PhSiH_3$ and subjected to one atmosphere of ethylene and heated to 100 °C, conversion of $PhSiH_3$ to $PhMeSiH_2$ is complete. After three hours, the ^1H NMR spectrum of the reaction mixture only contains resonances for $PhMeSiH_2$, excess $PhSiH_3$, and ethylene. Similar observations result when $To^{M}MgMe$ and $PhSiH_3$ are treated with *tert*-butyl ethylene, bis-trimethylsilyl acetylene, or *N*-benzylidene aniline (Eq. 5-3).

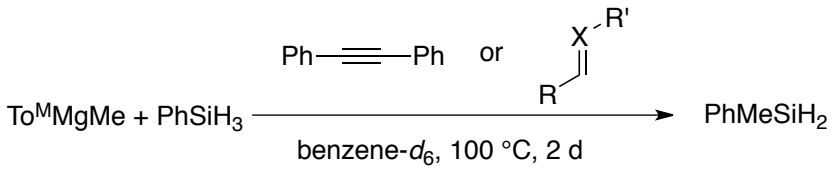

(Eq. 5-3)

Treating $To^{M}MgMe$ with 100 equivalents $PhSiH_3$ in benzene-d_6 and allowing the solution to stand for one hour then adding 100 equivalents of *tert*-butyl acrylate, the solution in the NMR tube immediately becomes viscous. Upon heating the NMR sample overnight at 60 °C, the solution becomes even more viscous. The ^1H NMR spectrum

displays a constant intensity for the $PhSiH_3$ resonance over the course of the reaction while the intensity of the olefin resonances decrease and new, broad, aliphatic resonances increase. Based on the sample becoming highly viscous, the product is proposed to be polymerized *tert*-butyl acrylate. However, investigations into the identification of the product and its physical properties have not been conducted. Meanwhile, heating a micromolar scale reaction between $To^{M}MgMe$ and *tert*-butyl acrylate at 60 °C for 20 hours produces a new To^{M} species. The ^{1}H NMR spectrum of the reaction mixture contained singlet resonances at 3.41, 1.61, and 1.10 ppm that integrate to 6:9:18 respectively. $To^{M}MgMe$ reacts with *tert*-butanol via protonolysis to give methane and a new To^{M} species that has identical chemical shifts to the product observed when $To^{M}MgMe$ reacts with *tert*-butyl acrylate. Although this species is not isolated, it is assigned as $To^{M}MgO^{t}Bu$ based on the matching ^{1}H NMR spectra from these two reactions. The likely origin of $To^{M}MgO^{t}Bu$ from the reaction of $To^{M}MgMe$ and *tert*-butyl acrylate is from a nucleophilic addition to the ester and subsequent loss of *tert*-butoxide that then binds to the metal center in a reaction similar to a Grignard addition to an ester.[61-62]

The reaction of $To^{M}MgNH^{t}Bu$ and $PhSiH_3$ is another route to generate $To^{M}MgH$. Therefore, the viability of $To^{M}MgNH^{t}Bu$ to function as a precatalyst for hydrosilylation was investigated. $To^{M}MgNH^{t}Bu$, generated in situ from $To^{M}MgMe$ and $t\text{-}BuNH_2$, reacts very rapidly with 10 equivalents of $PhSiH_3$ to generate $tBuHN–SiH_2Ph$ (the expected dehydrocoupling product) and a black precipitate. Upon addition of 10 equivalents of *tert*-butyl acrylate, the ^{1}H NMR spectrum of the reaction mixture only contains resonances for $tBuHN–SiH_2Ph$, excess $PhSiH_3$, and unreacted *tert*-butyl acrylate. Similar results are observed if *N*-benzylidene aniline or *para*-fluorostyrene are substituted for *tert*-butyl acrylate. Likely the reaction between $To^{M}MgNH^{t}Bu$ and excess $PhSiH_3$ is too rapid at

room temperature such that all $To^{M}MgH$ decomposes before the hydrosilylation substrate can be added.

Effect of Lewis acid on Si–C bond formation

Reports from Piers and co-workers show that $B(C_6F_5)_3$ can activate Si–H bonds through partial SiH abstraction that creates an electrophilic silicon center that is more prone to nucleophilic attack.[37] Based on our kinetic studies on magnesium mediated Si–C bond formation, a mechanism was proposed that involved nucleophilic attack of the magnesium methyl on silicon. A rate enhancement might be expected if $To^{M}MgMe$ were treated with $PhSiH_3$ in the presence of $B(C_6F_5)_3$. Addition of one equivalent of $B(C_6F_5)_3$ to a micromolar scale reaction of $To^{M}MgMe$ and $PhSiH_3$ produces $PhMeSiH_2$ faster than without $B(C_6F_5)_3$ present.

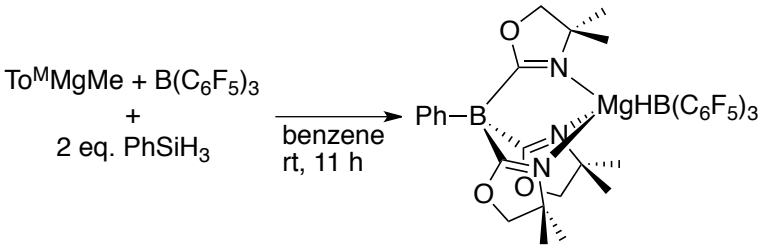

(Eq. 5-4)

Three resonances at -15.1, -18.5, and -21.1 ppm were observed in the ^{11}B NMR spectrum of the reaction mixture. The resonances at -18.5 and –15.1 ppm are broad singlets and are assigned to To^{M} and $H_3C–B(C_6F_5)_3$ respectively while the signal at -21.1 ppm (d, $^{1}J_{BH}$ = 66 Hz) is assigned to $H–B(C_6F_5)_3$.[63] Additionally, a broad quartet centered at 2.70 ppm (q, $^{1}J_{BH}$ = 66 Hz, ^{11}B: I = 3/2) in the ^{1}H NMR spectrum of the reaction mixture is assigned to the hydridoborate.[63] The ^{1}H NMR spectrum changes over several days at room temperature; the resonance at -15.1 ppm disappears while the resonances at -18.5 and -21.1 ppm persist. The ^{1}H NMR spectrum contains one set of To^{M} resonances at

3.30 (CH_2) and 0.82 ppm (CH_3), which is indicative of a pseudo-C_{3v} symmetric species in solution. Unfortunately, attempts to isolate crystals suitable for single crystal X-ray diffraction have been unsuccessful. Repeated preparations on microscale consistently provide the same species. A compound with identical ^1H and ^{11}B NMR chemical shifts is observed in micromolar scale reactions of $To^MMgSi(SiHMe_2)_3$ and $B(C_6F_5)_3$.[64] This compound is proposed to be $To^MMgHB(C_6F_5)_3$; speculating on the structure of $To^MMgHB(C_6F_5)_3$ provides three likely possibilities.

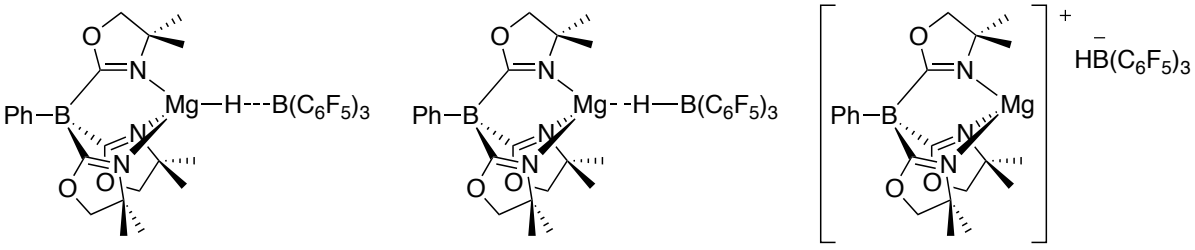

Figure 5-6. Possible structures for $To^MMgHB(C_6F_5)_3$

Preliminary studies using $To^MMgHB(C_6F_5)_3$ as a hydrosilylation catalyst began with *tert*-butyl acrylate. Quantitative formation of the insertion product from the reaction of $PhSiH_3$ and *tert*-butyl acrylate is complete in 11 hours at room temperature with 1 mol % $To^MMgHB(C_6F_5)_3$ (Eq. 5-5). The ^1H NMR spectrum is consistent with the structure of *tert*-butyl-2-(phenylsilyl)propanoate with resonances at 4.52 (SiH), 2.28 (CH), 1.30 ($C(CH_3)_3$), and 1.25 ppm (CH_3) with an integration ratio of 2:1:9:3 respectively. The IR spectrum (neat) displays the expected carbonyl and Si–H bands at 1716 cm^{-1} and 2152 cm^{-1} respectively.

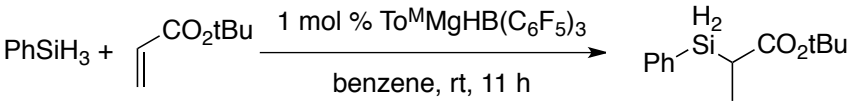

(Eq. 5-5)

The presence of only one product (α-insertion) in the ^{1}H NMR spectrum is interesting because the common hydrosilylation products from transition metal catalyzed hydrosilylation of α,β-unsaturated aldehydes, ketones, and esters are the β,γ-unsaturated silyl ether (1,2-addition) or silyl-enol ether (1,4-addition) [see (Eq. 5-6)].[22-23, 35]

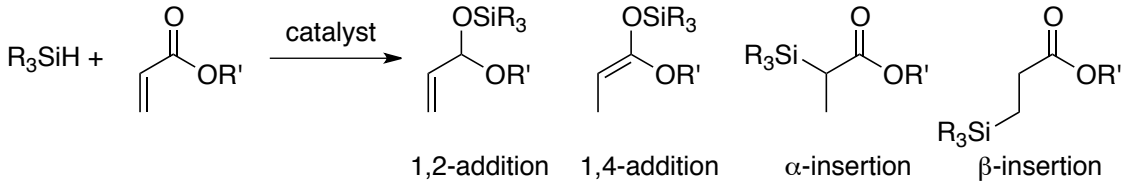

(Eq. 5-6)

H_2PtCl_4 has been shown to give mixtures of α- and β-insertion products as well as 1,4-addition with acyclic α,β-unsaturated esters,[25] while the insertion product is formed exclusively with cyclic maleic anhydride.[21] $B(C_6F_5)_3$ has also been reported to be a catalyst for the hydrosilylation of α,β-unsaturated ketones;[38] however, the only product obtained is the result of 1,4-addition. This implies that $To^MMgHB(C_6F_5)_3$ is acting as the hydrosilylation catalyst and not a source of $B(C_6F_5)_3$. Additionally, when $PhSiH_3$ and *tert*-butyl acrylate are treated with 10 mol % $B(C_6F_5)_3$, all resonances in the ^{1}H NMR spectrum of the reaction mixture are broad and unidentifiable with the exception of two assigned as 2-methylpropane; no resonances for the insertion product can be located.

Based on the product isolated from $To^MMgHB(C_6F_5)_3$ catalyzed hydrosilylation of *tert*-butyl acrylate with $PhSiH_3$ and the significantly different product observed in the absence of To^MMgMe, we propose the catalytic cycle shown in Scheme 5-2. Magnesium alkyl (**B**) should be an intermediate and the transformation from **B** to regenerate **A** is a Si–C cross-dehydrocoupling process akin to the reaction of To^MMgMe and $PhSiH_3$. The dehydrocoupling of To^MMgMe and $PhSiH_3$ is a slow process requiring elevated

temperatures and long reaction times; this process is accelerated by $B(C_6F_5)_3$. Thus, $B(C_6F_5)_3$ must participate in the *tert*-butyl acrylate hydrosilylation catalytic cycle to achieve turnover and greater than 95% conversion with 1 mol % $To^{M}MgMe$ and $B(C_6F_5)_3$ at room temperature in 11 hours.

Piers and co-workers have demonstrated that $B(C_6F_5)_3$ activates silanes by polarizing the Si–H bond making the silane more susceptible to nucleophilic attack.[37-38] Thus, the proposed catalytic cycle consists of an insertion of the hydride in compound **A** into the olefin of *tert*-butyl acrylate in a Markovnikov-type addition forming magnesium alkyl **B**. The fate of $B(C_6F_5)_3$ at this point is speculative, but even though a carbonyl-borane adduct is likely, kinetic evidence from Piers and co-workers shows a rapid equilibrium between free and bound $B(C_6F_5)_3$.[37, 65] Unbound $B(C_6F_5)_3$ can then form borane/silane complex **C** which is now more prone to nucleophilic attack from **B**. Attack of magnesium alkyl **B** followed by loss of the hydrosilylated product will regenerate $To^{M}MgHB(C_6F_5)_3$ (**A**).

Scheme 5-2. Possible catalytic cycle for magnesium-mediated hydrosilylation of *tert*-butyl acrylate

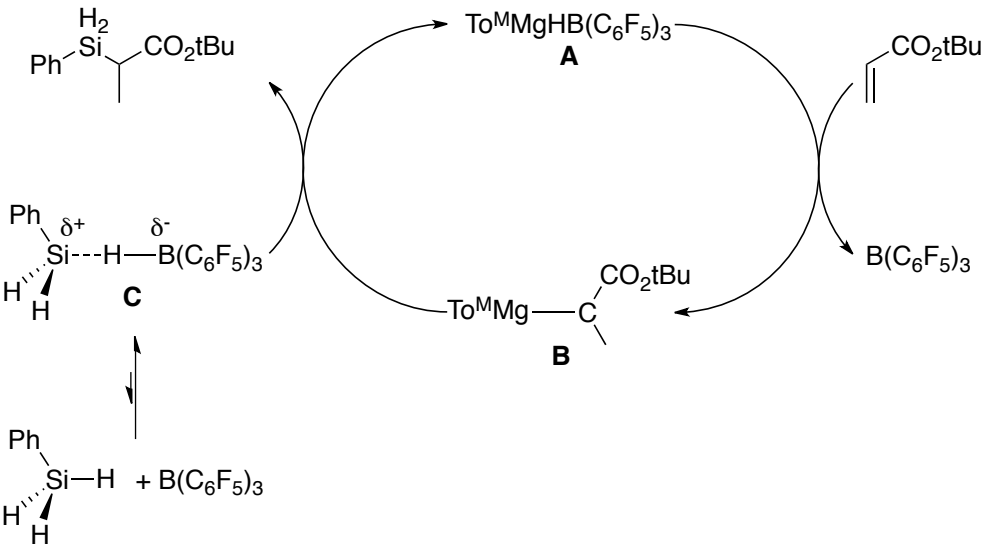

Conclusion

The similarity in kinetic features between Si–N and Si–C bond formation with $To^{M}MgMe$ as the precatalyst is intriguing. The kinetic evidence reveals that both processes undergo nucleophilic attack at silicon by the magnesium amide/alkyl; however, this similarity is contrasted by the valence change (i.e. three-coordinate nitrogen with a lone pair versus saturated four-coordinate carbon). The ability of $To^{M}MgMe$ to form a magnesium hydride upon reaction with $PhSiH_3$ that is suitable for insertion was studied. The apparent instability of this hydride prevented its use in hydrosilylation catalysis. However, the addition of $B(C_6F_5)_3$ provides a new $To^{M}Mg$ species that, preliminarily, appears to be a stabilized magnesium hydride. $To^{M}MgMe$ and $B(C6F5)_3$ react to form an active precatalyst for the hydrosilylation of an α,β-unsaturated ester, and this reactivity with *tert*-butyl acrylate provides further evidence of the composition of the newly formed hydride species.

Experimental

General. All reactions were performed under an inert atmosphere using standard Schlenk techniques or in a glovebox unless otherwise indicated. All glassware was pre-treated with a solution of 10% trimethylchlorosilane in chloroform, rinsed with water and acetone and dried overnight in an oven. Dry, oxygen-free solvents were used throughout. Benzene, toluene, pentane, diethyl ether, and tetrahydrofuran were degassed by sparging with nitrogen, filtered through activated alumina columns, and stored under N_2. Dioxane was dried over purple Na/benzophenone, distilled, and stored under N_2. Benzene-d_6 and toluene-d_8 were vacuum transferred from Na/K alloy and stored under N_2 in the glovebox. *o*-Xylenes-d_{10} was degassed by successive freeze-pump-thaw cycles then dried over freshly activated 4Å molecular sieves and stored

under N_2 in the glovebox. *para*-fluorostyrene was purchased from Aldrich and degassed and dried over freshly activated 4 Å molecular sieves and stored at -35 °C under N_2 in the glovebox. *tert*-Butyl acrylate was purchased from Aldrich and degassed and dried over freshly activated 4 Å molecular sieves and stored at -35 °C under N_2 in the glovebox. Trichlorophenylsilane was purchased from Gelest and reduced with $LiAlH_4$ to phenylsilane. Grignards used to synthesize the substituted silanes were prepared according to standard procedure using I_2 to activate the magnesium. (*p*-$OCH_3C_6H_4$)SiH_3 and (*p*-$CH_3C_6H_4$)SiH_3 were prepared according to a modified literature procedure and compared to published spectroscopic data.[66] (*para*-fluorophenyl)silane was prepared according to a modified literature procedure;[66] the spectroscopic data has not been reported and is given here. (*p*-$CF_3C_6H_4$)SiH_3 was prepared according to published procedure and compared to published spectroscopic data.[67] (*p*-$CH_3C_6H_4$)SiD_3 was prepared in an analogous manner to (*p*-$CH_3C_6H_4$)SiH_3 using $LiAlD_4$ in place of $LiAlH_4$. To^MMgMe was prepared according to published procedures.[15] All other reagents were purchased from standard suppliers and used as received. ^1H, $^{13}C\{^1H\}$, ^{11}B, $^{19}F\{^1H\}$, and $^{29}Si\{^1H\}$ NMR spectra were collected on a Bruker DRX400 spectrometer, Agilent MR400 spectrometer, or Bruker Avance III 600 spectrometer with a Bruker BBFO SmartProbe. ^{11}B NMR spectra were referenced to an external sample of $BF_3{\cdot}Et_2O$, $^{19}F\{^1H\}$ NMR spectra were referenced to an external sample of $C_6H_5CF_3$, and $^{29}Si\{^1H\}$ spectra were referenced to an external sample of $SiMe_4$. High-resolution mass spectrometry performed on a Waters GCT TOF mass spectrometer equipped with an Agilent 6890 GC.

***tert*-Butyl-2-(phenylsilyl)propanoate.** To^MMgMe (0.0065 g, 0.015 mmol) was added to a vial and dissolved in 1 mL of benzene. $B(C_6F_5)_3$ (0.0088 g, 0.017 mmol) was added to

a test tube and dissolved in 1 mL of benzene and added to the solution of To^{M}MgMe. $PhSiH_3$ (0.20 mL, 1.62 mmol) was immediately added, and the solution was allowed to stir 11 h. *tert*-Butyl acrylate (0.22 mL, 1.50 mmol) was added and the solution was allowed to stir. The reaction progress was monitored by NMR spectroscopy by taking aliquots of the reaction mixture and diluting them with benzene-d_6 and looking for the olefinic resonances corresponding to *tert*-butyl acrylate. After 11 hours, the solvent was evaporated to yield *tert*-butyl-2-(phenylsilyl)propanoate (0.301 g, 1.27 mmol, 85% yield). ^{1}H NMR (benzene-d_6, 600 MHz): δ 7.51 (m, 2 H, *ortho*-C_6H_5), 7.11 (m, 3 H, *meta*- and *para*-C_6H_5), 4.52 (m, $^1J_{SiH}$ = 201.9 Hz, 2 H, SiH_2), 2.28 (qt, $^3J_{HH}$ = 7.2 Hz, $^3J_{HH}$ = 3.1 Hz, 1 H, $CH_3CH(SiH_2Ph)CO_2CMe_3$), 1.30 (s, 9 H, $CH_3CH(SiH_2Ph)CO_2CMe_3$), 1.25 (d, ^3J_H = 7.2 Hz, 3 H, $CH_3CH(SiH_2Ph)CO_2CMe_3$). $^{13}C\{^1H\}$ (benzene-d_6, 151 MHz): δ 174.22 ($CH_3CH(SiH_2Ph)CO_2CMe_3$), 136.36 (*ortho*-C_6H_5), 130.64 (*ipso*-C_6H_5), 128.62 (*meta*- and *para*-C_6H_5), 79.97 ($CH_3CH(SiH_2Ph)CO_2CMe_3$), 28.46 ($CH_3CH(SiH_2Ph)CO_2CMe_3$), 26.94 ($CH_3CH(SiH_2Ph)CO_2CMe_3$), 12.93, ($CH_3CH(SiH_2Ph)CO_2CMe_3$). $^{29}Si\{^1H\}$ (benzene-d_6, 119 MHz): δ -24.02. IR (film, cm^{-1}): 3071 w, 3052 w, 3004 w, 2976 m, 2932 w, 2873 w, 2152 s (ν_{SiH}), 1716 s (ν_{CO}), 1457 m, 1429 m, 1367 m, 1316 m, 1255 w, 1212 w, 1141 br s, 1082 br s, 932 m, 901 m, 841 s, 737 m. MS (CI, CH_3) exact mass Calcd. for $C_{13}H_{21}O_2Si$: m/e 237.1311 ($[M+H]^+$), Found: 237.1311.

Modification to the published procedure for the synthesis of (p-XC_6H_4)SiH_3 (X = OCH_3, CH_3, F). *Caution.* In the absence of diethylether, $AlCl_3$-catalyzed silane redistribution reactions occur form SiH_4,[68] a pyrophoric gas. Therefore, reduction with $LiAlH_4$ or $LiAlD_4$ must be completed in ether solvent and quenched properly with water prior to distillation. The reported procedure[66] was followed with only a slight modification. The synthesized trichloro(aryl)silanes were carefully separated from the excess $SiCl_4$ in

the reaction mixture by distillation. They were then vacuum transferred to a collection flask and reduced to the corresponding organosilanes. The removal of $SiCl_4$ is critical, as pyrophoric SiH_4 will be formed upon addition of $SiCl_4$ to $LiAlH_4$.

(*p*-FC_6H_4)SiH_3. ^{1}H NMR (benzene-d_6, 600 MHz): δ 7.14-7.1 (m, 2 H, C_6H_4, *ortho*-F), 6.75-6.70 (m, 2 H, C_6H_4, *meta*-F), 4.12 (d, $^6J_{FH}$ = 0.7 Hz, $^1J_{SiH}$ = 199.8 Hz, 3 H, SiH_3). $^{13}C\{^1H\}$ NMR (benzene-d_6, 151 MHz): δ 165.02 (d, $^1J_{FC}$ = 249.3 Hz, C_6H_4, *ipso*-F), 138.45 (d, $^3J_{FC}$ = 7.67 Hz, C_6H_4, *meta*-F), 123.86 (d, $^4J_{FC}$ = 3.9 Hz, C_6H_4, *ipso*-SiH_3), 115.96 (d, $^2J_{FC}$ = 20.1 Hz, C_6H_4, *ortho*-F). $^{19}F\{^1H\}$ NMR (benzene-d_6, 565 MHz): δ -110.29. $^{29}Si\{^1H\}$ (benzene-d_6, 119 MHz): δ -60.39.

(*p*-$CF_3C_6H_4$)SiH_3. ^{1}H NMR (benzene-d_6, 600 MHz): δ 7.26 (d, $^3J_{HH}$ = 8.3 Hz, 2 H, C_6H_4, *ortho*-CF_3), 7.16 (d, $^3J_{HH}$ = 8.3 Hz, 2 H, C_6H_4, *meta*-CF_3), 4.05 (s, $^1J_{SiH}$ = 203.6 Hz, 3 H, SiH_3). $^{13}C\{^1H\}$ (benzene-d_6, 151 MHz): δ 136.65 (C_6H_4, *meta*-CF_3), 133.69 (C_6H_4, *ipso*-SiH_3), 132.39 (q, $^2J_{FC}$ = 32.3 Hz, C_6H_4, *ipso*-CF_3), 125.10 (q, $^1J_{FC}$ = 272.2 Hz, CF_3), 125.08 (q, $^3J_{FC}$ = 3.8 Hz, C_6H_4, *ortho*-CF_3). $^{19}F\{^1H\}$ (benzene-d_6, 565 MHz): δ -63.13. $^{29}Si\{^1H\}$ (benzene-d_6, 119 MHz): δ -60.06.

(*p*-$OCH_3C_6H_4$)SiH_3. ^{1}H NMR (benzene-d_6 600 MHz): δ 7.34 (m, 2 H, C_6H_4, *meta*-OCH_3), 6.72 (m, 2 H, C_6H_4, *ortho*-OCH_3), 4.30 (s, $^1J_{SiH}$ = 198.7 Hz, 3 H, SiH_3), 3.27 (s, 3 H, OCH_3). $^{13}C\{^1H\}$ (benzene-d_6, 151 MHz): δ 162.08 (C_6H_4, *ipso*-OCH_3), 138.02 (C_6H_4, *meta*-OCH_3), 118.69 (C_6H_4, *ipso*-SiH_3), 114.77 (C_6H_4, *ortho*-OCH_3), 54.86 (OCH_3). $^{29}Si\{^1H\}$ (benzene-d_6 119 MHz): δ -60.81.

Procedure for kinetic measurements

All kinetics measurements were conducted by monitoring the reaction with ^{1}H NMR spectroscopy using a Bruker DRX 400 MHz spectrometer. The reaction was monitored by taking a single ^{1}H NMR scans at regular preset intervals. Concentrations of

the reactants and products were determined by integration of resonances corresponding to the species of interest and integration of a 1,3,5-trimethoxybenzene standard of known concentration. Stock solutions of 1,3,5-trimethoxybenzene (10 to 30 mM) in either toluene-d_8 or *o*-xylene-d_{10} were prepared and used for a series of experiments; rate constants were obtained reproducibly through several batches of stock solutions. The NMR probe was pre-heated to the desired temperature, and the probe temperature was calibrated using an 80% ethylene glycol sample in 20% DMSO-d_6. The temperature was monitored during the course of the measurements using a thermocouple. Kinetic isotope measurements were performed in the same manner using the deuterated silane (*p*-$CH_3C_6H_4$)SiD_3.

Procedure for Si–C measurements

In a typical experiment, 0.040 mmol of To^{M}MgMe was dissolved in 0.6 mL of the stock solution. The solution was placed in a J. Young-style NMR tube and placed in the warmed NMR probe. Once the NMR solution had reached the desired temperature, the sample was locked and shimmed and a 1D-^{1}H NMR spectrum obtained to get the accurate concentration of To^{M}MgMe. The tube was pumped back into the glovebox and $PhSiH_3$ was added to the To^{M}MgMe solution. The tube was immediately placed back in the NMR probe. Rate constants were obtained by a nonweighted linear least-squares regression analysis of the integrated second-order rate law:

$$\ln\left(\frac{[\mathrm{PhSiH_3}]}{[\mathrm{To^MMgMe}]}\right) = \ln\left(\frac{[\mathrm{PhSiH_3}]_0}{[\mathrm{To^MMgMe}]_0}\right) + k\Delta_0 t$$

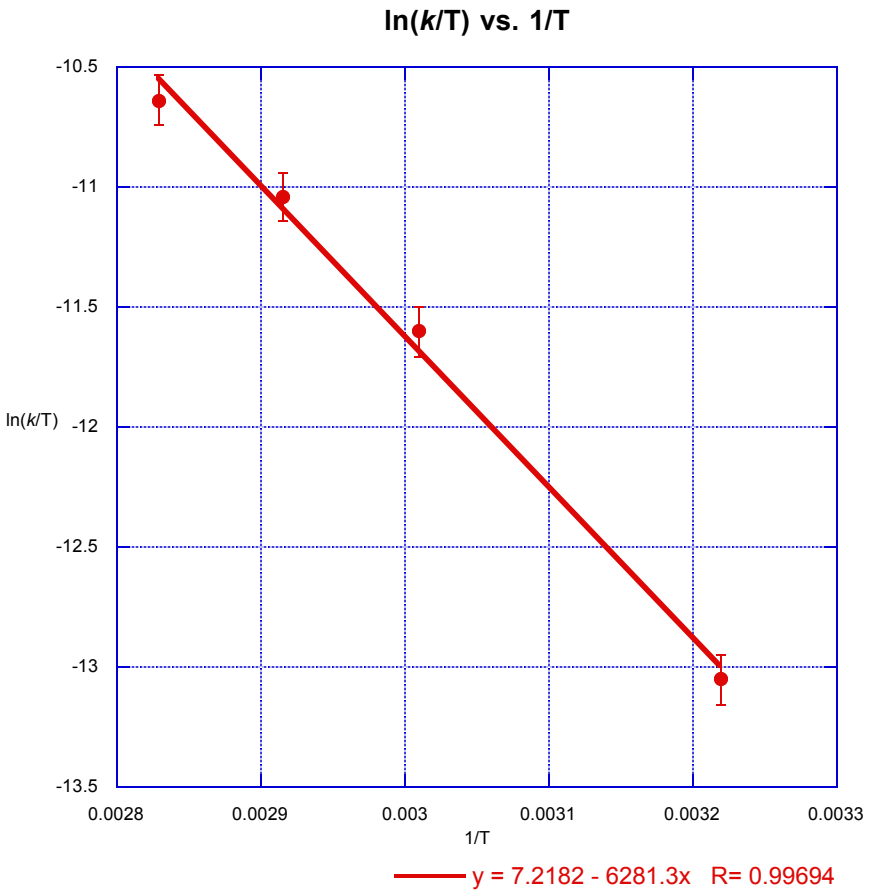

Figure 5-7. Plot showing the temperature dependence for the reaction of To^{M}MgMe and (p-$CF_3C_6H_4$)SiH_3 from 310 K to 353 K. Each k_{obs} value is obtained from a linear-least squares fit of ln([(p-$CF_3C_6H_4$)SiH_3]/[To^{M}MgMe]) versus time.

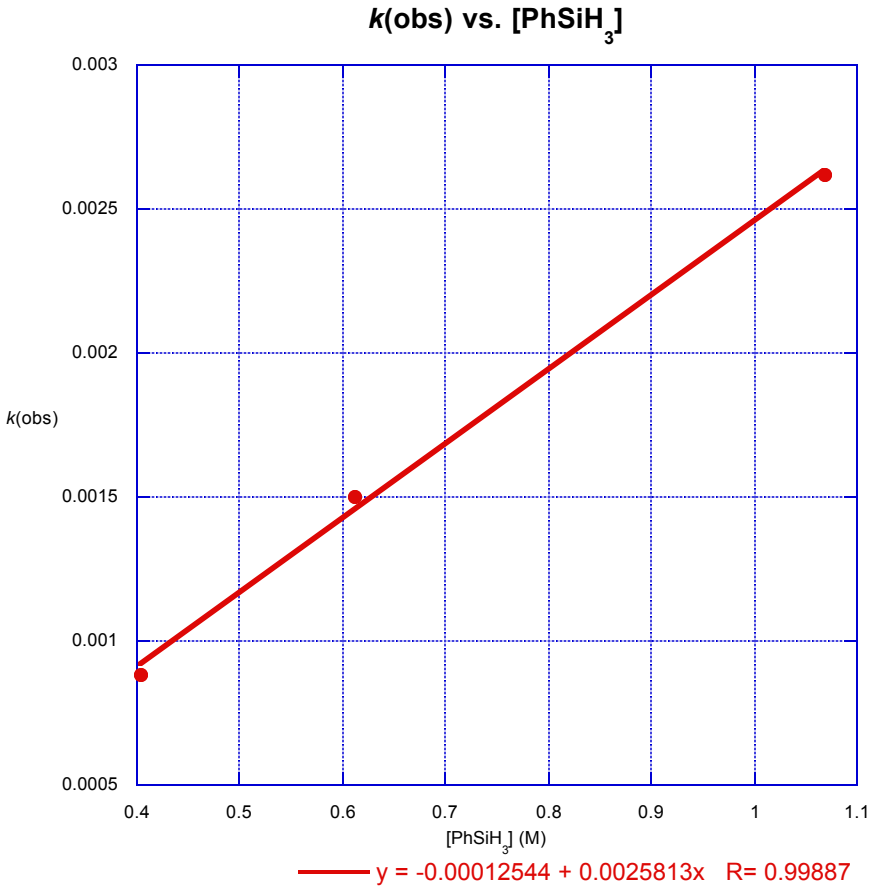

Figure 5-8. Plot showing linear dependence on [$PhSiH_3$] for the reaction of $To^{M}MgMe$ and $PhSiH_3$ at 373 K. Each k_{obs} value is obtained from a linear-least-squares fit of ln[$To^{M}MgMe$] versus time.

References

1. Jastrzebski, J. T. B. H.; Boersma, J.; van Koten, G., *The Chemistry of Organomagnesium Compounds*. Wiley: Hoboken, **2008**; Vol. 1.
2. Hanusa, T. P., *Comprehensive Organometallic Chemistry III*. Elsevier: Oxford, **2006**; Vol. 2.
3. Han, R.; Parkin, G., *J. Am. Chem. Soc.* **1990,** *112* (9), 3662-3663.
4. Han, R.; Parkin, G., *Organometallics* **1991,** *10* (4), 1010-1020.
5. Han, R.; Parkin, G., *J. Am. Chem. Soc.* **1992,** *114* (2), 748-757.
6. Chisholm, M. H.; Huffman, J. C.; Phomphrai, K., *J. Chem. Soc., Dalton Trans.* **2001,** (3), 222-224.
7. Chisholm, M. H.; Phomphrai, K., *Inorg. Chim. Acta* **2003,** *350* (0), 121-125.
8. Chisholm, M. H.; Gallucci, J.; Phomphrai, K., *Inorg. Chem.* **2002,** *41* (10), 2785-2794.
9. Crimmin, M. R.; Arrowsmith, M.; Barrett, A. G. M.; Casely, I. J.; Hill, M. S.; Procopiou, P. A., *J. Am. Chem. Soc.* **2009,** *131* (28), 9670-9685.

10. Hill, M. S.; Kociok-Kohn, G.; MacDougall, D. J.; Mahon, M. F.; Weetman, C., *Dalton Trans.* **2011,** *40* (46), 12500-12509.
11. Bailey, P. J.; Dick, C. M. E.; Fabre, S.; Parsons, S., *J. Chem. Soc., Dalton Trans.* **2000,** (10), 1655-1661.
12. Bailey, P. J.; Coxall, R. A.; Dick, C. M.; Fabre, S.; Parsons, S., *Organometallics* **2001,** *20* (4), 798-801.
13. Bailey, P. J.; Liddle, S. T.; Morrison, C. A.; Parsons, S., *Angew. Chem., Int. Ed. Engl.* **2001,** *40* (23), 4463-4466.
14. Bailey, P. J.; Coxall, R. A.; Dick, C. M.; Fabre, S.; Henderson, L. C.; Herber, C.; Liddle, S. T.; Loroño-González, D.; Parkin, A.; Parsons, S., *Chem. -Eur. J.* **2003,** *9* (19), 4820-4828.
15. Dunne, J. F.; Fulton, D. B.; Ellern, A.; Sadow, A. D., *J. Am. Chem. Soc.* **2010,** *132* (50), 17680-17683.
16. Neal, S. R.; Ellern, A.; Sadow, A. D., *J. Organomet. Chem.* **2011,** *696* (1), 228-234.
17. Gagne, M. R.; Stern, C. L.; Marks, T. J., *J. Am. Chem. Soc.* **1992,** *114* (1), 275-294.
18. Motta, A.; Lanza, G.; Fragalà, I. L.; Marks, T. J., *Organometallics* **2004,** *23* (17), 4097-4104.
19. Dunne, J. F.; Neal, S. R.; Engelkemier, J.; Ellern, A.; Sadow, A. D., *J. Am. Chem. Soc.* **2011,** *133* (42), 16782-16785.
20. Troegel, D.; Stohrer, J., *Coordination Chemistry Reviews* **2011,** *255* (13–14), 1440-1459.
21. Saxena, K.; Bisaria, C. S.; Saxena, A. K., *Appl. Organomet. Chem* **2009,** *23* (12), 535-540.
22. Ojima, I.; Nihonyanagi, M.; Kogure, T.; Kumagai, M.; Horiuchi, S.; Nakatsugawa, K.; Nagai, Y., *J. Organomet. Chem.* **1975,** *94* (3), 449-461.
23. Ojima, I.; Kogure, T., *Organometallics* **1982,** *1* (10), 1390-1399.
24. Sibi, M. P., Hydrogen Hexachloroplatinate. In *Encyclopedia of Reagents for Organic Synthesis*, Wiley: 2001.
25. Yoshii, E.; Kobayashi, Y.; Koizumi, T.; Oribe, T., *Chem. Pharm. Bull.* **1974,** *22*, 2767-2769.
26. Yun, J.; Buchwald, S. L., *J. Am. Chem. Soc.* **1999,** *121* (24), 5640-5644.
27. Hansen, M. C.; Buchwald, S. L., *Org. Lett.* **2000,** *2* (5), 713-715.
28. Roy, A. K., *Adv. Organomet. Chem.* **2007,** *Volume 55*, 1-59.
29. Bart, S. C.; Lobkovsky, E.; Chirik, P. J., *J. Am. Chem. Soc.* **2004,** *126* (42), 13794-13807.
30. Riant, O.; Mostefaï, N.; Courmarcel, J., *Synthesis* **2004,** *2004* (EFirst), 2943,2958.
31. Mimoun, H.; de Saint Laumer, J. Y.; Giannini, L.; Scopelliti, R.; Floriani, C., *J. Am. Chem. Soc.* **1999,** *121* (26), 6158-6166.
32. Mimoun, H., *J. Org. Chem.* **1999,** *64* (7), 2582-2589.
33. Albright, A.; Gawley, R. E., *J. Am. Chem. Soc.* **2011,** *133* (49), 19680-19683.
34. Díez-González, S.; Nolan, S. P., *Acc. Chem. Res.* **2008,** *41* (2), 349-358.
35. Koller, J. r.; Bergman, R. G., *Organometallics* **2011,** *ASAP - Published on web 9/14/11*.
36. Blackwell, J. M.; Sonmor, E. R.; Scoccitti, T.; Piers, W. E., *Org. Lett.* **2000,** *2* (24), 3921-3923.
37. Parks, D. J.; Blackwell, J. M.; Piers, W. E., *J. Org. Chem.* **2000,** *65*, 3090-3098.

38. Blackwell, J. M.; Morrison, D. J.; Piers, W. E., *Tetrahedron* **2002,** *58* (41), 8247-8254.
39. Warren E, P., *Adv. Organomet. Chem.* **2004,** *Volume 52*, 1-76.
40. Rubin, M.; Schwier, T.; Gevorgyan, V., *J. Org. Chem.* **2002,** *67*, 1936-1940.
41. Gountchev, T. I.; Tilley, T. D., *Organometallics* **1999,** *18* (26), 5661-5667.
42. Molander, G. A.; Nichols, P. J., *Journal of the American Chemical Society* **1995,** *117* (15), 4415-4416.
43. Fu, P.-F.; Brard, L.; Li, Y.; Marks, T. J., *Journal of the American Chemical Society* **1995,** *117* (27), 7157-7168.
44. Voskoboynikov, A. Z.; Shestakova, A. K.; Beletskaya, I. P., *Organometallics* **2001,** *20* (13), 2794-2801.
45. Dash, A. K.; Gourevich, I.; Wang, J. Q.; Wang, J.; Kapon, M.; Eisen, M. S., *Organometallics* **2001,** *20* (24), 5084-5104.
46. Radu, N. S.; Don Tilley, T.; Rheingold, A. L., *J. Organomet. Chem.* **1996,** *516* (1-2), 41-49.
47. Sadow, A. D.; Tilley, T. D., *J. Am. Chem. Soc.* **2005,** *127* (2), 643-656.
48. Sadow, A. D.; Tilley, T. D., *Angew. Chem., Int. Ed. Engl.* **2003,** *42* (7), 803-805.
49. Castillo, I.; Tilley, T. D., *J. Am. Chem. Soc.* **2001,** *123* (43), 10526-10534.
50. Castillo, I.; Tilley, T. D., *Organometallics* **2001,** *20* (26), 5598-5605.
51. Radu, N. S.; Tilley, T. D.; Rheingold, A. L., *J. Am. Chem. Soc.* **1992,** *114* (21), 8293-8295.
52. Buch, F.; Brettar, J.; Harder, S., *Angew. Chem., Int. Ed. Engl.* **2006,** *45* (17), 2741-2745.
53. Spielmann, J.; Harder, S., *Eur. J. Inorg. Chem.* **2008,** *2008* (9), 1480-1486.
54. Harder, S.; Brettar, J., *Angew. Chem., Int. Ed. Engl.* **2006,** *45* (21), 3474-3478.
55. Spielmann, J.; Harder, S., *Chem. -Eur. J.* **2007,** *13* (32), 8928-8938.
56. Bonyhady, S. J.; Jones, C.; Nembenna, S.; Stasch, A.; Edwards, A. J.; McIntyre, G. J., *Chem. -Eur. J.* **2010,** *16* (3), 938-955.
57. Green, S. P.; Jones, C.; Stasch, A., *Angew. Chem., Int. Ed. Engl.* **2008,** *47* (47), 9079-9083.
58. Hill, M. S.; MacDougall, D. J.; Mahon, M. F., *Dalton Trans.* **2010,** *39* (46), 11129-11131.
59. Espenson, J. H., *Chemical Kinetics and Reaction Mechanisms*. 2nd ed.; McGraw-Hill: New York, **1995**.
60. Hansch, C.; Leo, A.; Taft, R. W., *Chem. Rev.* **1991,** *91* (2), 165-195.
61. Fieser, L. F.; Fieser, M., *Reagents for Organic Synthesis*. Wiley: New York, **1967**.
62. Smith, M. B.; March, J., *March's Advanced Organic Chemistry*. 5th ed.; Wiley: New York, **2001**.
63. Yan, K.; Upton, B. M.; Ellern, A.; Sadow, A. D., *J. Am. Chem. Soc.* **2009,** *131* (42), 15110-15111.
64. Lampland, N. L., Unpublished work. 2012.
65. Parks, D. J.; Piers, W. E.; Parvez, M.; Atencio, R.; Zaworotko, M. J., *Organometallics* **1998,** *17* (7), 1369-1377.
66. Banovetz, J. P.; Suzuki, H.; Waymouth, R. M., *Organometallics* **1993,** *12* (11), 4700-4703.
67. Molander, G. A.; Corrette, C. P., *Organometallics* **1998,** *17* (25), 5504-5512.
68. Speier, J. L.; Zimmerman, R. E., *J. Am. Chem. Soc.* **1955,** *77* (23), 6395-6396.

Chapter 6: Conclusion

General conclusions

The design of oxazoline containing ligands continues to be a popular area of development in metal-catalyzed chemistry. In particular, the area of bis-oxazolines has seen drastic growth in the past two decades. Our work has shown that all aspects of ligand design are of critical importance. This is exemplified by comparing the bis(oxazolinyl)propane and 1,5-bis(phosphino)pentane ligands and their aptitude to form 16-membered bimetallic macrocycles and cyclometalated palladium(II) pincer complexes. The difference in reactivity is likely due to the difference in donor groups. Additionally, a Probox containing pincer complex of rhodium(III) is isolated but in very low yield while the analogous bis-oxazoline ligands containing aromatic backbones cyclometalate readily and in good yield. Thus, the backbone of the ligand can also significantly impact the reactivity of the ligand.

Likewise, the synthesis of a chiral C_3-symmetric ligand for magnesium and calcium provides access to thermally robust group 2 metal complexes that are active for the hydroamination/cyclization of aminoalkenes to their corresponding pyrrolidines. Unfortunately, the stereoselectivity was rather poor compared to known group 3 and group 4 metal complexes that can achieve greater than 90% ee for the same substrates. The lack of significant stereoselectivity observed is an interesting comparison to the highly stereoselective polymerization catalysts based on dicationic ‘trisox’ lanthanide compounds.

The tris(oxazolinyl)phenylborate ligand is highly effective at stabilizing reactive magnesium compounds in order to investigate their stoichiometric reactivity. Kinetic studies on magnesium amide and magnesium alkyl compounds have allowed us to

propose a nucleophilic attack mechanism for magnesium mediated Si–N and Si–C bond forming reactions. Additionally, $To^{M}MgMe$ catalyzes the hydrosilylation of *tert*-butyl acrylate in the presence of $B(C6F5)_3$.

Future directions

The study of the reactivity of $To^{M}MgMe$ is far from complete. As discussed in Chapter 5, we have discovered that a system containing $To^{M}MgMe$ and $B(C_6F_5)_3$ is a good hydrosilylation catalyst for *tert*-butyl acrylate. We have been unable to structurally characterize $To^{M}MgHB(C_6F_5)_3$; therefore, its proposed structure was based on reactivity and spectroscopic studies. This would be a valuable compound to isolate and structurally characterize so its stoichiometric reactivity can be studied. The scope of the hydrosilylation catalysis has only begun and a significant amount of effort should go into the development of this catalyst system. Kinetic studies on the stoichiometric steps and the overall catalytic cycle need to be conducted to elucidate the mechanism for the hydrosilylation of *tert*-butyl acrylate. A mechanistic comparison between the reaction of $To^{M}MgMe/PhSiH_3$ and the hydrosilylation of *tert*-butyl acrylate would be interesting as both involve Si–C bond formation steps.

Additionally, chiral centers are generated upon hydrosilylation of α,β-unsaturated carbonyl compounds, thus a chiral ligand (e.g. $[To^{T}]$) should be utilized to investigate the possible stereoselective transformations. The % ee's observed for the hydroamination/cyclization of aminoalkenes are low; however, the stereochemical-determining step for hydroamination/cyclization involves an intramolecular cyclization versus an intermolecular nucleophilic attack as is proposed for Si–C bond formation.

Finally, olefin insertion into the Mg–H bond should be expanded to other Mg–X compounds. For example, catalytic hydrophosphination of C=X multiple bonds with

To^{M}MgMe could yield interesting secondary and tertiary phosphines. New chiral ligands for metal-catalyzed transformations could be accessed if the C=X multiple bonded species contains another donor group (e.g. imine).

Appendix: NMR spectra used to determine % ee of pyrrolidines

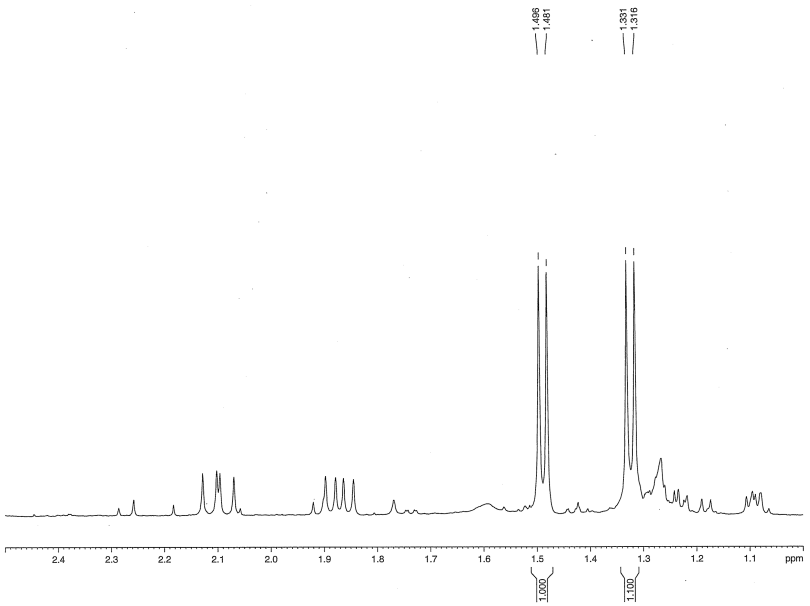

Figure A-1. ^{1}H NMR of the (+)-Mosher amide of racemic 2-methyl-4,4-diphenylpyrrolidine via $MgMe_2{\cdot}(O_2C_4H_8)_2$.

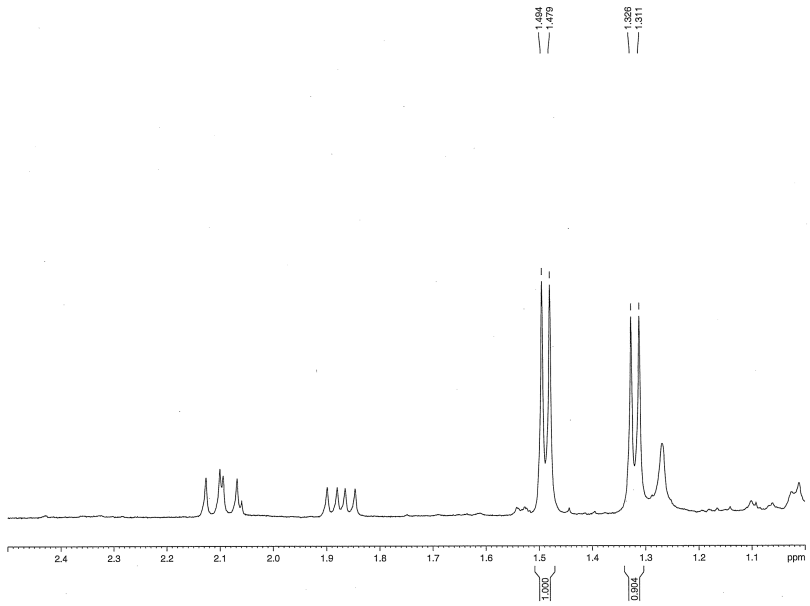

Figure A-2. ^{1}H NMR spectrum of the (+)-Mosher amide of 2-methyl-4,4-diphenylpyrrolidine via $To^{T}MgMe$. 0 % ee.

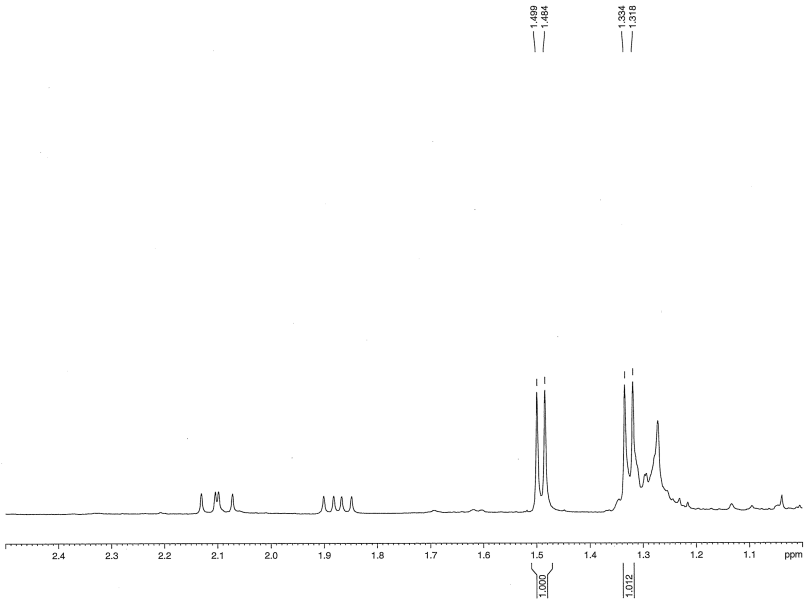

Figure A- 3. ^{1}H NMR spectrum of the (+)-Mosher amide of 2-methyl-4,4-diphenylpyrrolidine via $To^{T}CaC(SiHMe_2)_3$. 0 % ee.

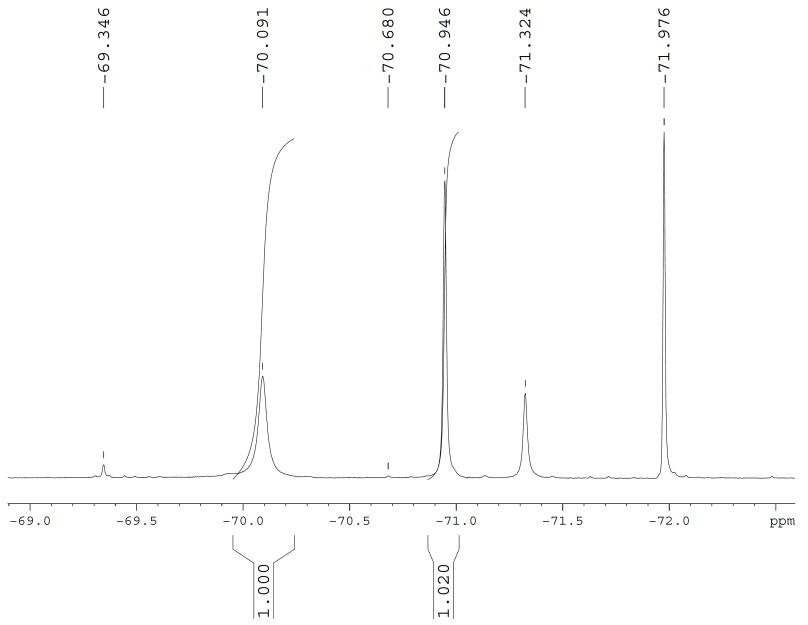

Figure A- 4. $^{19}F\{^{1}H\}$ NMR spectrum of the (+)-Mosher amide of racemic 3-methyl-2-azaspiro[4.5]decane via $MgMe_2{\cdot}(O_2C_4H_8)_2$.

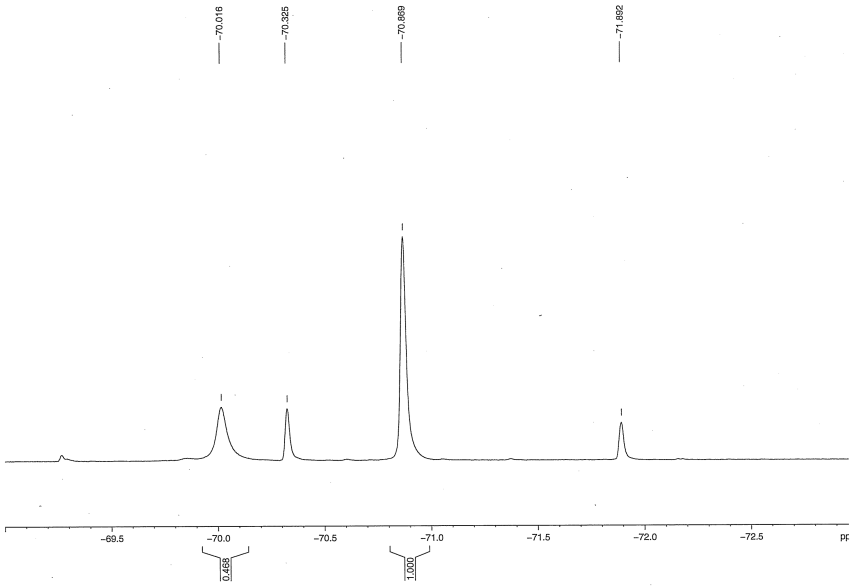

Figure A- 5. $^{19}F\{^{1}H\}$ NMR spectrum of the (+)-Mosher amide of 3-methyl-2-azaspiro[4.5]decane via $To^{T}MgMe$. 36 % ee.

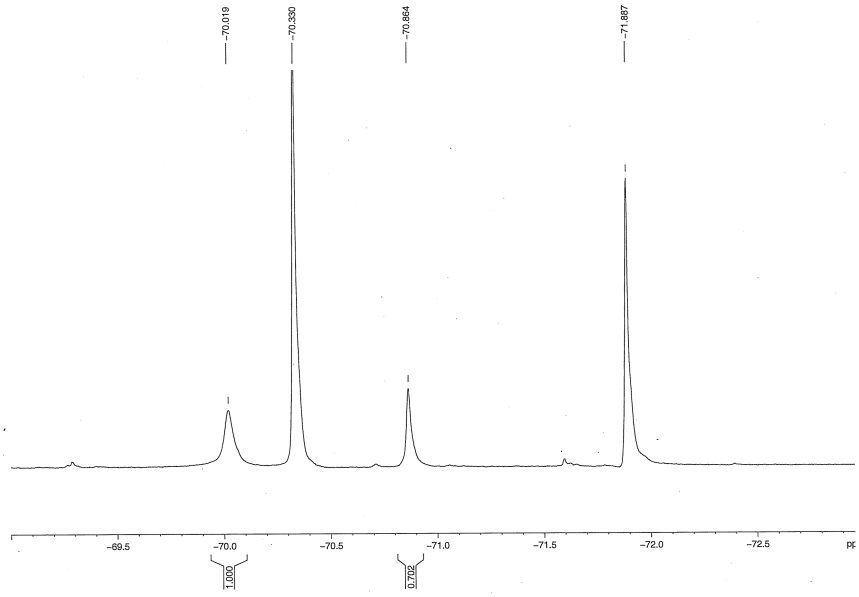

Figure A- 6. $^{19}F\{^{1}H\}$ NMR spectrum of the (+)-Mosher amide of 3-methyl-2-azaspiro[4.5]decane via $To^{T}CaC(SiHMe_2)_3$. 18 % ee.

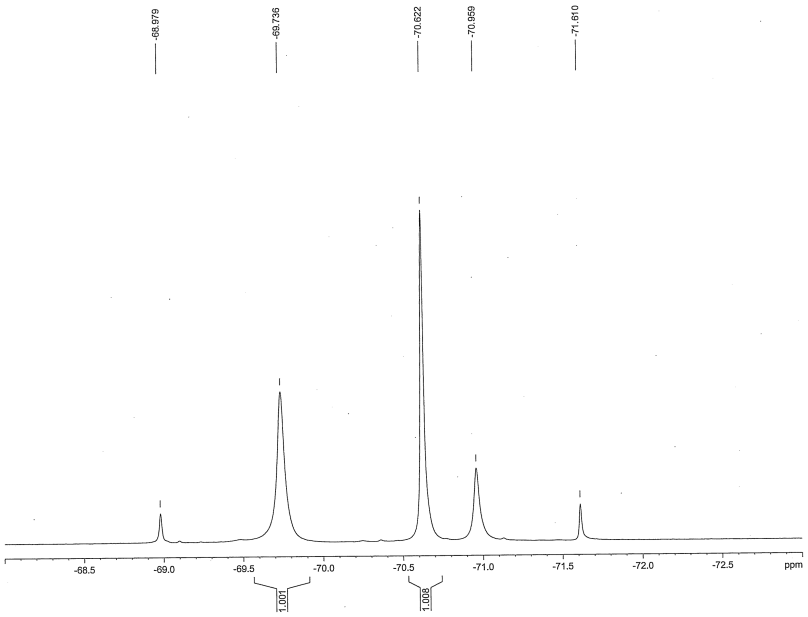

Figure A- 7. $^{19}F\{^{1}H\}$ NMR spectrum of the (+)-Mosher amide of racemic 2,4,4-trimethylpyrrolidine via $MgMe_2{\cdot}(O_2C_4H_8)_2$.

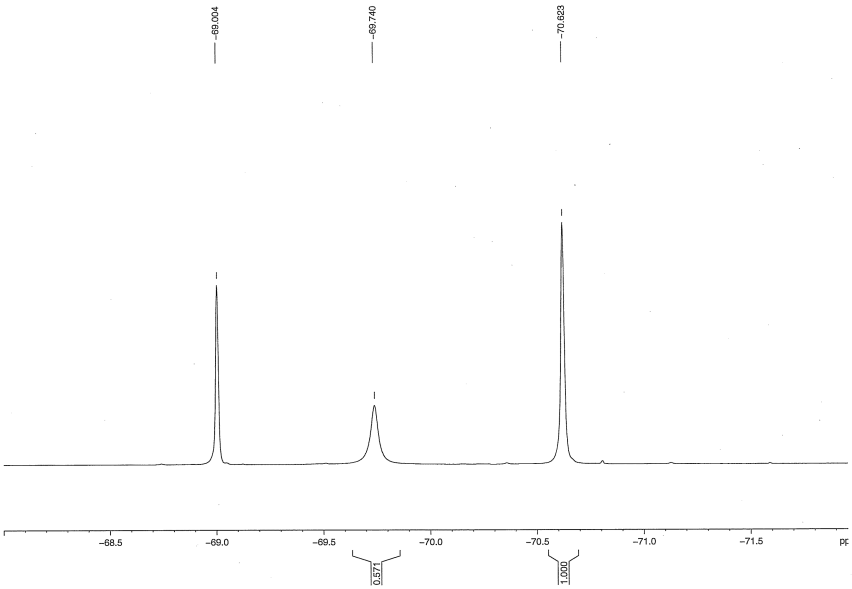

Figure A- 8. $^{19}F\{^{1}H\}$ NMR spectrum of the (+)-Mosher amide of 2,4,4-trimethylpyrrolidine via $To^{T}MgMe$. 27 % ee.

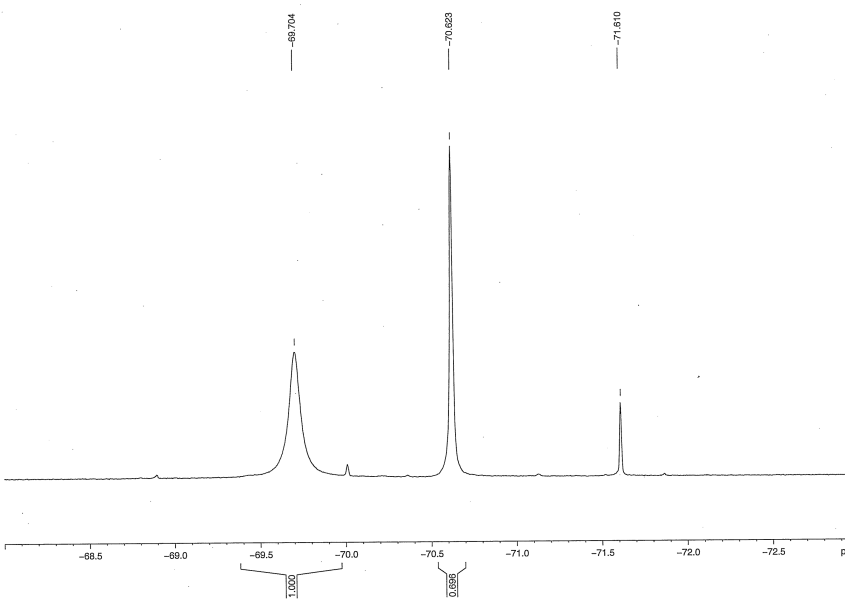

Figure A- 9. $^{19}F\{^{1}H\}$ NMR spectrum of the (+)-Mosher amide of 2,4,4-trimethylpyrrolidine via $To^{T}CaC(SiHMe_2)_3$. 18 % ee.